CHEMICAL COVALENT LABELING AND TANDEM MASS SPECTROMETRY FOR TARGETED PROTEIN CHARACTERIZATION, QUANTIFICATION AND STRUCTURAL ANALYSIS

By

YALI LU

A DISSERTATION

Submitted to
Michigan State University
in partial fulfillment of the requirements
for the degree of

DOCTOR OF PHILOSOPHY

Chemistry

2010

ABSTRACT

CHEMICAL COVALENT LABELING AND TANDEM MASS SPECTROMETRY FOR TARGETED PROTEIN CHARACTERIZATION, QUANTIFICATION AND STRUCTURAL ANALYSIS

By

YALI LU

A major goal within the emerging field of proteomics is the systematic identification, characterization and quantitative analysis of protein expression, protein post-translational modifications (PTMs) and specific functional protein-protein interactions that are involved in the regulation/deregulation of normal cellular function. To date, the application of mass spectrometry (MS) and tandem mass spectrometry (MS/MS) based approaches have achieved remarkable progress with regard to the investigation of biological problems. However, the enormous sample mixture complexity and the presence of various PTMs that regulate cellular processes present formidable challenges for the comprehensive analysis of cellular proteomes. Chemical labeling has been a valuable tool to assist in MS-based proteomics, to achieve the goal such as the improved peptide/protein sequence analysis, the enrichment and characterization of protein PTMs, the quantitation of protein expressions or to probe protein structure and protein-protein interactions. Here, the development of fixed charge chemical labeling strategies for selective control of the multistage gas-phase fragmentation reactions of peptide ions is described. In one study, a novel 'fixed charge' sulfonium ion-containing 'amine reactive' cross-linking reagent *S*-methyl 5,5′-thiodipentanoylhydroxysuccinimide was synthesized, characterized, and initially applied to model peptides, in order to develop a 'targeted' multistage tandem mass spectrometry based approach for the identification and characterization of protein-protein interactions. Under low energy collision induced dissociation (CID)-MS/MS conditions, peptide

ions containing this cross-linker are shown to exclusively fragment via facile cleavage of the bond directly adjacent to the 'fixed charge', which was found to be independent of the precursor ion charge state or amino acid composition (i.e., proton mobility). Thus, the cross-linked peptides can be effectively identified from unmodified peptides, and the various types of cross-linked products (i.e., intra, inter, and dead-end) that may be formed from a cross-linking reaction are readily distinguished via recognition of their distinct fragmentation patterns. Another study was focused on the development and application of a peptide derivatization strategy using an amine specific sulfonium ion containing reagent *S,S*′-dimethylthiobutanoylhydroxysuccinimide ester iodide (DMBNHS) combined with CID-MS/MS and electron transfer dissociation (ETD)-MS/MS for the enhanced characterization and quantitative analysis of protein phosphorylation. The introduction of this fixed charge to phosphopeptides is shown to lead to improved ionization efficiencies, and an increase in the abundance of higher charge state precursor ions following electrospray ionization (ESI). Upon CID-MS/MS, the exclusive neutral loss(es) of dimethylsulfide are observed, without loss of the phosphate group(s). The relative abundances of "light" versus "heavy" neutral loss product ions generated from CID-MS/MS of D_6-light and D_6-heavy DMBNHS stable isotope labeled phosphopeptides enables their differential quantitative analysis, whereas subsequent ETD-MS/MS of the intact precursor ion(s) allows phosphopeptide sequence identification and phosphorylation site characterization, suggesting the reagent holds great promise for studies of protein post-translational modifications.

ACKNOWLEDGMENTS

I would like to express my deep thanks to all those who gave me the possibility to reach the end of the road leading to the completion of this dissertation. First and foremost, I would like to thank my advisor, Professor Gavin E. Reid, for his guidance and constant support during my research and study at Michigan State University. His perpetual energy and dedication in research had motivated me throughout the whole process. I also wish to express my sincere thanks to other committee members, Professor Gary J. Blanchard, Professor Babak Borhan, and Professor A Daniel Jones for their valuable advice and friendly help through extensive discussions around my work. Many thanks to the collaborators who have contributed to the research work for many interesting findings. Professor Paul M. Stemmer and Dr. Joe Caruso at Wayne State University generously provided the instruments and supports for enabling the analysis of many phosphopeptides by electron transfer dissociation. I would like to also thank Mr. Yujing Tan and Professor Merlin L. Bruening for their phosphopeptide enrichment strategy. I would like to give my particular thanks to Professor Babak Borhan and Dr. Marina Tanasova for support in the preparation of ionic cross-linking reagents. I would like to thank the previous and current members of the Reid research group, for their friendship, encouragement, and helpful discussions along this journey. Finally, I wish to thank my family and friends for helping me get through the difficult times, and for all the emotional support and caring they provided. I owe my deepest thanks to my parents, Yunhong Lu and Qiuzhi Sun, for being along with me during this not easy but rewarding journey.

TABLE OF CONTENTS

LIST OF TABLES

LIST OF FIGURES

LIST OF SCHEMES

CHAPTER ONE

A BRIEF INTRODUCTION TO CHEMICAL LABELING AND MASS SPECTROMETRY STRATEGIES EMPLOYED FOR PROTEOMIC ANALYSIS

1.1 Introduction to Proteomics

Proteomics has become one of the key technologies in the postgenomic era. The goal of proteomics is to comprehensively identify, characterize and quantify changes in protein expression, as well as to characterize protein-protein interactions, under the influence of biological perturbations [1, 2]. Over the past decade, mass spectrometry (MS) has emerged as the most efficient and versatile tool in the field of proteomics [3-6]. With the development of the electrospray ionization (ESI) [7] and matrix-assisted laser desorption/ionization (MALDI) [8, 9] techniques, large biological molecules may be ionized with minimal fragmentation, readily amenable for MS analysis. MS-based proteomics has achieved remarkable progress with regard to the investigation of biological problems; however there is still a long way to go for the comprehensive and complete characterization of cellular proteomes and their post-translational modifications (PTMs) [2, 10, 11]. The increase in sample mixture complexity, resulting from proteolytic digestion and the dynamic range associated with the proteome, presents formidable challenges for protein identification and characterization. Various PTMs that regulate cellular processes further complicate the analysis. The ability to form a series of 'sequence' product ions, via fragmentation of the peptide amide bonds during low-energy collision induced dissociation-tandem mass spectrometry (CID-MS/MS) is typically required for database analysis and protein

identification. However, it is well documented that the gas-phase fragmentation reactions of protonated peptide ions are influenced strongly by both the amino acid composition and charge state of the precursor ion (i.e., proton mobility) [12-14]. In addition, under certain conditions of proton mobility, the presence of several common PTMs may result in the formation of dominant 'non-sequence' neutral loss product ions, via fragmentations occurring at the modified amino acid side chain [15], such as the neutral loss of H_3PO_4 (98 Da) from phosphoserine or phosphothreonine containing peptides [16, 17], or the loss of CH_3SOH (64 Da) from methionine sulfoxide containing peptides [18, 19]. The formation of these non-sequence neutral loss product ions in high relative abundance may limit the amount of sequence information that is available for the unambiguous identification of a peptide, or for localization of the modification site(s) within the peptide sequence.

The ability to perform comprehensive quantitation of protein expression and its changes under biological perturbations is one of the most important goals of proteomics [20, 21]. However, MS is not an inherently quantitative technique. Due to the strong dependence of ionization on the physical and chemical nature of the analyte, the intensity of a peptide ion introduced into the mass spectrometer via ESI or MALDI does not necessarily reflect the amount of that peptide present in the sample mixture. Thus, the development of methods for accurate protein quantification is currently another challenging area of MS-based proteomics.

Mass spectrometry is relatively a new technique in the field of protein structural analysis. In recent years, affinity purification combining mass spectrometry (AP-MS) has been used to characterize protein complexes and protein-protein interactions [22]. With the AP-MS method, multi-protein complexes are isolated from cell lysates using single or multiple AP experiments,

subjected to proteolytic cleavage and then the complex components are identified by MS. The AP-MS approach allows the protein interacting networks to be mapped, however, only those protein-protein interactions that are stable enough to survive the subsequent lysis and purifications could be detected. In addition, information regarding the specific interacting site(s) of the protein is typically not obtainable by this approach.

1.2 Introduction to Chemical Labeling

To address the challenges associated with mass spectrometry-based proteomics, chemical labeling has become a valuable tool to assist in identification, characterization and quantification of protein expression as well as structural analysis of protein complexes [22-29]. Chemical labeling is a strategy to covalently modify specific functional group(s) residing on amino acid side chains, or on the protein termini. Ideal labeling reactions would modify the target functional groups without side reactions on other residues or degradation of the analytes, and complete derivatization should be achievable without using a high excess of derivatizing reagents in a short reaction period.

Chemical labeling methods have been widely employed to address challenges associated with protein identification and characterization. Numerous chemical labeling approaches [26, 30] have been developed to direct the formation of a desired series of sequence product ions in order to facilitate protein sequencing by conventional "bottom up" strategies [31, 32] upon CID-MS/MS. The low stoichiometry of the PTM peptides present in the large majority of non-PTM peptides requires efficient enrichment procedures prior to MS analysis. Chemical labeling can facilitate enrichment by converting PTMs into tractable sites for the purpose of affinity

enrichment [27]. Chemical labeling has also played an essential role in quantitative proteomics, whereby relative or absolute quantitative analysis can be realized in a mass spectrometer by introducing isotope labels into the samples via chemical labeling approaches at either the protein or the peptide level [28]. Finally, via covalent labeling, structural information about proteins or protein complexes can be obtained by measuring the differential reactivity of amino acid side chains or the spatial relationship between two amino acid side chains [29, 33]; such strategies are especially useful for capturing transient and labile protein-protein interactions under physiological conditions. According to these aspects, the applications of chemical labeling strategies in the field of MS-based proteomics are summarized below in the remainder of this brief introduction, with particular attention given to analysis strategies using labeling reagents containing fixed charges.

1.3 Chemical Labeling Strategies to Improve the Sequence Analysis of Peptide Ions

1.3.1 Chemical Labeling Strategies to Improve Peptide Sequencing using Collision Induced Dissociation-Tandem Mass Spectrometry (CID-MS/MS)

A major challenge facing strategies for protein identification and PTM characterization is the ability to form a series of sequence product ions from protonated peptides during CID-MS/MS. Although the mechanisms of peptide ion fragmentation by low energy CID will be discussed in detail in the next chapter, it should be noted here that complete sequence coverage is not usually achieved during CID-MS/MS. The reason for incomplete sequence coverage is that

the CID mechanism is highly dependent on the proton mobility of the peptide ions and the presence of labile PTMs [12-14, 17, 18].

To improve peptide identification and characterization by *de novo* sequencing or database searching, a number of chemical labeling methods have been developed in an effort to enhance product ion sequence coverage and to reduce complexity in CID-MS/MS spectra. Modification of the side chains of basic amino acid residues within a peptide to alter proton affinity is one such approach [34-36]. For example, Foettinger *et al.* have demonstrated that the proton affinity of the strongly basic guanidine group of arginine residues is decreased by modification with malondialdehyde [35]. Therefore, the ionizing proton is less likely to be sequestered and allows the "mobility" of the proton along the peptide backbone to initiate the backbone cleavage. As a result of the investigation of a set of modified standard peptides, it was found that significantly more sequence product ions were observed after derivatization of arginine side chains in most cases.

Introducing fixed negative or positive charges to peptide N- or C-termini via chemical labeling is another efficient strategy to simplify and direct fragmentation towards a single series of sequence product ions [26, 37-40]. Because of the primary amine nucleophilicity and basicity, the N-termini of peptides are usually the target for the modification reactions. By adding a negative charge on the N-termini of peptides via sulfonation, it is possible to direct the location of the ionizing proton(s) to the C-terminus, such that when the peptide backbone is cleaved the formation of y-ions will be favored when using CID [40]. This approach is especially effective when applied to tryptic peptides, due to the high proton affinity of the arginine or lysine residues on tryptic peptide C-termini. Thus, a range of sulfonation reagents such as chlorosulfonylacetyl chloride [37, 41], 2-sulfobenzoic acid cyclic anhydride [42], 3-sulfopropionic acid N-

hydroxysuccinimide (NHS) ester [43], 4-sulfophenyl isothiocyanate (SPITC) [44-47] and 3-sulfobenzoic acid NHS ester [48, 49] have been applied to add anionic sulfonic acid groups to the N-terminus of tryptic peptides. These derivatization reactions are simple and can be performed quickly with good reaction yields. Among these approaches, 3-sulfobenzoic acid NHS ester appears to be most advantageous since no loss of the derivative is observed during the fragmentation process of modified peptides; for example, a complete series of y-ions were formed by this method during MALDI tissue imaging analysis [49]. The addition of a positively charged group to the N-terminus of peptides, using tris(2,4,6-trimethoxyphenyl)phosphonium acetic acid N-hydroxysuccinimide ester (TMPP-Ac-OSu) has also been successfully applied to simplify CID-MS/MS spectra [49]. Compared to sulfonation modification, introducing a positively charged tris(2,4,6-trimethoxyphenyl)phosphonium acetyl (TMPP-Ac) group to the N-termini of the peptides (Scheme 1.1) orients fragmentation towards the formation of N-terminal fragment ions, which is independent of the presence and/or position of basic residues in the peptide sequence, and therefore the method has found wide use in the analysis of non-tryptic peptides [38, 50-55].

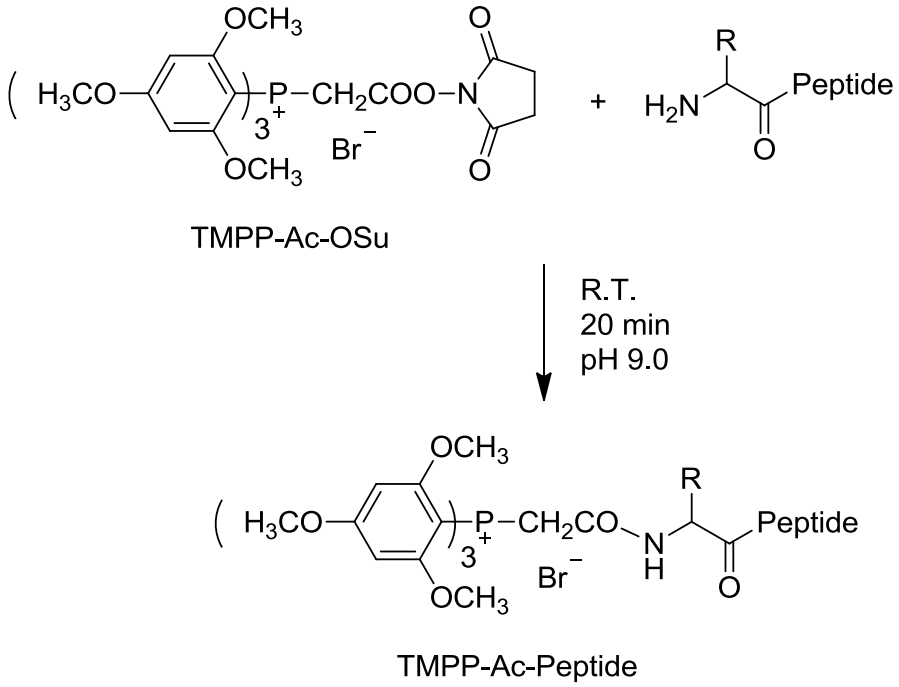

Scheme 1.1 Reaction of the TMPP-Ac-OSu Reagent with the N-terminus of a peptide. Adapted from Reference [55].

During the time scale of CID activation/dissociation, cyclic ions may be formed in the gas phase via head-to-tail interaction of b-ions resulting from the dissociation of short peptides [56]. The presence of "nondirect sequence ions" via ring opening at various amide bonds can complicate peptide and protein identification or even lead to erroneous results. The formation of such interfering ions can be avoided by peptide N-terminal modification. In a recent work by Samgina and coworkers, N-terminal modification via acetylation, sulfobenzoylation or the addition of a 2,4,6-trimethylpyridinium group successfully blocked gas-phase cyclization of short peptides from the tryptophyllin family, thereby improving the *de novo* sequencing of these short peptides [57].

1.3.2 Chemical Labeling Strategies to Improve Peptide Sequencing using Electron Capture Dissociation- (ECD-) and Electron Transfer Dissociation-Tandem Mass Spectrometry (ETD-MS/MS)

Recently, electron capture dissociation (ECD) [58] and electron transfer dissociation (ETD) [59] have been introduced as new ion activation techniques for MS/MS experiments. ECD and ETD can be regarded as complementary approaches to CID for peptide/protein sequence analysis [60-66]. ECD/ETD techniques are based on the interaction of multiply charged peptides with either free electrons (ECD) or anionic species (ETD). As a result of the non-selective nature of electron transfer to the peptide, free radical sites may form anywhere along the length of the peptide backbone. Consequently, radical-directed cleavage results in a homogeneous series of complementary N- and C-terminal fragment ions in a manner which allows labile PTM information to be retained. ECD/ETD techniques hold great promise for the analysis of protein PTMs; however, the efficiency of such electron-based dissociation methods is highly dependent on the charge density of the precursor peptide ions [62, 65-68], which limits their applicability for the dissociation of singly or doubly charged tryptic peptides.

Several recent studies have demonstrated the success of chemical labeling strategies to improve ECD/ETD fragmentations. One such way is to increase the charge state of peptide ions via the attachment of fixed positive charge sites so that the dissociation efficiency becomes enhanced. For example, the introduction of a positive charge on the thiol side chain of cysteine containing peptides by using either *N*,*N*-dimethyl-2-chloro-ethylamine [69] or (3-acrylamidopropyl)-trimethyl ammonium chloride [70] yielded peptide precursor ions of higher charge states and striking enhancements of ETD fragmentation for improved sequence coverage.

To enhance *de novo* sequencing, chemical labeling strategies have been employed to simplify fragmentation patterns of doubly charged peptides while using electron based dissociation methods, similar to those carried out for CID-MS/MS. By converting the N-terminus to an acidic sulfonate derivative with either 4-sulfophenyl isothiocyanate (SPITC) or 4-(chlorosulfonyl)phenyl isocyanate (SPC), the presence of N-terminal fragments were eliminated and resulted in the enhanced generation of C-terminal product ions with high sequence coverage [71]. However, in such an approach the sensitivity might be compromised in positive ion mode due to the ionization of acidic N-termini after modification. The attachment of basic groups via several common approaches to Lys-N and/or tryptic peptides has been investigated by Hennrich and coworkers under ETD conditions [72]. The dissociation of doubly charged peptide ions by dimethylation, guanidination, and imidazolinylation showed simplified product ion spectra and enhanced sequence coverage, especially for imidazolinylated peptides.

It has been previously shown that modification of *O*-glycosylated and *O*-phosphorylated peptides with positively charged TMPP-Ac at the N-termini improves the sequence coverage and simplifies data interpretation from ECD fragmentation of doubly charged peptide ions [73]. However, suppressed peptide backbone cleavage was observed in doubly TMPP-Ac modified dipeptides in the 2+ charge state [74]. Such an observation was also reported during ECD-MS/MS of doubly and triply protonated peptide ions modified with a bi-pyridine derivative at the N-termini [75]. Similarly, O'Connor and co-workers have demonstrated that the attachment of a positively charged trimethylpyridinium (TMP) group to the N-termini and/or lysine side chains resulted in fewer backbone cleavages and more abundant side-chain cleavages upon ECD [76]. From these reports, it appears that the electronic properties and stability of the charged groups introduced to the peptides following electron attachment has a significant impact on the

ECD/ETD fragmentation pathways. In this regard, a number of experimental studies and theoretical calculations have been carried out, to help understand the fundamentals of ECD/ETD, from the dissociation of doubly protonated peptide ions modified with varying electron affinity tags [77], to answer questions such as the effect of charge site-identity (ionizing proton vs. fixed charge) on electron-transfer ion/ion reactions [78] and to investigate the mechanism of specific disulfide bond cleavage upon ETD [79]. Based on these results, consideration of criteria such as recombination energy and hydrogen atom affinity compared to those of peptide amide groups has been proposed for the selection of chemical tags to facilitate future targeted ECD/ETD fragmentation approaches [80].

1.3.3 Chemical Labeling Strategies to Improve Peptide Sequencing using Photo Dissociation-Tandem Mass Spectrometry (PD-MS/MS)

Photodissociation (PD) strategies, including infrared multiphoton dissociation (IRMPD) and ultraviolet photodissociation (UVPD), have shown their particular strength for biomolecule sequencing because of their great potential for selective bond cleavage by using tunable laser sources [81-84]. It was observed that PD efficiency is highly dependent on the deposited laser energy and intensity [85]. The use of chemical labeling for efficient PD of peptide ions can be traced back more than twenty years ago. In an early study, photodissociaton of singly-charged dinitrophenyl (DNP) modified amino acids and peptides was evaluated using visible and UV photons [86]. Peptide backbone cleavage with little side chain cleavage of the DNP tag was observed from visible PD of DNP modified peptides; however, side chain loss within the tag often dominated UVPD spectra, suggesting photodissociation of peptide ions is an energy

dependent process. The modification of peptide N-termini using the Edman reagent phenyl isothiocyanate (PITC) and its derivative 4-sulfophenyl isothiocyanate (SPITC) provides good chromophores at 266 nm for UVPD. By this approach, the intensity required for efficient UVPD was greatly reduced with minor interference to peptide backbone dissociation [87]. To improve photoabsorptivities of the peptides and/or to reduce the complexity in product ion spectra, peptide N-terminal sulfonation approaches have been developed and explored by Brodbelt et al. with both IRMPD [88] and UVPD [89] methods. Recently, the Brodbelt group reported a new IR-chromogenic reagent, 4-methylphosphonophenylisothiocyanate (PPITC), which bears a negative charge site similar to the sulfonation reagents [90]. The PPITC labeled peptides were found to have enhanced photoabsorptivities at a wavelength of 10.6 μm, compared to SPITC and TIPC derivatized peptides, and higher sequence coverage was generally obtained upon IRMPD-MS/MS.

To achieve site-selective fragmentation of unmodified peptides and proteins is a formidable task given the current understanding of the techniques available for photodissociation of peptide bonds. As such, chemical labeling provides an attractive alternative way to facilitate selective fragmentation in the field of PD-MS/MS [91]. It has been shown that selective cleavage can occur at protein tyrosine or histidine residue sites using UVPD following the conversion of the sites to iodinated derivatives [91]. Photoactivation of iodinated protein at a wavelength of 266 nm specifically dissociates C-I bonds and generates a highly localized radical site which directs subsequent CID dissociation of the protein backbone to occur selectively at the modified tyrosine or histidine residue sites. Another example of label-assisted PD-MS/MS has shown that the attachment of a quinone moiety to cysteine residues can lead to selective photodissociation of the

backbone at the modified cysteines upon UVPD, allowing the presence and location(s) of free or disulfide bound cysteine residues to be easily identified from within peptides or proteins [92].

1.4 Chemical Labeling Strategies for the Enrichment and Characterization of Post-Translational Modifications

Protein post-translational modifications (PTMs) play an essential role in the co-regulation of biological events. The global identification and characterization of protein PTMs is often a difficult task for MS-based proteomics due to their low stoichiometry and typical labile and transient characteristics [11, 93]. The chemical labeling strategies described above for improved peptide sequencing may also be able to assist in characterization of post-translationally modified proteins [73]. For example, Czeszak *et al.* has demonstrated that the use of a positively charged phosphonium tag enables the unambiguous localization of *O*-glycosylation sites without cleaving labile glycans upon matrix-assisted laser desorption ionization/postsource decay (MALDI/PSD) analysis of modified *O*-glycopeptides [94].

Many efforts have been devoted to the development of modification-specific enrichment techniques for mapping protein PTMs [27]. A PTM can be chemically modified for the purpose of affinity enrichment, improved MS identification or/and quantitative analysis. The PTM phosphate group can be converted into a functional moiety by β-elimination/Michael addition reaction [95] or by phosphoamidate chemistry [96, 97]. Phosphoserine and phosphothreonine can undergo β-elimination reactions under alkaline conditions. The resultant dehydroalanine or dehydroamino-2-butyric acid intermediate can readily react with a nucleophile (usually thio) as a Michael acceptor thus converting the original phosphates into various functional entities. If an

affinity tag (such as biotin) [98] or an affinity tag reactive group (such as thiol) [99-102] is introduced, selective enrichment of phospho-Ser/Thr-containing peptides/proteins is enabled. Functional groups that give rise to unique reporter ions upon CID-MS/MS have also been introduced at the original phosphorylation site(s) by the same manner, for enhanced phosphopeptide identification [103-106]. A representative example is shown in Figure 1.2 [103], where the β-elimination/Michael addition is performed using 2-dimethylaminoethanethiol as nucleophile and the resultant thioether is converted into the corresponding sulfoxide derivative via the treatment with hydrogen peroxide. The sulfoxide undergoes facile gas phase fragmentation and allows the formation of a unique product ion at m/z 122.06. This enables use of sensitive and specific precursor ion scan MS/MS for detection of phosphorylated species within complex peptide mixtures. Another derivatization reagent, *N*-(4-bromobenzoyl)aminoethanethiol was reported recently by Mano *et al.* for its characteristic isotopic pattern [107]. The product ions which contain modified phospho-Ser/Thr sites are readily identified from their characteristic twin peaks with an intensity ratio of approximately 1:1 and a two-mass unit difference. In addition, double pseudoneutral loss experiments, during which both ^{79}Br- and ^{81}Br-containing neutral losses from product ion mass spectra are detected, can be performed for the selective identification of modified phosphopeptides in a highly complex mixture [107]. Interestingly, the Hathaway group described a chemical-enzymatic approach by using 2-aminoethanethiol as a Michael addition reagent [108, 109]. Enzymatic cleavage sites at original phospho-Ser/Thr residues are generated from the resultant aminoethylcysteine analogs by using a lysine-specific protease, which can lead to the modified residues being the only cleavage sites if lysine residues are deliberately blocked. *O*-glycosylated peptides are reported by the Hathaway group to follow the same approach as well. Successful

application of this method has been shown for the identification of phosphorylaion sites in several phosphoproteins, for example bovine α- and β-casein, α-tubulin, and GP kinase 2 by Knight *et al.* [110] and bovine α-S1 casein by McCormick and coworkers [111].

As a side benefit, an enhanced ionization efficiency of derivatized peptides is usually observed when negatively charged phosphate groups are substituted by basic functional moieties using β-elimination/Michael addition approaches, thereby increasing the sensitivity of the analysis [104, 105, 112]. In addition, the incorporation of isotope labels into nucleophilic derivatization reagent for quantitative analysis of the phosphorylation state of proteomes can be achieved [112-114], following the same manner of protein quantitative analysis which will be discussed in the next section.

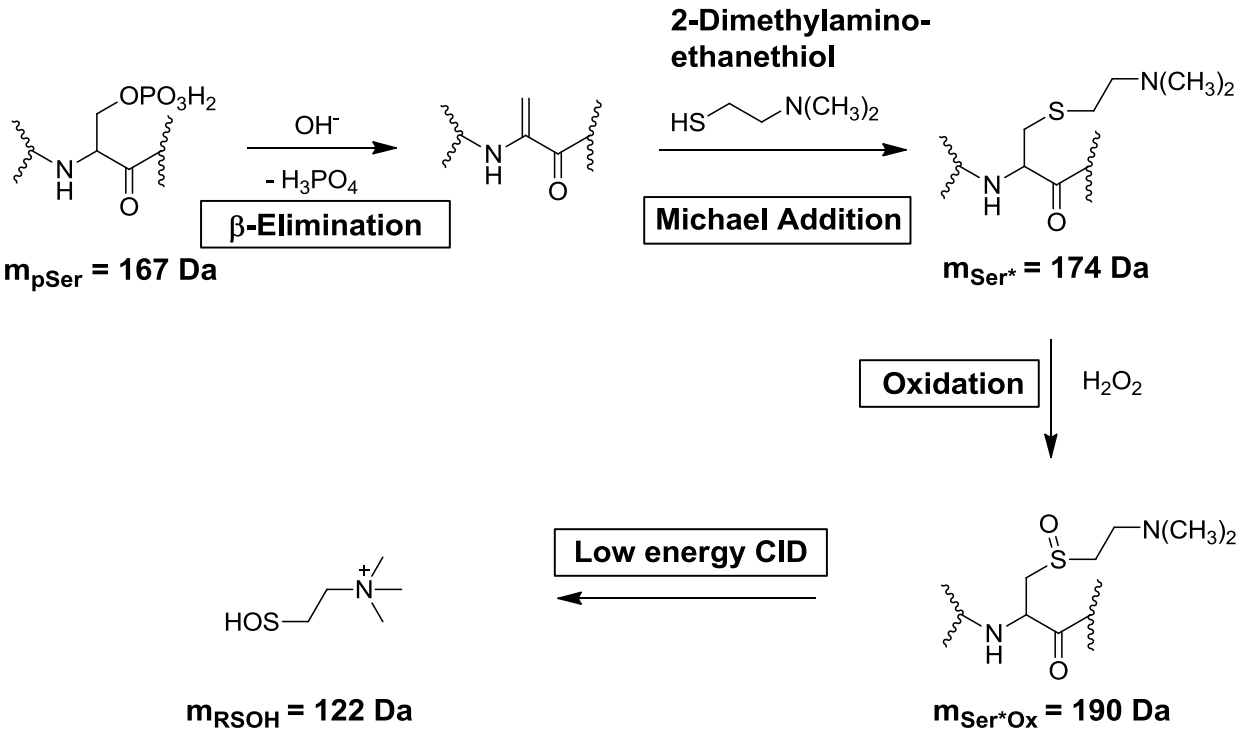

Figure 1.1 Derivatization strategy for phosphoserine-containing peptides. Phosphoserine undergoes β-elimination upon treatment with strong bases. The resulting Michael system reacts with the nucleophilic thiol group of 2-dimethylaminoethanethiol which introduces a highly basic functional group at the former phosphorylation site. Controlled oxidation of the thioether to the sulfoxide is accomplished by short incubation with 3% H_2O_2. The generated 2-dimethylaminoethanesulfoxide derivative gives rise to a characteristic fragment ion (sulfenic acid derivative) at m/z 122.06 upon low energy CID. Adapted from Reference [103].

Due to the high lability of the sugar-Ser/Thr linkage, conventional CID-MS/MS often fails in *O*-glycan site identification. Alkaline induced β-elimination with NaOH has been used to liberate *O*-linked glycans from peptides or proteins for identification of *O*-glycosylation sites [115]. Later, this method was optimized by using mild and volatile basic alkylamines to convert *O*-glycosylated Ser and Thr residues into amine derivatives [116-118]. When combined with a concomitant Michael-type addition of nucleophilic reagent, such as ethanethiol, the strategy is more efficient at localizing the initial glycosylation site due to the higher mass increment

compared with the resultant amine derivatives [119, 120]. Likewise, biotin pentylamine (BAP) or dithiothreitol (DTT) was employed by Wells et al. to tag *O*-linked β-*N*-acetylglucosamine (*O*-GlcNAc) sites following β-elimination reaction to facilitate affinity chromatography. This method was suggested as being amenable to quantitative analysis by using differential isotopic DTT labeling [121]. Recently, chemical approaches have been demonstrated to convert nitrotyrosine [122], *S*-nitrosylation [123] and *S*-palmitoylation [124, 125] modifications into a tractable tag for affinity enrichment and subsequent LC-MS/MS analysis. However, these strategies typically involve multiple reactions, sample loss during each step can be a problem, and unwanted side products are often observed.

1.5 Quantitative Analysis of Protein Expression through Chemical Labeling Strategies

The accurate quantitative analysis of protein expression in responding to stimulus is one of the major goals of proteomics. There are two categories of quantitative proteomics: absolute quantitation which determines the absolute amount of the protein in the sample, and relative quantitation which compares the protein amount among different states [126]. MS can obtain quantitative proteomic information by measuring mass spectral peak intensities or spectral counts from a particular peptide under different conditions, i.e. label-free quantitation [127, 128], or more accurate analysis can be achieved by comparing peptides from different states with predictable mass differences introduced by stable isotope labels [20, 21, 129]. Isotope labels can be introduced into the peptide or protein metabolically, enzymatically or chemically. For accurate quantitation, no matter what labeling method is used, the resulting mass difference between “light” and “heavy” labeled peptides should be at least 3-4 Da to minimize isotope

overlap [20]. In addition, the "light" and "heavy" forms of labeled peptides should co-elute from a chromatographic column. However, the commonly used D-labeled peptides tend to elute earlier than the H-labeled counterparts from commonly used reverse phase column because of the slightly weaker deuterium-bonding compared to hydrogen bonding [130-134]. Due to this concern, more expensive ^{13}C- and ^{15}N-labeled reagents may be preferred [19]. Numerous methods have been developed for stable isotope-based quantification in proteomics. However, only those employing chemical labeling strategies are included in this brief introduction.

1.5.1 Chemical and Stable Isotope Labeling Approaches for MS-Based Quantification

In a typical approach, "light" or "heavy" isotope labels are introduced to the sample at either the protein or peptide level via derivatization with an isotope coded chemical reagent. The two proteomes are then pooled together for subsequent enrichment, separation and MS analysis. Quantitative information is then obtained by measuring the relative abundances of light- and heavy-labeled target peptides following acquisition of a mass spectrum. A range of functional groups within the protein or peptide can be the targets for the isotope labeling reaction. A general overview of commonly employed chemical labeling strategies is listed in Table 1.1, and a more detailed discussion of each of these approaches can be found in a review article by Ong and Mann[20] and references cited therein.

Table 1.1 Chemical-labeling strategies for quantitative proteomics. Adapted from Reference [20].

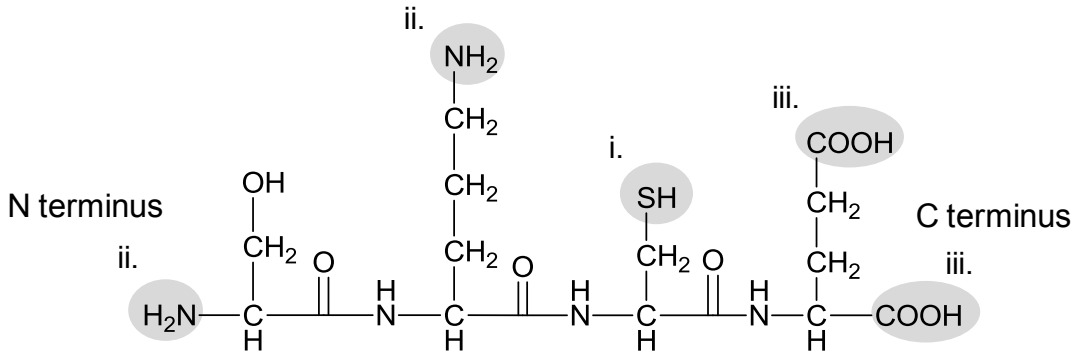

i. Sulfhydryl group-directed (cysteine)

ii. Amine-directed (amino terminus and ε–amino group of lysine)

iii. Carboxyl-directed (carboxyl terminus, aspartic and glutamic acid)

Target	Name of method or reagent	Isotopes	Refs.
Sulfhydryl	Isotope-coded affinity tag (ICAT)	D	45
	Cleavable ICAT	^{13}C	46-48
	Acrylamide	D	101
	Isotope-coded reduction off of a chromatographic support (ICROC)	D	102
	2-vinyl-pyridine	D	103
	N-t-butyliodoacetamide	D	104
	Iodoacetanilide	D	104
	Hys Tag	D	49,50
	Solid-phase ICAT	D	105
	Acid-labile isotope-coded extractants (ALICE)	D	106
	Solid phase mass tagging	^{13}C	107,108

Table 1.1 (cont'd)

Target	Name of method or reagent	Isotopes	Refs.
Amines	Tandem mass tags (TMT)	D	109
	Succinic anhydride	D	110
	N-acetoxysuccinamide	D	56
	Acetic anhydride	D	111
	Propionic anhydride	D	58
	Nicotinoyloxy succinimide (Nic-NHS)	D	55
	Isotope-coded protein label (ICPL, Nic-NHS)	D	57
	Phenyl isocyanate	D	112
	Isotope-coded *n*-terminal sulfonation (ICenS) 4-sulfophenyl isothiocyanate	^{13}C	113
	Sulfo-NHS-SS-biotin and $^{13}C,D_3$-methyl iodide	^{13}C, D	114
	Formaldehyde	D	115
	Isobaric tag for relative and absolute quantitation (iTRAQ)	^{13}C, ^{15}N, ^{18}O	59
Lysines	Guanidination (*O*-methyl-isourea) mass coded abundance tagging (MCAT)	No isotope	116
	Guanidination (*O*-methyl-isourea)	^{13}C, ^{15}N	117,118
	Quantitation using enhanced sequence tags (QUEST)	No isotope	119
	2-Methoxy-4,5-1*H*-imidazole	D	120
Carboxyl	Methyl esterification	D	51
	Ethyl esterification	D	121
Trytophan	2-nitrobenzenesulfenyl chloride (NBSCl)	^{13}C	122
pSer/pThr	Phosphoprotein isotope-coded affinity tag (PhIAT)	D	123
	Phosphoprotein isotope-coded solid-phase tag (PhIST)	^{13}C, ^{15}N	124
O-GlcNac	Beta elimination and Michael addition with dithiothreitol (BEMAD)	D	125-127

The high nucleophilicity of the sulfhydryl group makes cysteine residues attractive targets for chemical labeling. ICAT (Isotope Coded Affinity Tag), including a thio-specific reactive group, an eightfold deuterated linker and a biotin affinity tag, is one of the earliest chemical reagents introduced for quantitative proteomics [130]. The incorporation of a biotin moiety allows avidin affinity purification of labeled peptides, thus improving quantification of complex mixtures by mass analysis. ICAT has been successfully applied in the quantitative studies of low abundance-proteins [135], the proteins contained in the microsomal fraction of cells [136] and differential expression of *Pseudomonas aeruginosa* proteins on limitation of magnesium [137]. However, the fragmentation of the large ICAT tag during CID-MS/MS significantly complicates peptide identification, and the deuterium tags result in separation of "light" and "heavy" labeled peptides during reverse phase chromatography. These limitations were addressed by the development of a cleavable version of ICAT the reagent, which contains nine ^{13}C instead of eight deuteriums and an acid-cleavable biotin moiety [138, 139]. The use of stable ^{13}C labels eliminates the retention shift in reverse phase chromatography. Removal of the biotin moiety after affinity purification results in minimum fragmentation in the residual part of the tag during CID-MS/MS, allowing a larger number of proteins to be identified compared to the first generation of ICAT reagent [140].

Enhanced peptide sequencing can be achieved while performing protein quantitative analysis, by incorporating differential stable isotopes into the "fragmentation-directing" reagents as described above. The James group has described the use of 1-([H_4/D_4]nicotinoyloxy)succinimide esters for relative quantitation and enhanced *de novo* sequencing of proteins [39]. More recently, Che and Fricker demonstrated the quantitative

peptidomics analysis of mouse pituitary by using amine-reactive H_4/D_4-succinic anhydride and H_9/D_9-[3-(2,5-dioxopyrrolidin-1-yloxycarbonyl)propyl]trimethylammonium chloride [134]. From analysis of negatively charged succinyl and positively charged 4-trimethylammoniumbutyryl (TMAB) labeled mouse pituitary peptides, the relative levels of two largely independent peptide sets were obtained. Thus, the use of both labels is preferable for better sequence coverage.

1.5.2 Chemical and Stable Isotope Labeling Approaches for MS/MS-Based Quantification

In a complex mixture, MS-based quantitative analysis, i.e., quantitation achieved in the mass scan, is often hampered by the presence of interfering components which overlap with differentially-labeled peptide ion peaks or which reduce the signal to noise ratio (S/N) of mass detection. To address these issues, a novel class of labeling reagents has been developed, whereby quantification is performed in an MS/MS scan. The isobaric Tag for Relative and Absolute Quantitation (iTRAQ) is one family of such reagents [141-145]. The iTRAQ approach utilizes a 4-plex or 8-plex set of amine-reactive isobaric tags to quantitate expression levels of multiple protein populations. As shown in Figure 1.1 for a 4-plex iTRAQ reagents, the differential isotope labels are incorporated into the reporter group (variable mass of 114-117 Da for 4-plex or 113-121 Da for 8-plex) and the balance group, so that the overall mass of each reagent is the same while the reporter ions formed upon CID-MS/MS are differentially isotope-labeled [141]. The isobaric nature of iTRAQ-labeled peptides allows their co-elution during

reverse-phase chromatography. In addition, these iTRAQ-labeled peptides appear as single peaks in MS scans, leading to an increased peak capacity and improved sensitivity.

Another tagging technique employing the same concept has also gained popularity, namely, the tandem mass tags (TMTs) [146, 147]. TMTs are a multiplexed set of isobaric labeling reagents, which comprise an isotopic reporter group tethered to a mass normalization group with a cleavable linker, allowing quantification to be carried out by comparing the ratio of differentially labeled reporter ions released during CID-MS/MS. The Other MS/MS-based quantitative analysis strategies have been developed such as Cleavable Isobaric Labeled Affinity Tag (CILAT), which is a hybrid of the ICAT and iTRAQ approaches [148]. However, the TMT reagents from Thermo Scientific and iTRAQ reagents from Applied Biosystems are currently the only labeling technologies commercially available where quantification is carried out in MS/MS mode.

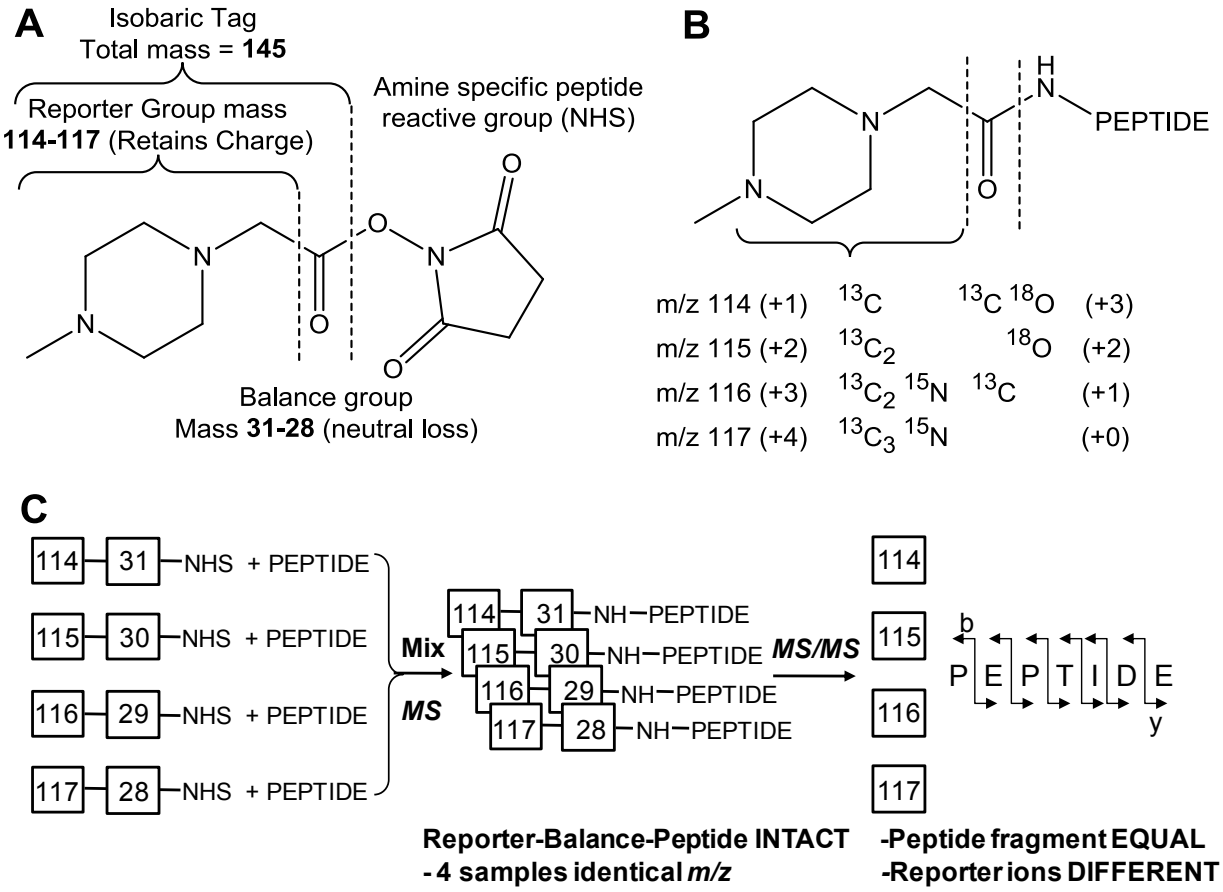

Figure 1.2 (A) Structure of the iTRAQ reagent that consists of a reporter group, a mass balance group, and a peptide-reactive group. The overall mass of reporter and balance components of the molecule are kept constant (145.1 Da) using differential isotopic enrichment with ^{13}C, ^{15}N, and ^{18}O atoms. (B) Upon reaction with a peptide, the tag forms an amide linkage to any peptide amine (N-terminus or ε amino group of lysine). When subjected to CID, fragmentation of the tag amide bond results in the loss of balance group as a neutral species, while the charge is retained by the reporter group fragment. The numbers in parentheses indicate the number of enriched centers in either the reporter group or balance group of the molecule. (C) A mixture of four identical peptides, each labeled with one member of the mixture set, appears as a single, unresolved precursor ion in a mass scan (identical m/z). Following CID, the four reporter group ions appear as distinct masses (m/z 114-117). All other sequence-informative fragment ions (that is, b- and y-type ions) remain isobaric. Adapted from Reference [141].

Only a few labeling strategies have been investigated to date in combination with ETD for quantification. It has been reported that fewer channels are available from ETD-MS/MS analysis

of iTRAQ labeled peptides, i.e., 3 from 4-plex and 5 from 8-plex for peptide and protein quantification [149-151]. Similar results are obtained when using TMTs, as only four unique reporter ions can be generated from ETD fragmentation of TMT 6-plex labeled peptides [152]. Fortunately, both the McLuckey [149] and the Coon [151] groups have demonstrated that more channels are open for iTRAQ differentially labeled peptides, when specific reporter-ion-containing fragments resulting from ETD are further subjected to resonant excitation CID. Furthermore, the addition of iTRAQ or TMT tags to a peptide showed minor deleterious effects on ETD fragmentation of peptide backbone. Thus, with respect to compatibility with these quantitation techniques, ETD holds great potential for protein quantitative analysis as well as peptide sequencing, which is especially beneficial for studies of post-translationally modified peptides and proteins [152].

1.6 Studies of Protein Structure, Protein Folding and Protein-Protein Interactions via Chemical Labeling Strategies

For many years, chemical labeling combined with mass spectrometry has been a valuable tool to probe protein structure and protein interactions, especially when protein systems are not amenable to conventional high resolution techniques such as NMR and X-ray crystallography [29]. A variety of approaches have been developed, typically based on the use of hydrogen-deuterium exchange (HDX) [153-155], or chemical covalent labeling [29, 156-158] to change the mass of the protein in a structure dependent manner prior to HPLC-MS and/or -MS/MS analysis. HDX is typically used to probe the entire protein backbone via targeting of the main chain amide hydrogens. However, the accurate interpretation of protein structure based on the

results obtained from HDX is hampered by possible back-exchange and scrambling in solution-phase and gas-phase experiments. In another way, chemical labeling approaches measure the differential reactivities of amino acid side chains towards non-specific [156, 157] or amino acid-specific labels [29, 158] for mapping protein structure and interactions, due to the fact that the reactivity of individual amino acids within the protein is highly dependent on their solvent accessibilities.

Nonspecific oxidative modification of protein side chains has been widely used to examine protein folding and conformational changes by monitoring a wide range of target sites [156, 157]. Various methods have been used for generating the hydroxyl radicals required for oxidative labeling, such as photolysis of H_2O_2 using a pulsed UV laser [155], radiolysis of water by electron pulses or synchrotron X-ray pulses [156] or Fenton and Fenton-link reactions [159]. However, due to the nonspecific nature of the reaction, highly complex products often result from oxidative protein labeling, presenting significant challenges for their analysis.

In contrast to hydroxyl radical meditated non-specific labeling approaches, varying amino acid-specific reagents are employed for targeting particular amino acid side chains or functional groups involved in protein active inter-phases. Amino acid-specific labeling reactions are usually carried out with the reagents employing established organic chemistry. Currently, only eight out of twenty naturally occurring amino acids have been used as the targets for such specific labeling reactions [29]. Among them, the ε-NH_2 group on lysine side chains is most commonly modified owing to the large number of lysine residues present on the surface of most proteins [160, 161]. A range of chemical labeling strategies have been developed for the modification of lysine

residues, involving reactions with organic acid anhydrides [162, 163], *N*- hydroxysuccinimide (NHS) deriviatives [164-168] and imido esters [169] as shown in Scheme 1.2 [29].

Amidination of lysine residues by using S-methylthioacetimidate and propioimidate has been reported by the Reilly group for probing protein solvent-accessible regions [169]. As illustrated in Scheme 1.2, the positive charge on the lysine polar side chain is retained after amidination at physiological pH. Thus, the use of imido esters such as *S*-methylthioacetimidate has potential advantages over previously investigated lysine modification reagents in terms of minimizing the extents of disturbance in protein conformation upon labeling reaction and without compromising ionization efficiency of modified peptides for MS analysis.

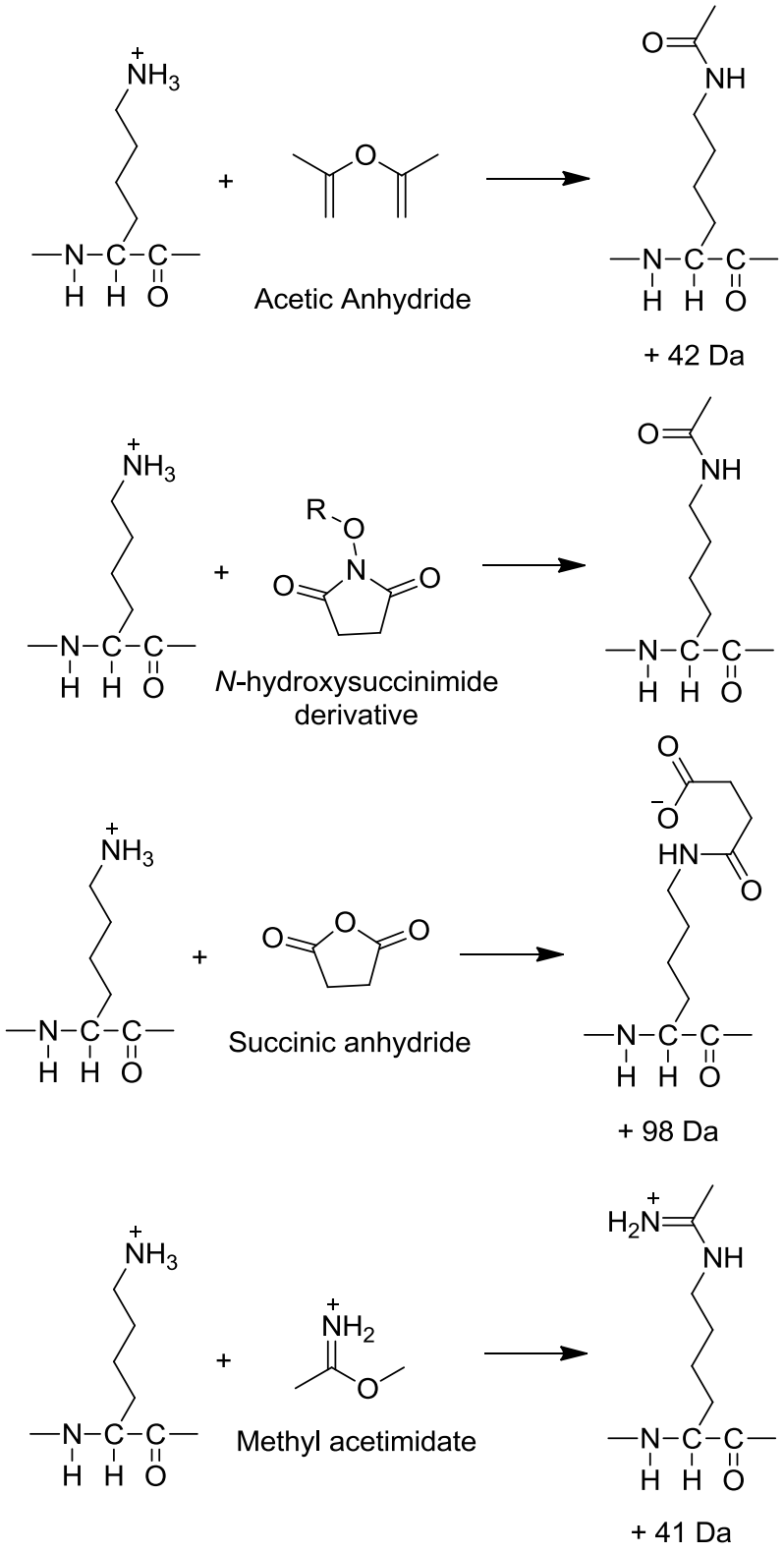

Scheme 1.2 Modification reactions of lysine residues. Adapted from Reference [29].

Zhou *et al.* have recently demonstrated the use of a 'fixed-charge' sulfonium containing amine-specific modification reagent, *S,S'*-dimethylthiobutanoylhydroxysuccinimide ester (DMBNHS), for the improved analysis of higher order protein structures [170]. Exclusive neutral loss(es) of dimethylsulfide (62 Da) is observed upon CID-MS/MS of the 'fixed-charge' derivatized peptide ions, allowing an analysis strategy involving HPLC-MS coupled with automated CID-MS/MS and data dependent neutral loss triggered MS^3 in a quadrupole ion trap mass spectrometer to be developed for the improved identification and characterization of the peptide derivatization site(s) (Scheme 1.3).

By determining particular modification sites, chemical labeling provides information about the region(s) that are on the protein surface or are involved in an interface with other molecules. The use of isotope labeled derivatizing reagents can also help to obtain information regarding the degree of modification [171, 172], which usually reflects the extent to which the specific region is involved in ligand binding interactions.

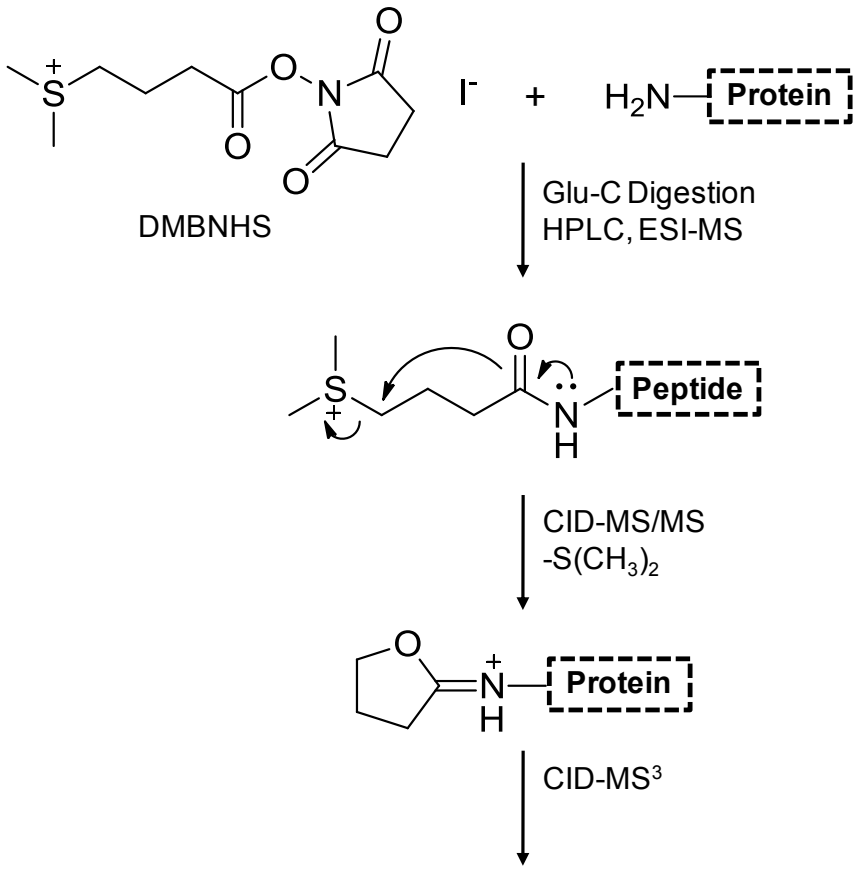

Scheme 1.3 Schematic of the solution phase DMBNHS protein modification and gas phase CID-MS/MS and -MS^3 fragmentation reactions of DMBNHS modified peptide ions. Adapted from Reference [170].

Chemical cross-linking is principally a specific chemical labeling approach for studying the low-resolution structure of protein topology and protein interactions. It not only relies on the differential reactivity of amino acids upon exposure to the label, but it also depends on the spatial relationship between two amino acid side chains [158, 173]. A detailed discussion of chemical cross-linking strategies will be discussed in the following chapters.

1.7 Future Prospects

Chemical labeling in conjunction with MS has been extensively used in recent years to address challenges associated with protein identification, characterization, quantification, as well as structural analysis. Despite the success of current chemical labeling methods, further improvements to this approach are desired. One of the needed improvements is the development of new amino acid-specific labeling reagents to improve the identification of modified peptides. One common problem associated with the chemical labeling approach is that the modified peptides may be difficult to detect amongst the largely unmodified peptide population. This is especially severe when a complicated peptide mixture resulting from a large protein or protein mixture is analyzed. Therefore, the research included in this dissertation was directed toward the development of new chemical labeling reagents and associated methodologies for improved cross-linking strategies and for enhanced quantitative phosphoproteome analysis.

CHAPTER TWO

CHEMICAL CROSS-LINKING STRATEGIES FOR MAPPING PROTEIN STRUCTURE AND PROTEIN-PROTEIN INTERACTIONS

2.1 Protein Structure and Function

The study of proteins has fascinated biochemists and chemists for over a century. Understanding the compositions, three-dimensional structures, and chemical activities of proteins are among some of the most pressing scientific issues, which ultimately aim at R&D of new drugs for human healthcare [174].

Proteins perform a wide variety of roles. The most important biological functions of proteins involve the catalysis of biochemical reactions, i.e., function as enzymes. Some proteins have structural functions for providing support and shape to cells. Other proteins are important for transport and storage of particular small biomolecules. Proteins are also essential in information processing in the cells, via their roles as messengers or receptor proteins [174]. The key to appreciating how different proteins function in different ways lies in an understanding of their structures. Protein structure is defined at four levels [174]. Primary structure describes the linear sequence of amino acid residues in a protein molecule. Secondary structure relates to the

---

Some of the concepts described in Chapter Two were published in: Froelich, J. M.; Lu, Y. ; Reid, G. E., Chemical Derivatization and Multistage Tandem Mass Spectrometry for Protein Structural Characterization. In: Practical Aspects of Trapped Ion Mass Spectrometry. Vol. 5: Applications. (March R. E. and Todd J. F. J. Ed), 2009, CRC Press.

regularities maintained by hydrogen bonds between amide hydrogens and carbonyl oxygens of the peptide backbone. α helices and β sheets are two major secondary structures. The shape of the fully folded polypeptide chain defines the tertiary structure, which is stabilized by non-covalent interactions between amino acid side chains within the molecule and with water molecules surrounding it. Proteins can also work together to achieve a particular function by forming transient or stable multi-subunit complexes, resulting in the highest level of organization, quaternary structure. Identification of the interacting partners and further mapping of the specific interaction sites are crucial to understand how proteins function together as biological assemblies [174].

2.2 Current Methods Employed for Protein Structure Analysis

Numerous techniques have been developed to probe protein-protein interactions. X-ray crystallography and multidimensional NMR are currently primarily applied due to their very high structural resolution. X-ray crystallography uses the diffraction pattern produced by bombarding a single crystal with beam of collimated X-rays to solve the crystal structure; therefore, a single crystal has to be obtained for X-ray studies. Alternatively, nuclear magnetic resonance (NMR) spectroscopy is capable of three-dimensional structure determination of proteins in solution. However, limitations of NMR spectroscopy result from its low inherent sensitivity and from the high complexity and information content of NMR spectra. Other methods such as yeast two-hybrid screens and protein microarrays provide very high throughput, but structural resolution is low [175], large numbers of non-specific interactions are often detected, and little information is provided regarding specific interacting sites between the

protein subunits [176]. In recent years, computational biology has shown great promise in predicting *ab initio* protein structures from amino acid sequences; however there remains a need for further developments in this field prior to its widespread application, such that experimental data are still required for validation [177].

2.3 Chemical Cross-Linking

Because of the high sensitivity and rapid analysis of MS techniqies, chemical cross-linking followed by proteolytic digestion and subsequent characterization by mass spectrometry has shown great promise in providing distance constrains, albeit at relatively low resolution, for assigning protein topologies and protein interactions [158, 173, 178]. Cross-linkers can covalently link interacting regions within a protein or interacting regions between the individual components of multi-protein complexes. Most importantly, non-covalent protein-protein interactions, which may be transient or dependent on specific physiological conditions, can be captured into long-lived covalent complexes [22, 175]. Typically in a bottom-up strategy, cross-linked proteins or protein complexes are separated by one-dimensional gel electrophoresis (SDS-PAGE), and then subjected to enzymatic in-gel digestion, chromatographic fractionation and mass spectrometry analysis [178]. Ultimately the assignment of distance constraints within a single protein or protein complexes can be employed to provide information regarding the protein-protein interactions and three-dimensional structure of the protein or protein complex. This strategy is represented schematically in Figure 2.1 [179].

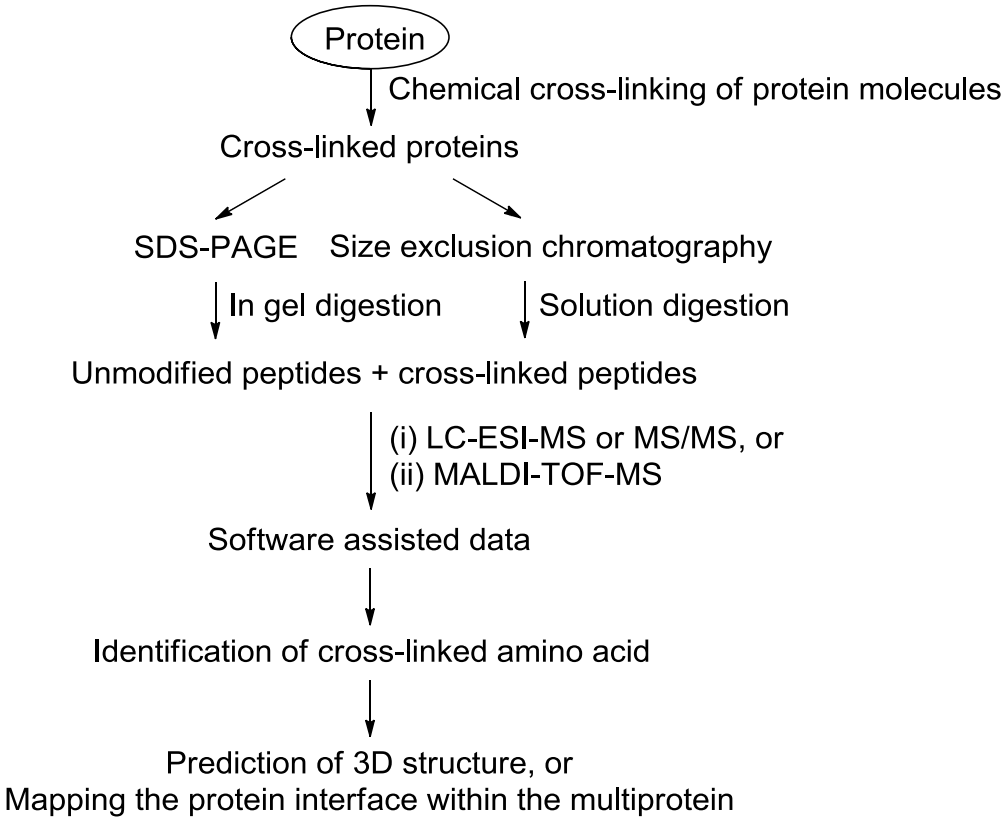

Figure 2.1 Cross-linking methodology flowchart by the bottom-up approach. Adapted from Reference [179].

2.3.1 Cross-Linking Reagents

Cross-linking reagents contain two or more reactive ends to specific functional groups on proteins or other molecules. A large number of reagents have been described in the literature, and many are now commercially available [180]. Major target functional groups for cross-linking reactions include primary amines, sulfhydryls, carbonyls, carbohydrates and carboxylic acids. The commonly used reactive groups of cross-linkers are summarized in Table 2.1 [173]. As mentioned previously, modification of lysine with the use of NHS-esters has been the most commonly used labeling strategy to probe protein structure due to their rapid reaction rates and

physiological reaction conditions [158, 181]. Therefore, NHS-esters have been the most frequently used reactive group implemented in cross-linkers. Recently, *N*-hydroxyphthalimide, hydroxybenzotriazole, and 1-hydroxy-7-azabenzotriazole have been introduced by Bich and coworkers as new reactive groups of amine specific cross-linkers [182]. These new cross-linkers showed a better efficiency and reacted about 10 times faster than commercially available disuccinimidyl suberate (DSS) when used to covalently cross-link the gluthatione-S-transferase (GST) dimer, illustrating the feasibility of their applications in the kinetic studies of protein complexe formation.

Table 2.1 Cross-linker reactive groups and their functional targets. Adapted from Reference [173].

Reactive Group	Features
Haloacetyl	Thio-reactive
Maleimide	Thio-reactive
Acryl	Thio-reactive
Aldehyde	Amine-reactive
Imidoester	Amine-reactive
N-hydroxysuccinimide ester	Amine-reactive
Glyoxal	Arginine-specific
Phenylazide	Non-selective, photo-reactive
Tetraflurophenylazide	Non-selective, photo-reactive

Cross-linkers can be either homobifunctional, with two identical reactive groups at both reactive sites, or heterobifunctional, containing different reactive groups. Otherwise, relatively newly developed tri-functional cross-linking reagents incorporate a third functional group for reacting with a third target group, or for affinity purification of cross-linked products; a biotin moiety is commonly used for such purpose [183, 184]. Usually, cross-linking reagents have a spacer carbon chain; however zero-length cross-linkers may be employed to catalyze the

formation of a chemical bond between two target groups without introducing an intervening linker. For example, carbodiimides are applied to mediate the direct formation of amide bonds between a carboxyl group and an amine group [185].

Besides the reactive functional groups of cross-linking reagents, the spacer arm length, water solubility or cell membrane permeability and additional modules for the separation and purification of cross-linked products are significant characteristics that should be taken into account for a specific application. The spacer arm length defines the distance relationship between two target groups on amino acid residues of a protein or protein complexes, which indicates the folding pattern of a protein or interacting sites between two subunits, i.e. protein-protein interactions. The solubility of cross-linking reagents in aqueous solution expands their applications to large proteins and protein complexes with poor solubility in organic solvents. The specific tags contained in cross-linking reagents that are used to facilitate the identification of cross-linked products will be discussed in the following section.

2.3.2 Possible Cross-linked Products from a Cross-Linking Reaction

Following the chemical cross-linking reaction, a variety of products may be produced. As shown in Figure 2.2 [186], after proteolysis even for a single cross-linking reaction, three distinct types of cross-linked peptides might be formed:

(1) dead-end modified peptides (Type 0) with only one of the reactive groups of cross-linker reacted with the protein and the other one hydrolyzed. A type 0 modification doesn't

provide any information related to the distance constrains between two amino acid residues but may indicate reactive groups exposed on the protein surface;

(2) intramolecular cross-linked peptides (Type 1) with both reactive groups of cross-linker reacted with two amino acids on the same peptide chain. Type 1 cross-link can be applied to map three-dimensional structure of proteins.

(3) intermolecular cross-linked peptides (Type 2) with both reactive groups of cross-linker reacted with two amino acids on the two different peptide chains after proteolysis. If these two peptide chains come from two proteins within the complex, the important information about interacting sites will be obtained.

Combinations of type 0, 1, or 2 modifications give rise to a large number of possible cross-linked products, whereas the yields of multiple cross-linking reactions are usually low. The results from double modifications are also presented in Figure 1.2, where the α chain can be either same as, or different from, the β chain.

A Single modifications

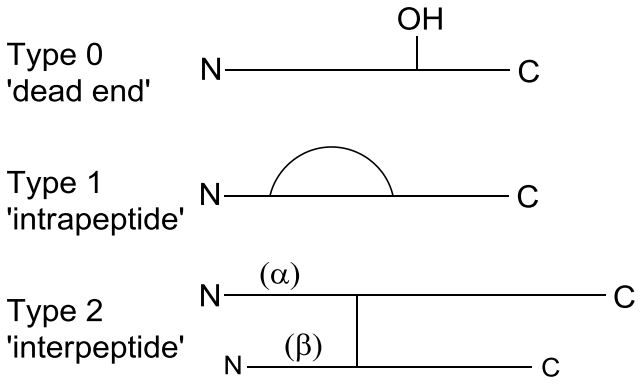

B Multiple modifications

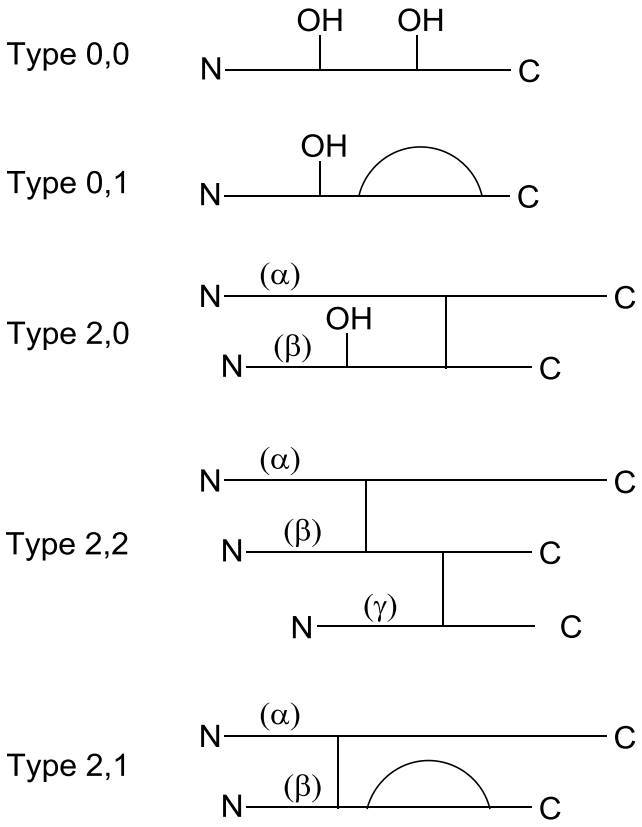

Figure 2.2 (A) Classification of cross-linked peptides into Type 0, Type 1 and Type 2. (B) Multiple modifications by the combinations of Type 0, 1 and 2. Adapted from Reference [186].

2.3.3 Chalenges Associated with the Identification and Characterization of Chemically Cross-Linked Peptides

As described above, despite the relative straightforwardness of cross-linking approaches, the identification of cross-linked products by mass spectrometry is not straightforward due to the high complexity of the resultant peptide mixtures.

For analysis of the cross-linking reaction products from protein or protein complexes, enzymatic digestion is usually performed prior to mass spectrometry analysis [bottom-up]. This process increases the complexity because cross-linked peptides are present along with a large number of unmodified peptides. The well known term, 'looking for a needle in a haystack', is often used to describe the challenges associated with the identification of cross-linked peptides resulting from this complexity.

To date, a number of techniques have been developed to facilitate the unambiguous assignment of cross-linked peptides, involving the enrichment of cross-linker-containing species by specific affinity tags [183, 184, 187-193] or via the introduction of discriminating properties such as differential isotope labels [194-202], specific 'solution-phase' [201, 203-206] or 'gas-phase' [190, 192, 207-213] cleavage sites, within the cross-linking reagent itself, or within the cross-linked peptides.

2.3.4 Affinity Cross-Linking Reagents

Affinity enrichment methods have typically incorporated a biotin functional group into the cross-linker, allowing affinity purification of cross-linked peptides by avidin affinity column or

on avidin beads to reduce the complexity of the mixtures for subsequent mass spectrometry analysis [183, 184, 187-192]. Recently, Chowdhury and coworkers have developed an alkyne tag containing reagent termed click-enabled linker for interacting proteins (CLIP) [193]. This cross-linker enables subsequent enrichment of cross-linked species through alkyne-azido click chemistry [214] with a biotin affinity reagent. Another distinct feature of CLIP is the incorporation of a small NO_2 moiety that can be released during MS/MS analysis, providing additional confidence for the identification of cross-linked peptides.

2.3.5 Isotope Labeling of Cross-Linked Peptides

The incorporation of differential isotope labels has been employed to enable the detection of cross-linked peptides via identification of their distinct isotope patterns during MS analysis [194-202]. This can be realized by incorporation of the isotope label within the protein or peptide [194-197], or within the cross-linker itself [198-202].

2.3.5.1 Isotope Labeling on Polypeptide Chain

One approach involves the introduction of ^{18}O to the C-terminal carboxyl group(s) of the polypeptide chain(s) formed during proteolytic digestion in ^{18}O enriched water [194, 195]. Intermolecular cross-linked peptides (Type 2, Figure 2.2) are readily distinguished by a characteristic 8-Da mass shift compared to peptides formed by proteolysis using naturally

abundant water. However, non-modified, dead-end and intramolecular cross-linked peptides are not able to be distinguished, as they will all exhibit a common 4-Da mass increment.

Another approach described by Chen and coworkers [196] involves reductive di-methylation of primary amino groups within a protein, followed by enzymatic hydrolysis and derivatization of the newly formed N-termini with a 1:1 (w/w) mixture of 2,4-dinitrofluorobenzene-d_0/d_3. Due to the incorporation of two dinitrophenyl groups, intermolecular cross-linked peptides will be distinguished by a characteristic 1:2:1 isotope pattern in the mass spectra from the 1:1 isotope pattern of other cross-linked types and non-modified peptides containing only one peptide chain. Similarly, for visualizing intermolecular cross-linked peptides, a mixed isotope cross-linking (MIX) strategy was designed by Taverner *et al.*, by mixing 1:1 uniformly ^{15}N-labeled and unlabeled proteins to form a mixture of homodimers [197]. Cross-linked peptides from an intermolecular origin exhibit triplet/quadruplet MS peaks (triplet for homodimeric intermolecular cross-link, quadruplet for heterodimeric intermolecular cross-link), that are unique from the doublet peaks of all other peptide species.

Identification of intermolecular cross-linked products by introducing isotope labels on the protein or peptide is feasible for the study of protein-protein interactions; however intramolecular cross-links cannot be distinguished by this method.

2.3.5.2 Isotope Labeled Cross-Linking Reagents

Incorporation of the isotope label within the cross-linking reagent potentially allows all cross-linked peptides to be detected, via identification of their distinct isotope patterns upon

reaction with 1:1 mixtures of stable isotope-labeled and nonlabeled cross-linking reagents [198, 199, 202]. Isotope-labeled cross-linkers could be easily combined with other strategies for further identification of cross-link types [200, 201]. Recently, Seebacher *et al.* have developed a new integrative method employing isotope-labeled cross-linking reagents in the presence of isotope-labeled water [200]. In this way, deadend cross-linked peptides could be discriminated by an additional 2-Da splitting from hydrolysis of the cross-linking reagent's free reactive ester in $[^{16}O]H_2O/[^{18}O]H_2O$ (1:1) buffer. Similarly, employing isotope labeled cross-linking reagents followed by ^{18}O labeling could further distinguish intermolecular cross-link from all the cross-linked products.

Isotope-labeling technologies have been widely employed to assist in finding cross-linked peptides in mixtures. However, limitations to these approaches may be encountered when m/z values of differentially labeled cross-linked peptide products overlap with unlabeled peptides also present in the mixture, thereby precluding identification of the characteristic isotopic multiplets. Moreover, the use of only one isotope labeling process is not capable to identify all the cross-linked types at once.

2.3.6 Cleavable Cross-Linking Reagents

The use of cross-linking reagents containing solution-phase cleavage sites has also demonstrated to result in an improved ability to identify the presence of cross-linked peptides from within complex mixtures [201, 203-206]. These cleavage reactions may be performed by hydrolysis [201], or by the use of reducing agents in the case of disulfide containing cross-

linking reagents [203-205], thereby allowing cross-linked peptides to be identified during subsequent MS analysis via the mass shifts observed before and after the cleavage reaction.

2.3.6.1 Solution Phase Cleavable Cross-Linking Reagents

The thiol-cleavable cross-linking reagent 3,3′-dithio-*bis*(succinimidylpropionate) (DTSSP) has been applied to a number of proteins and protein complexes [203-205]. After reduction of the cross-linker disulfide bond, intermolecular cross-linked peptides give rise to two separated components, each containing a reduced linker. Intra-molecular cross-links yield two reduced linker halves on the same peptide, whereas deadend type only have one present. Different cross-link types are distinguished by their characteristic mass shifts before and after reduction.

Another interesting example involves cleavable cross-linkers combined with isotope-coding strategies [201]. The isotope-labeled cleavable cross-linker is applied with its unlabeled counterpart to provide additional discriminating information because of the distinct isotope-pairs thus formed, allowing unambiguous identification of cross-linked products. However, the application of cleavable cross-linkers by a chemical reaction relies on mass spectrometry analysis before and after the cleavage reaction takes place. Thus, the identification of cross-linked products might be complicated if the corresponding signals of reduced cross-link species are not observed, or if they overlap with non-cross-linked peptides.

Recently, the de Jong group has designed a cross-linker containing an azido group to enable reducing reagent tris(2-carboxyethyl)phosphine (TCEP) induced cleavage of cross-linked peptides along with reduction of the azide without cleavage in parallel (Scheme 2.1) [206]. Thus,

all three types of cross-linked peptides are able to be identified by the defined mass difference between products from two reduction pathways in one analysis.

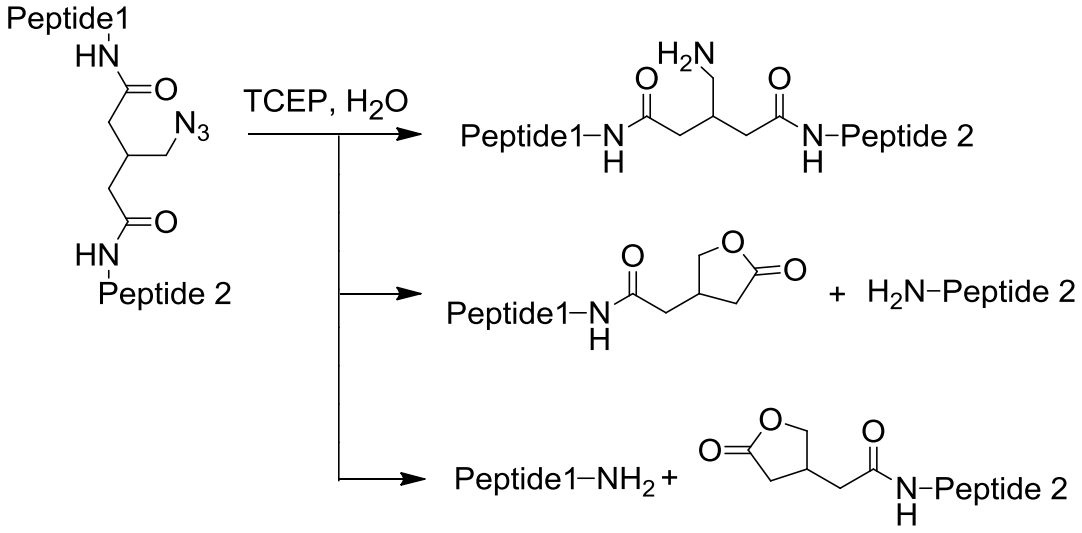

Scheme 2.1 Phosphine-induced reactions of cross-linked peptides resulting from reaction with bis(succinimidyl)-3-azidomethyl glutarate (BAMG). Two parallel reaction pathways occur in the presence of reducing reagent tris(2-carboxyethyl)phosphine (TCEP). In one pathway, TCEP reduces the azido group to form an amino group (upper pathway). In the other pathway, the two peptides of the cross-link are separated in the form of either a free peptide or a lactone modified peptide (center and lower pathways). Adapted from Reference [206].

The solution phase enrichment/cleavage and isotope labeling methods each involve several chemical reactions and sample handling steps prior to and/or following the cross-linking process. Thus unintended by-reactions should be avoided in those reactions for unambiguous identification of cross-links.

To simplify the problem, effort has been placed on the use of gas phase dissociation methodologies for the discrimination and subsequent amino acid sequence analysis of cross-linked products.

2.3.6.2 Gas Phase Cleavable Cross-Linking Reagents (Using MS/MS)

In recent years, several groups have initiated the development and application of novel classes of gas-phase cleavable cross-linking reagents, whereby cross-linked reaction products are identified and characterized based on their characteristic fragmentation behavior observed during tandem mass spectrometry (MS/MS) [190, 192, 207-213]. These gas-phase cleavable sites may be incorporated into a side chain on the cross-linking reagent [207], resulting in formation of a stable "reporter ion" (thereby maintaining the cross-linked peptide linkages), or incorporated directly into the cross-linker spacer chain [190, 192, 208-212], thereby resulting in cleavage of the cross-link upon MS/MS. In each case, further structure interrogation of the peptide product ions formed following the initial cleavage reaction can be achieved by MS^n analysis. These strategies, though still needing improvement, are promising and could serve as basis for the second generation of cross-linking reagents [158].

Back *et al.* described the use of a bifunctional lysine reactive cross-linker, *N*-benzyliminodiacetoylhydroxysuccinimide (BID; Figure 2.3), which yields a stable benzyl cation marker ion under MS/MS conditions, to successfully identify inter- and intra-molecular cross-linked peptides [207]. However, formation of the benzyl cation at low m/z results in an inability to employ this strategy in quadrupole ion trap instruments, due to the low mass cut off inherent to this instrumentation. In addition, the benzyl cation is only observed as a dominant product for certain charge states of a protonated peptide.

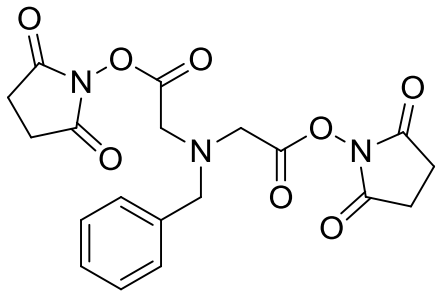

Figure 2.3 Structure of the cross-linker *N*-benzyliminodiacetoylhydroxysuccinimide (BID). Adapted from Reference [207].

In another study by Seebacher *et al.*, a diagnostic ion at m/z 222 was reported upon CID of cross-linked peptides formed by reaction with the commercially available cross-linker disuccinimidyl suberate (DSS) (Figure 2.4) [200]. Recently, the Gozzo group demonstrated the pathway for formation of this diagnostic ion, as well as two other distinct fragment ions from DSS-containing peptides [215]. Based on the presence of these diagnostic ions, an approach involving precursor ion scan (PIS) on a quadrupole time-of-flight (Q-TOF) instrument was developed [216]. The approach could also be applied for the identification of cross-linked peptides with DSS-homologous cross-linkers.

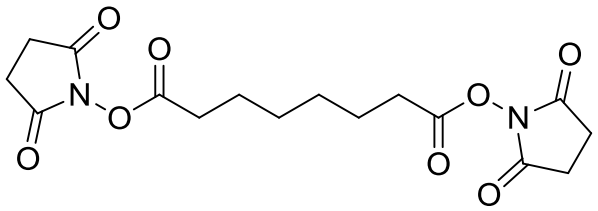

DSS

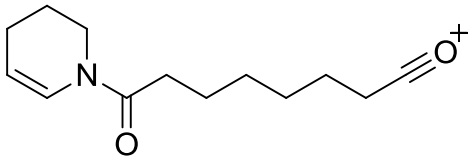

***m/z* 222.1494**

Figure 2.4 Structure of the commercially available cross-linker disuccinimidyl suberate (DSS) and the diagnostic ion at m/z 222.1494 resulting from fragmentation of DSS cross-linked peptides with the modification on lysine side chain. Adapted from Reference [216].

Bruce *et al*. introduced a cross-linker strategy, termed protein interaction reporters (PIRs; Figure 2.4) [217]. PIRs contain two low-energy MS/MS cleavable bonds within the spacer arm [208]. Upon CID MS/MS, PIR intermolecular cross-linked peptides fragment at two cleavage sites within the linker giving rise to two separated peptides each with an additional mass and a reporter ion. PIRs have also been combined together with other chemical features, such as an affinity tag, a hydrophilic group or a photocleavable group to produce a series of tri- and multi-functional group cross-linking reagents [190, 192, 209]. With assistance of bioinformatics platform, PIRs strategy has been successfully applied to map interactions and interacting sites from native cell in a large scale for the first time [192]. However, PIRs are a series of molecules with spacer arm chain length of nearly 43 Å [208], making these reagents less informative to determine the specific interaction points of protein-protein interactions.

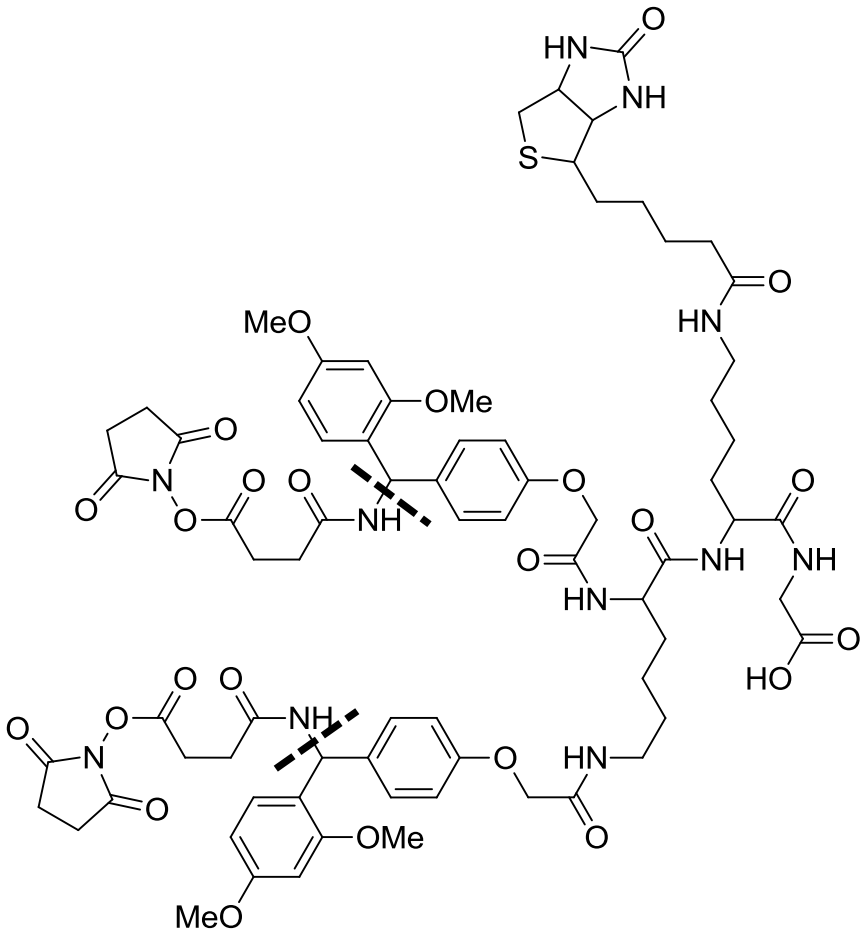

Figure 2.5 A representative example of protein interaction reporters (PIRs). The MS/MS labile bonds are indicated by dashed lines, the reactive groups are *N*-hydroxysuccinimide (NHS) esters and the affinity group is biotin. Adapted from Reference [217].

To reduce the cross-linker length, Soderblom *et al*. [210, 211] have developed a set of single site gas phase cleavable cross-linking reagents that can be selectively fragmented in the source region of the mass spectrometer. As shown in Scheme 2.2, the designed cleavage site at an aspartyl-prolyl bond is thought to be meditated by proton transfer from the aspartyl side chain to the basic amine of the adjacent prolyl residue to realize the preferential cleavage. Therefore, the selectivity of cleavage at the cross-linker is expected to be dependent on the charge state and amino composition of the cross-linked peptide precursor ions [14].

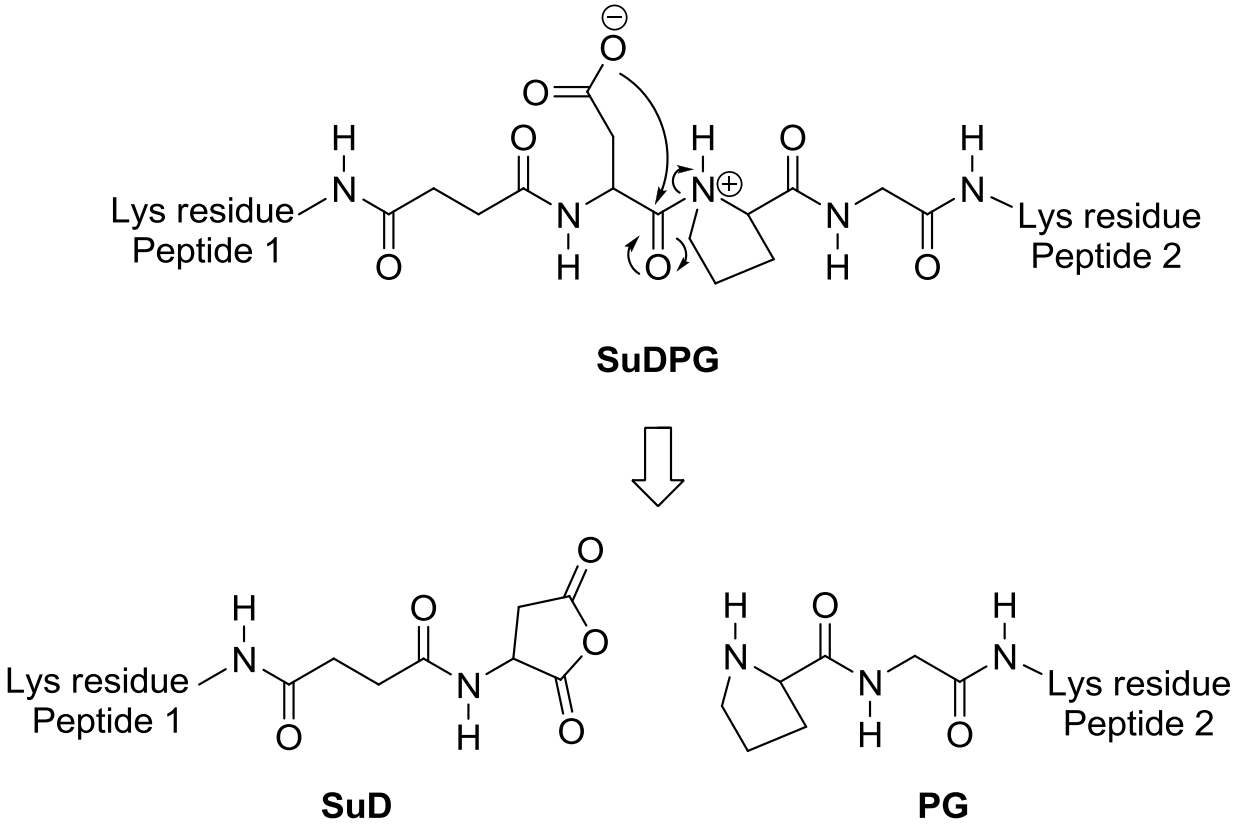

Scheme 2.2 CID-MS/MS fragmentation mechanism at aspartyl-prolyl bond within SuDPG cross-linked peptides. Adapted from Reference [210].

Recently, Dreiocker *et al.* designed a cross-linker based on Edman degradation chemistry, which contains a highly nucleophilic thiourea moiety connected to proline via glycine, with subsequent cleavage of the glycyl-prolyl amide bond upon CID-MS/MS [212]. The resultant peptide fragment ions contain characteristic mass shifts; in addition, they can generate distinct neutral losses upon further fragmentation, allowing the unambiguous identification of the cross-linked peptides. However, the selectivity of this cross-linker also relies on initial protonation at the proline imide nitrogen to achieve the desired cleavage.

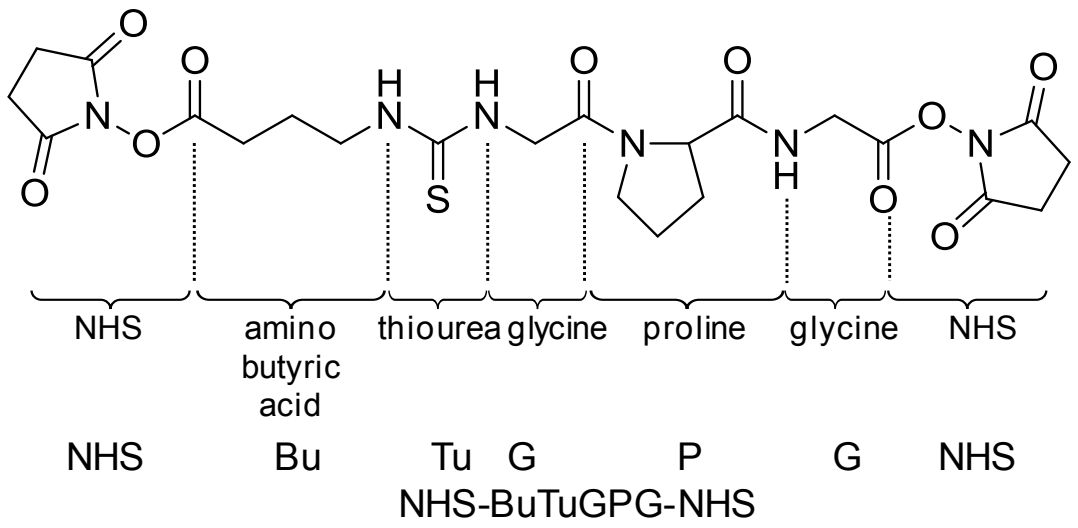

Figure 2.6 Structure of the cross-linking reagent NHS-BuTuGPG-NHS. Preferred cleavage of the Gly-Pro amide bond of the linker can be realized by selective nucleophilic attack of sulfur upon CID-MS/MS. Adapted from Reference [212].

As an alternative to gas phase cleavable cross-linking reagents using CID, an IR active chromogenic cross-linker (IRCX) has been employed to facilitate the identification of cross-linked peptides. Recently, Gardner and coworkers developed a new IRCX which incorporates a phosphate functional group into the cross-linker for its characteristic absorption at 10.6-μm (Figure 2.7) [213]. Therefore, all the peptides which contain IRCX would undergo photodissociation and be readily distinguished by a dramatic decrease in their ion abundances upon IR irradiation. Whereafter, the identified IRCX-containing peptides could be further interrogated by infrared multiphoton dissociation (IRMPD), CID, or both methods. The capability of this IRCX was experimentally demonstrated by its application to ubiquitin cross-link analysis, opening another promising pathway for the structural analysis of biological assemblies by chemical cross-linking methods.

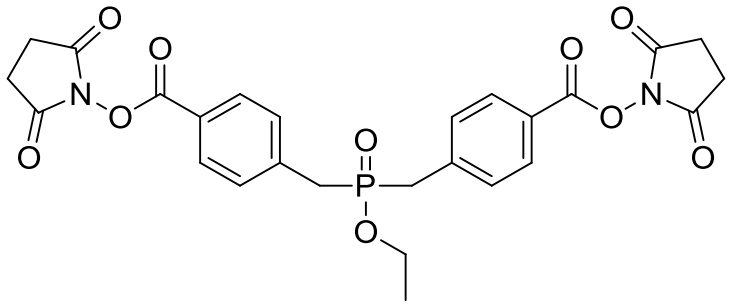

Figure 2.7 Structure of an IR chromogenic cross-linking reagent (IRCX). Adapted from Reference [213].

Recently, another photocleavable cross-linker bimane bisthiopropionic acid N-succinimidyl ester (BiPS) was introduced by Borchers and coworkers (Figure 2.8) [218]. BiPS can be photocleaved under MALDI conditions. With the incorporation of isotope labels and fluorophore elements into the molecule, BiPS provides a powerful tool to aid in rapidly distinguishing cross-linked peptides based on MALDI analysis.

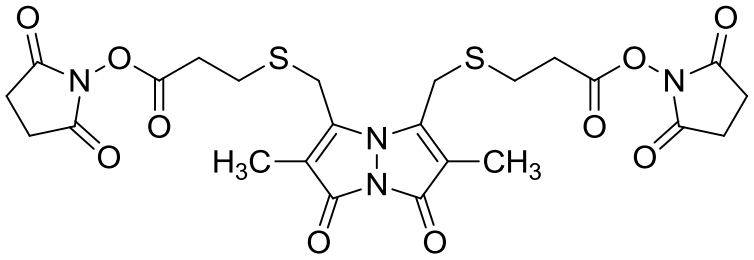

Figure 2.8 Structure of MALDI photocleavable cross-linking reagent bimane bisthiopropionic acid *N*-succinimidyl ester (BiPS). Adapted from Reference [218].

For more conveniently used MS/MS cleavable cross-linkers, regardless of whether the cleavage site is incorporated on the cross-linker side-chain or in the cross-linker spacer chain, the gas-phase cleavage is required to take place prior to cleavage of the peptide backbone. However, the mechanisms responsible for the gas-phase fragmentation reactions that give rise to the

product ions of interest are typically highly dependent on the charge state and amino acid composition of the peptide (i.e., proton mobility), thus the product ions required for crosslink identification may only be observed in low abundance from total peptide ions or many dissociation channels [207, 208, 210, 212].

To obtain further insights into this issue, the mechanisms likely to be responsible for the fragmentation of protonated cross-linked peptide ions by tandem mass spectrometry are briefly described below.

2.4 Gas Phase Fragmentation Reactions of Protonated Cross-linked Peptide Ions

Proteins may be identified by 'fingerprinting' analysis of the masses obtained from their proteolytically derived peptides [219]. Most commonly however, protein identification is achieved by tandem mass spectrometry of selected peptide ions to obtain peptide sequence information, which is interpreted by either database analysis [220, 221] or by using *de novo* sequence analysis methods [31, 222]. The successful sequence analysis of protonated peptide ions relies heavily on the formation of a complete series of product ions resulted from the cleavage along the peptide backbone. However, other product ions resulting from cleavage of the amino acid side chains, multiple cleavages of the peptidic chain or involving rearrangement reactions are also observed, complicating the mass spectrum and hindering peptide sequence analysis [223]. An understanding of the mechanisms responsible for protonated peptide fragmentation, and how they control the types of fragment ions observed, is key to increasing the accuracy of protein identification methods and for the determination of post-translational modifications [15, 224, 225] or modifications involving peptide cross-linking.

2.4.1 Mechanisms for the Fragmentation of Protonated Peptide Ions

The nomenclature for peptide fragment ions formed from dissociations along the peptide backbone is shown in Scheme 2.3 [226]. Product ions corresponding to cleavage of the Cα-C, the C-N amide bond and the N- Cα bond, are termed a-, b-, and c-types ions if the charge is retained on the N-terminal fragment or x-, y- and z- type ions if the C-terminal fragment retains the charge. Collision induced dissociation (CID) is the most commonly used technique for energy transfer required for gas phase fragmentation reactions. Under the low energy CID conditions employed in triple quadrupole and quadrupole ion trap mass spectrometers, b- and y-type ions are typically the dominant product ions produced [227].

Protonation is typically required to occur at each of the amide bonds along the peptide backbone for a complete sequence information under low energy activation conditions. The mechanism for the cleavage process is generally described using the "mobile proton model" described by Dongre *at*. *el*. [228] and extended by Kapp *et al*. [14], which defines 3 categories; "non mobile" when the total number of protons ≤ the number of Arg residues, "mobile" when the total number of protons > the total number of basic residues (i.e. combined number of Arg, Lys and His), or "partially mobile" when the number of Arg residues < the total number of protons ≤ the total number of basic residues [14, 18].

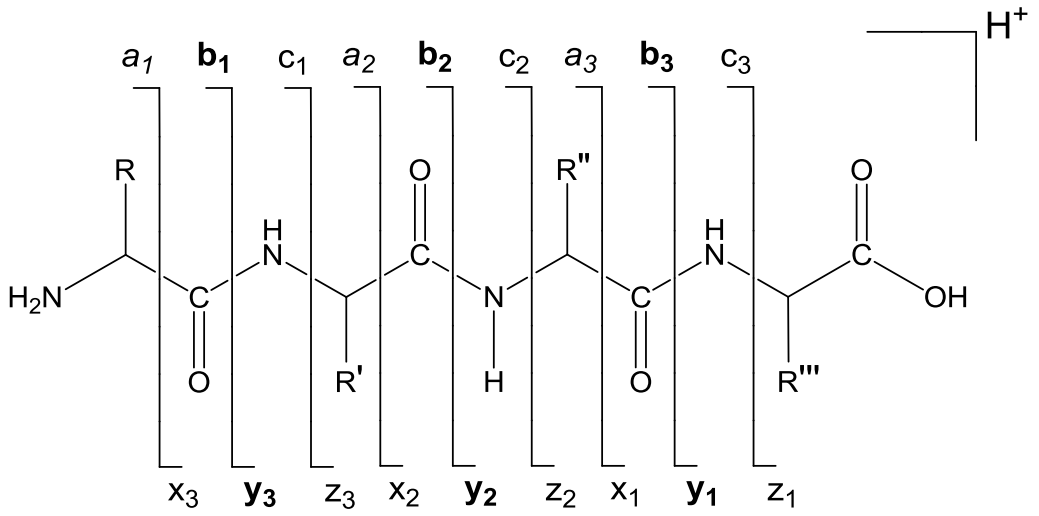

Scheme 2.3 Nomenclature for peptide fragment ions. Adapted from Reference [226].

Under "mobile" or "partially-mobile" proton conditions, fragmentation of most protonated peptides requires the involvement of an ionizing proton at the cleavage site, i.e. the cleavages are "charge-directed" [229, 230], whereas under "non-mobile" proton conditions, "charge-remote" fragmentation pathways (i.e. no ionizing proton involvement) can dominate [14, 231].

As shown in Scheme 2.4, during a "charge-directed" process, after the proton is transferred to the cleavage site, dissociation of the amide bond is initiated by nucleophilic attack from an adjacent nucleophile, e.g. amide carbonyl, resulting in an ion-molecule complex, followed by further dissociation without or with intermolecular proton transfer giving b- and/or y- type ions.

However, the propensities for each amide bond cleavage along the peptide backbone are usually not the same. It has been observed that enhanced amide bond cleavage usually occurs at the N-terminal side of a proline residue under the "mobile" proton conditions [14]. This is probably due to the higher proton affinity of the proline imide bond compared to an amide bond. Under "non-mobile" proton conditions, enhanced dissociation at the C-terminal side of aspartic

acid residues is often observed, as a result of a "charge-remote" process involving proton transfer from the carboxyl group of the aspartic acid residue to the adjacent amide bond [14]. A "charge-remote" fragmentation process is also responsible for the dominant neutral loss of CH_3SOH (64 Da) observed from the dissociation of side chain of methionine sulfoxide residues under low proton mobility conditions, which is reported to be a more favorable process compared to the C-terminal aspartic acid cleavage [18]. Thus, the propensities for peptide bond cleavage (amide bond and side chain) are highly dependent on the proton mobility conditions of the peptide ions.

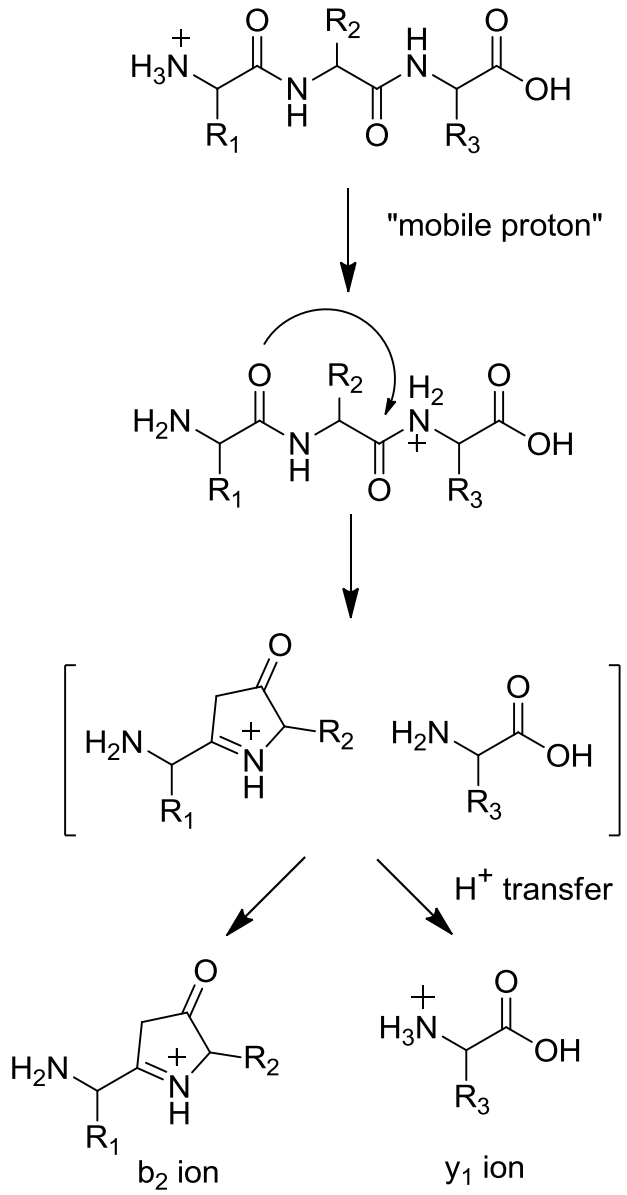

Scheme 2.4 The general mechanism for the competition between y- and b-type product ion formation in protonated peptides. Adapted from Reference [227].

2.4.2 Gas-Phase Fragmentation Reactions of Protonated Cross-Linked Peptide Ions

Back *et al.* has studied the CID fragmentation behavior of BID intramolecular cross-linked tyrlysbradykinin (YKRPPGFSPFR) at different charge states [207]. It was found that the marker benzyl cation was observed from dissociation of triply charged precursor peptide ions but not from doubly charged species, indicating the desired fragmentation pathway at the side chain of the BID requires "mobile" proton conditions. In addition, the observation of this marker ion is only one of many fragmentation pathways, thus limiting its sensitivity for the identification of cross-linked peptides.

The cross-linking reagent (SuDPG) developed by Soderblom *et al*. [210] is based on the incorporation of an aspartyl-prolyl bond within the linker region for specific gas-cleavage site. As shown in Scheme 2.2, cleavage is initiated by transferring a labile proton from the aspartyl side chain to the basic backbone amine of the adjacent prolyl residue, and then the carboxy anion attacks the carbonyl carbon, resulting in a cyclized anhydride and a free prolyl residue. However the Kapp *et al*. study indicated that fragmentation of Asp-Pro bonds is significantly enhanced only for peptides under non-mobile conditions [14]. As a result, realizing preference cleavage in both BID and SuDPG cross-linked peptides is limited by their charge states. Similarly, the desired cleavage of cross-linked peptides obtained from reaction with PIRs and NHS-BuTuGPG-NHS are also dependent on the proton mobility conditions of the precursor ions.

2.5 Bioinformatics Strategies in the Field of Chemical Cross-Linking

With the improvements in cross-linking reagents, extracting structure information from cross-linking experiments is still a formidable task. As another emerging and rapid growing area, bioinformatics tools play an important role in data analysis. Two recent reviews on cross-linking

mass spectrometry highlighted recent advances of the technology with emphasis on data analysis by computer software [232, 233]. Typical programs firstly identify cross-link candidates from matching results of experimental MS spectrum against calculated possible cross-links and then MS/MS spectra are analyzed for confirmation. For example, Pro-CrossLink [234] and XLINK [200] were developed for LC-ESI-MS data and LC-MALDI-MS data using isotope labeling. The recently developed xQuest program is able to detect cross-linked peptides from large protein databases [235], probably most sophisticated software reported so far. However, xQuest requires isotope labeling to work satisfactionly and the process can be computationally expensive, especially for complex mixtures. Among all cross-link types, inter-peptide cross-links are most informative type for protein structure detection, but are probably most challenging to identify. Mono-links and intra-peptide cross-links could be identified by running regular protein identification tools such as SEQUEST [220] with post-translational modification options. Inter-peptide cross-links from gas-phase cleavable cross-linker result in the formation of two separated peptide chains, which could be identified by regular protein identification software as well. Thus computational processing could be simplified and more confidence obtained, by using these cross-linking strategies.

2.6 Aims of the Chemical Cross-Linking Project

To develop improved chemical cross-linking and tandem mass spectrometry methodologies for the analysis of protein structures and protein-protein interactions, the aims of this project are:

1. Synthesis of a series of novel water soluble ‘fixed charge’ sulfonium ion containing cross-linking reagents.

2. Evaluation of the multistage gas-phase fragmentation reactions of cross-linked peptide ions formed by reaction with these reagents, using synthetic peptides as models for standard proteins and protein complexes.

CHAPTER THREE

DEVELOPMENT OF NOVEL IONIC REAGENTS FOR CONTROLLING THE GAS-PHASE FRAGMENTATION REACTIONS OF CROSS-LINKED PEPTIDES

3.1 Introduction

Chemical cross-linking combined with proteolytic digestion and mass spectrometry is a promising approach to provide inter- and intramolecular distance constraints for the structural characterization of protein topologies and functional multiprotein complexes. Despite the relative straightforwardness of these methodologies, the identification and characterization of cross-linked proteins presents a significant analytical challenge, due to the complexity of the resultant peptide mixtures, as well as the array of inter-, intra-, or "dead-end"-cross-linked peptides that may be generated from a single cross-linking experiment. Based on results from recent studies aimed at the development of fixed charge sulfonium ion chemical derivatization strategies for "targeted" MS/MS-based identification, characterization, and quantitative analysis of peptides containing specific functional groups (e.g., the side chains of methionine or cysteine) [19, 170, 236-239], and as a first step toward the development of an improved MS/MS-based approach for the comprehensive analysis of protein-protein interactions using chemical cross-linking and multistage tandem mass spectrometry, this chapter describes the synthesis, characterization, and

---

Part of the results described in Chapter Three were published in: Lu, Y.; Tanasova, M.; Borhan, B.; Reid, G. E., Ionic Reagent for Controlling the Gas-Phase Fragmentation Reactions of Cross-Linked Peptides. Anal. Chem. 2008, 80, 9279-9287.

initial demonstration of the selective CID-MS/MS gas-phase fragmentation behavior of cross-linked peptide ions formed by reaction with a novel amine reactive, sulfonium ion containing cross-linking reagent, *S*-methyl 5,5′-thiodipentanoylhydroxysuccinimide.

3.2 Cross-Linker Design and Rationale

A cross-linking reagent that demonstrates preferential gas-phase fragmentation **r**eactions under low-energy CID-MS/MS conditions must satisfy a number of criteria. The reagent must be soluble and stable when subjected to cross-linking reaction conditions in aqueous solutions at mild pH values. The cross-linker should contain an appropriate linker length for detecting informative protein-protein interaction sites within protein complexes (typical commercially available cross-linking reagents have a spacer arm less than 20 Å). The structure of the cross-linker (or a functional group within the cross-linker) should facilitate enrichment of the cross-linked reaction products in solution, in order to allow their observation during MS and to enable subsequent selection of the precursor ions for MS/MS analysis. Finally, a requirement that is specific to a gas-phase cleavable cross-linking reagent is that fragmentation of the cross-linker during MS/MS should occur exclusively and independently of the proton mobility of the cross-linked peptide precursor ion; i.e., the energy required for cleavage within the linker region should be lower than that for cleavage within the peptide backbone or side chains, regardless of the number of protons, the amino acid composition, or the sequence of the peptide.

NHS esters are commonly employed as the reactive groups of cross-linking reagents in order to target primary amino groups, (i.e., the ε-amino groups of lysine amino acid side chains or the α-amino group of the N-terminus), located within the protein or proteins of interest [175,

240]. However, the application of NHS esters to the analysis of large protein complexes is typically limited by their poor solubility under "native" aqueous conditions, thereby requiring the use of sulfo-NHS esters. However, simple members of ionic sulfonium salts typically exhibit high solubilities in water [241]. Thus, a sulfonium ion containing cross-linker would be expected to offer an advantage for the mapping of large protein complexes due to its substantial solubility under aqueous conditions. The presence of the sulfonium ion would also facilitate enrichment of cross-linked peptides using strong cation-exchange chromatography prior to MS and MS/MS analysis [242].

3.2.1 Incorporation of a 'Fixed Charge' Sulfonium Ion into an Amine Functional Group Specific Cross-Linking Reagent *S*-Methyl 5,5′-Thiodipentanoylhydroxysuccinimide

Previous studies carried out in the Reid group have demonstrated that peptide ions containing fixed-charge sulfonium ion derivatives introduced to the side chains of certain amino acid residues (e.g., methionine and cysteine) undergo exclusive loss of a dialkylsulfide moiety during the time scale of ion activation in either ion trap or quadrupole mass spectrometers, via selective cleavage at the site of the fixed charge [19, 170, 236-239]. Using a combination of experimental data and theoretical calculations, the mechanism for this loss has been proposed to proceed via neighboring group participation reactions involving nucleophilic attack from an adjacent amide bond, resulting in the formation of 6-membered oxazoline or 5-membered iminohydrofuran product ions, depending on the alkyl chain length linking the nucleophile with the sulfonium ion leaving group (Scheme 3.1) [237, 239]. Importantly, these selective fragmentation reactions have been demonstrated to occur independently of the proton mobility of

the peptide precursor ions containing the sulfonium ion derivatives [19, 170, 236-239]. These results suggest that the incorporation of a fixed charge sulfonium ion into the backbone of a chemical cross-linking reagent, containing an NHS ester (that subsequently reacts with a primary amino group within the protein of interest to form a nucleophilic amide bond) and that has an appropriate alkyl chain (propyl or butyl) linker attached to the electrophilic sulfonium ion, would result in selective fragmentation of the cross-linker upon CID-MS/MS.

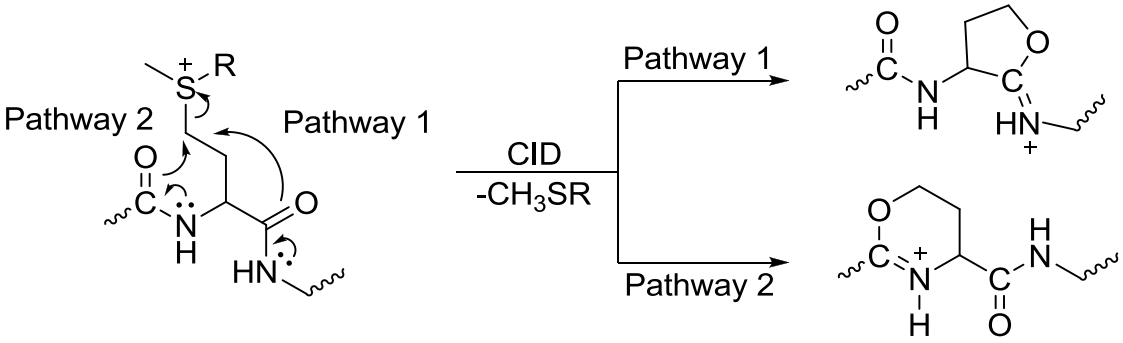

Scheme 3.1 Gas-phase fragmentation behavior of the sulfonium ion derivative of methionine-containing peptides. Adapted from Reference [237].

3.2.2 Gas-Phase Fragmentation Reactions of Cross-linked Peptides Formed by Reaction with the Ionic Cross-Linking Reagent *S*-Methyl 5,5′-Thiodipentanoylhydroxysuccinimide

Synthesis of *S*-methyl 5,5′-thiodipentanoylhydroxysuccinimide (**1;** Scheme 3.2) was carried out as described in Experimental Chapter Four. ESI-MS analysis in a quadrupole ion trap of this reagent revealed a single ion at m/z 443.3, corresponding to the M^+ precursor ion. CID-MS/MS of the m/z 443.3 precursor ion resulted in the formation of a dominant product ion at m/z

197.9 (see Figure 4.4), via the neutral loss of 5-(methylthio)pentanoylhydroxysuccinimide (see Scheme 4.5).

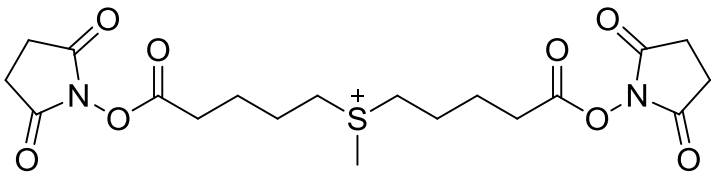

S-Methyl 5,5′-Thiodipentanoylhydroxysuccinimide (**1**)

Scheme 3.2 Structure of ionic cross-linking reagent *S*-methyl 5,5′-thiodipentanoylhydroxysuccinimide (**1**).

Potential mechanisms for the gas-phase fragmentation reactions of the various types of peptide products formed by reaction with cross-linking reagent **1** (i.e., intermolecular, dead-end, and intramolecular) are shown in Scheme 3.3. For intermolecular peptide cross-links (Scheme 3.3A), the two peptide chains are connected by a cross-linker arm (designated here as **I**-**S**) between two amide nitrogens. Fragmentation of a labile C-S bond on either side of the fixed charge upon low-energy CID MS/MS would result in the formation of two separated peptide chains containing unique modifications, one containing a protonated six-membered iminotetrahydropyran (**I**) with a mass increment of 83 Da, and the other containing a neutral S-methylthiopentanoyl (**S**) group with a mass increment of 130 Da. Note that fragmentation of the cross-linker in Scheme 3.3A may occur on either side of the sulfonium ion linkage. Therefore, due to the symmetrical structure of the cross-linking reagent, the dissociation of a homodimeric intermolecular cross-linked precursor ion (i.e., when $peptide_1$ and $peptide_2$ are the same) would result in the formation of a single pair of **I** and **S** modified peptide product ions. In contrast, dissociation of a heterodimeric cross-linked precursor would yield two pairs of **I** and **S** modified

products. This difference in fragmentation therefore allows these two types of reaction products to be readily differentiated.

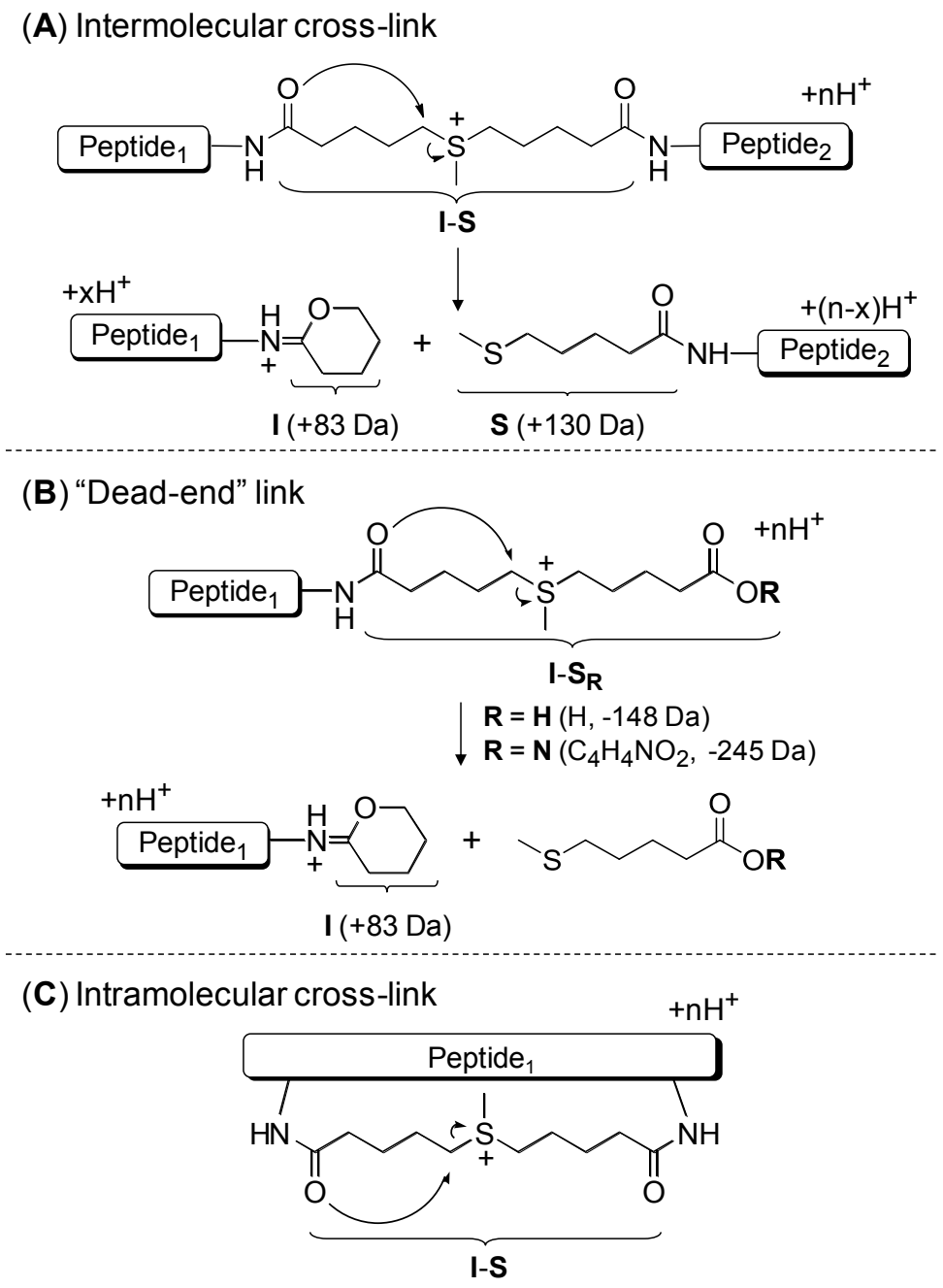

Scheme 3.3 Selective gas-phase fragmentation reactions of intermolecular, dead-end, and intramolecular cross-linked peptide products formed by reaction with ionic cross-linking reagent **1**. The linker formed upon cross-linking is denoted as **I-S**. Cleavage of the C-S bond within the linker region results in two specific peptide modifications, one corresponding to a 6-membered iminotetrahydropyran (**I**) and the other corresponding to S-methylthiopentanoyl (**S**) group. A "dead-end" modification ($\mathbf{I\text{-}S_R}$) on an intact peptide is labeled $\mathbf{I\text{-}S_N}$ when an unreacted NHS functional group is retained, and $\mathbf{I\text{-}S_H}$ when a carboxyl group is formed via hydrolysis of the NHS ester.

For "dead-end" cross-links (designated in Scheme 3.3 as **I-S_R**), where one reactive NHS group has undergone a cross-linking reaction and where the other ester remains intact (**I-S_N**) or has undergone hydrolysis (**I-S_H**) (Scheme 3.3B), CID-MS/MS would result in the neutral loss of 5-(methylthio)pentanoic acid (148 Da, where R = H) or the loss of 5-(methylthio)pentanoylhydroxysuccinimide (245 Da, where R = $C_4H_4NO_2$). In both cases, it is predicted that the cleavage would preferentially take place at the C-S bond closest to the peptide chain, since an amide carbonyl oxygen is expected to be a better nucleophile compared to either an ester or acid carbonyl oxygen [230]. For both intermolecular and dead-end cross-linked peptide products, subsequent isolation and MS^3 dissociation of the initial MS/MS product ions can then be used to provide additional structural information required for identification of the peptide sequences involved in the cross-linking reactions, as well as for characterization of the specific site(s) at which cross-linking has occurred.

For an intramolecular peptide cross-link (Scheme 3.3C), the desired C-S bond cleavage is expected to be the energetically favored process. However, as no change in m/z would be observed upon initial dissociation of these bonds, immediate further fragmentation would occur during CID-MS/MS to yield b- and y-type sequence ions. The symmetrical structure of the cross-linking reagent **1**, would again be expected to result in similar fragmentation efficiencies at the two possible C-S bond cleavage sites. Thus, a given b- or y-type product ion may be observed with either **I** or **S** modifications. The factors that influence the ions that are observed will be discussed later in this chapter.

3.3 Multistage Tandem Mass Spectrometry Analysis of Sulfonium Ion Containing Cross-Linked Peptide Ions

In order to initially examine the multistage CID-MS/MS gas-phase fragmentation behavior of the peptide products formed by reaction with cross-linking reagent **1′** or **1″**, the model synthetic peptide VTMAHFWNFGK (pep_{VWK}) was subjected to cross-linking as described above. The ESI mass spectrum obtained following a 30-min cross-linking reaction with reagent **1′** (iodide counter ion) is shown in Figure 3.1. Reaction with reagent **1″** (methylsulfate counter ion) was found to proceed more slowly (probably due to counterion effect), with similar yields of the various cross-linked peptide products obtained only after 90 min using 2.5 equiv of cross-linker (data not shown).

Figure 3.1 ESI-mass spectrometry analysis of cross-linked VTMAHFWNFGK (pep_{VWK}) formed by reaction with reagent **1′**. Intermolecular cross-linked ions (structure **a**) are indicated as $[2M + nH + (I\text{-}S)]^{(n+1)+}$. Intramolecular cross-linked ions (structure **b**) are indicated as $[M + nH + (I\text{-}S)]^{(n+1)+}$. Unhydrolyzed monolinked ions (structure **c**) are indicated as $[M + nH + (I\text{-}S_N)]^{(n+1)+}$. Hydrolyzed monolinked ions (structure **d**) are indicated as $[M + nH + (I\text{-}S_H)]^{(n+1)+}$. Hydrolyzed dilinked ions (structure **e**) are indicated as $[M + nH + 2(I\text{-}S_H)]^{(n+2)+}$. The residual unreacted cross-linking reagent is labeled $(I\text{-}S)_{NN}^{+}$. Hydrolyzed cross-linking reagent is labeled $(I\text{-}S)_{NH}^{+}$. Doubly hydrolyzed cross-linking reagent is labeled $(I\text{-}S)_{HH}^{+}$.

Figure 3.1 (cont'd)

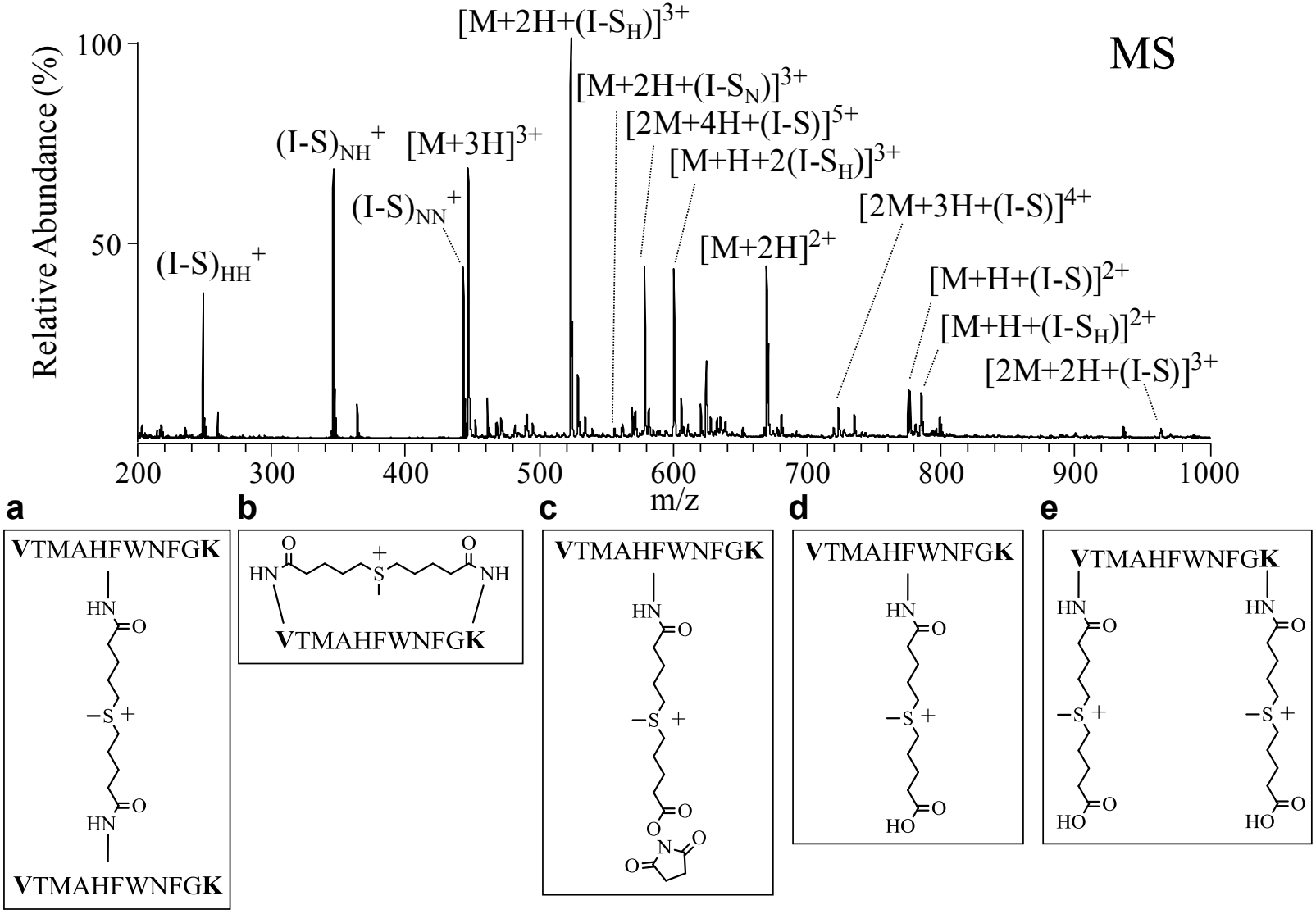

The complexity of the mass spectrum in Figure 3.1 arises due to the formation of multiple reaction products, including intermolecular (**a** in Figure 3.1; 15.6 % relative abundance) and intramolecular **b** in Figure 3.1; 3.7 % relative abundance) crosslinks (labeled $[2M + nH + (I\text{-}S)]^{(n+1)+}$ and $[M + nH + (I\text{-}S)]^{(n+1)+}$, respectively), monolinked unhydrolyzed (**c** in Figure 3.1; 0.7 % relative abundance) dead-end links ($[M + nH + (I\text{-}S_N)]^{(n+1)+}$), and mono- (**d** in Figure 3.1; 33.8 % relative abundance) and dilinked (**e** in Figure 3.1; 12.8 % relative abundance) hydrolyzed dead-end links ($[M + nH + (I\text{-}S_H)]^{(n+1)+}$ and $[M + nH + 2(I\text{-}S_H)]^{(n+2)+}$, respectively), as well as due to the presence of unreacted peptide $[M + nH]^{n+}$ (33.3 % relative abundance), residual unreacted cross-linking reagent $(I\text{-}S)_{NN}^{+}$, hydrolyzed cross-linking reagent $(I\text{-}S)_{NH}^{+}$, and doubly hydrolyzed cross-linking reagent $(I\text{-}S)_{HH}^{+}$. Thus, the cross-linking reagent in intact and hydrolyzed forms was remained from Sep-paking elution procedure. Note that the relative abundance of each type of cross-linked product will be varied with changing the reaction conditions, such as the concentrations of the peptide solutions, reaction time and with or without quenching. Most importantly, the formation of each type of cross-linked product is directly related to protein structure of interst. Despite this complexity, the identification and characterization of each of these products was readily achieved by examination of the characteristic fragmentation behavior of each of their respective precursor ions.

3.3.1 Analysis of Intermolecular Cross-Linked Reaction Products

Dissociation of the +5 charge state of the homodimeric intermolecular cross-linked precursor ion of pep_{VWK} ($[2M + 4H + (I\text{-}S)]^{5+}$ in Figure 3.1) resulted in exclusive fragmentation of the cross-link to yield a single pair of product ions containing iminotetrahydropyran (**I**) and S-methylthiopentanoyl (**S**) modifications ($[M + 2H + \mathbf{I}]^{3+}$ and $[M + 2H + \mathbf{S}]^{2+}$ in Figure 3.2A, respectively), consistent with that outlined in Scheme 3.3A. Importantly, the specificity of this fragmentation was found to be independent of the precursor ion charge state (see the product ion spectra obtained from the +4 and +3 charge states of the homodimeric intermolecular cross-linked precursor ion of pep_{VWK} ($[2M + 3H + (I\text{-}S)]^{4+}$ and ($[2M + 2H + (I\text{-}S)]^{3+}$ in Figure 3.2B and C, respectively). Due to the presence of a single peptide in this reaction, and the symmetrical structure of the cross-linking reagent **1**, dissociation of the homodimeric intermolecular cross-linked precursor ions resulted in the formation of a single pair of **I** and **S** modified product ions.

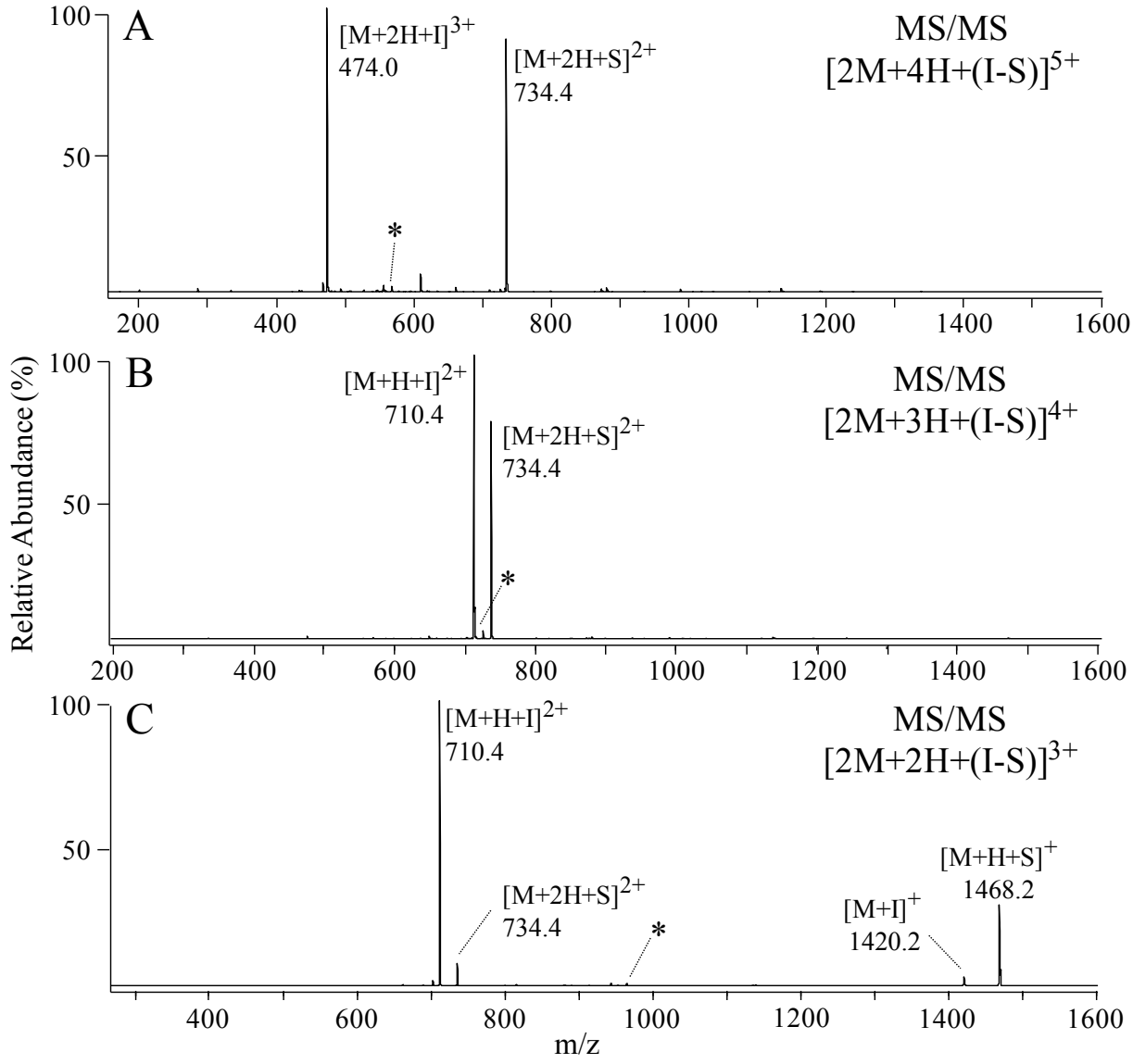

Figure 3.2 CID-MS/MS product ion spectra of intermolecular cross-linked ions formed from the model peptide (pep_{VWK}). (A) $[2M + 4H + (I\text{-}S)]^{5+}$, (B) $[2M + 3H + (I\text{-}S)]^{4+}$, and (C) $[2M + 2H + (I\text{-}S)]^{3+}$ from Figure 3.1. The m/z of the precursor ions selected for dissociation in each spectrum are indicated by an asterisk.

A result similar to that described above was also observed upon CID-MS/MS analysis of the homodimeric reaction products formed by cross-linking of the aspartic acid containing peptide pep_{GDR} (GAILDGAILR). Panels A and B in Figure 3.3, show the product ion spectra

obtained from the $[2M + 2H + (I\text{-}S)]^{3+}$ and $[2M + H + (I\text{-}S)]^{2+}$ precursor ions. Importantly, essentially exclusive cleavage of the cross-linker was observed for these ions, even though an aspartic acid residue that was observed to undergo preferential cleavage giving rise to a single dominant product ion upon dissociation of its unmodified protonated precursor ion (Figure 3.3C) was present within the peptide sequences. Previous studies to examine the global factors influencing the fragmentation reactions of protonated peptide ions have demonstrated that cleavage at the C-terminal side of aspartic acid residues is significantly enhanced under "partially mobile" and "nonmobile" proton conditions [14]. The +3 and +2 precursor ion charge states of the cross-linked sulfonium ion containing pep_{GDR} homodimer would both be classified as nonmobile, as would the +1 precursor ion charge state of the monomeric pep_{GDR} peptide. Thus, the observation of only low-abundance product ions corresponding to cleavage at the C-terminal side of an aspartic acid residue in the homodimeric cross-linked peptide in Figure 3.3B is consistent with our previous studies demonstrating that fragmentation of sulfonium ion derivatives is an energetically favorable process compared to those for amide bond cleavage reactions [237, 239].

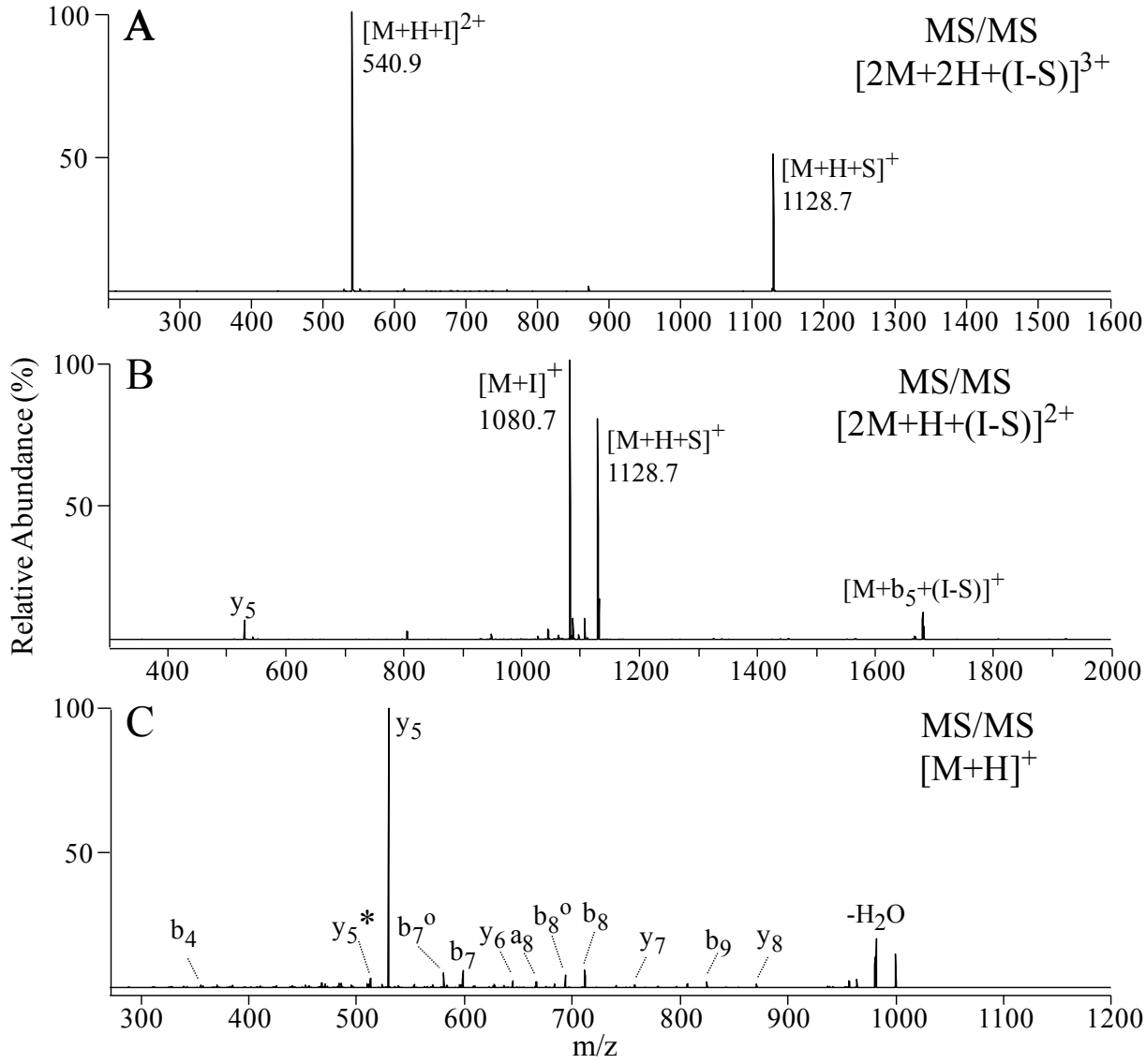

Figure 3.3 CID-MS/MS product ion spectra of (A) intermolecular cross-linked ion [2M + 2H + (I-S)]$^{3+}$ formed from the model peptide (pep_{GDR}) with **1**, (B) intermolecular cross-linked ion [2M + H + (I-S)]$^{2+}$ formed from the model peptide (pep_{GDR}) with with **1′**, and (C) [M + H]$^{+}$ ion of pep_{GDR}. A superscript "o" indicates the neutral loss of H_2O. A superscript "*" indicates the neutral loss of NH_3.

The mass spectrum obtained by ESI-MS analysis following cross-linking of a 1:1 mixture of neurotensin (α, *p*ELYENKPRRPYIL) and angiotensin II (β, DRVYIHPF) with reagent **1** is

shown in Figure 3.4A. CID-MS/MS analysis of the homodimeric cross-linked precursor ions from neurotensin ($[2\alpha + 4H + (I\text{-}S)]^{5+}$) and angiotensin II ($[2\beta + 4H + (I\text{-}S)]^{5+}$) are shown in Figure 3.4B and C, respectively. Similar to that discussed above, a single pair of product ions containing **I** and **S** modifications were observed as the dominant fragmentation pathway in each case. In contrast, dissociation of the heterodimeric intermolecular crosslinked peptide product ($[\alpha + \beta + 3H + (I\text{-}S)]^{4+}$) resulted in the formation of two pairs of characteristic **I** and **S** modified product ions (Figure 3.4D). Therefore, the characteristic products formed from the dissociation of homo- and heterodimeric cross-linking reactions allow these products to be readily differentiated. A similar result was also obtained upon CID-MS/MS of the intermolecular heterodimeric cross-linked peptide product formed by reaction between [Glu^1]-fibrinopeptide B and substance P (Figure 3.5).

Figure 3.4 (A) ESI-mass spectrometry analysis of cross-linked neurotensin (α) and angiotensin II (β) formed by reaction with reagent **1**. CID-MS/MS of (B) the $[2\alpha + 4H + (I\text{-}S)]^{5+}$ precursor ion of neurotensin containing a homodimeric intermolecular cross-link, (C) the $[2\beta + 4H + (I\text{-}S)]^{5+}$ precursor ion of angiotensin II containing a homodimeric intermolecular cross-link, and (D) the $[\alpha + \beta + 3H + (I\text{-}S)]^{4+}$ precursor ion of neurotensin and angiotensin II containing a heterodimeric intermolecular cross-link. The m/z of the precursor ions selected for dissociation in each spectrum are indicated by an asterisk. A † indicates product ions containing an **I** modification.

Figure 3.4 (cont'd)

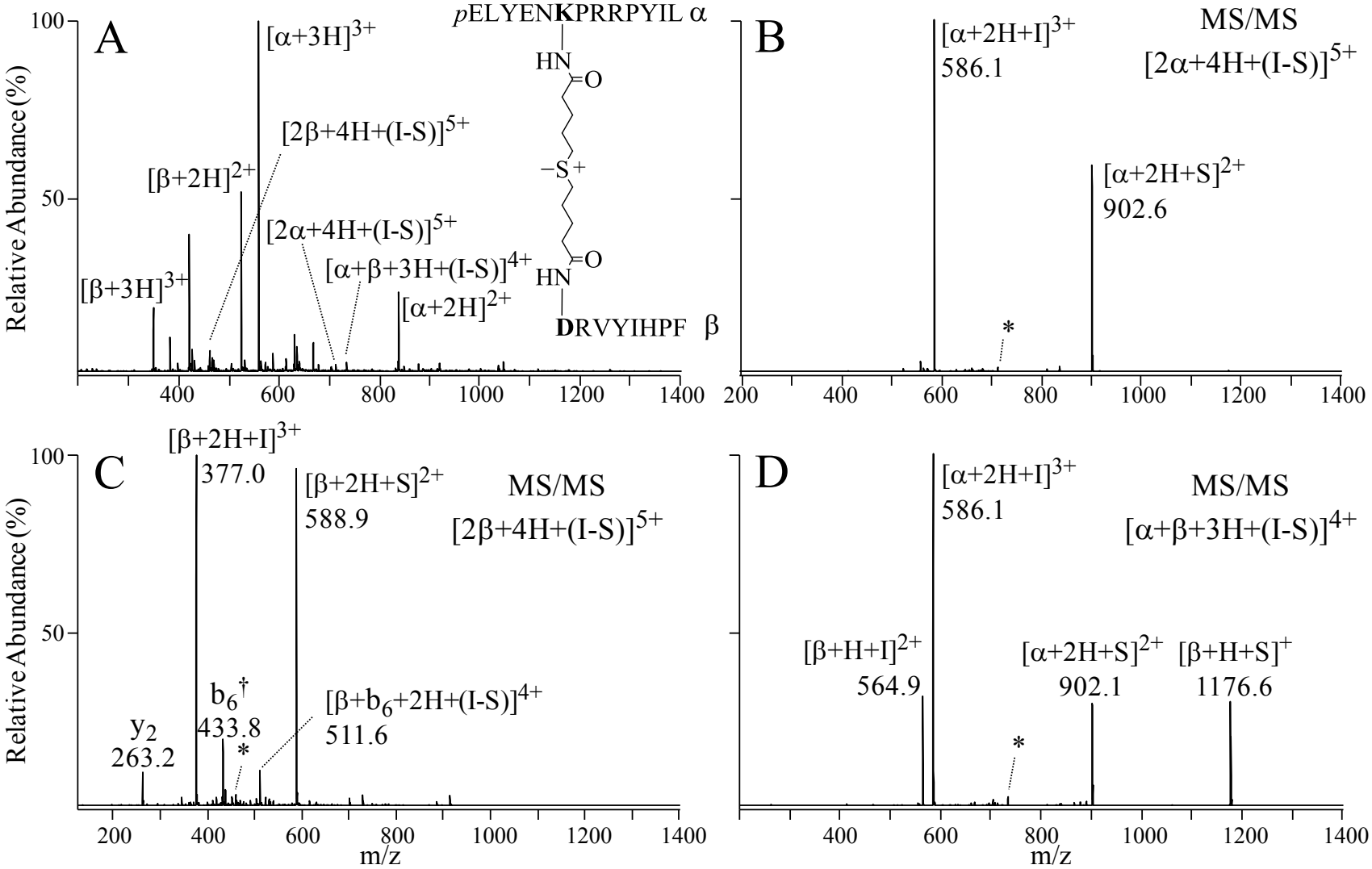

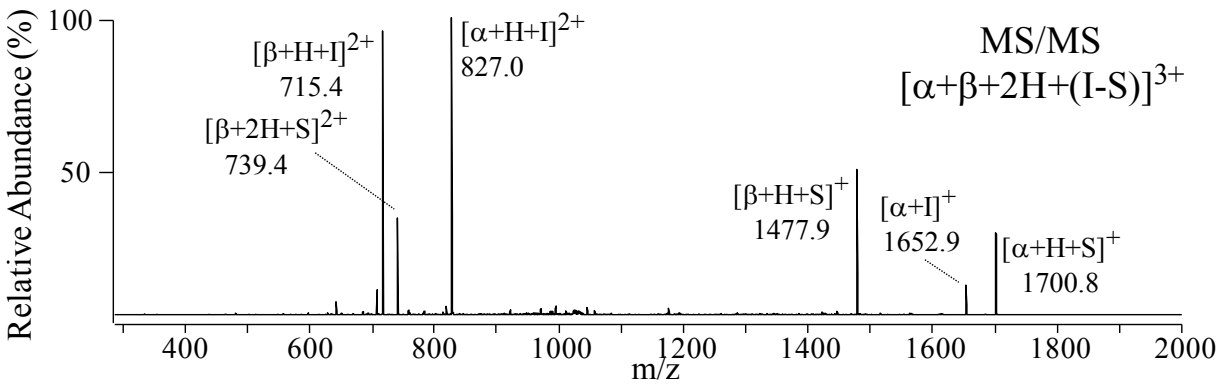

Figure 3.5 CID-MS/MS product ion spectra of the hetero-dimeric $[\alpha+\beta+2H+(I-S)]^{3+}$ precursor ion formed by reaction of reagent **1** with [Glu^1]- fibrinopeptide B (α) and Substance P (β).

Note that in addition to cleavage of the cross-linker for the homodimeric cross-linked angiotensin II peptide reaction product in Figure 3.4C, several minor product ions formed by cleavage at the His_6-Pro_7 amide bond within the angiotensin II peptide sequence ($[\beta + b_6 + 2H + (I-S)]^{4+}$ and y_2) as well as by sequential fragmentation of the cross-linker and the His_6-Pro_7 amide bond ($b_6^{\dagger}$, where † indicates the presence of an **I** modification) were also observed (Figure 4.3C). Previous studies to examine the global factors influencing the fragmentation reactions of protonated peptide ions have demonstrated that cleavage at the N-terminal side of proline residues is significantly enhanced under "mobile" and "partially mobile" proton conditions [14] (the +5 charge state of the sulfonium ion containing crosslinked angiotensin II homodimer would be classified as partially mobile). Again, therefore, the observation of these ions at only low abundance in Figure 3.4C is consistent with fragmentation of sulfonium ion derivatives being an energetically favorable process [237, 239].

Neurotensin and angiotensin II each contain only a single amino group amenable for reaction with the NHS ester of the cross-linking reagent. Thus, it was not necessary to obtain

further evidence to assign the sites at which the cross-linking reactions had occurred for the reaction products in Figure 3.4. In contrast, the model peptide pep_{VWK} could undergo reaction at either the α-amino or ε-amino groups to yield an isomeric mixture of intermolecular cross-linked homodimeric products (i.e., α-amino to ε-amino, ε-amino to ε-amino, or α-amino to ε-amino). Therefore, in order to determine the modification site(s) at which the homodimeric cross-linking reaction had occurred, as well as to estimate the extent of reaction occurring at each site, both of the MS/MS peptide products shown in Figure 3.2A were isolated then subjected to further dissociation by MS^3, followed by analysis of the resultant b- and y-type product ions (Figure 3.6A and B). The CID-MS^3 spectra from the $[M + H + I]^{2+}$ product ions from Figure 3.2B and C and the $[M + H + S]^+$ product ion from Figure 3.2C are shown in Figure 3.7. In all cases, both b- and y-type product ions containing **I** (labeled with a † in Figure 3.6A and Figure 3.7A) or **S** (labeled with a ‡ in Figure 3.6B and Figure 3.7B) modifications were observed, indicating that cross-linking had occurred on both α-amino and ε-amino functional groups.

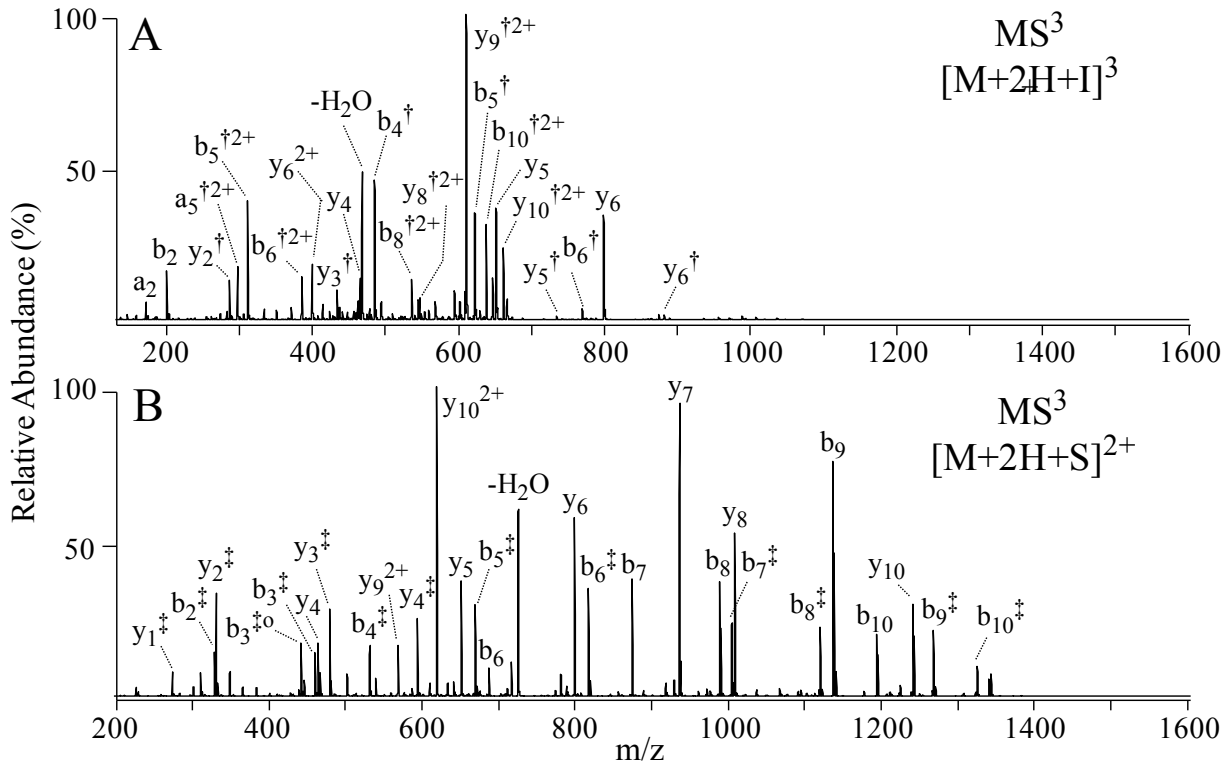

Figure 3.6 CID-MS^3 spectra of (A) the $[M + 2H + I]^{3+}$ product ion and (B) the $[M + 2H + S]^{2+}$ product ions from Figure 3.2A. A † indicates product ions containing an **I** modification. A ‡ indicates product ions containing an **S** modification. A superscript "o" indicates the neutral loss of H_2O.

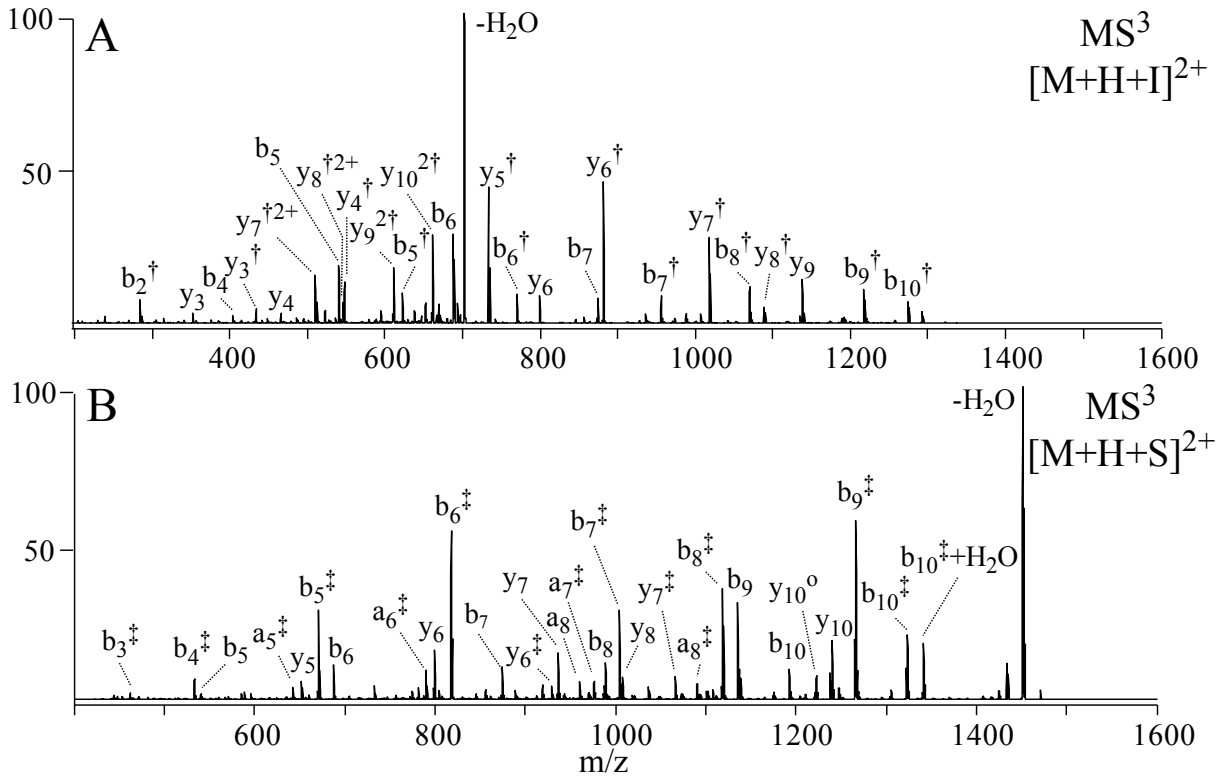

Figure 3.7 CID-MS^3 spectra of (A) the $[M+H+I]^{2+}$ product ion from Figures 3.2B and 3.2C, and (B) the $[M+H+S]^{+}$ product ion from Figure 3.2C. A † indicates product ions containing an **I** modification. A ‡ indicates product ions containing an **S** modification. A superscript "o" indicates the neutral loss of H_2O.

An attempt to estimate the extent to which the cross-linking reactions had occurred at the α- or ε-amino groups of the pep_{VWK} peptide was made by measuring the ratio of the summed relative abundances of the modified b-type ions and unmodified y-type ions (i.e, α-amino modified), to the summed relative abundances of the unmodified b-type ions and modified y-type ions (i.e., ε-amino modified) in Figure 3.6 and Figure 3.7. However, as ion detection efficiency in ion trap mass spectrometers is affected by both the charge state and product ion mass (some product ions fall below the low-mass cutoff of the instrument so are not observed), some

variability was observed (63:37 for the $[M + 2H+ I]^{3+}$ ion in Figure 3.6A, 68:32 for the $[M + 2H + S]^{2+}$ ion in Figure 3.6B, 25:75 for the $[M + H + I]^{2+}$ ion in Figure 3.7A, and 79:21 for the $[M + H + S]^{+}$ ion in Figure 3.7B), depending on the specific product ions that were observed in each case. Overall, however, there was a preference for reaction at the α-amino position, consistent with its lower pK_a compared to that of the ε-amino group.

Importantly, in all cases, as the individual peptide chains involved in intermolecular cross-linking reactions are separated upon cleavage of the sulfonium ion linker upon performing MS/MS, characterization of the peptide sequences by MS^3 is greatly simplified (i.e., no product ions are generated that contain amino acid residues from both peptides) [243]. Furthermore, the presence of **I** or **S** modifications was found to have only a minimal influence on the appearance of the product ions produced following MS^3, compared to their unmodified peptides.

3.3.2 Analysis of Dead-End Cross-Linked Reaction Products

Dissociation of the triply charged precursor ions from the intact (i.e., unhydrolyzed) and hydrolyzed monolinked products formed by reaction of the model peptide pep_{VWK} with the sulfonium ion containing crosslinking reagent **1** ($[M + 2H + (I\text{-}S_N)]^{3+}$ and $[M + 2H + (I\text{-}S_H)]^{3+}$ from Figure 3.1, respectively) each resulted in essentially exclusive neutral losses of 5-(methylthio)pentanoylhydroxysuccinimde (245 Da) or 5-(methylthio)pentanoic acid (148 Da), respectively (Figure 3.8A and B). This is consistent with the mechanism proposed in Scheme 3.3B where the major cleavage was expected to take place on the C-S bond closest to the peptide chain due to the greater nucleophilic strength of the amide carbonyl oxygen compared to either

the acid or ester carbonyl oxygen [230]. However, a minor product ion corresponding to cleavage on the "outer" C-S bond ($[M + 2H + S]^{2+}$ in Figure 3.8B), involving nucleophilic attack from the acid oxygen, was also observed from the hydrolyzed monolinked ion, indicating that some, albeit minor, competition between these cleavage sites is possible for this reaction product. Similar fragmentation behavior was also observed upon MS/MS dissociation of the doubly charged precursor ions from the intact and hydrolyzed monolinked reaction product from the pep_{VWK} peptide (data not shown), as well as for the doubly and singly charged precursor ions from the hydrolyzed monolinked reaction product from the pep_{GDR} peptide (Figure 3.9). Notably, the specificity associated with fragmentation of the cross-linker from the triply and doubly charged precursor ions of the intact monolinked reaction product from the phosphoserine containing pep_{LpSR} peptide was found not to be significantly affected by the potentially competing loss of H_3PO_4 (Figure 3.10). Interestingly, comparison of the spectra obtained by CID-MS^3 of the $[M + 2H + I]^{3+}$ product ions (shown in Figure 3.8C) from Figure 3.8A and B with that observed from the intermolecular cross-linked product ion in Figure 3.6A revealed a significantly higher abundance of b-type ions containing the **I** modification for the monolinked products (labeled in the spectra with a †; a ratio of α-amino modified : ε-amino modified of 83:17 was determined from Figure 3.8C), suggesting a somewhat greater specificity for modification of the α-amino functional group.

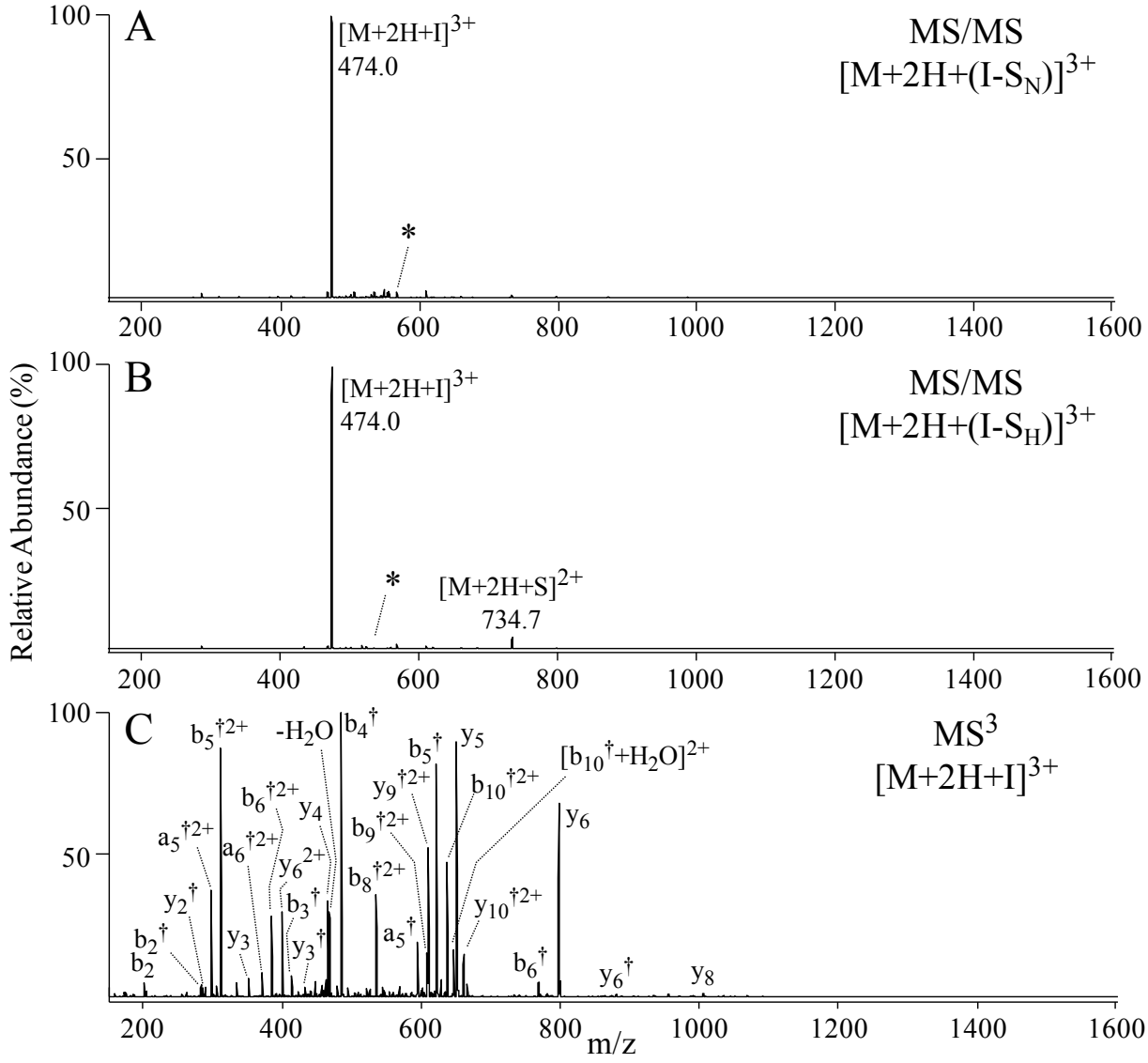

Figure 3.8 CID-MS/MS and MS^3 of pep_{VWK} containing unhydrolyzed ($I\text{-}S_N$) and hydrolyzed ($I\text{-}S_H$) monolinks. (A) MS/MS of the $[M + 2H + (I\text{-}S_N)]^{3+}$precursor ion, and (B) MS/MS of the $[M + 2H + (I\text{-}S_H)]^{3+}$precursor ion from Figure 3.1. The m/z of the precursor ions selected for dissociation in each spectrum are indicated by an asterisk. (C) MS^3 of the $[M + 2H + I]^{3+}$ product ion from panel A. Note that an identical spectrum was obtained by MS^3 of the $[M + 2H + I]^{3+}$ product ion from panel B. A † indicates product ions containing an **I** modification.

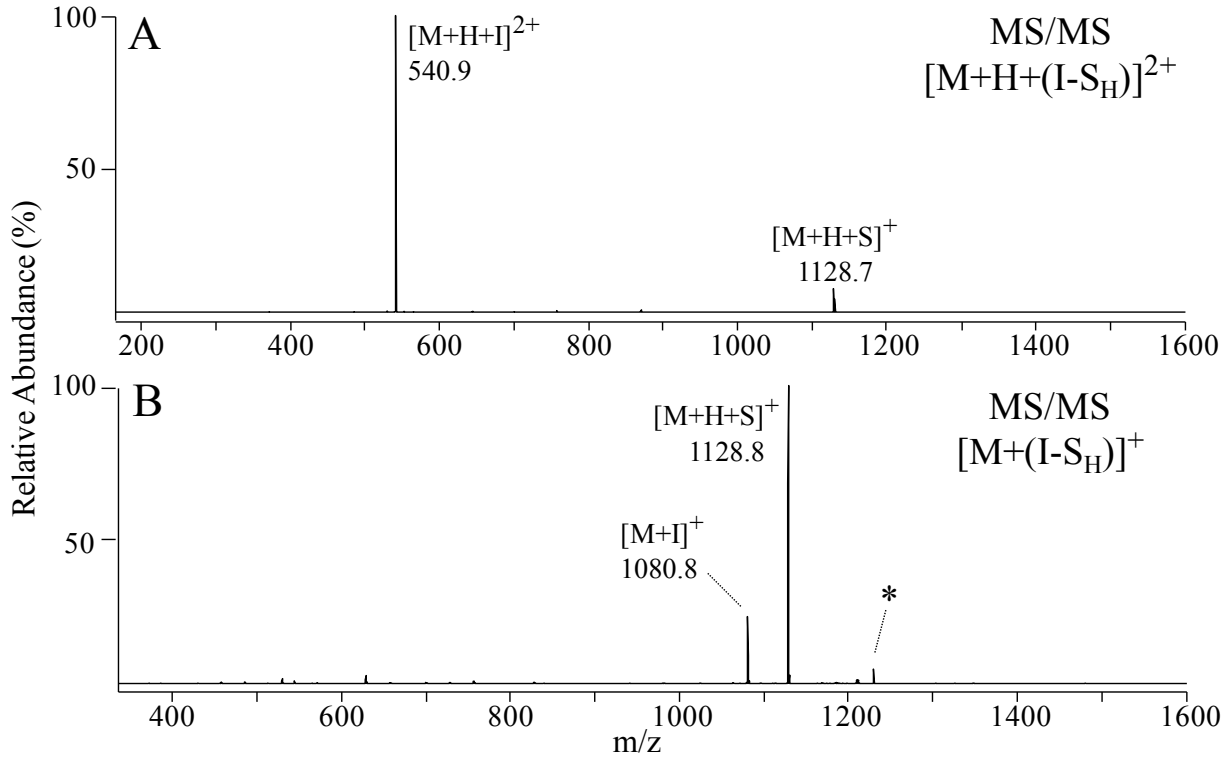

Figure 3.9 CID-MS/MS product ion spectra of (A) the $[M+H+(I\text{-}S_H)]^{2+}$ and (B) the $[M+(I\text{-}S_H)]^{+}$ precursor ions from the hydrolyzed mono-linked product formed by reaction of reagent **1′** with the pep_{GDR} peptide.

Figure 3.10 CID-MS/MS product ion spectra of the (A) $[M+2H+(I\text{-}S_N)]^{3+}$, (B) $[M+H+(I\text{-}S_N)]^{2+}$ precursor ion from the intact mono-linked reaction product formed by reaction of reagent **1** with the phosphoserine containing pep_{LpSR} peptide. (C) CID-MS^3 product ion spectrum of the $[M+2H+I]^{3+}$ product ion from panel A. (D) CID-MS^3 product ion spectrum of the $[M+H+I]^{2+}$ product ion from panel B. A † indicates product ions containing an **I** modification. A ‡ indicates product ions containing an **S** modification.

Figure 3.10 (cont'd)

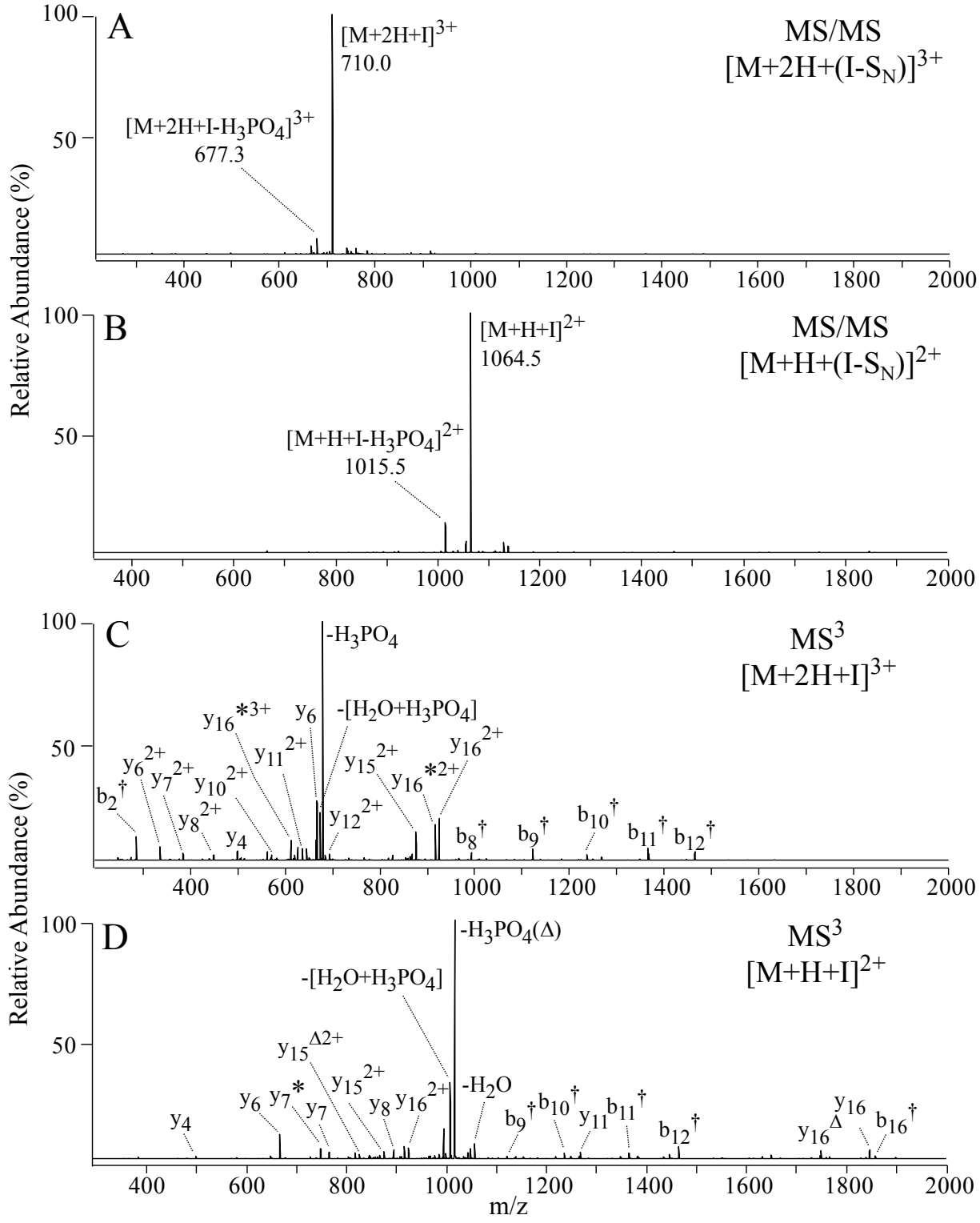

Although the cross-linking reactions were carried out at a low (1.5:1) cross-linker to peptide ratio, a relatively abundant hydrolyzed dilinked peptide reaction product was also observed in Figure 3.1 ($[M + H + 2(I\text{-}S_H)]^{3+}$; 12.8% relative abundance among all identified peptide species). A particular feature of this dilinked product, which distinguishes it from monolinked modifications, is its multistage MS/MS behavior. As predicted, a major neutral loss of 148 Da was observed from MS/MS of the $[M + H + 2(I\text{-}S_H)]^{3+}$ precursor ion (Figure 3.11A). However, the sequential fragmentation of a second 148-Da neutral species was also observed in this spectrum, indicating the presence of a second $I\text{-}S_H$ modification in this ion. MS^3 of the $[M+ H + I + (I\text{-}S_H)]^{3+}$ product ion from Figure 3.11A confirmed the presence of this additional modification (Figure 3.11B), while MS^4 of the $[M + H + 2I]^{3+}$ ion (Figure 3.11C) was employed to confirm the sites of modification to the N-terminal α-amino and lysine side chain ε-amino functional groups. Note that while peptide ions containing mono- or di- dead-end links do not provide information regarding the spatial relationships of target functional groups within the protein of interest, the identification of these products can yield useful information regarding the surface accessibility of these functional groups [170, 186, 244].

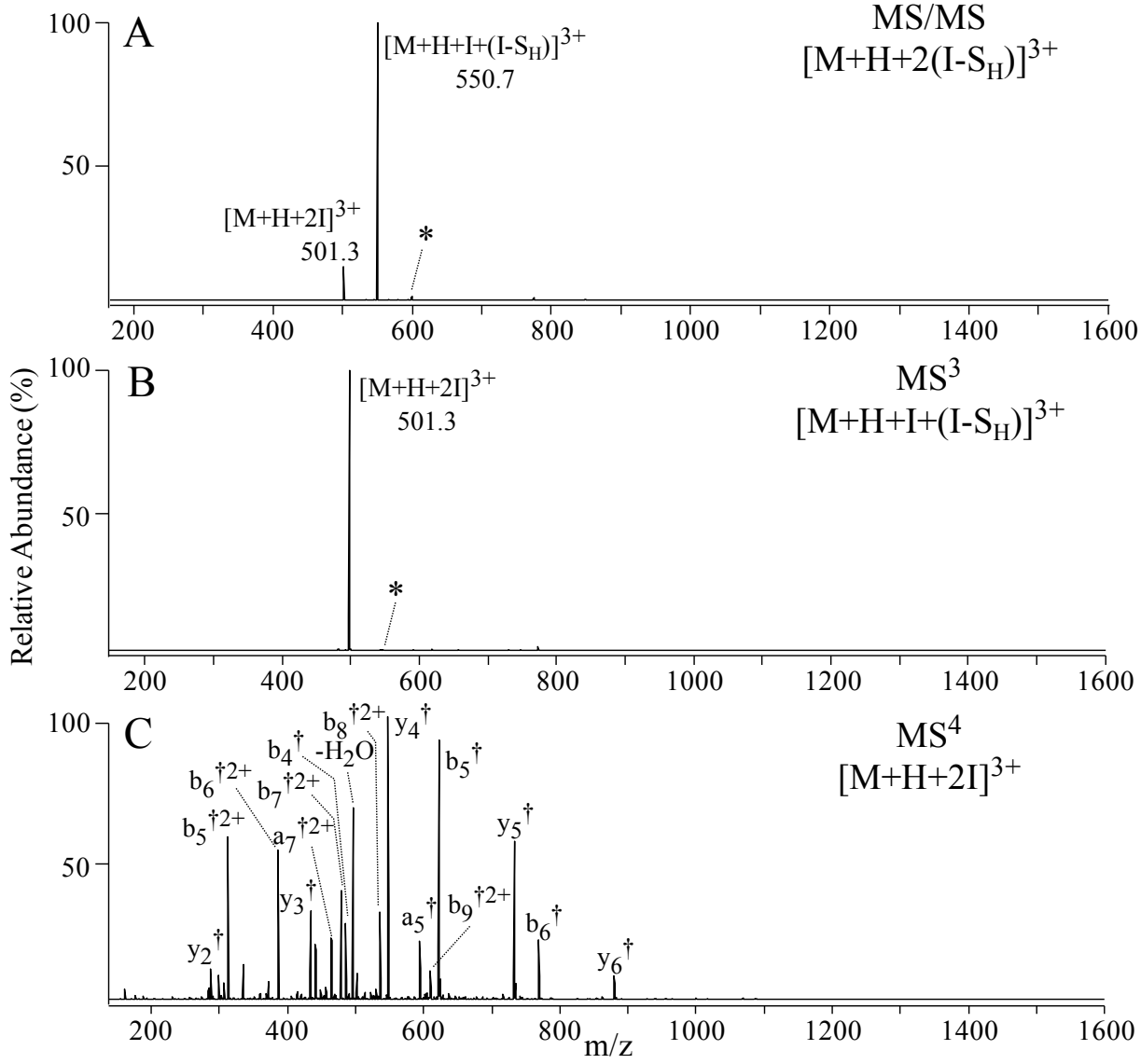

Figure 3.11 (A) CID MS/MS of the $[M + H + 2(I\text{-}S_H)]^{3+}$ precursor ion of pep_{VWK} containing a hydrolyzed ($I\text{-}S_H$) dilink from Figure 3.1. (B) MS^3 of the $[M + H + I + (I\text{-} S_H)]^{3+}$ product ion from panel A. The m/z of the precursor ions selected for dissociation in each spectrum are indicated by an asterisk. (C) MS^4 of the $[M + H + 2I]^{3+}$ product ion from panel B. A † indicates product ions containing an **I** modification.

3.3.3 Analysis of Intramolecular Cross-Linked Reaction Products

Consistent with the proposal outlined in Scheme 3.3C, MS/MS of the intramolecular cross-linked ($[M + H + (I-S)]^{2+}$) precursor ion from the pep_{VWK} peptide from Figure 3.1 resulted in initial cleavage of the crosslinker, followed by immediate further fragmentation within the peptide backbone, thereby allowing detailed structural information to be obtained by direct analysis of the MS/MS product ion spectrum (Figure 3.12). Similar results were also obtained following CID-MS/MS of the intramolecular cross-linked ($[M + H + (I-S)]^{2+}$) precursor ions observed following reaction of **1** with either substance P (Figure 3.13A) or the phosphoserine containing pep_{LpSR} peptide (Figure 3.13B).

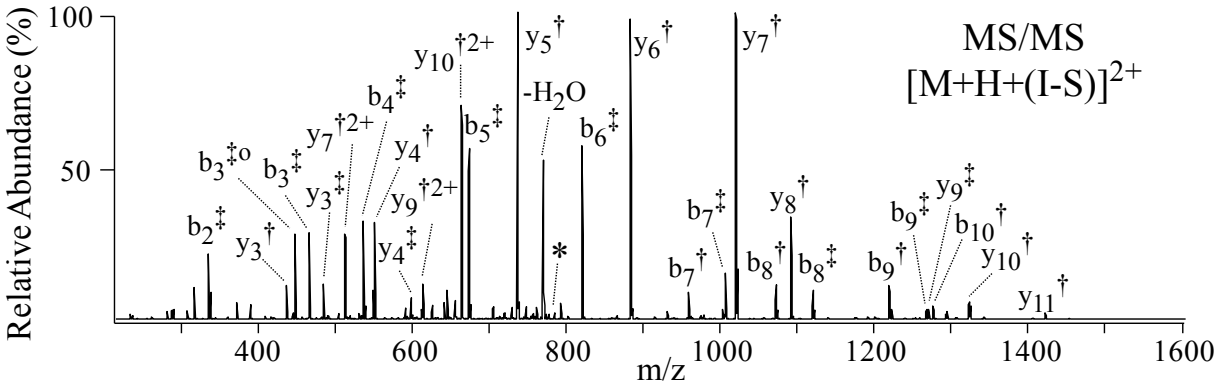

Figure 3.12 CID-MS/MS of the $[M + H + (I-S)]^{2+}$ precursor ion of pep_{VWK} containing an intramolecular cross-link from Figure 3.1. The m/z of the precursor ions selected for dissociation in the spectrum is indicated by an asterisk. A † indicates product ions containing an **I** modification. A ‡ indicates product ions containing an **S** modification.

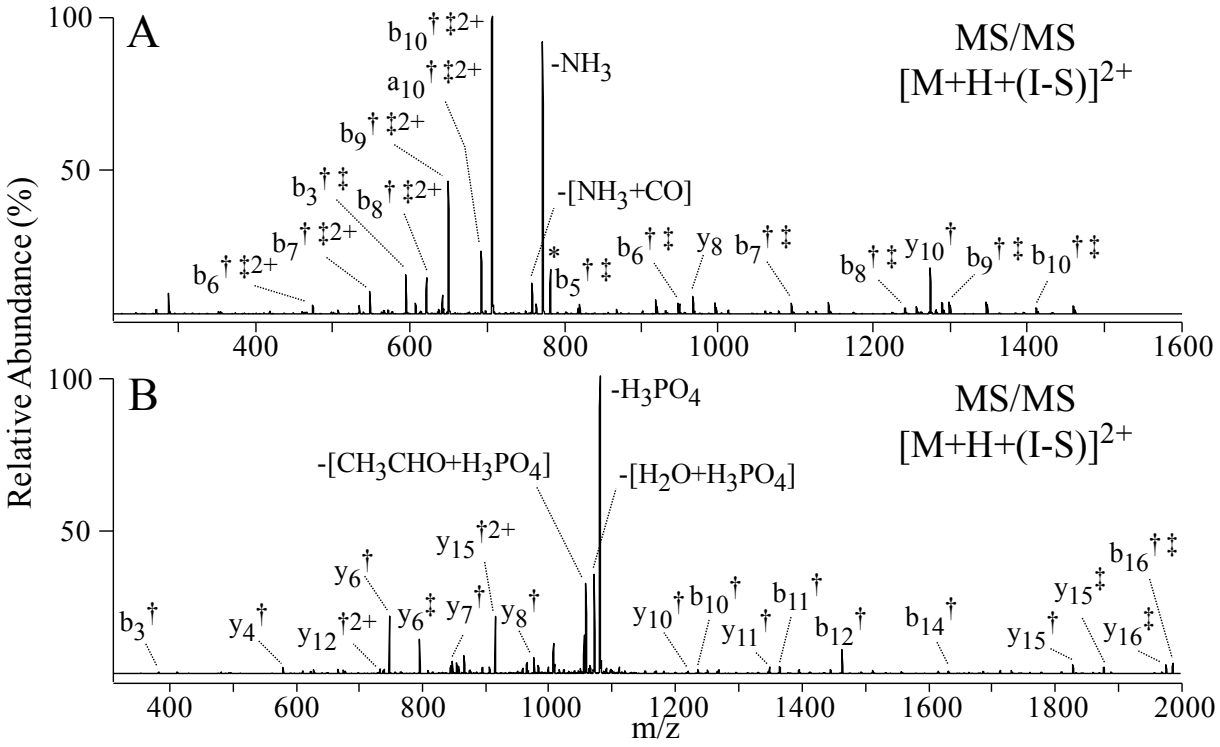

Figure 3.13 CID-MS/MS of the intramolecular cross-linked ($[M+H+(I-S)]^{2+}$) precursor ions formed following reaction of **1** with (A) substance P and (B) the phosphoserine containing pep_{LpSR} peptide.

3.4 Multiple Cross-Linking Reactions

Although the cross-linking reactions were carried out at a low cross-linker to peptide ratio (1.5:1), several peptide ions resulting from multiple cross-linking reactions, such as the hydrolyzed dilinked peptides discussed above, were observed. The identification of multiply cross-linked peptides involving intermolecular or intramolecular cross-links is a challenging task and seldomly reported [245].

3.4.1 Analysis of Intermolecular Cross-Linking Reaction Together with Dead-End Modification Products

Dissociation of an intermolecular cross-linked peptide product ion containing one dead-end modification involves fragmentation reactions taking place at two low energy cleavage sites. Similar to the dissociation of a heterodimeric intermolecular cross-link discussed above, two pairs of peptide product ions were observed upon CID-MS/MS analysis of $[2M+3H+(I-S)+(I-S_H)]^{5+}$ precursor ion resulting from cross-linking reaction of pep_{VWK}. Among them, one pair of peptide product ions corresponded to **I** or **S** modified pep_{VWK} and the other pair of peptide ions contained an **I** or **S** modification together with the modification from dead-end cross-link (intact (**I**-$\mathbf{S_H}$) or after neutral loss (**I**)) as shown in Figure 3.14. Also, a neutral loss of 148 Da was observed from dissociation of the precursor ion, similar to that of a dead-end cross-link, with the intermolecular cross-link remaining intact. The observation of multiple fragmentation pathways complicated the product ion spectra; however, they follow the same mechanism as proposed for the dissociation of single cross-link bond shown in Scheme 3.3 and could be easily identified.

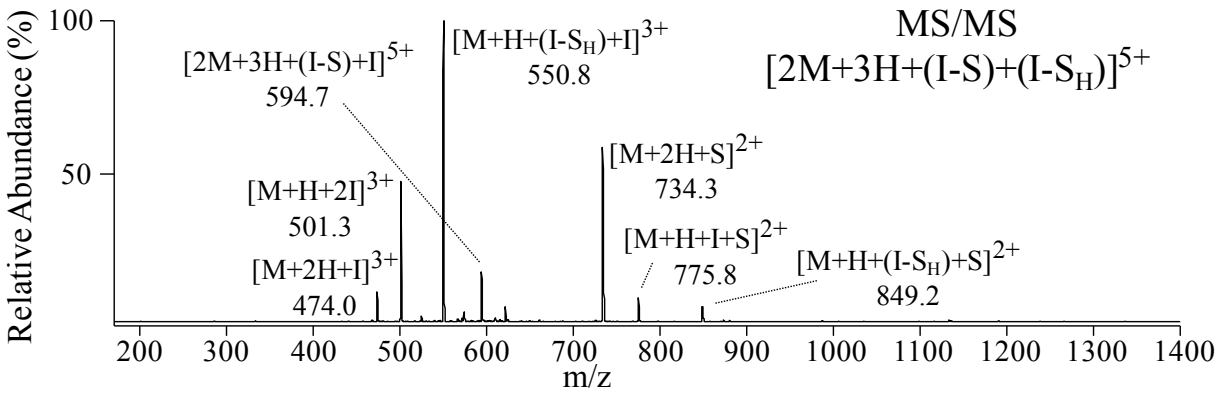

Figure 3.14 CID-MS/MS of the intermolecular cross-linked pep_{VWK} containing one hydrolyzed monolink ($[2M+3H+(I-S)+(I-S_H)]^{5+}$) precursor ion formed following reaction of **1**.

3.4.2 Analysis of Intramolecular Cross-Linking Reaction Together with Dead-End Modification Products

The model peptide insulin-like growth factor I (57-70) (pep_{IGF}, ALLETYCATPAKSE) is expected to contain two reactive sites towards the NHS-ester groups of cross-linking reagent **1**, i.e., the α-amino group on the N-terminus and the ε-amino group on the lysine side chain. However, a peptide product was observed corresponding to the introduction of an intramolecular cross-link and a hydrolyzed monolink, indicating the presence of a third reactive functional group towards **1**. Consistent with the proposed mechanism described in Scheme 3.3B and C, MS/MS of the intramolecular and dead-end cross-linked ($[M+(I-S)+(I-S_H)]^{2+}$) precursor ion from the pep_{IGF} resulted in the neutral loss of 148 Da from the hydrolyzed mono-link modification and initial cleavage of the intramolecular-cross-linker (Figure 3.15A). The neutral loss product ions were isolated then subjected to further dissociation by MS^3, indicating that cross-linking had

occurred not only with the N-terminus and lysine amine groups, but also with the Cys_7 thiol group, based on the observation of $b_6^{\dagger}$, $b_7^{\dagger\ddagger}$ and $y_7^{\dagger}$, $y_8^{\dagger\ddagger}$ ions (Figure 3.15B).

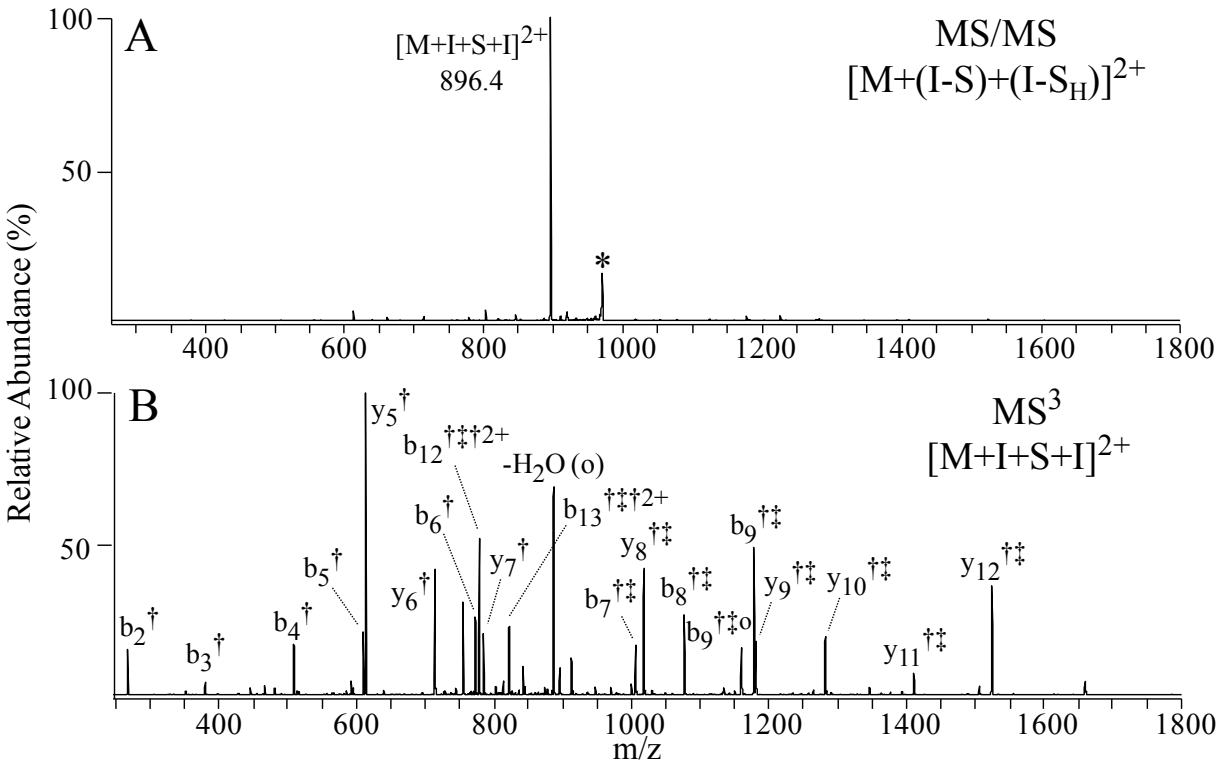

Figure 3.15 (A) CID-MS/MS and (B) CID-MS^3 of the intramolecular cross-linked pep_{IGF} containing one hydrolyzed monolink ($[M+(I-S)+(I-S_H)]^{2+}$) precursor ion formed following reaction of **1.** The m/z of the precursor ions selected for dissociation in each spectrum is indicated by an asterisk. A † indicates product ions containing an **I** modification. A ‡ indicates product ions containing an **S** modification.

It has been reported recently by several groups that NHS esters also show significant reactivity towards serine, tyrosine and threonine hydroxyl groups as well as histidine imidazole groups [246-250]. Additional effects such as local pH and hydrogen bonding are demonstrated to influence the reactivity of the amino acid side chains. Therefore, the reactivity of NHS ester group of cross-linker **1** towards cysteine is probably due to the nucleophilic character of thiol

group under the conditions employed (phosphate buffered saline, pH = 7.5). Thus, in a more complex system of protein cross-linking reactions, a much richer pattern of reactivity is expected as primary amines (N-terminus and Lys residues) are not the only sites that react with NHS esters.

3.5 Effects of Neighboring Group Participation Reactions on the Gas Phase Fragmentation of Cross-Linked Peptides

Due to the symmetrical structure of the cross-linking reagent **1**, two C-S bonds adjacent to a fixed charge site are expected to have equal possibilities for preferential cleavage from an intra-molecular or heterodimeric inter-molecular cross-linked peptide under low energy CID-MS/MS conditions. However, from analysis of the spectrum in Figure 3.12, it appeared that **I** modifications (labeled in the spectra with a †) were mainly located on y-type product ions while **S** modifications (labeled in the spectra with a ‡) were mainly located on the b-type product ions. These data indicate that the two C-S bonds do not have identical cleavage efficiencies. We hypothesize that this is due to the individual intramolecular "solvation" environments of the nucleophilic α-amide bond and ε-amide bond that are responsible for the sulfonium ion bond cleavage reactions that subsequently affects the nucleophilic reactivity of these groups. Below, more detailed insights into this observation will be discussed.

3.5.1 Gas Phase Fragmentation Behavior of Dead-End Cross-Linked Reaction Products

Cleavage of dead-end cross-links are predicted to preferentially take place at the C-S bond closest to the peptide chain, as shown in Scheme 3.3B, due to the greater nucleophilic strength of the amide nitrogen compared to an acid or ester oxygen on the terminal end of the cross-link. However, dominant product ions corresponding to cleavage on the "outer" C-S bond involving nucleophilic attack from the acid oxygen were also observed from hydrolyzed monolinked peptide ions, for particular charge states. For example, the product ion spectra from doubly and singly charged hydrolyzed monolink of pep_{GDR} revealed a significant change of major product ions from **I** to **S** modified peptides (see Figure 3.9A and B). In addition, the **S** modified pep_{GDR} product ion was observed to retain the same charge state as the precursor ion, suggesting tetrahydropyran-2-one was lost as a neutral species during CID-MS/MS. A similar result was also observed upon CID-MS/MS analysis of the hydrolyzed monolink reaction products of neurotensin from the comparison of triply and doubly charged precursor ions (Figure 3.16). The observation of the preferential cleavage shifting from the "inner" to the "outer" C-S bond with decreasing charge states of the hydrolyzed monolinked peptide ions is probably due to the change of proton mobility status of the selected precursor ion [14].

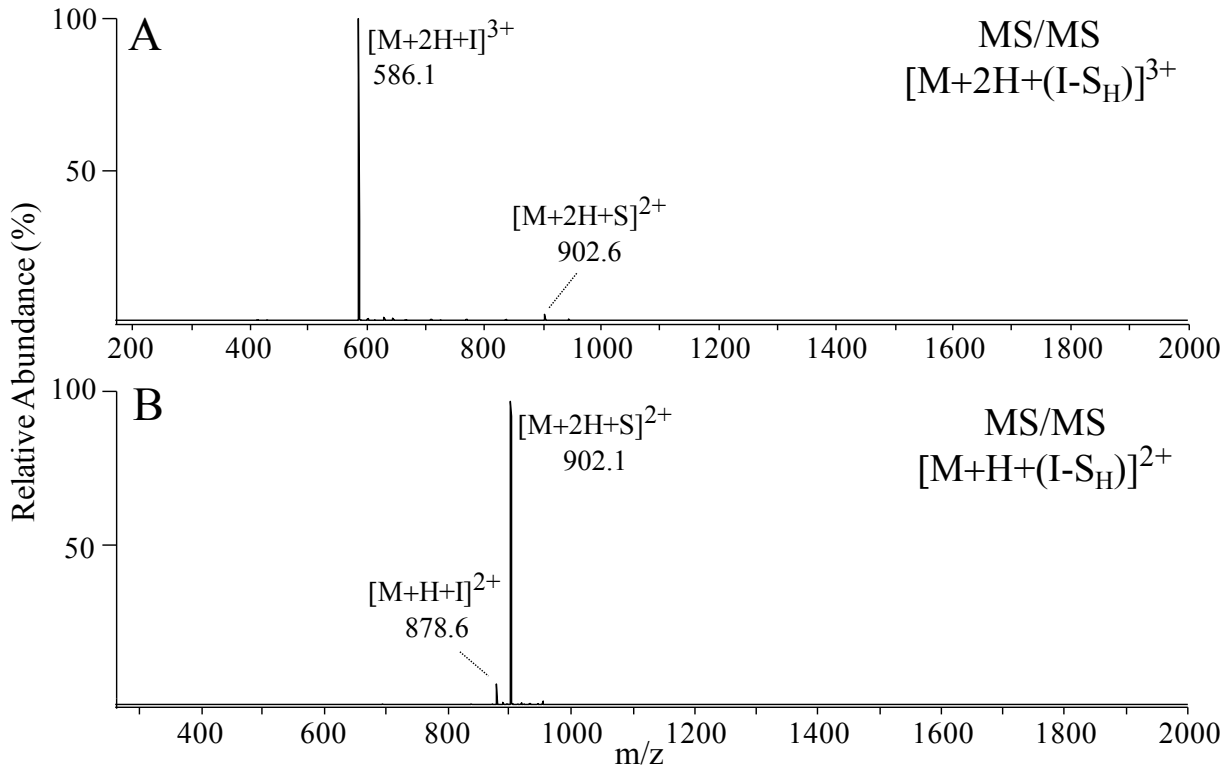

Figure 3.16 CID-MS/MS product ion spectra of (A) the $[M+2H+(I-S_H)]^{3+}$ and (B) the $[M+H+(I-S_H)]^{2+}$ precursor ions from the hydrolyzed mono-linked product formed by reaction of reagent **1** with neurotensin.

It is widely acknowledged that when ionizing protons are strongly "sequestered" at the initial site of protonation (i.e., "non-mobile" proton condition), preferential fragmentation at the C-terminal side of an aspartic acid residue may occur [251-253], resulting from a "charge-remote" process involving proton transfer from the aspartyl side chain to the adjacent amide bond [254]. Similarly, the hydrolyzed monolink modification contains a carboxyl group, which may undergo a proton transfer process if there is a basic group present in the peptide that is eagerly "looking for" a proton. Note that for singly charged pep_{GDR} and doubly charged neurotensin containing a hydrolyzed monolink modification, the arginine residue(s) present in both peptide ions do not all

contain ionizing protons. Thus the labile proton in the carboxyl group residing on hydrolyzed monolink may be transferred to the side chain of an arginine residue. The resultant carboxylate group is a better nucleophile than the amide nitrogen, which then initiates the nucleophilic attack responsible for the cleavage on the "outer" C-S bond.

This competing fragmentation pathway may potentially be blocked by derivatizing the carboxyl group of the hydrolyzed monolink modification. To determine whether the observation of gas-phase cleavage of the "outer" C-S bond requires the carboxyl group on the hydrolyzed monolink, peptides were esterified with methanolic HCl as described in Chapter Four. Since the C-terminal carboxyl group is esterified as well, the esterification experiment was applied to neurotensin before and after the cross-linking reaction, thus the role of carboxyl group within the hydrolyzed monolink was able to be differentiated from that on the C-terminus. As shown in Figure 3.17A, dissociation of the doubly charged precursor ion from the hydrolyzed monolinked product formed by a cross-linking reaction of methyl esterified neurotensin resulted in the dominant **S** modified product peptide ion. This is consistent with the fragmentation behavior of the unesterified counterpart (Figure 3.16B). However, when the carboxyl group within the hydrolyzed monolink was modified, the **I** modified neurotensin became the exclusive product ion, indicating a different fragmentation pathway upon esterification of the carboxyl group of the hydrolyzed monolink from doubly charged monolinked neurotensin.

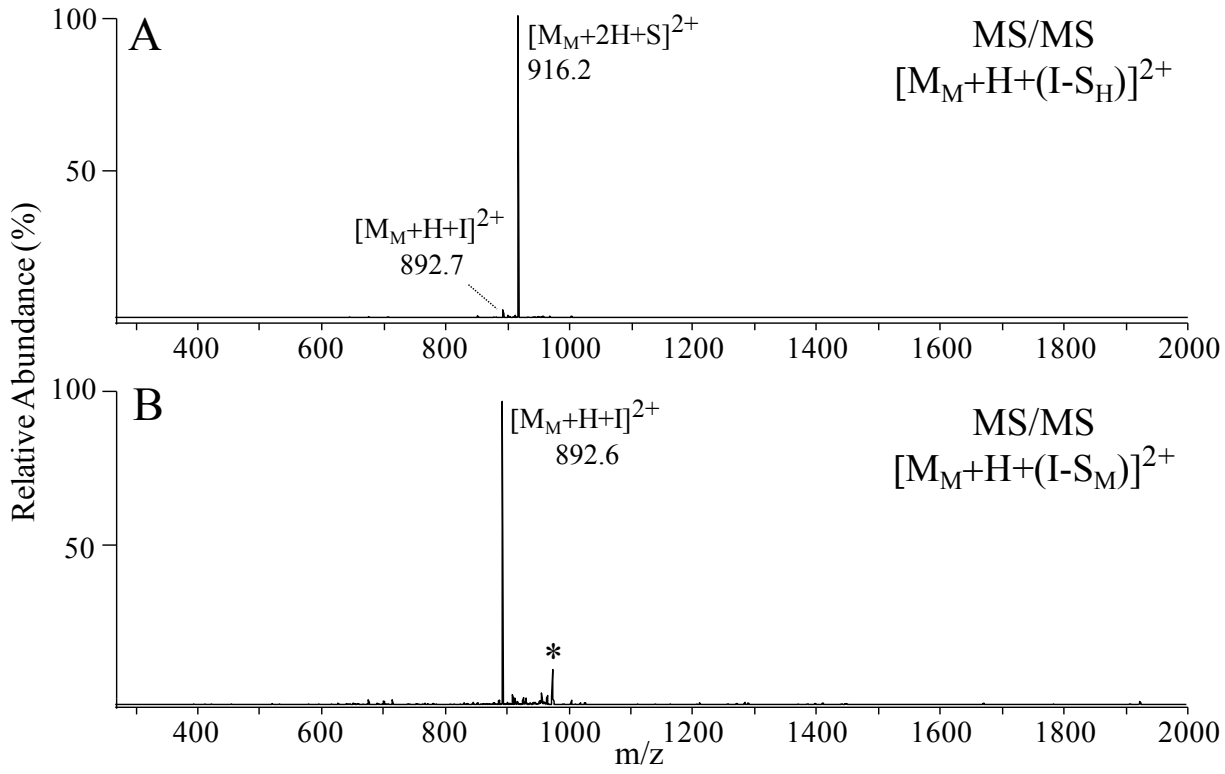

Figure 3.17 CID-MS/MS product ion spectra of (A) the $[M_M+H+(I-S_H)]^{2+}$ and (B) the $[M_M+H+(I-S_M)]^{2+}$ precursor ions from the hydrolyzed mono-linked product formed by reaction of reagent **1** with neurotensin. A subscript "M" indicates methyl esterification of carboxyl group. The m/z of the precursor ion selected for dissociation is indicated by an asterisk.

The above results clearly indicate that the cleavage at the "outer" C-S bond within the hydrolyzed monolink involves the carboxyl group of the hydrolyzed cross-link. A mechanism for the gas-phase cleavage of the "outer" C-S bond adjacent to the fixed charge is illustrated in Scheme 3.4.

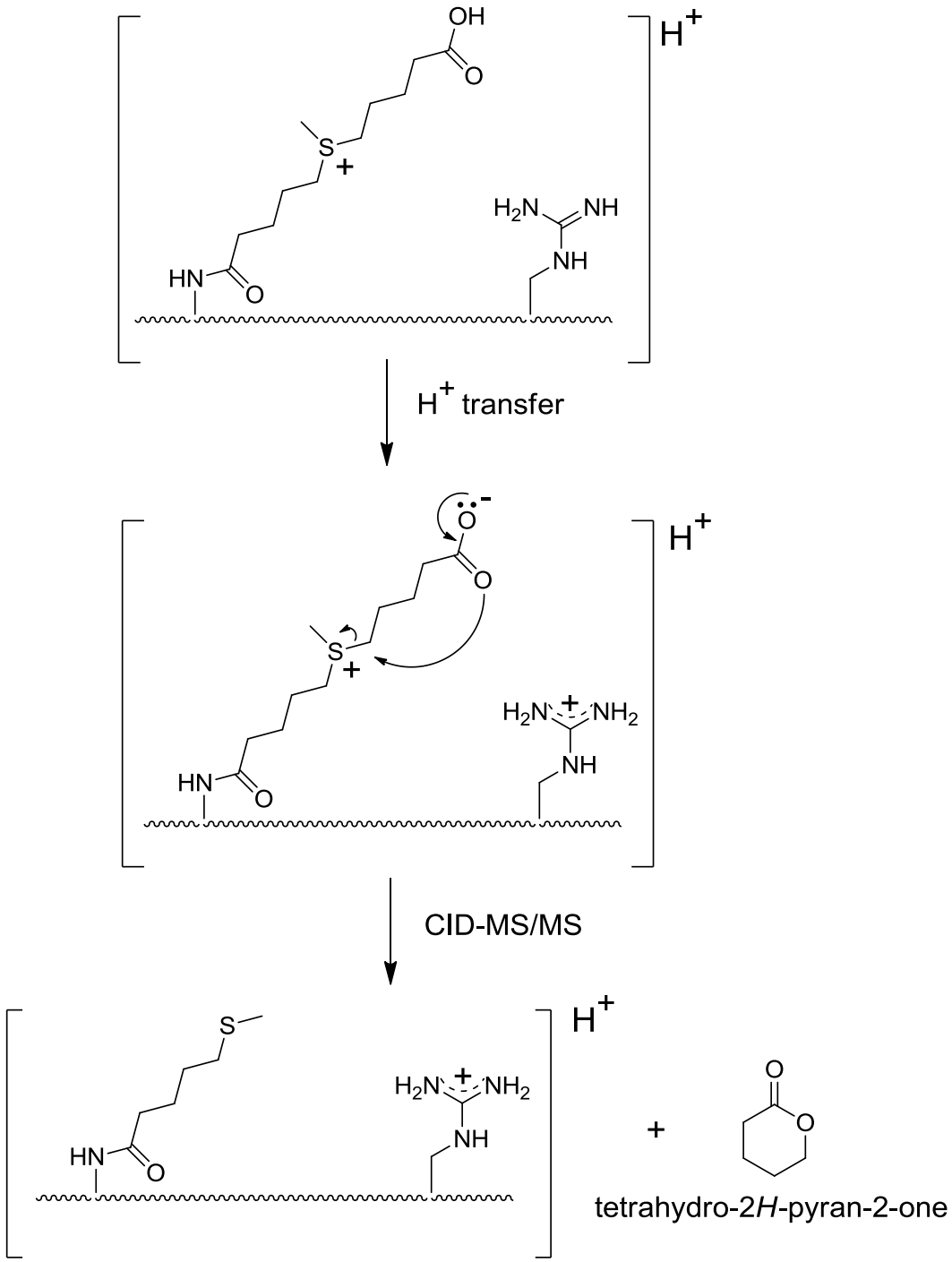

Scheme 3.4 Proposed mechanism for the gas phase fragmentation at the "outer" C-S bond in a hydrolyzed mono-linked peptide.

In some circumstances, dominant fragmentation at the "outer" C-S bond may also be observed from hydrolyzed mono-linked peptides even when the number of ionizing protons is no less than that of basic residues (i.e., under mobile or partially mobile proton conditions). A notable example of such behavior was observed from the fragmentation of triply charged hydrolyzed mono-linked angiotensin II. Figure 3.18A shows a representative spectrum. In order to estimate the extent to which C-S bond fragmentation had occurred, the relative abundances of **I** and **S** modified angiotensin II product ions were measured. Specificity in the localization of cleavage between the two labile C-S bonds indicates the relative nucleophilic strength of the amide nitrogen or carboxylate oxygen that initiates the nucleophilic attack. For the triply charged hydrolyzed mono-linked angiotensin II, the product ion with an **I** modification only accounts for 19.5±0.6 % of the product ion abundance; a result from triplicate experiments. This indicates the nucleophilic strength of the amide nitrogen which initiates the formation of the **I** modified product ion was decreased compared to that of triply charged hydrolyzed mono-linked neurotensin. In principle, the individual intramolecular "solvation" environment, such as hydrogen bonding or other noncovalent interactions involving acidic or basic residues, can influence the activity of nucleophiles due to the distribution of electron density. We now take an insight into the possible role of the acidic and basic residues present in angiotensin II in the fragmentation of the triply charged hydrolyzed mono-link. Methyl esterification of carboxyl groups present in the angiotensin II peptide chain (Figure 3.18B) or together with the carboxyl group on the cross-linker dead-end (Figure 3.18C) was observed to yield similar abundances of the **I** modified product ion (19.4±3.9 % and 18.4±0.2 % respectively), compared to the non-esterified species. However, when the basicity of the imidazolyl group of the histidine residue was decreased via modification with diethyl pyrocarbonate (DEPC), the relative abundance of

the **I** modified product ion increased to 46.8±2.7 %, suggesting that the "solvation" environment surrounding the cross-linker amide nitrogen was moderated upon modification of the basic imidazolyl group of the histidine.

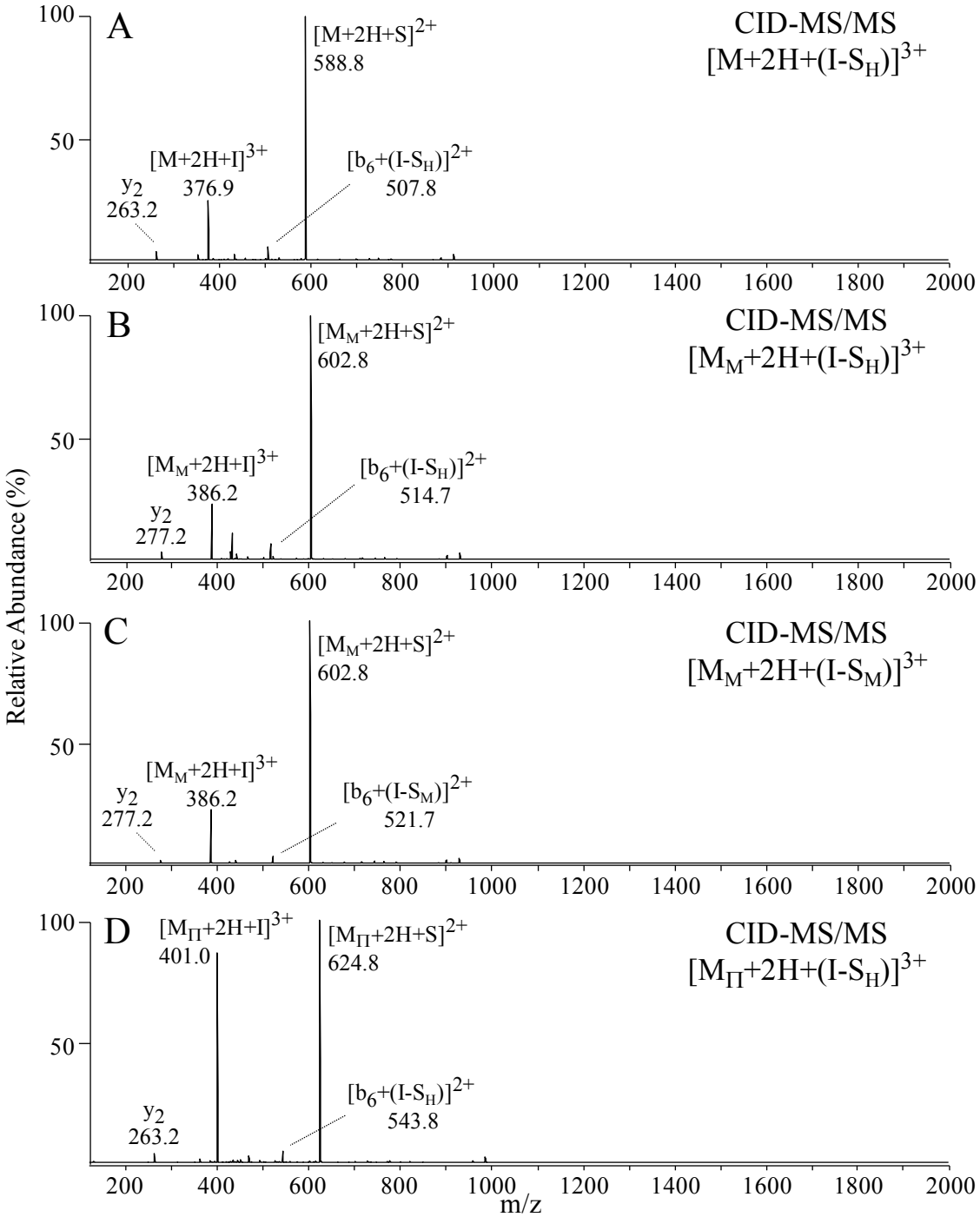

Figure 3.18 Representative CID-MS/MS product ion spectra of (A) the $[M+2H+(I\text{-}S_H)]^{3+}$, (B) the $[M_M+2H+(I\text{-}S_H)]^{3+}$, (C) the $[M_M+2H+(I\text{-}S_M)]^{3+}$ and (D) the $[M_\Pi+2H+(I\text{-}S_H)]^{3+}$ precursor ions from the hydrolyzed mono-linked product formed by reaction of reagent **1** with angiotensin II. A subscript "M" indicates methyl esterification of carboxyl group. A subscript "Π" indicates DEPC modification on imidazolyl group of histidine residue.

A further look into the role of the histidine residue to affect the nucleophilic strength of peptide-linker amide bond was taken by investigating the fragmentation behavior of the doubly charged hydrolyzed mono-linked angiotensin II. As the representative product ion spectrum in Figure 3.19A shows, the **I** modified peptide is still the minor product, accounting for 35.5±1.1 % of total C-S bond cleavage. The major product ion, **S** modified angiotensin II, retained the same charge state as the precursor ion, suggesting that proton transfer had occurred from the carboxyl group of the cross-linker dead-end to the peptide during the fragmentation process. As previously mentioned, the observation of proton transfer is probably due to the lack of ionizing protons for the basic residues present in the peptide. For doubly charged dead-end cross-linked angiotensin II, which contains one arginine and one histidine residue, however there is only one ionizing proton available. Based on the bascicity of arginine and histidine, this ionizing proton is most possibly sequestered by the arginine guanidino group. Thus it is suggested that the proton affinity of the basic imidazolyl group of histidine is the driving force responsible for the occurrence of intramolecular proton transfer. Consistent with this proposal, an average of 82.5±2.0 % **I** modified angiotensin II was observed upon DEPC modification of the histidine residue (a representative spectrum is shown in Figure 3.19B). These results indicate that the cleavage efficiencies of two the C-S bonds could be altered by controlling the individual "solvation" environment.

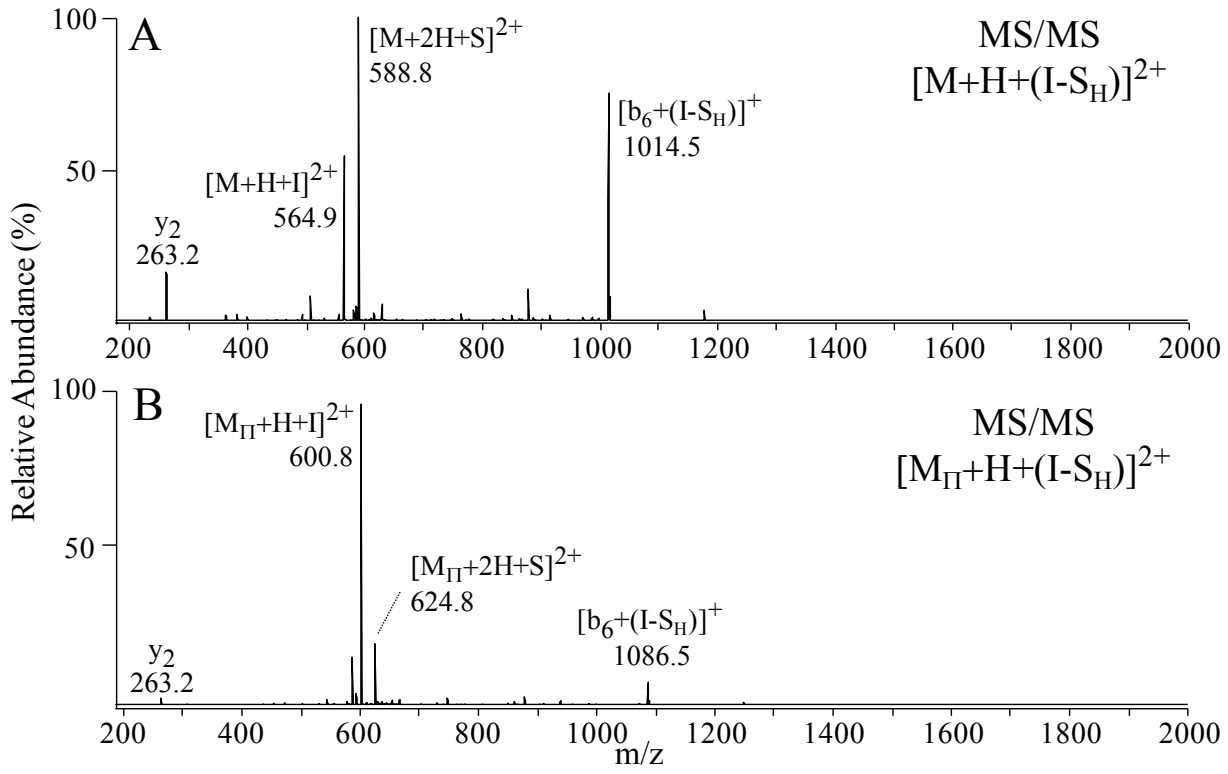

Figure 3.19 Representative CID-MS/MS product ion spectra of (A) the $[M+H+(I-S_H)]^{2+}$, and (B) the $[M_\Pi+H+(I-S_H)]^{2+}$ precursor ions from the hydrolyzed mono-linked product formed by reaction of reagent **1** with angiotensin II. A subscript "Π" indicates DEPC modification on imidazolyl group of histidine residue.

3.5.2 Gas Phase Fragmentation Behavior of an Intermolecular Cross-Linked Reaction Product

The dissociation of heterodimeric intermolecular cross-linked neurotensin (α) and angiotensin II (β) was investigated to determine if similar "solvation" conditions affected the fragmentation pathways as described above for hydrolyzed mono-linked peptides. The product ion spectrum of the $[\alpha+\beta+3H+(I-S)]^{4+}$ ion was shown in Figure 3.4D. The product ions corresponding to cleavage of C-S bond at the neurotensin side (**I** modified neorotensin and **S**

modified angiotensin II) (α C-S bond) are noticeably more abundant than those formed from cleavage at the C-S bond at the angiotensin II side (β C-S bond), indicating the cross-linker amide nitrogen at the neurotensin side (α amide nitrogen) has a greater nucleophilic strength than that at the angiotensin II side (β amide nitrogen). As discussed above for the fragmentation of hydrolyzed mono-linked angiotensin II, the nucleophilic strength of the β amide nitrogen is probably weakened due to the individual "solvation" environment involving the imidazolyl group of the histidine residue. In order to determine whether the histidine residue affects the fragmentation behavior of the quadruply charged heterodimeric cross-link, the relative abundance of product ions generated from cleavage at the C-S bonds was calculated before and after DEPC modification (representative spectra are shown in Figure 3.20). The relative abundance of product ions upon cleavage at the β C-S bond accounted for 37.0±1.6 % for the native heterodimeric cross-link and increased to 64.2±0.8 % following DEPC modification of the histidine residue contained in the β peptide, angiotensin II. The significant difference between the fragmentation efficiency of the β C-S bond demonstrates the role of the histidine residue and nucleophilic strength of the β amide nitrogen, which is consistent with the results obtained from the hydrolyzed mono-linked angiotensin II.

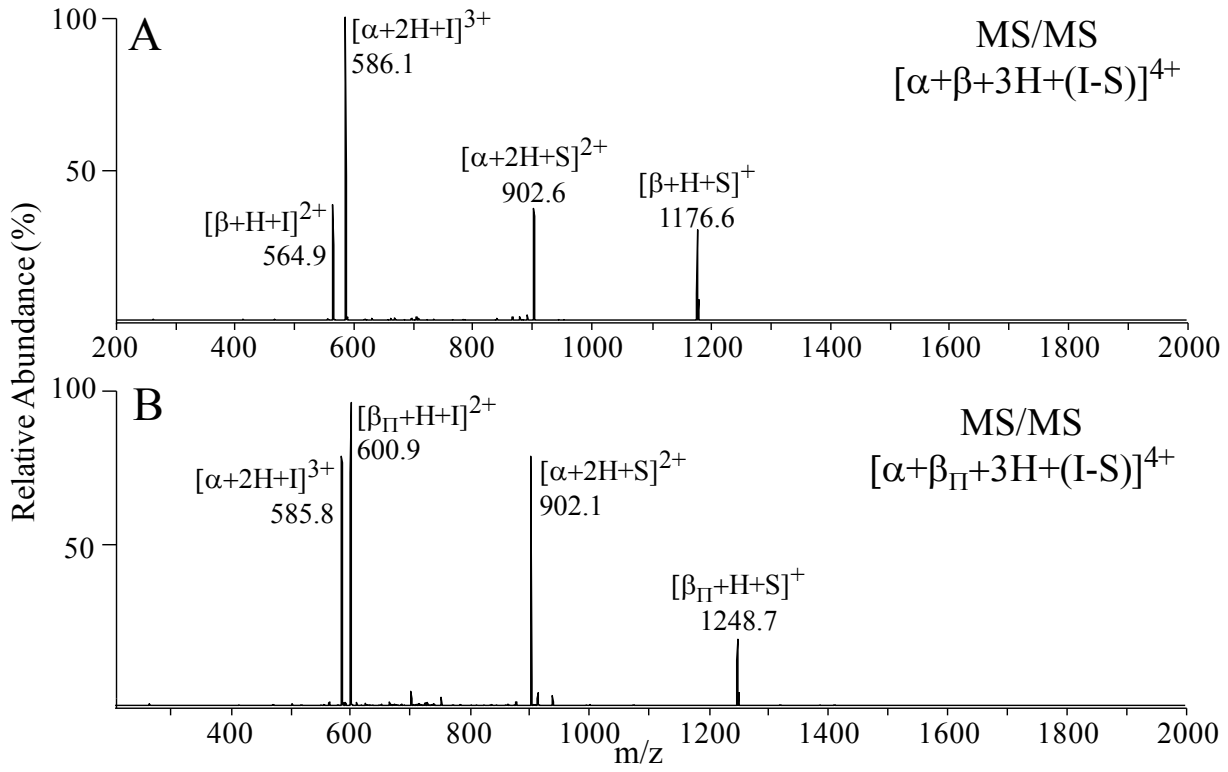

Figure 3.20 Representative CID-MS/MS product ion spectra of (A) the $[\alpha + \beta + 3H + (I\text{-}S)]^{4+}$, and (B) the $[\alpha + \beta_{\Pi} + 3H + (I\text{-}S)]^{4+}$ precursor ions of heterodimeric intermolecular cross-links containing of neurotensin (α) and angiotensin II (β) formed by reaction of reagent **1**. A subscript "Π" indicates DEPC modification on imidazolyl group of histidine residue.

These findings indicate that the individual "solvation" environment, which is related to the charge state and amino acid composition of peptide ions, affects the nucleophilic strength of the amide or acid/ester bond that is responsible for the sulfonium bond cleavage reactions. This "solvation" can occur due to noncovalent interactions such as hydrogen bonding which involve, most probably, acidic or basic amino acid residues. Based on the fact that the fragmentation behavior of sulfonium bonds was changed by blocking particular functional groups, it provides a tool to control the gas phase sulfonium bond cleavage by altering the "solvation" environment. Although there is a difference in fragmentation efficiency of the two C-S bonds adjacent to the

sulfonium ion, fragmentation of the sulfonium ion is an energetically favorable process compared to those for peptide backbone and side chain cleavage reactions. Most importantly, this fact is not changed with the peptide charge state and amino acid composition.

3.6 Summary and Future Aspects

The results presented above illustrate that CID-MS/MS of cross-linked peptides containing a fixed charge sulfonium ion can be employed to effectively identify cross-linked peptides from unmodified peptides, via recognition of their distinct fragmentation patterns, as well as to distinguish between the various types of cross-linked products (i.e., intra, inter, and dead-end) that may be formed from a cross-linking reaction. Homodimeric intermolecular cross-linked peptides are readily identified by the formation of a single pair of characteristic product ions, while heterodimeric intermolecular cross-linked peptides are identified by the formation of two pairs of product ions. Peptides containing intact or hydrolyzed dead-end cross-links are identified based on the observation of their characteristic neutral losses. MS^3 of these initial products can be used to provide information required for characterization of the peptide sequences and localization of the modification site(s) involved in the cross-linking reactions. MS/MS of intramolecular cross-linked peptides results in initial cleavage of the cross-linker, followed by immediate further fragmentation of the peptide backbone, thereby allowing detailed structural information to be obtained by direct analysis of the MS/MS product ion spectrum. Multiple cross-linking reaction products, albeit containing multiple low energy gas phase cleavable sites which complicates MS/MS product ion spectrum, are able to be identified based on distinct fragmentation behaviors of single cross-linking reaction products. The competition between two

labile bonds adjacent to sulfonium ion suggests that the two C-S bonds do not have identical cleavage efficiencies. This is probably due to the individual intramolecular "solvation" environments of amide or acid/ester bond; that are responsible for sulfonium ion bond cleavage. Preliminary experiments indicate that the modification of the "solvation" environment by blocking a particular functional group within the cross-linked peptide may provide a tool for controlling the competition between two low energy gas phase cleavable sites of the sulfonium ion.

The specificity of these gas-phase fragmentation reactions, along with the solubility and stability of the sulfonium ion containing cross-linking reagent under aqueous conditions, suggests that this reagent holds great promise for the mass spectrometry based structural analysis of large proteins or multiprotein assemblies in future studies. In addition, the concepts of complementary techniques introduced recently (see below) could also be integrated into this sulfonium ion containing cross-linking reagent, providing more opportunities for discovering protein structure and protein-protein interactions. For example, new types of reactive groups within cross-linking reagents, such as 1-hydroxy-7-azabenzotriazole show better reactivities and faster reaction rates compared to commonly used NHS esters [182]. By introducing this type of reactive group into a sulfonium ion containing cross-linking reagent, kinetic studies of protein complexes might be attempted. In another aspect, the cross-linking reaction strategy may be improved for targeting low-reactivity functional groups within the protein of interest. Intra- and inter-molecular cross-link products are usually of most relevance for providing information regarding spatial relationships of target functional groups. However, the variable and uneven nucleophilic reactivity of these groups typically limits the diversity of intra- or inter-protein cross-linking reactions. A recent study by the Gibson group employing partial acetylation of the

most reactive lysines prior to cross-linking was shown to improve the diversity of the cross-linking reactions effectively [244]. This result suggests that by modifying the reactive "hot-spots" that dominate the cross-linking reaction profile without disturbing protein native structure, more distance constraints required for reliable protein structural modeling could be obtained. Finally, it is also worth considering the strategies for relative quantitative measurement of protein structures and protein interactions [217]. Isotope labels can be incorporated into cross-linking reagent **1** using the currently employed synthesis route, by using iodomethane-d_3 as the final alkylating reagent. Thus chemical cross-linking can be carried out with two different states of protein assembly by using "light" and "heavy" labeled cross-linking reagents. A quantitative chemical cross-linking strategy would be useful for visualization of protein structural changes associated with biological perturbations which may enable better understanding of protein functions. In summary, with its unique gas-phase fragmentation behavior and continued development, this sulfonium ion containing cross-linking reagent holds great potential for mass spectrometry based structural analysis of large proteins and protein-protein complexes.

CHAPTER FOUR

EXPERIMENTAL METHODS FOR CHAPTER THREE

4.1 Materials

All chemicals were analytical reagent (AR), or of a comparable or higher grade and used without further purification. *N,N*′-Dicyclohexylcarbodiimide (DCC) was purchased from Fluka (Switzerland). 5-Bromovaleric acid, thiourea and diethyl pyrocarbonate (DEPC) were from Sigma-Aldrich (St. Louis, MO, USA). N-hydroxysuccinimide (NHS) was purchased from Pierce (Rockford, IL, USA). Sodium hydroxide, sodium phosphate dibasic (crystal), potassium phosphate monobasic (crystal), dimethyl sulfate and N,N'-dimethyl formamide (DMF) were purchased from Spectrum Chemicals (Gardena, CA, USA). DMF was dried over 3-Å molecular sieves (Spectrum Chemicals) and filtered prior to use. Sodium chloride, sodium sulfate anhydrous, hydrochloric acid and ethyl acetate were purchased from Columbus Chemical Industries (Columbus, WI, USA). Potassium chloride, sulfuric acid and ethyl ether were purchased from Jade Scientific (Canton, MI, USA). Glacial acetic acid, dichloromethane, chloroform, methanol (anhydrous) and ethanol were purchased from Mallinckrodt Chemicals (Phillipsburg, NJ, USA). Iodomethane was purchased from EMD Chemicals (San Diego, CA, USA), and acetonitrile was from Fisher Scientific (Hampton, NH, USA).

The synthetic peptide VTMAHFWNFGK (pep_{VWK}) and GAILDGAILR (pep_{GDR}) were obtained from Auspep (Parkville, Australia). Neurotensin, angiotensin II, and [Glu^1]-

fibrinopeptide B were purchased from Sigma-Aldrich (St. Louis, MO, USA). Insulin-like growth factor I (57-70) was purchased from American Peptide Company (Sunnyvale, CA). Substance P was obtained from Bachem (Torrance, CA). The phosphoserine containing peptide LSVPTpSDEEDEVPAPKPR (pep_{LpSR}) was synthesized by Sigma-Genosys (The Woodlands, TX). All peptides were used without further purification.

Water was deionized and purified by a Barnstead nanopure diamond purification system (Dubuque, Iowa, USA). All reactions were performed in oven dried glassware.

^{1}H-NMR spectra were obtained on Varian Inova 300 MHz or 500 MHz instruments and are reported in parts per million (ppm) relative to the solvents resonances (δ), with coupling constants (*J*) in Hertz (Hz).

4.2 Synthesis of Ionic Cross-Linking Reagent *S*-Methyl 5,5′-Thiodipentanoylhydroxysuccinimide (1)

Synthesis of the ionic cross-linking reagents *S*-Methyl 5,5′-dipentanoylhydroxysuccinimide **(1;** *S*-Methyl 5,5′-thiodipentanoylhydroxysuccinimide iodide **1′** or *S*-Methyl 5,5′-thiodipentanoylhydroxysuccinimide methylsulfate **1′′**) was achieved by initial preparation of 5-mercaptopentanoic acid (**2**), followed by alkylation with 5-bromovaleric acid. Then, esterification of the resultant 5,5′-thiodipentanoic acid (**3**) using NHS yielded 5,5′-thiodipentanoylhydroxysuccinimide (**4**). Finally, alkylation of 4 with either iodomethane or dimethyl sulfate provided the target molecule (Scheme 4.1). A detailed description of the synthesis of **1′** and **1′′** are provided below.

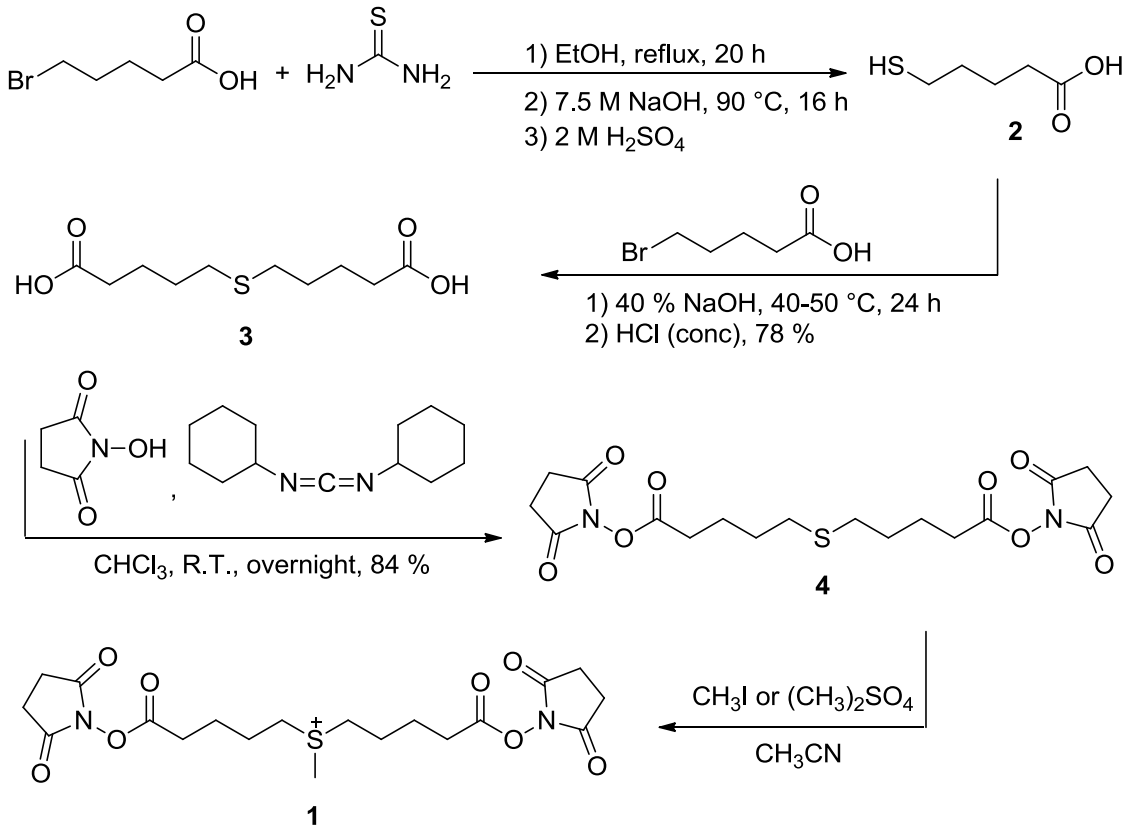

Scheme 4.1 Synthesis of ionic cross-linking reagent *S*-Methyl 5,5′-dipentanoylhydroxysuccinimide (**1**).

4.2.1 Synthesis of 5-Mercaptopentanoic Acid (2)

Using a procedure adapted from Jessing et al. [255], 5-bromovaleric acid (2.2 g, 12.1 mmol) and thiourea (1.4 g, 18.4 mmol) were dissolved in ethanol (25 ml) and refluxed for 20 h. The solvent was removed under reduced pressure and 7.5 M NaOH (aq) (25 ml, 187 mmol) was added. The mixture was stirred for an additional 16 h at 90 °C. Then with cooling on an ice bath, 2M H_2SO_4 (aq) was added slowly under stirring to pH 1 and the product was extracted twice with dichloromethane (2×100 mL). The combined extracts were then dried with anhydrous

Na_2SO_4 and concentrated by rotary evaporation to give the title acid (**2**) as a colorless oil in quantitative yield. The product was then used without further purification. ^{1}H NMR (300 MHz, $CDCl_3$): δ 1.32(t, 1H, *J* = 7.8 Hz), 1.59-1.73 (m, 4H), 2.32 (t, 2H, *J* = 7.5 Hz), 2.49 (q, 2H, *J* = 6.9 Hz), 8.95 (s, broad, 1H); ^{13}C NMR (75 MHz, $CDCl_3$): δ 23.21, 24.06, 33.07, 33.35 and 179.49.

The characterization by ESI-MS and CID-MS/MS analysis is shown in Figure 4.1A and B, respectively. The gas-phase fragmentation behavior of the deprotonated $[M-H]^-$ precursor ion at m/z 133 is consistent with the expected structure, yielding a product ion at m/z 99 via the neutral loss of H_2S, as displayed in Scheme 4.2.

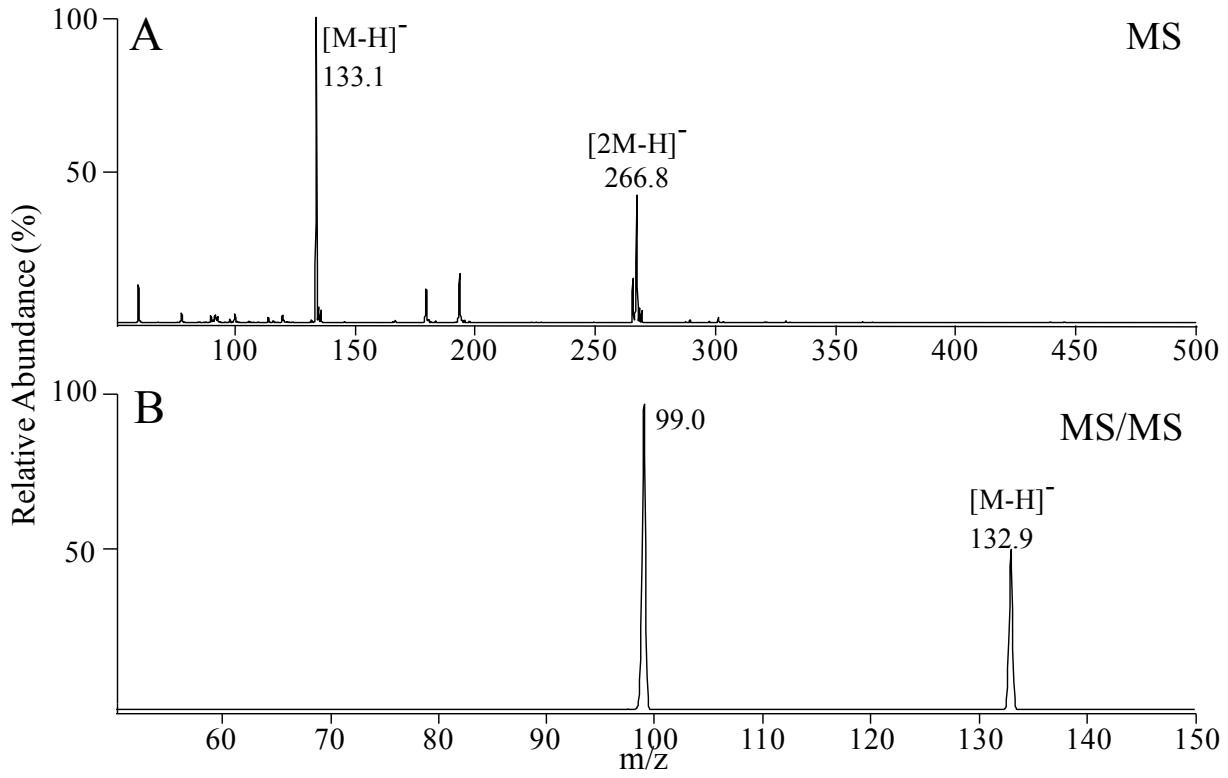

Figure 4.1 Characterization of **2** by nanoelectrospray quadrupole ion trap mass spectrometry. (A) The pseudomolecular ion $[M-H]^-$ at m/z 133.1 and the dimer at m/z 266.8; (B) CID-MS/MS of selected parent ion at m/z 132.9.

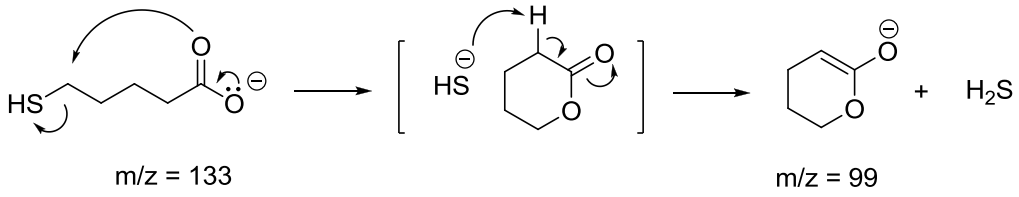

Scheme 4.2 Fragmentation mechanism of **2** anion. The spectrum is displayed in Figure 2.8B. Square brackets indicate ion-molecule complexes.

4.2.2 Synthesis of 5,5'-Thiodipentanoic Acid (3)

Following the method of Rabinovich et al. [256], a freshly prepared solution of 5-bromovaleric acid (3.4 g, 18.8 mmol) in 16.7 M NaOH (8 mL) was added dropwise to an ice bath cold solution of freshly prepared **2** (2.5 g, 18.7 mmol) dissolved in 16.7 M NaOH (8 mL). The resulting reaction mixture was stirred at 40-50 °C for 24 h. After the heating was terminated, the product mixture was acidified with concentrated hydrochloric acid to pH 1 and repeatedly extracted with dichloromethane (5×50 mL). Extracts were combined, dried over anhydrous Na_2SO_4, filtered, and evaporated under reduced pressure to give **3** as a white solid in 78 % (3.4 g) yield. ^{1}H NMR (300 MHz, $CDCl_3$): δ 1.49-1.67 (m, 8H), 2.26 (t, 4H, J = 7.2 Hz), 2.44 (t, 4H, J = 7.2 Hz); ^{13}C NMR (75 MHz, $CDCl_3$): δ 23.84, 28.80, 31.42, 33.39 and 176.79.

The characterization by mass spectrometry and MS/MS is shown in Figure 4.2. The deprotonated pseudo-molecular ion $[M-H]^-$ at m/z 233 (Figure 4.2A) was selected for fragmentation by CID-MS/MS, the fragments obtained were consistent with the expected structure, and the fragmentation pathways are demonstrated in Scheme 4.3.

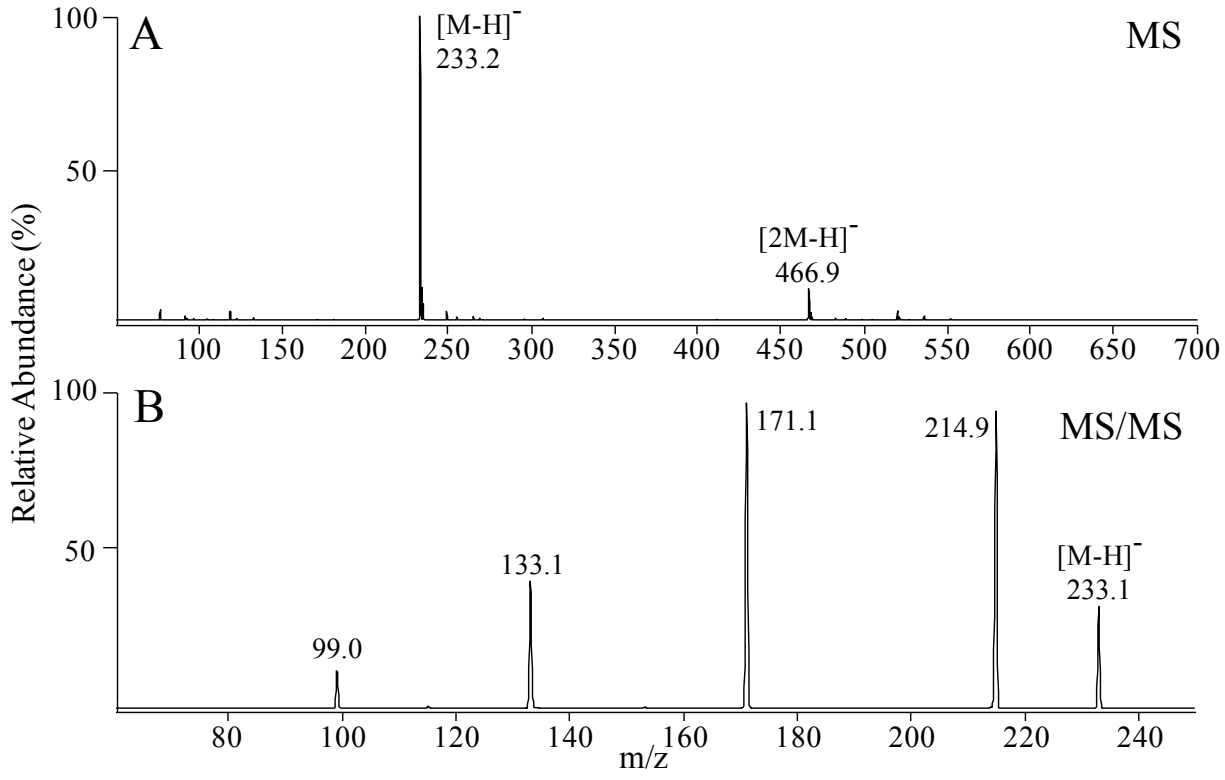

Figure 4.2 Characterization of compound **3** by nanoelectrospray quadrupole ion trap mass spectrometry. (A) ESI-MS spectrum. Abundant ions corresponding to the deprotonated precursor ion ($[M-H]^-$) at m/z 233.2 and a deprotonated non-covalent dimer (m/z 466.9) were observed. (B) CID-MS/MS product ion spectrum of the $[M-H]^-$ precursor ion.

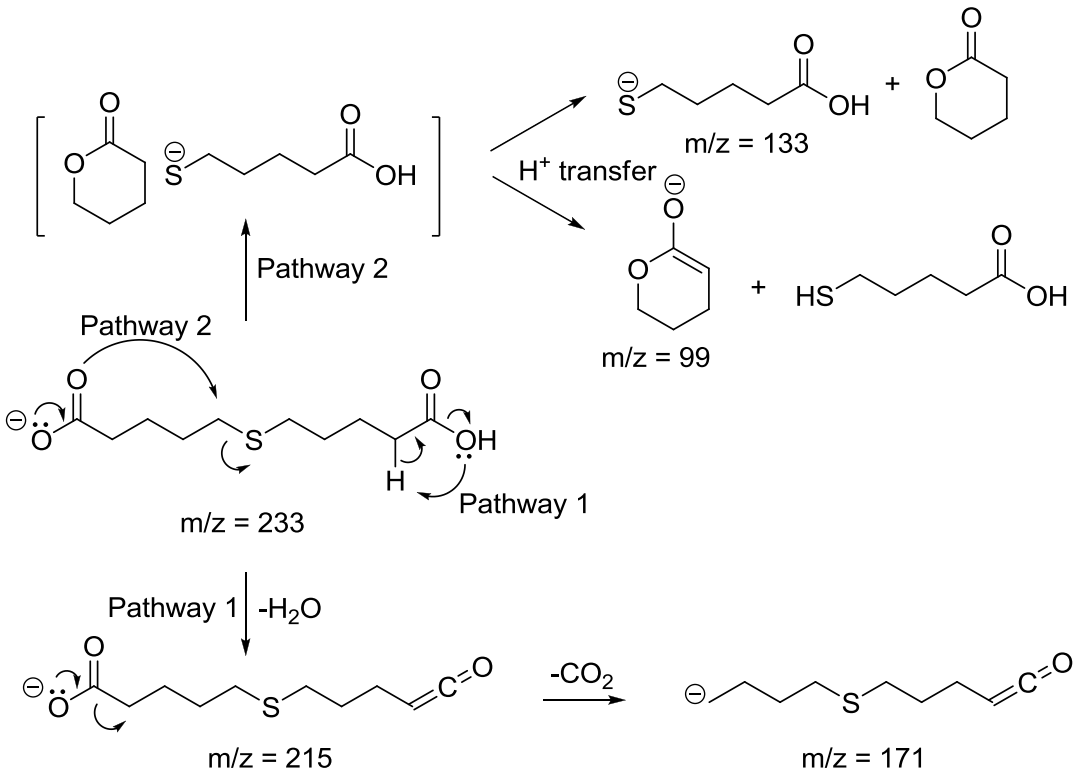

Scheme 4.3 Proposed fragmentation mechanism of **3** anion. The spectrum is displayed in Figure 4.2B. Square brackets indicate ion-molecule complexes.

4.2.3 Synthesis of 5,5'-Thiodipentanoylhydroxysuccinimide (4)

Following methods analogous to other NHS-esters [240, 257, 258], compound **3** (1.17 g, 5.0 mmol) and NHS (1.44 g, 12.5 mmol) were dissolved in 10:1 v/v mixture of chloroform and dichloromethane (55 ml) and stirred for 5 min at room temperature. DCC (2.58 g, 12.5 mmol) was then added, and the mixture was stirred overnight. After filtration of dicyclohexylurea (DCU) precipitate and solvent removed under reduced pressure, the oily residue was dissolved in a minimum amount of ethyl acetate. The remaining DCU was precipitated and removed by filtration. Following rotary evaporation of the ethyl acetate, the residue was dissolved in

dichloromethane, washed with 1 M NaOH and H_2O, and then evaporated to near dryness. The residue was then recrystallized with ethyl ether containing a trace amount of acetone to give a light yellow solid in 84 % (1.8 g) yield. ^{1}H NMR (300 MHz, $CDCl_3$): δ 1.63-1.71 (m, 4H), 1.76-1.84 (m, 4H), 2.50 (t, 4H, J = 7.5 Hz), 2.60 (t, 4H, J = 7.5 Hz), 2.78 (s, 8H); ^{13}C NMR (75 MHz, $CDCl_3$): δ 23.60, 25.50, 28.35, 30.42, 31.03, 168.32 and 169.14.

Upon characterization by mass spectrometry and MS/MS, the singly charged $[M+H]^+$ ion at m/z 429.1 was the most abundant ion, the NH_4^+ and Na^+ adducts were also present. The peak of m/z at 314.2 corresponds to an in source fragment of the $[M+H]^+$ ion, via the neutral loss of 115 (NHS), the dominant product ion present in the MS/MS spectrum in Figure 4.3B. The fragmentation pathway is displayed in Scheme 4.4.

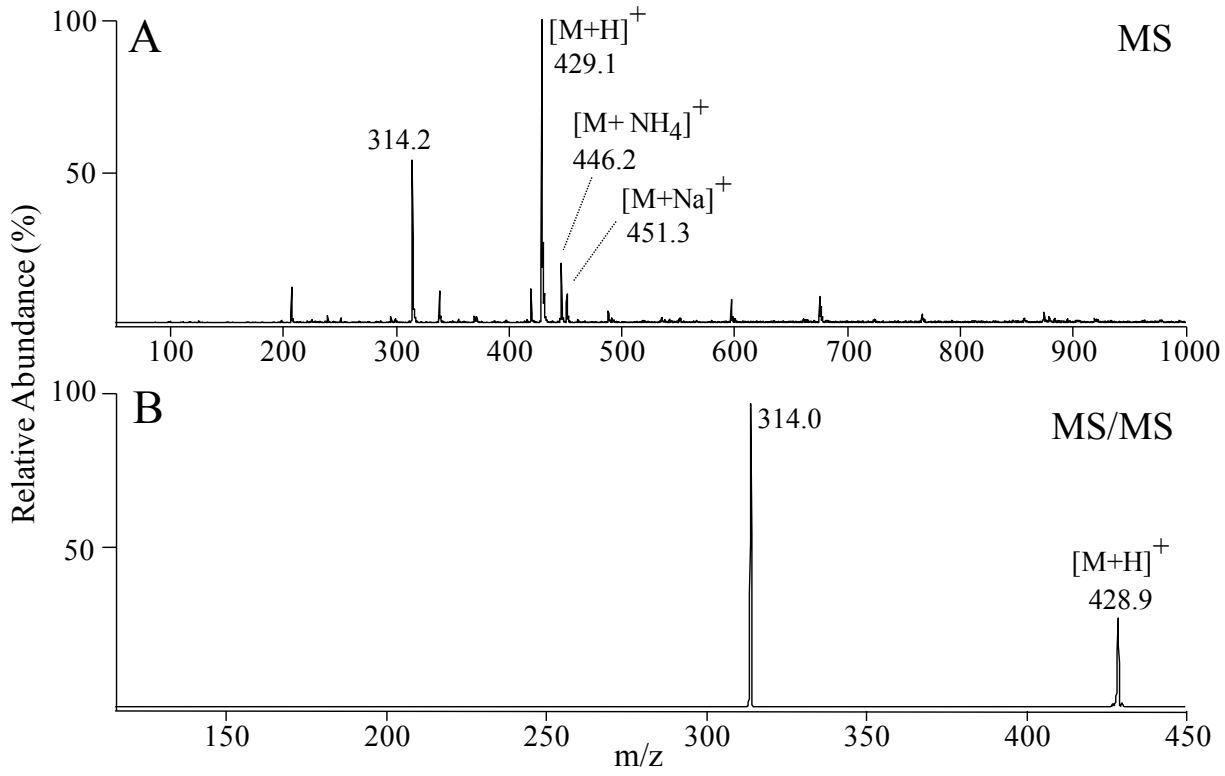

Figure 4.3 Characterization of **4** by nanoelectrospray quadrupole ion trap mass spectrometry. (A) ESI-MS spectrum. The pseudomolecular ion $[M+H]^+$ at m/z 429.1, as well as the NH_4^+ and Na^+ adducts are present; (B) CID-MS/MS of protonated precursor ion at m/z 428.9.

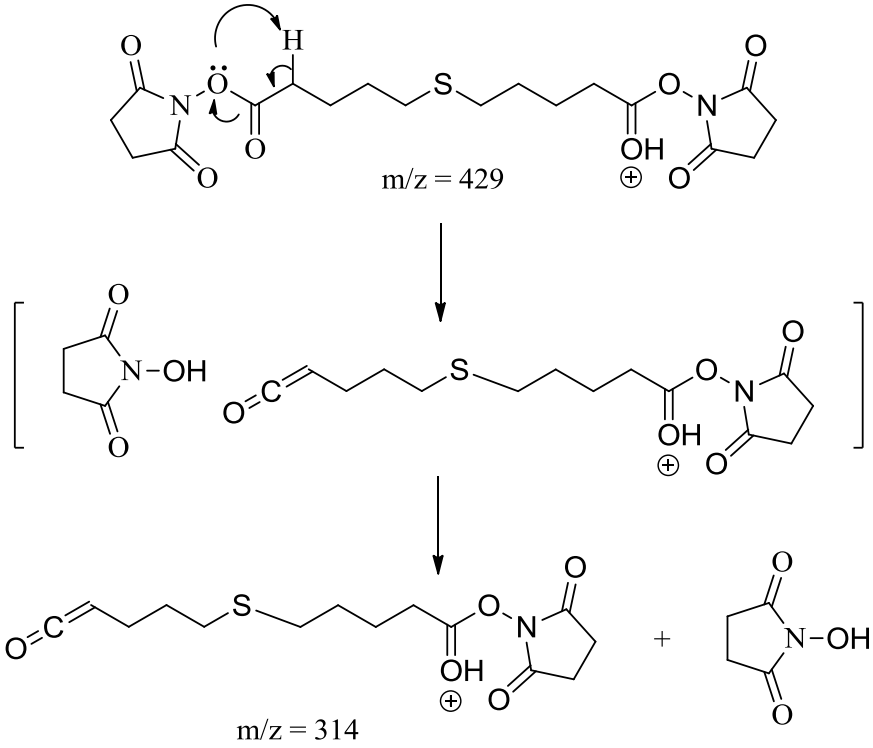

Scheme 4.4 Fragmentation of protonated **4**. The spectrum is displayed in Figure 4.3B. Square brackets indicate ion-molecule complexes.

4.2.4 Synthesis of *S*-Methyl 5,5'-Thiodipentanoylhydroxysuccinimide

A mixture of **4** (214 mg, 0.5 mmol) and iodomethane (160 mg, 1.1 mmol) in acetonitrile (1.5 mL) was allowed to react at room temperature for 4 days. Following removal of the solvent under vacuum, a pale yellow solid was obtained to give *S*-methyl 5,5'-thiodipentanoylhydroxysuccinimide iodide (**1′**), which was used for cross-linking reactions without further purification. ^{1}H NMR (500 MHz, $CDCl_3$ + CD_3OD): δ 1.89-1.91 (m, 8H), 2.68 (t, 4H, J = 6.5), 2.78 (s, 8H), 3.02 (s, 3H), 3.53 (t, 4H, J = 7.5); ^{13}C NMR (125 MHz, $CDCl_3$ + CD_3OD): δ 22.51, 22.66, 23.00, 25.53, 29.99, 40.34, 168.21 and 169.73.

Alternatively, a mixture of **4** (214 mg, 0.5 mmol) and dimethyl sulfate (0.63 g, 5mmol) in acetonitrile (2 mL) was allowed to react at room temperature for 4 days. Following freeze-drying, a dark brown oily residue was obtained to provide *S*-methyl 5,5'-thiodipentanoylhydroxysuccinimide methylsulfate (**1′′**), which was used for cross-linking reactions without further purification. ^{1}H NMR (500 MHz, CD_3CN): same as for **1′** above.

Alkylation with either iodomethane or dimethyl sulfate provided the target sulfonium ion **1** with different counter ions; identical fragmentation behavior was observed following low energy CID MS/MS. Figure 4.4 demonstrates positive mode mass spectrometry of molecular ion at m/z 433 and MS/MS spectra obtained by analysis of **1′′**. The major product ion is observed at m/z 197.9 as shown in Figure 4.4B. This ion is formed upon cleavage of C-S bond adjacent to 'fixed charge', resulting in an oxonium ion with 6-membered ring (Scheme 4.5). Fragment ion at m/z 131 is possibly due to a neutral loss of 115 (NHS) from further fragmentation of complementary product ion of 198.

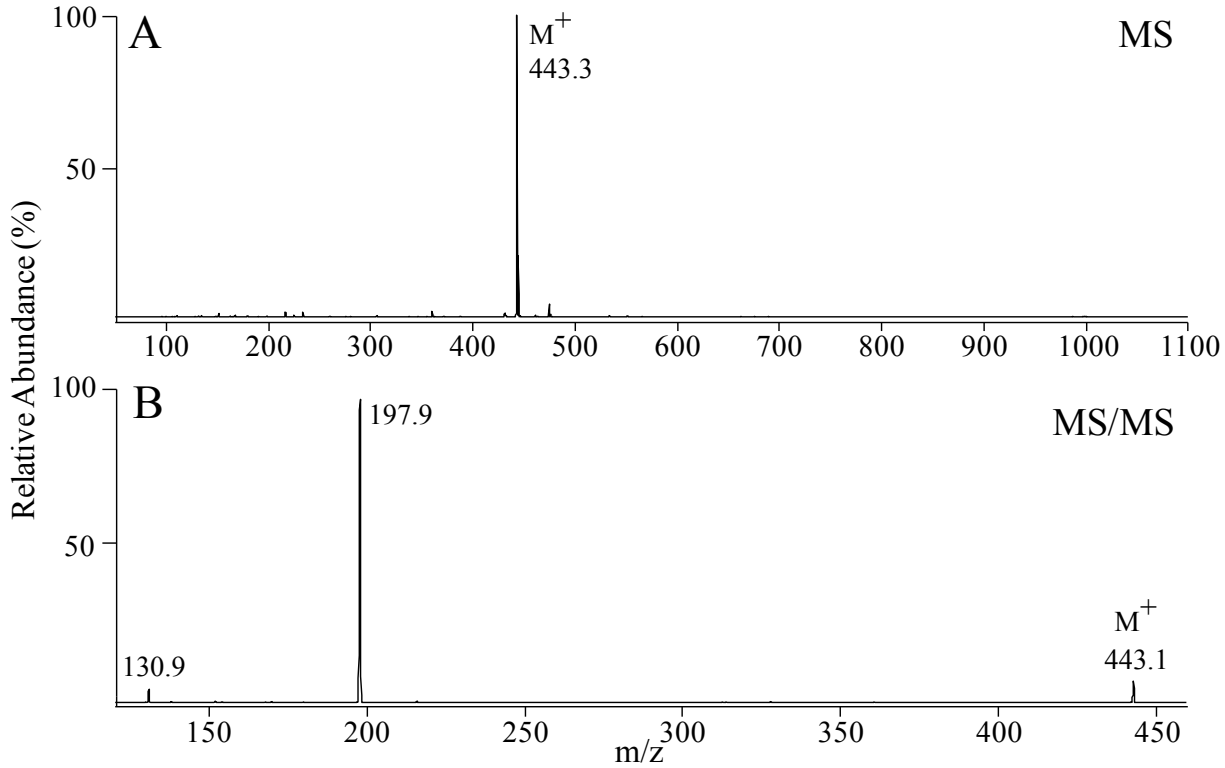

Figure 4.4 Characterization of ionic cross-linking reagent **1** by nanoelectrospray quadrupole ion trap mass spectrometry. (A) The 'fixed charge' M^+ sulfonium ion precursor is observed at m/z 443; (B) CID-MS/MS product ion spectrum of the M^+ precursor ion.

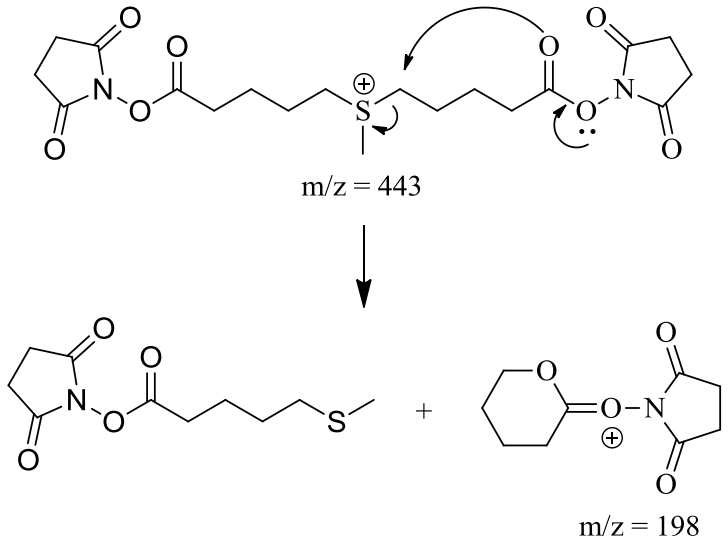

Scheme 4.5 Fragmentation pathway of sulfonium ion **1**. The spectrum is displayed in Figure 4.4B. Formation of the ion at m/z 198 is the major process.

4.3 Peptide Cross-Linking Reactions

For single peptide cross-linking reactions, peptides were dissolved in phosphate-buffered saline (PBS, 800 mg of NaCl, 217 mg of $Na_2HPO_4 \bullet 7H_2O$, 20 mg of KCl, and 20 mg of KH_2PO_4 per 100 ml, pH 7.5) to a concentration of 0.5 mM. Cross-linking reagent **1′** or **1″** was dissolved in DMF and then immediately added to the peptide solution to a concentration of 0.75 mM (the final concentration of DMF was 1%), and the reaction allowed to proceed at room temperature for 30-120 min. Multipeptide cross-linking reactions (5.0 mM each in phosphate-buffered saline) were carried out using **1′** or **1″** at a peptides/cross-linking reagent molar ratio of 1.6:1 and allowed to proceed at room temperature for 2 h. A series of synthetic peptides were employed. As the primary goal of the current study was to examine the utility of a sulfonium ion containing cross-linking reagent for controlling the specificity of the gas-phase fragmentation reactions of inter-, intra-, or dead-end cross-linked peptides, as well as to examine the potential competition between cleavage of the cross-linker and cleavage of facile bonds within the peptide sequence (e.g., enhanced cleavage at the C-terminal side of aspartic acid residues, at the N-terminal side of proline residues, or at the side chain of post-translational modified residues such as loss of H_3PO_4 from phosphoserine or phosphothreonine). Thus, only limited evaluation of the reaction conditions required to optimize the abundances of specific types of cross-linking reaction products was carried out. Furthermore, the concentrations of the peptide solutions subjected to cross-linking reactions in this study were ~1 order of magnitude higher than that used in prior protein cross-linking studies (in native protein structures or protein complexes, lower concentrations may be employed as the “local concentration” of the reactive groups subjected to

cross-linking are defined by the structural fold of the protein or protein complex of interest). Note, however, that the other conditions employed for the peptide cross-linking reactions (i.e., the use of a biologically relevant solution composition, pH, peptide/reagent molar ratio, etc.) are similar to those employed in previous protein cross-linking studies, thereby allowing the current methods to be readily applied to future studies involving the analysis of intact proteins. All reaction products were desalted by Sep-pak (Waters, Milford, MA) purification, with elution in 40, 60, and 80% acetonitrile (aq) containing 0.05% formic acid prior to mass spectrometry analysis.

4.4 Methyl Esterification of Peptides

Methyl esterification of peptides was carried out as previous reported [259, 260] with minor modifications. Reagent methanolic hydrochloric acid was prepared by dropwise addition of 320 μL of acetyl chloride with stirring to 2 mL of anhydrous methanol. The model peptide, typically 100 μg, was thoroughly dried by vacuum centrifugation prior to the esterification reaction and reacted with 200 μL of the reagent at room temperature for 2 h. Then, the reagent was removed by evaporation under vacuum.

4.5 Diethyl Pyrocarbonate (DEPC) Modification of Cross-Linked Peptides

DEPC modification was carried out using a procedure adapted from Hnízda *et al.* [261]. 40 μL of freshly prepared DEPC solution (12.5 mM) in methanol was added to the 40 μL of peptide mixture solution (5 mM) resulting from a cross-linking reaction performed in PBS buffer and

subjected to a 2-fold dilution with H_2O. The reaction proceeded at room temperature for 1h. Then, reaction products were desalted by Sep-pak purification as described previously and further diluted in a solution of methanol:water:acetic acid 50:50:1 v/v for nanoelectrospray mass spectrometry analysis.

DEPC is most frequently used for modification of histidine residues in proteins, by substitution at one of the nitrogen positions on the imidazole ring (Scheme 4.6). At higher DEPC concentration levels, the imidazole ring may be disrupted upon the formation of multiple substitution by-products. DEPC modification can also occur with other nucleophiles such as tyrosine and primary amines [262].

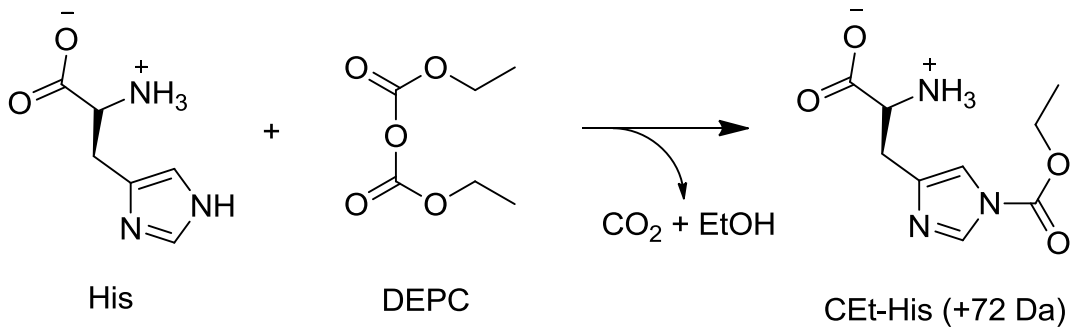

Scheme 4.6 Modification of histidine residue by diethyl pyrocarbonate (DEPC). CEt-His denotes carbethoxyhistidine. Adapted from Reference [262].

4.6 Mass Spectrometry

Mass spectrometry analysis of cross-linked peptide ions was performed using (i) a Thermo Scientific model LCQ Deca 3D quadrupole ion trap or (ii) a Thermo Scientific model LTQ linear quadrupole ion trap mass spectrometer (San Jose, CA), each equipped with nanoelectrospray

(nESI) sources. Samples (~10 μM) were introduced into the mass spectrometers at a flow rate of 0.5 μL / min. The spray voltage was maintained at 2.0-2.5 kV, while the capillary temperature was in the range of 150 to 200 ˚C. Collision-induced dissociation (CID)-MS/MS and -MS^n experiments performed using helium as a collision gas, at an activation q value of 0.25 and an activation time of 30 ms. Collision energies were individually optimized for each compound of interest. The spectra shown are typically the average of 20-50 scans. Repeated analysis of individual sample was found to result in less than 5% variation in relative product ion abundances.

A brief discussion of the principles of operation of the instrumentation in which these tandem mass spectrometry measurements are performed is given below.

4.6.1 Tandem Mass Spectrometry (MS/MS)

Tandem mass spectrometry (MS/MS) is a method involving selection of a precursor ion in a first stage of mass analysis, an intermediate reaction event (typically dissociation) followed by a second stage of mass analysis. These experiments can be realized in space, in instruments containing distinct mass analyzer regions, such as a triple quadrupole, or in time, by performing a sequence of analysis steps in an ion storage device such as an ion trap. For in space MS/MS experiments, four main scan modes, product ion scan (daughter scan), precursor ion scan (parent scan), neutral loss scan, and selected reaction monitoring (SRM), are available [263]. However, mass analysis involving more than two stages can not be realized by this type of instrument. The identification of cross-linked peptides often requires multiple stages of tandem mass spectrometry to be employed. The quadrupole ion trap could satisfy such purpose. To understand

the principles of how a quadrupole ion trap works, we can first consider the general operating principles of the quadrupole mass analyzer.

4.6.2 Quadrupole Mass Analyzer

The quadrupole mass analyzer separates ions based on achieving a stable trajectory in oscillating electric fields according to the ions' m/z ratio. Four parallel hyperbolic or cylindrical rods are employed with a variable amplitude oscillating AC (RF) voltage and variable DC voltage superimposed to pairs of opposite rods.

When ions are accelerated along the z-axis into the space between the quadrupole rods, they are also subjected to accelerations along the x and y axis resulting from forces induced by the electric fields, which are a function of the position of the ion from the center of the rods, i.e. x and y. If the values of x and y never reach the quadrupole field radius r_0, the ion will have a stable trajectory. The motion of ions within a quadrupole mass analyzer is described by a second-order differential equation named after the 19th century French physicist E. Mathieu: the Mathieu equation. The solutions to the equation described in the following formulas define the regions of stability and instability for ions as a function of the operating conditions in a quadrupole mass analyzer,

$$a_u = a_x = -a_y = \frac{8zeU}{m\omega^2 {r_0}^2}$$

$$q_u = q_x = -q_y = \frac{4zeV}{m\omega^2 {r_0}^2}$$

where U is the amplitude of the DC potential, V is the amplitude of the AC potential, $\omega = 2\pi\upsilon$ is the angular frequency (υ is the frequency of the applied AC potential), and t is time.

a_u and q_u values define whether the ions have stable trajectories when passing through the quadrupole electric field at given instrumental conditions. Therefore after rearranging these equations, the operating parameters for the quadrupole mass analyzer are derived.

$$U = a_u \frac{m\omega^2 r_0^2}{z8e}$$

$$V = q_u \frac{m\omega^2 r_0^2}{z4e}$$

As shown above, the stability of an ion at a given m/z value, for a particular operating frequency and r_0 value, can be determined simply as a function of U and V. More straightforwardly, a combination of U and V values determines whether an ion at a specific m/z has a stable trajectory through the quadrupole, which is defined by solutions of a_u and q_u values as shown in Figure 4.5. When the quadrupole is operating at a certain combination of U and V near the apex of the stability diagram (a_u = 0.237, q_u = 0.706), only one m/z ion will have a stable trajectory. Thus a mass spectrum is obtained by scanning a constant U/V ratio near the apex of the stability diagram, allowing only one m/z ion at a time to be stable and pass through the quadrupole, whereas others are unstable and then lost.

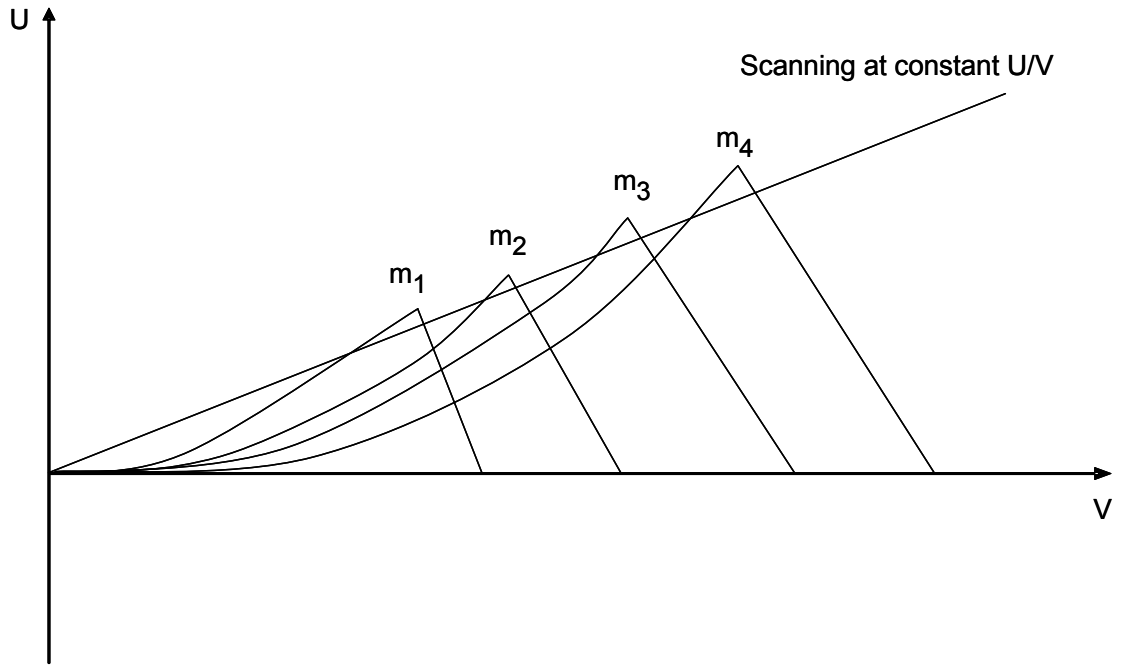

Figure 4.5 Quadrupole stability regions for positively charged ions with different masses ($m_1 < m_2 < m_3 < m_4$), as a function of U and V. Each ion can be detected successively by scanning U and V near the apex with a constant ratio of U/V. Adapted from Reference [263].

4.6.3 The Quadrupole Ion Trap

The quadrupole ion trap is based on the same principle as the quadrupole mass analyzer, where an oscillating electric field is generated in three-dimensions resulting from the application of an RF potential to a hyperbolic ring electrode, while two hyperbolic end cap electrodes are held at ground as displayed in Figure 4.6.

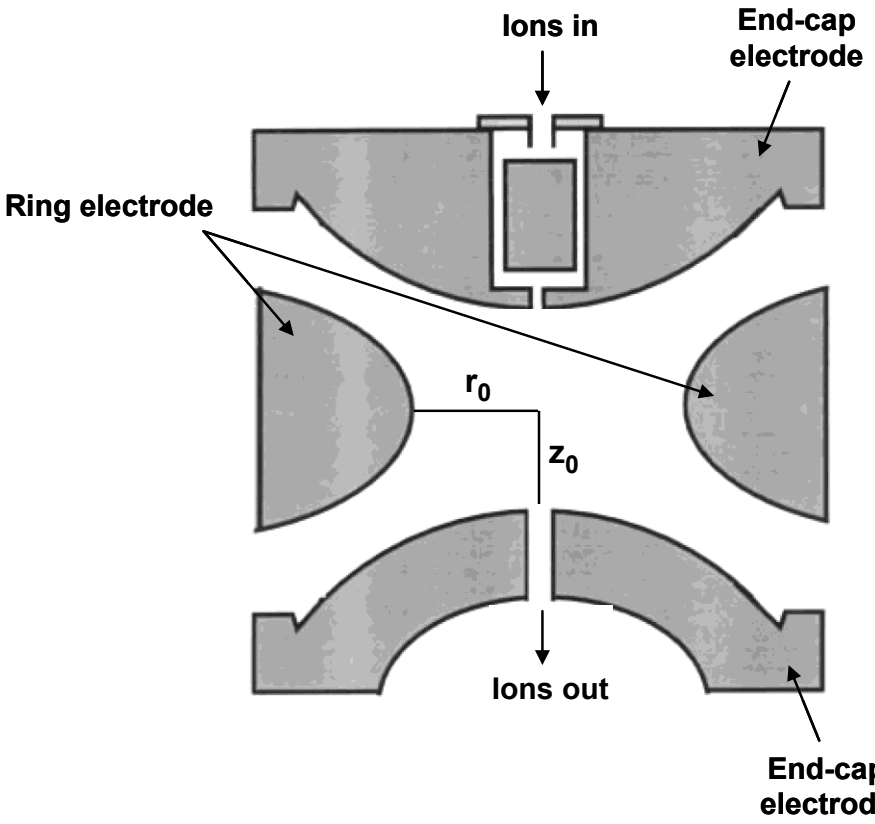

Figure 4.6 Cross-section of a three-dimensional quadrupole ion trap. Adapted from Reference [264].

The solution of the Mathieu equation can also be used to describe the ion motion in three dimensional ion traps. Since the DC potential applied to the end caps is usually zero, the solution for a_u is equal to zero whereas q is given by the following equation,

$$q_u = -2q_r = \frac{8zeV}{m(r_0^2 + 2z_0^2)\omega^2}$$

where r_0 and z_0 are the distances from the centre of the trap to the ring electrode and end cap electrodes, respectively, V is the amplitude of the RF potential, and ω is the angular velocity of the RF potential applied a fixed frequency. For an ideal geometry of the quadrupole ion trap, r_0 and z_0 are defined by the following equation,

$$r_0^2 = 2z_0^2$$

However, this ideal geometry is not usually employed due to truncation of the electrodes of the ion trap, and due to the holes in the ion exit and the entrance lenses.

To have a stable trajectory, ions must have motions such that their coordinates never reach or exceed r_0 and z_0, which are defined by a_u and q_u values shown as stability diagram in Figure 4.7. According to the equation above, high m/z ions are represented by larger balls with low q values and low m/z ions by small balls with high q values under the same RF potential. Since there is no DC voltage applied, the ion trap is operated along the V (q) axis. Thus ions with different m/z values are retained inside the trap as long as their q values are less than the q = 0.908 at the stability boundary.

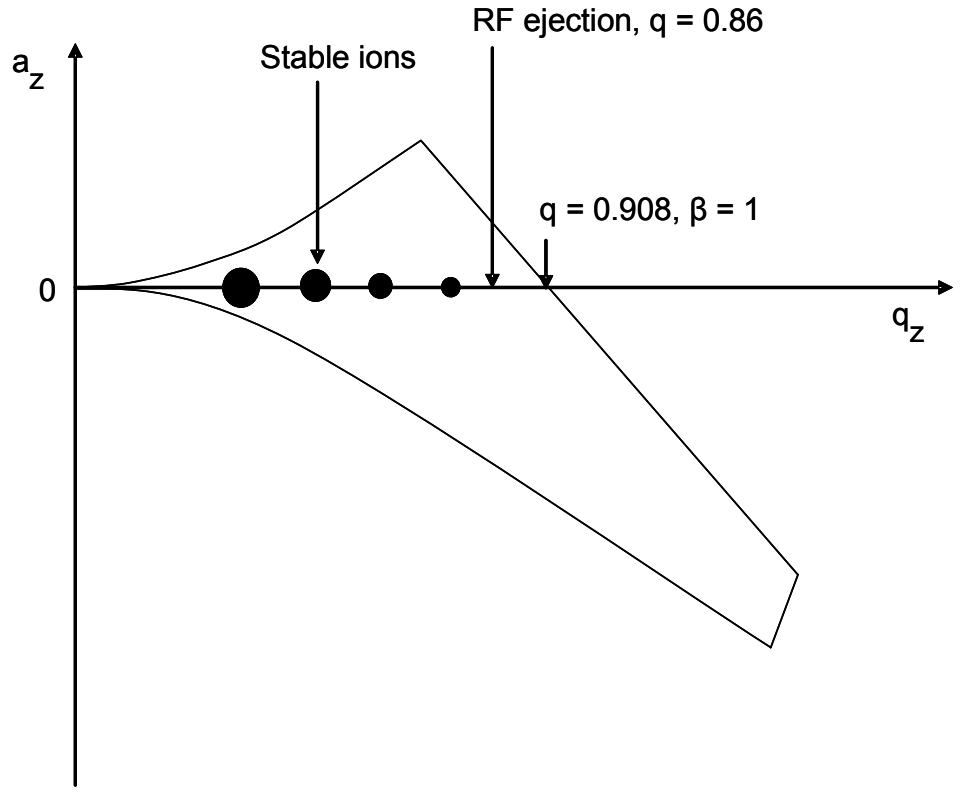

Figure 4.7 Mathieu stability diagram for a quadrupole ion trap. The larger balls represent high m/z ions whereas smaller balls represent the low m/z ions. Adapted from Reference [263].

To acquire a mass spectrum in the quadrupole ion trap, the amplitude of the applied RF potential is increased while simultaneously applying a supplementary (auxiliary) radio frequency to the end cap electrodes at a frequency corresponding to a q value of 0.86. As ions of different m/z successively achieve a q value of 0.86, they are excited due to their secular frequency and become resonantly ejected. The maximum RF operating voltage and the q-eject value determines the highest m/z value that can be analyzed.

Due to their inertia, the ions oscilate at a 'secular' frequency, which is lower than the frequency of RF field, as expressed by the following equation,

$$f_z = \frac{\beta_z v}{2}$$

where β_z is a fundamental stability parameter and is approximated by the following equation for q values less than 0.4.

$$\beta_z = \left[a_z + \left(\frac{q_z^2}{2} \right) \right]^{1/2}$$

When the supplementary frequency applied to the end-cap electrodes matches the secular frequency of an ion, the kinetic energy of the ion will increase rapidly and the ion's trajectory becomes unstable until it is ejected. Thus, the ion is designated to be ejected at a q value of 0.86, in order to achieve higher mass resolution compared to mass analysis via ion ejection at the stability limit.

4.6.4 Multiple Stage Tandem Mass Spectrometry (MS^n) Realized in an Ion Trap Mass Spectrometer

The main advantage of the ion trap is the ability to perform multistage tandem mass spectrometry (MS^n) experiments. This can be achieved by first selecting a precursor ion by expelling all other ions via the application of supplementary AC frequencies at their secular frequencies. Then the isolated ions are subjected to resonance excitation via the application of a low amplitude supplementary AC frequency at the ions secular frequency of motion, resulting in energetic collisions with the inert He bath gas present in the trap. The product ion spectrum is

then obtained by resonant ejection. This time-dependant tandem mass spectrometry can be repeated to provide MS^n spectra if one of the product ions is selected for further fragmentation.

In order to fragment the ions by resonance excitation, an RF voltage must be applied so that the q value of the m/z of interest can be adjusted to the value of the supplemental RF frequency. However, if the applied V voltage is increased, the low mass cut-off which is proportional to V is also increased. Thus, it is advantageous to work at lower V to allow a wider mass detection range. The Dehmelt potential defined by the following equation,

$$\overline{D_z} = q_z \frac{V}{8} = \frac{zeV^2}{m(r_0^2 + 2z_0^2)\omega^2}$$

is also increased as a function of V^2. The Dehmelt potential determines the trapping efficiency of the ions. Thus, an appropriate q value must be selected for ion resonance excitation to achieve a compromise between the sensitivity and the low mass cut-off.

Due to the low injection and trapping efficiencies and limited ion storage capacity related to the 3D quadrupole ion trap, the two-dimensional linear quadrupole ion trap (LIT) has been developed and become more widely used [265, 266]. As illustrated in Figure 4.8, the LIT stores ions in a two-dimensional electric field, which is created by applying an RF potential to four hyperbolic rods in the x- and y-dimensions, and static DC potentials to each end of the rods in the z-dimension. The geometry of the LIT allows ions to be stored along the entire length of the trap, thus improving the ion storage capacity. In addition, the ions can be ejected and detected at the both sides of the LIT resulting in improved sensitivity. In the studies described here, a 3D quadrupole ion trap and a 2D linear quadrupole ion trap were both employed.

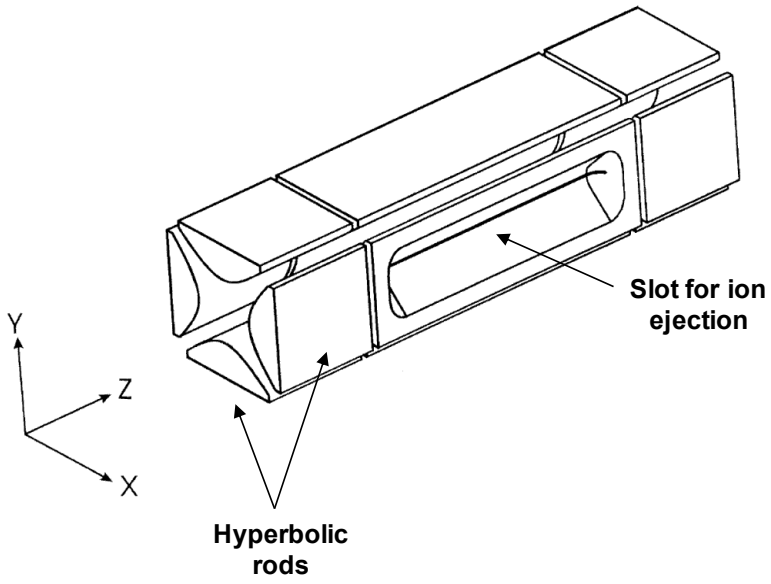

Figure 4.8 Diagram of a two-dimensional linear quadrupole ion trap. Adapted from Reference [266].

CHAPTER FIVE

INTRODUCTION TO PHOSPHOPROTEOME ANALYSIS

5.1 Protein Phosphorylation

Post-translational modifications (PTMs) involve the enzymatic, or to a lesser extent, chemical addition and/or removal of functional groups onto protein amino acid residues [11, 93, 267]. The presence of PTMs greatly increases proteome complexity; however, they play an essential role in the regulation of biological functions. Protein phosphorylation represents one of the most important classes of protein PTM. Reversible protein phosphorylation, which is regulated by protein kinases and phosphatases, serves a critical role in coordinating and regulating virtually all cellular processes. *O*-phosphorylated serine, threonine and tyrosine residues are the most common phosphorylation forms in eukaryotes (Figure 5.1) [268]. Phosphorylation also occurs at arginine, histidine, and lysine residues as well as aspartic and glutamic acid residues, although present in less abundance [269, 270]. A comprehensive analysis of protein phosphorylation should include identification of phosphorylated proteins and peptides, localization of the specific sites of phosphorylation and quantitation of phosphorylation site occupancies under the specific biological environment.

However, protein phosphorylation analysis is still one of the most challenging tasks for contemporary MS techniques due to its low stoichiometry and dynamic nature. Typically only a small fraction of the proteins are phosphorylated and they are present at very low abundance, thus separating them from large amount of non-phosphorylated proteins is usually a prerequisite

before analysis [270-273]. The co-regulation of kinases and phosphotases is highly dynamic, some proteins may only be transiently phosphorylated, and therefore need to be captured instantaneously for analysis [274]. In addition, most proteins undergo phosphorylation at different sites; this heterogeneity further complicates the characterization of protein phosphorylation. To address these challenges, numerous approaches have been developed and applied for the targeted analysis of protein phosphorylation. Comprehensive review articles on various aspects of phopshoprotein and phosphopeptide analysis have recently appeared in the literature [224, 225, 269-273, 275-279]. Therefore, this brief introduction only aims to give a general overview of MS-based phosphoproteome analysis, emphasizing approaches which have recently gained popularity, and those approaches involving chemical labeling strategies.

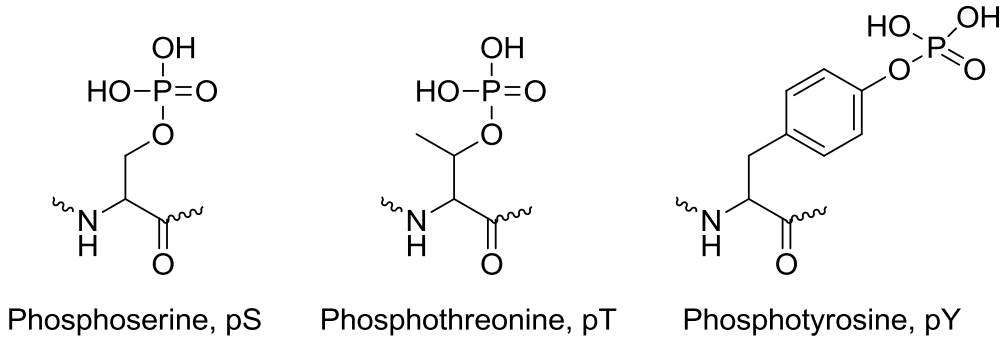

Figure 5.1 Structures of *O*-phosphorylated serine, threonine and tyrosine residues.

5.2 Enrichment Methods for Phosphorylated Peptides

Phosphoproteome analysis is generally based on the identification and characterization of phosphopeptides using MS methods following proteolytic processing of intact phosphoproteins [272]. However, phosphopeptides are notorious difficult for MS detection, due to their low

abundance and lower ionization efficiency compared to the non-phosphorylated peptide ions [270, 271]. Thus, enrichment of phosphopeptides is usually required prior to MS analysis for improved detection and more efficient characterization. There are various strategies available for this, such as immunoprecipitation of phosphotyrosine-containing proteins/peptides [280, 281], ion exchange chromatography [282], immobilized metal ion affinity chromatography (IMAC) [283, 284], metal oxide affinity chromatography (MOAC) [285-288], and chemical derivatization by β-elimination/Michael addition reaction [98-102] or by phosphoamidation [96, 97] which were already discribed in Chapter One. Comprehensive discussions of phosphopeptide enrichment approaches can be found in recent review articles [277, 278]. Several commonly used strategies are outlined in Figure 5.2 [277], and only IMAC and MOAC will be highlighted in the following.

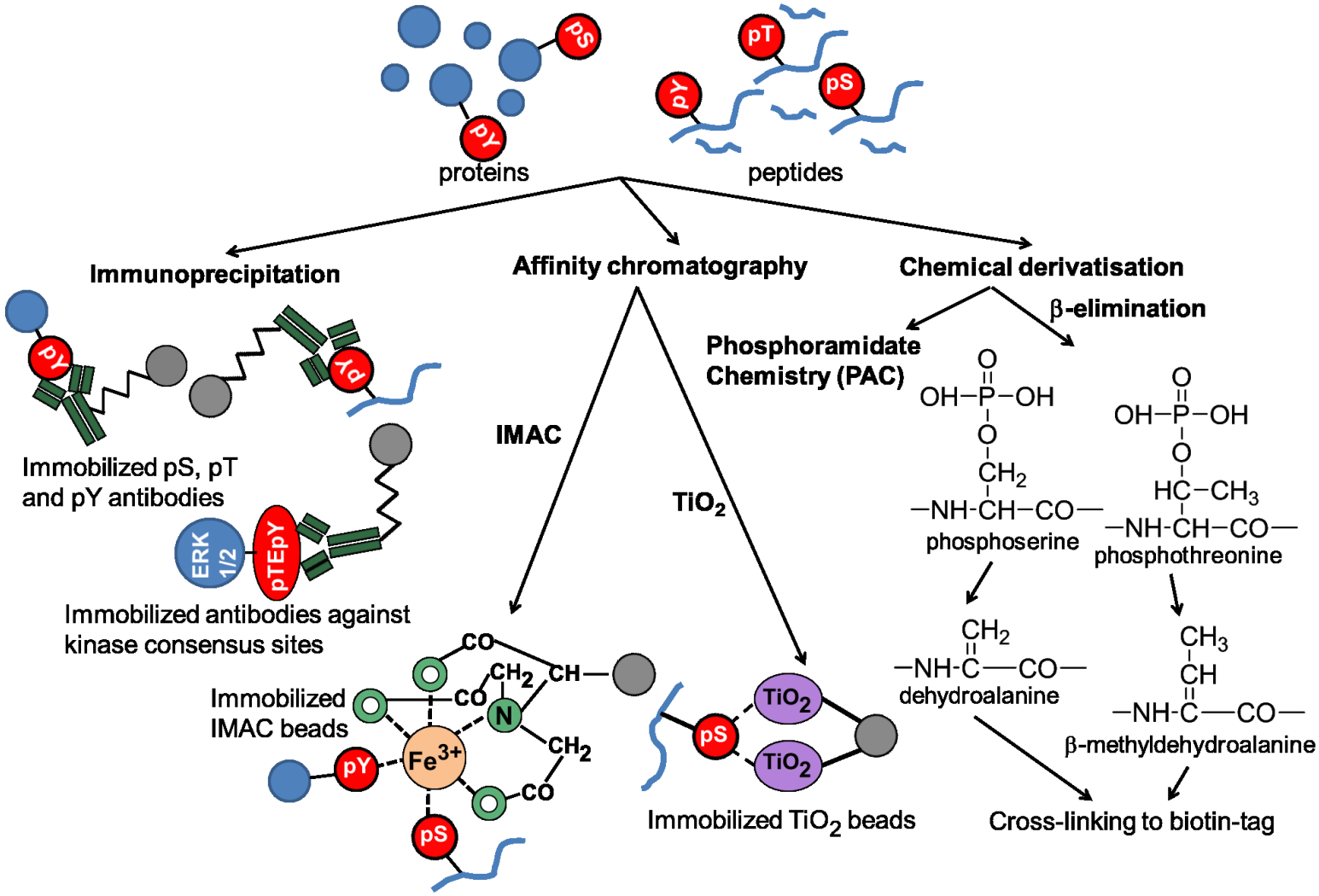

Figure 5.2 Strategies for specific phospho-protein or -peptide enrichment. Adapted from reference [277]. For interpretation of the references to color in this and all other figures, the reader is referred to the electronic version of this dissertation.

5.2.1 Immobilized Metal Ion Affinity Chromatography (IMAC)

IMAC is one of the most frequently used techniques for phosphopeptide and phosphoprotein enrichment prior to MS analysis [283, 289, 290]. IMAC is based on the electrostatic interactions of the negatively charged phosphate group with positively charged metal ions. These metal ions are bound to the column material via nitriloacetic acid (NTA), iminodiacetic acid (IDA), or tris(carboxymethyl)ethylenediamine (TED) linkers. Various immobilized metal ions have been employed to enrich phosphopeptides. Of these, Fe^{3+} is most frequently used, although Ga^{3+}, Al^{3+}, or Zr^{4+} have also been employed [284, 291-293]. IMAC procedures have been widely used due to their compatibility with subsequent separation and MS detection techniques such as LC-ESI-MS/MS [294-296] and MALDI-MS [297].

However, there are a number of problems associated with IMAC-based strategies. One of the major limitations is nonspecific binding of peptides containing acidic amino acid residues, i.e., glutamic acid and aspartic acid. It has been reported that nonspecific binding can be alleviated by converting the carboxyl groups of amino acid residues to their methyl esters using methanolic HCl [259] or thionyl chloride in methanol [298, 299]. Unfortunately, incomplete esterification and side reactions may increase sample complexity, and sample may be lost during sample handling steps [300].

Although IMAC employs typical binding, washing and eluting chromatography procedures, consideration should be made to control experimental conditions such as pH, ionic strength and organic composition of the solvents, to reduce nonspecific binding and improve the specificity toward phosphopeptides [301]. By carefully selecting appropriate experimental conditions,

enhanced phosphopeptide recovery and separate detection of multiply and singly phosphorylated peptides may be achieved [299].

5.2.2 Metal Oxide Affinity Chromatography (MOAC)

MOAC has appeared in recent years whose use has grown rapidly for phosphopeptide enrichment, based on the particular affinity of metal oxides to phosphate groups. Titanium dioxide was first used as the affinity material and is currently the most popular one employed for MOAC [286, 302-304]. The approach exhibits high recoveries and selectivity for phosphopeptides, due to the specific interaction of porous titanium dioxide microspheres with phosphate groups, via bidentate binding at the TiO_2 surface [273]. When coupled with appropriate solutions such as substituted organic acid as modifiers for sample loading, or by purposely increasing the pH of the elution buffer, TiO_2 appears to be highly selective to bind with phosphopeptides over acidic peptides, even without methyl esterification of peptides [305-308].

Several other metal oxides have also been shown to be useful for phosphopeptide enrichment, including zirconium dioxide (ZrO_2) [287, 309-311], aluminum hydroxide ($Al(OH)_3$) [312, 313], aluminum oxide (Al_2O_3) [314], and niobium oxide (Nb_2O_5) [288]. Since metal oxides act as Lewis acids, their differences in acidity scale may contribute to the different selectivity for phosphopeptide enrichment [315].

5.2.3 Selection of Enrichment Methods

As briefly described above, various methods are available for phosphopeptide enrichment. These methods usually provide complementary information [316]. For example, immunoprecipitation is highly effective for enrichment of phosphotyrosine-containing peptides by using phosphotyrosine-specific antibodies. Otherwise, chemical derivatization strategies based on β-elimination/Michael addition work well for phosphoserine/phosphothreonine-containing peptides. It has also been reported that TiO_2-based MOAC techniques are more efficient for enrichment of mono-phosphorylated peptides compared to multiply phosphorylated peptides, because the strong binding of the latter hampers their efficient recovery [277]. In contrast, IMAC preferably enriches multiply phopshorylated peptides, but the approach is limited by nonspecific binding when dealing with highly complex samples [277]. Thus the selection of enrichment methods should be based on the sample type and specific aims of the study. If global phosphoproteome analysis is the goal, a combination of multiple approaches will allow more phosphopeptides to be identified.

5.3 Phosphopeptide Identification and Characterization by Mass Spectrometry

In recent years, rapid improvements in technology have allowed MS become a powerful tool for phosphoproteome analysis [3, 317, 318]. These include the use of soft ionization techniques for introducing phosphopeptides into the mass spectrometer, and the identification and characterization of phosphopeptides using MS, MS/MS and multistage tandem mass

spectrometry (MS^n) techniques on various instrument platforms, which will be introduced briefly below. A detailed discussion of mass spectrometry approaches for phosphoproteome characterization can be found in recent review articles [224, 225].

5.3.1 MS Analysis of Phosphorylated Peptides

Identification of the presence of a phosphopeptide can be achieved via MS analysis of a sample before and after phosphatase treatment [319, 320]. The observed reduction in mass of one or multiple units of 80 Da due to dephosphorylation is indicative of the presence of phosphorylation site(s). Alternatively, chemical modification of the phosphate group by a mass tag such as trimethoxyborate (TMB) via ion-molecule reactions (IMR) in negative ion mode has been reported for rapid diagnosis of the presence of phosphopeptides in mixture [321]. However, for unambiguous identification of the peptide sequence and localization of phosphorylation site(s), the majority of analysis strategies rely on the use of tandem mass spectrometry (MS/MS).

5.3.2 Tandem Mass Spectrometry for Phosphopeptide Analysis

The dissociation methods most widely employed for phosphoproteome analysis include collision-induced dissociation (CID) [322], electron capture dissociation (ECD) [63, 323], and electron transfer dissociation (ETD) [64, 324]. In addition, infrared multi-photon dissociation (IRMPD) [83], ultraviolet photodissociation (UVPD) [84], and femto-second laser-induced photodissociation (fsLID) [325, 326] have also been applied to characterization of phosphopeptide ions. Phosphopeptide ions have distinct fragmentation behaviors when using

these different dissociation techniques. Understanding the gas phase ion chemistry associated with phosphopeptide fragmentation using different MS/MS methods is critical for successful phosphopeptide analysis.

5.3.2.1 Collision Induced Dissociation (CID)

5.3.2.1.1 Limitations of CID

CID is the most established and widely used MS/MS method employed for peptide sequencing. During CID, peptide ions are activated upon collision with an inert neutral gas. By this manner, the kinetic energy of the peptide ions is converted into internal energy which is redistributed over the whole molecule, leading to bond cleavage when the internal energy exceeds the bond activation barrier [327]. Due to its lower energy barrier for phosphoester bond cleavage [328, 329], phosphorylated peptide ions often undergo selective and preferential fragmentation at the phosphate group, giving rise to dominant nonsequence neutral losses from the precursor ions. The observation of these dominant nonsequence ions can be beneficial for enhanced detection of phosphopeptide ions. For example, the presence of phospho-serine, -threonine, and -tyrosine peptides can be detected with high specificity by the observation of a m/z 79 PO_3^- product ion formed by CID of negatively charged precursor ions [330, 331], or by the neutral loss of 80 or 98 Da (HPO_3 or H_3PO_4 respectively) in either positive or negative mode [16, 282, 296, 332-334]. Further identification of peptide sequence and localization of phosphorylation sites can be achieved using data dependent CID-MS/MS or CID-MS^3 methods

based on the observation of these "diagnostic" ions [335-339]. Alternatively, precursor ion scanning by monitoring the formation of phosphotyrosine-specific immonium ions at m/z 216.043 has been used for selective identification of phosphotyrosine-containing peptides within complex peptide mixtures [340-342].

However, the presence of prominent phosphate neutral losses can complicate the CID-MS/MS spectra and limit the sequence information obtained. The mechanisms responsible for the gas-phase neutral loss of H_3PO_4 have been evaluated recently [17]. It was demonstrated that the phosphate loss is more dominant under limited proton mobility conditions due to a charge-directed reaction mechanism involving the formation of strong hydrogen bonding between the phosphate group and the side chain of a protonated arginine or lysine residue [17]. It has also been reported that competing phosphate fragmentation reactions involving the combined neutral losses of HPO_3 and H_2O (98 Da) can provide neutral loss product ions with the same m/z; but corresponding to unmodified residues at original phosphorylation sites and dehydrated residues at original hydroxyl (or carboxyl)-containing amino acid residues [343]. Thus, CID-MS^3 of the 98 Da neutral loss product ions may not provide information to correctly locate the phosphorylation site(s) [344]. In addition, the potential for intramolecular gas phase phosphate transfer under CID-MS/MS may also compromise the unambiguous localization of phosphorylation sites, because phosphate groups migrate between side chains before cleavage of the peptide backbone [343-345].

5.3.2.1.2 Chemical Labeling Strategies to Enhance Phosphopeptide Identification and Characterization by CID-MS/MS

To overcome limitations due to the lability of the phosphate groups upon CID-MS/MS, chemical derivatization strategies have been developed to enhance phosphopeptide identification and characterization. The majorities of these derivatization approaches are based on β-elimination/Michael addition chemistry, by conversion of the phosphate group into functional moieties which can facilitate affinity enrichment [98-102], to become lysine mimics for selective cleavage by lysine-specific proteases [108-110], or lead to the formation of characteristic reporter ions during CID-MS/MS [103-106].

Other derivatization approaches involve the use of malondialdehyde to decrease the basicity of arginine residues in phosphorylated peptides [346]. As a result, a decreased relative abundance of 98 Da neutral losses and increased peptide sequence product ions can be observed from CID of modified phosphopeptides. It has also been reported that protonated phosphopeptides react with trivalent boron species via ion-molecule reactions in the gas phase [347, 348]. The resultant boron-derivatized phosphopeptides preferentially undergo backbone cleavage when subject to CID, therefore improving the capability for unambiguous phosphorylation site assignment.

5.3.2.2 Electron-Based Dissociation

Electron-based dissociation methods have been recently developed and introduced as complementary techniques for phosphoproteome analysis [63, 64, 323, 324]. These techniques including electron capture dissociation (ECD) and electron transfer dissociation (ETD), allow phosphopeptide fragmentation without the frequently observed dominant neutral loss of phosphate group when using CID, thus providing highly informative MS/MS spectra. However,

it should be noted that these approaches are limited to the analysis of multiply charged precursor ions due to charge state reduction occurring upon the attachment of an electron.

5.3.2.2.1 Electron Capture Dissociation (ECD)

Electron capture dissociation (ECD) involves exothermic capture of low energy electrons (< 0.2 eV) by positively charged peptide ions which give rise to charge reduced peptide radical cations (Scheme 5.1) [58]. Following electron capture, abstraction of the resultant $H^{\bullet}$ from the neutralized charged group (e.g., ammonium group as shown in Scheme 5.1) to a nearby amide oxygen atom will yield a labile aminoketyl intermediate which dissociates by N-C_{α} bond cleavage, resulting in a homogeneous series of c- and z-type ions [349]. This dissociation-recapture mechanism is under debate since the cross section for gas-phase peptide ions to recapture a free hydrogen atom is low, therefore the mechanisms responsible for ECD are continually being refined [350].

As a non-ergodic fragmentation technique, ECD allows the labile phosphate group to be retained [351, 352]. ECD has been applied to phosphopeptide identification and phosphorylation site assignment in a wide range of biological samples [323, 353]. A data-dependent ECD-MS/MS strategy has been demonstrated by Cooper and co-workers, in which observation of the neutral loss of 98 Da by CID is used to trigger subsequent ECD to facilitate phosphopeptide sequencing [354, 355].

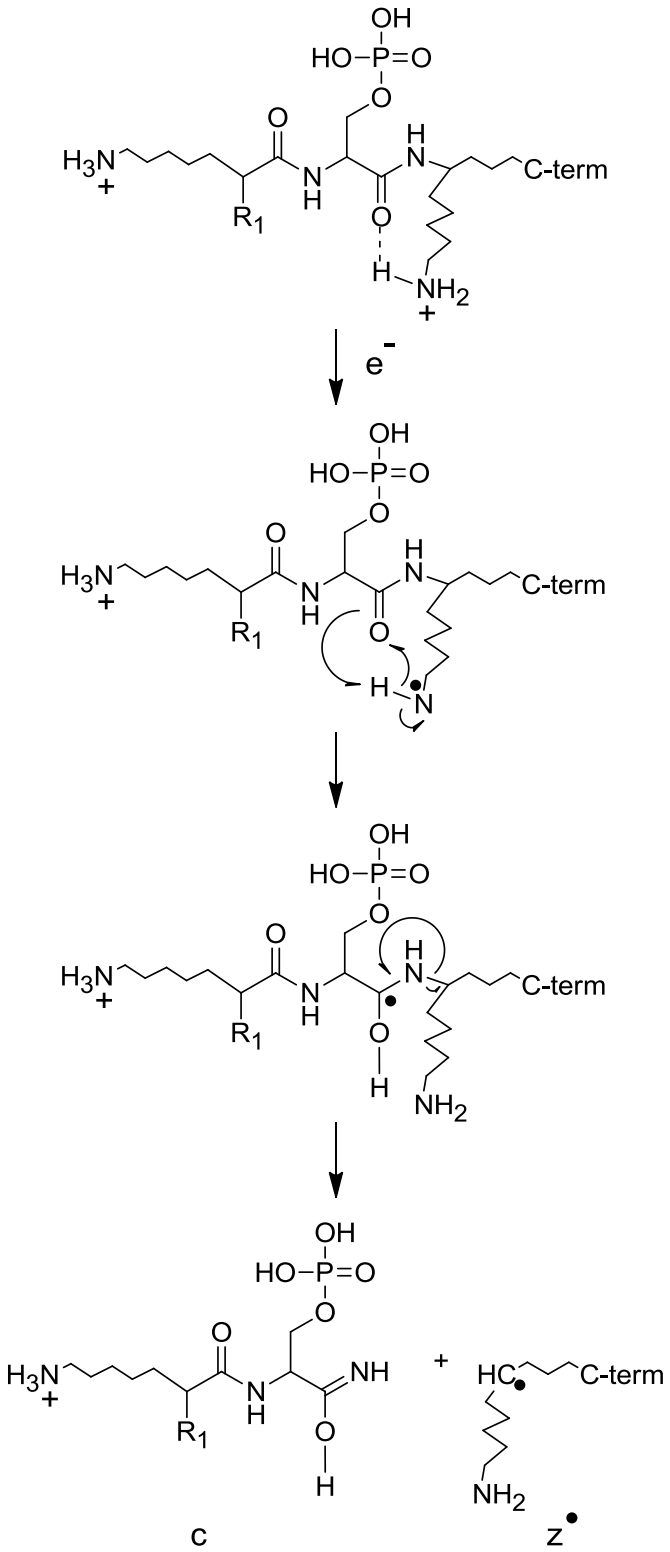

Scheme 5.1 Proposed ECD/ETD fragmentation mechanism of phosphorylated peptides for the formation of c- and z-type product ions. Adapted from Reference [224].

5.3.2.2.2 Electron Transfer Dissociation (ETD)

Electron transfer dissociation (ETD) is based on ion-ion interactions of multiply charged peptide ions with anionic species formed from the use of electron donors (e.g., anthracene, fluoranthene, and azobenzene), allowing widely used quandrupole ion trap mass spectrometers to be amenable for use in electron-based dissociation techiniques [59]. The fragmentation mechanism of ETD is thought to be analogous to ECD, in which the free radical site introduced upon electron transfer induces non-specific cleavage of the N-Cα bond on a peptide's backbone, resulting in c- and z-type product ions, with phosphate groups or other potentially labile modifications maintained (Scheme 5.1) [59, 224]. ETD has been successfully applied for the global phosphoprotome analysis of *Saccharomyces cerevisiae* yeast [356], human embryonic kidney cells 293T [357], and human embryonic stem cells [358], with the assistance of phosphopeptide enrichment techniques.

5.3.2.2.3 Limitations of Electron Based Dissociation

ECD and ETD techniques are advantageous for characterization of protein phosphorylation due to their primary backbone cleavage and no loss of labile PTMs. However, the fragmentation efficiency of these electron based methods is highly dependent on the charge density of the precursor ions. Specifically, the electron capture cross section for ECD is proportional to the square of the ion charge [62]. In addition, even with the expected high efficiency of electron capture, limited dissociation of doubly protonated precursor ions may occur [359, 360]. Similar to ECD, the efficiency of ETD is improved by increasing charge/residue ratios. Because less

energy is released upon electron transfer to low charge density peptide ions (for example, 2+), it might not be enough energy to overcome the non-covalent interactions within the charge reduced species, resulting in electron transfer without dissociation [65, 361]. Thus, the requirement for higher-charged precursor ions compromises the ECD/ETD performance for phosphopeptide analysis because peptides with acidic phosphate groups are less likely to form multiply protonated species [224].

To overcome the non-covalent interactions within low charged peptide radical cations and to increase the extent of dissociation, activated ion-ECD (AI-ECD) has been developed which involves collisional ion heating with or following the ECD process [362]. For ETD, one of the ways to improve fragmentation of doubly charged peptide ions is the application of supplemental low-energy collisional activation to charge reduced radical cations [363, 364]. More recently, an analogous ECD+CID method has been demonstrated to improve fragmentation efficiency via performing CID on charge reduced precursor ions in ion traps [365].

5.3.2.2.4 Chemical Labeling Strategies to Enhance Phosphopeptide Identification and Characterization by Electron-Based Dissociation -MS/MS

One other way to alleviate the charge state dependence of ECD/ETD efficiencies is to increase the charge states of the peptide ions, by adding charged tags. A method was recently described for the analysis of phosphopeptides by derivatization of carboxyl groups with 1-(2-pyrimidyl) piperazine (PP), which converts acidic carboxyl groups to highly basic PP moieties, leading to higher charge states of peptide ions [366] and enhanced analysis upon ETD [367]. The benefits of fixed charge derivatization have also been demonstrated from ECD of doubly charged

precursor ions. For example, the addition of trimethyl-phenyl phosphonium cations to the N-termini of phosphorylated peptides increased the sequence coverage and simplified data interpretation upon ECD [73].

Alternatively, the addition of 0.1% *m*-nitrobenzyl alcohol (*m*-NBA) to the LC solvents promotes supercharging of phosphopeptide ions as a result of low vapor pressure and high surface tension of *m*-NBA. The subsequent ETD analysis of these highly charged precursor ions was enhanced and was reflected by increased database searching scores [368].

5.3.2.3 Photo-Dissociation (PD)

Photodissociation (PD) techniques provide an attractive alternative for peptide ion fragmentation [83, 84]. Ions in the gas phase are irradiated with UV, visible, or IR photons and thus are activated and subsequently dissociated by internal energy deposition based on the number and wavelengths of the photons absorbed. Therefore, by using tunable laser sources, selective bond cleavage may be achieved. PD techniques can be performed on a number of mass spectrometer platforms; ion trapping and time-of-flight mass spectrometer are most often used.

5.3.2.3.1 Infrared Multiphoton Dissociation (IRMPD)

Infrared multiphoton dissociation (IRMPD) employs low energy photons (~ 0.1 eV/photon) and is classified as a "slow heating" method since tens or hundreds of IR photons are required for ion dissociation [83]. Irradiation typically takes from a few milliseconds to several seconds for a continuous-wave CO_2 (10.6 μm) laser, in order to induce effective peptide amide bond

cleavage. Energy re-distribution is allowed within the IR activated ions, leading to an ergodic dissociation process and the resultant MS/MS spectra are comparable with those obtained by CID [83].

IRMPD has particular strength for the characterization of phosphopeptides, since the phosphate groups are strong chromophores for efficient absorption of 10.6 μm photons by P-O bonds [81, 329, 369]. IRMPD has been successfully applied for selective detection of phosphopeptides from mixtures, via the observation of characteristic neutral losses of the phosphate group [370-373]. In addition, the low mass cutoff associated with resonant excitation in ion traps can be circumvented by using IRMPD, allowing the observation of more product ions in the low m/z region compared to CID [373]. However, IRMPD can suffer from similar limitations to those discussed above for CID, such as the observation of dominant neutral loss of phosphate group, particularly from the dissociation of precursor ions under limited proton mobility conditions.

5.3.2.3.2 Ultraviolet Photodissociation (UV-PD)

The higher photon energy of ultraviolet light (157-355 nm; 7.9-3.5 eV) may allow single-photon fragmentation processes [84]. The energies deposited to peptide ions by UV photons are more clearly defined. By using different wavelengths of UV photons, UVPD may selectively target residue-specific chromophores such as aromatic amino acids, or common chromophores such as the peptide amide bonds. Since UVPD has not been incorporated into commercial mass spectrometers, limited studies have been applied for phosphopeptide analysis. Kim and Reilly have investigated the timescale dependence for the formation of neutral loss and sequence

product ions from UVPD of singly charged arginine-terminated phosphopeptides [374]. It was found that the neutral loss of 98 Da from precursor ions appeared at considerable abundance after only a 300 ns post-photoexcitation; however loss of 98 Da from sequence product ions was not observed until 1 μs post-photoexcitation. Thus, by using appropriate post-photoexcitation time, the characteristic neutral loss non-sequence ions as well as the sequence ions containing intact phosphate groups can be both observed, allowing phosphopeptides to be easily identified and characterized.

Site-specific dissociation at the site of the phosphorylated residues has been achieved by conversion of the phosphate group to a UV-absorbing sulfhydryl-containing naphthyl chromophore via β-elimination/Michael addition reactions (Scheme 5.2) [375]. Photodissociation of singly deprotonated or multiply protonated derivatized phosphopeptide ions at a wavelength of 266 nm led to homolytic cleavage of the C-S bond which connects the label to the peptide. The resultant highly localized radical site directs the subsequent backbone cleavage at the two sides of the original phosphorylation site(s). The formation of such site specific sequence ions allows unambiguous localization of phosphorylation site(s).

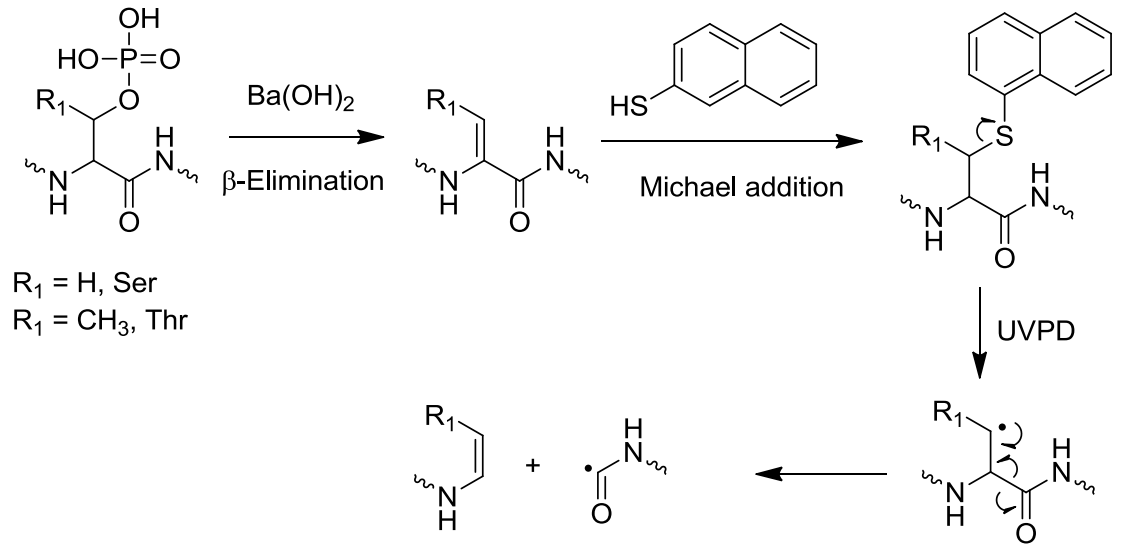

R_1 = H, Ser
R_1 = CH_3, Thr

Scheme 5.2 Phosphorylated serine and threonine peptides derivatization via β-elimination/Michael addition chemistry for introduction of a naphthyl chromophore and analysis by UVPD at 266 nm in an ion trap. Adapted from Reference [375].

Interestingly, site-specific diagnostic product ions have been recently reported from 193 nm UVPD of phosphorylated peptides in a tandem time-of-flight instrument [376]. The formation of these characteristic a_n+1-98 product ions are solely resulting from the cleavage at the phosphorylation site(s), clearly indictate that the n^{th} amino acid residue is phosphorylated. Recently, these diagnostic a_n+1-98 product ions have also been observed upon ETD-MS/MS of triply charged phosphopeptide ions, and upon fs-LID of singly charged phosphopeptide ions, suggesting the potential of these techniques for phosphorylation site assignment [326].

5.4 Quantitative Proteome Analysis

A critical task of phosphoproteomics is determination of relative changes in protein phosphorylation involved in regulating biological response to cellular perturbations [279]. There are a variety of different methods that have been developed and applied for quantitative phosphoproteome analysis, such as one- or two-dimensional gel electrophoresis based strategies using phosphorylation specific stains [377, 378]. However, the most widely employed quantitative techniques involve the incorporation of various isotopic labels into the phosphopeptides to allow quantitative measurement by MS. Phosphopeptides can be differentially isotopic labeled via metabolic labeling *in vivo* or by chemical derivatization *in vitro*. It should be noted that differentially isotopic labeled phosphopeptides should have nearly identical chemical properties (e.g., retention time) to ensure the relative abundances of their MS peaks are directly related to their abundances present in biological samples [133].

5.4.1 Metabolic Labeling Approaches for Stable Isotope Incorporation

In one commonly employed method of metabolic isotope labeling, cells are cultured in a medium with $^{15}N/^{14}N$ or $^{13}C/^{12}C$ forms of an amino acid (typically arginine or lysine), such that the differential isotope labels are incorporated when proteins are expressed by the cell [379, 380]. By this method, all peptides resulting from tryptic digestion carry at least one C-terminal labeled amino acid and the same peptides become mass distinguishable from different sample pools. This technique is generally termed Stable Isotope Labeling by Amino acids in Cell culture, i.e., SILAC. SILAC enables comparison of up to three samples in a single analysis, and has been successfully applied to the global study of phosphorylation dynamics in signaling networks of HeLa cells [282] and phosphorylation dynamics during early differentiation of human embryonic

stem cells [381]. However, SILAC and other metabolic labeling approaches are restricted to situations where cells or animal models (e.g., the SILAC mouse [382]) can be grown on labeled media and may not be directly applied to compare human tissue samples [270, 279].

5.4.2 Chemical Labeling Approaches for Stable Isotope Incorporation

A variety of chemical labeling approaches have been utilized to incorporate stable isotopes to peptides or proteins *ex vitro*. The majority of these isotope coded labeling reagents facilitate quantitative analysis via measuring the relative abundances of "light" and "heavy" labeled peptides in the mass spectra, i.e., MS-based quantitation. Reagents containing stable isotopes can be attached to common peptide functional groups such as N-terminal amino groups [383] or C-terminal carboxylic groups [260, 384]. Typically enrichment is required for target quantitative analysis of phosphoprotein using these global labeling reagents. Alternatively, phosphate groups themselves can be converted to isotopically labeled moieties via β-elimination/Michael addition reactions [112-114]. If affinity tags are also incorporated into the nucleophilic Michael addition reagents, the enrichment and quantitation of phosphorylation can be simultaneously achieved, for example by the phosphoprotein isotope-coded affinity tag (PhIAT) [100, 385] or phosphoprotein isotope-coded solid-phase tag (PhIST) [386] techniques.

An enzymatic $^{16}O/^{18}O$-labeling approach has been reported by Yao *et al.* for global isotope coding of peptides [387]. With this approach, enzymatic digestion of proteins is carried out in the presence of $H_2{}^{16}O$ or $H_2{}^{18}O$, thus the C-terminal carboxylic group of each newly generated peptide will incorporate two ^{18}O atoms for the latter case. The approach has been evaluated by

comparison of known virion proteins from two serotypes (Ad5 and Ad2) of adenovirus, showing its potential for comparative proteomic studies of complex proteins.

Due to the limitations of MS-based quantitative approaches encountered for analysis of complex protein mixture (discussed in Chapter One), MS/MS-based quantitation techniques have been developed and widely applied for phosphoprotoeme studies. The commercial available iTRAQ has become one of the most commonly used approaches due to its multiplex capability (4-plex or 8-plex). Coupled with IMAC enrichment strategies, iTRAQ has been successfully applied for quantitation of phosphotyrosine in a time resolved manner upon epidermal growth factor receptor (EGFR) activation to reveal ErbB signaling network [388]. The 8-plex iTRAQ has also been applied to longitudinal studies of protein expression, demonstrating the potential for high throughput quantitative analysis [144]. However, a reduced identification efficiency of phosphopeptides was reported recently when using isobaric tags such as iTRAQ and TMT for quantitative analysis based on the use of CID-MS/MS methods [389]. In this study, higher charge state distributions for iTRAQ or TMT labeled phosphopeptides were demonstrated. Thus, one possible reason for a decreased identification efficiency might be due to the occurrence of decreased base peak intensities after labeling, resulting in less frequent identifications of lower abundant peptides. On the other hand, due to the high proton affinity of the isobaric tags, the formation of highly abundant reporter ions from the fragmentation of labeled peptides might suppress the formation of peptide backbone derived fragments, thereby limiting the sequence information that could be obtained.

Interestingly, another MS/MS-based quantitative approach was introduced by converting the phosphate groups to phosphoramidates with the assistance of carbodiimide, followed by acid-catalyzed hydrolysis in $H_2{}^{16}O$ or $H_2{}^{18}O$ waters. Thus, the phosphate groups are regenerated with

one ^{18}O atom incorporated [390]. The direct incorporation of the isotope atoms to phosphate group allows the quantitative analysis of phosphorylation via the measurement of isotope ratios of phosphate-specific marker ions generated upon tandem parallel collision-induced dissociation mass spectrometry (p^2CID-MS) [390, 391].

5.5 Specific Aims

Numerous techniques have been developed and applied to achieve the goal of comprehensive phosphoprotome analysis. Unfortunately, no existing technique has been demonstrated to be perfect. Chemical labeling approaches have been a valuable tool to assist in the field of phosphoprotome analysis. For this reason, the major goals of the research described in the following chapter are to develop improved chemical labeling and tandem mass spectrometry methodologies for enhanced phosphoprotein identification, characterization and quantitative analysis, including:

1. Synthesis of a 'fixed charge' sulfonium ion containing peptide derivatization reagent and its isobaric isotope coded derivatives.
2. Evaluation of the effect of chemical labeling on the ionization efficiency, charge state distribution, and retention time of a range of phosphopeptides.
3. Evaluation of the multistage gas-phase fragmentation reactions of modified phosphopeptides employing collision induced dissociation (CID) and electron transfer dissociation (ETD).

4. Evaluation of the quantitative capability of isobaric isotope coded sulfonium ion reagents based on CID and ETD techniques.

CHAPTER SIX

FIXED CHARGE DERIVATIZATION FOR ENHANCED COLLISION INDUCED DISSOCIATION (CID) QUANTITATION AND ELECTRON TRANSFER DISSOCIATION (ETD) CHARACTERIZATION OF PHOSPHOPEPTIDES

6.1 Introduction

Protein phosphorylation is involved in the regulation of a wide variety of *in-vivo* biological functions. These functions are highly dependent on the locations at which proteins are phosphorylated. Commonly, phosphorylation sites are identified by tandem mass spectrometry (MS/MS), typically employing collision induced dissociation (CID) or electron transfer dissociation (ETD) as the ion activation technique. Unfortunately, unambiguous phosphate group localization by using CID-MS/MS can be hampered due to facile loss of the PTM or the potential for intrapeptide phosphate group rearrangements, particularly for low charge state precursor ions (pathway A in Scheme 6.1) [344]. ETD has an improved ability to localize phosphate groups, but can be limited in that it optimally requires the precursor ions to be highly multiply-charged (pathway B in Scheme 6.1). In addition, due to their acidic nature, the ionization efficiency of phosphopeptides is usually suppressed, limiting the sensitivity for their detection. Thus, strategies to improve the ionization efficiency of phosphopeptides by introducing positively charged tags onto phosphopeptides using chemical labeling approaches have been examined [366, 367]. Here, the development and initial application of a peptide labeling strategy (pathway C in Scheme 6.1) coupled with ESI-MS, CID-MS/MS and ETD-MS/MS are demonstrated for

the enhanced quantitation and identification of protein phosphorylation, including characterization the modification site(s).

6.2 Strategies for Phosphopeptide Analysis using DMBNHS Labeling

An amine specific sulfonium ion containing reagent DMBNHS (*S,S*′-dimethylthiobutanoylhydroxysuccinimide ester iodide) has recently been applied toward the 'targeted' identification and characterization of protein surface "active" lysine residues [170]. It has previously been shown that CID-MS/MS of DMBNHS modified peptide ions give rise to the exclusive neutral loss of dimethylsulfide ($S(CH_3)_2$; 62 Da) under low energy CID-MS/MS conditions, independently of the amino acid composition and precursor ion charge state (i.e., proton mobility) of the peptide [170]. The attributes of the DMBNHS reagent include good solution phase reactivity and specificity towards primary amines, an incorporated fixed charge sulfonium ion moiety and the characteristic gas-phase fragmentation reaction. These features suggest this reagent could be employed in the field of phosphoproteome analysis, as demonstrated in Scheme 6.1.

The results described in Chapter Three for the gas-phase fragmentation of a monolinked phosphoserine containing pep_{LpSR} (LSVPTpSDEEDEVPAPKPR) peptide formed by reaction with sulfonium ion containing cross-linking reagent, demonstrated that the specificity associated with fragmentation of the labile C-S bond adjacent to the sulfonium ion was not significantly affected by the potentially competing loss of H_3PO_4 [392]. Thus, under low energy CID-MS/MS conditions, the dissociation of DMBNHS modified phosphopeptides preferably occur at the fixed

charge sulfonium ion site, leading to the neutral loss of $S(CH_3)_2$, while the phosphate group(s) remain intact (Scheme 6.1). The number of neutral losses of $S(CH_3)_2$ observed during CID-MS/MS indicates the number of modified residues, providing information about the presence of Lys residues within the peptide; that is, besides one common modification on the peptide's N-terminus the other modification(s) are generally on lysine residues. The incorporation of "light" and "heavy" isotope labels into the DMBNHS reagent would allow the differential quantitative analysis of phosphopeptide, via the measurement of the relative abundances of "light" and "heavy" labeled neutral loss product ions generated from fragmentation of labeled phosphopeptides [19, 236]. Finally, introduction of the 'fixed charge' into the phosphopeptide may potentially lead to improved ionization efficiencies and increase the abundance of high charge state precursor ions amenable to ETD [367, 393].

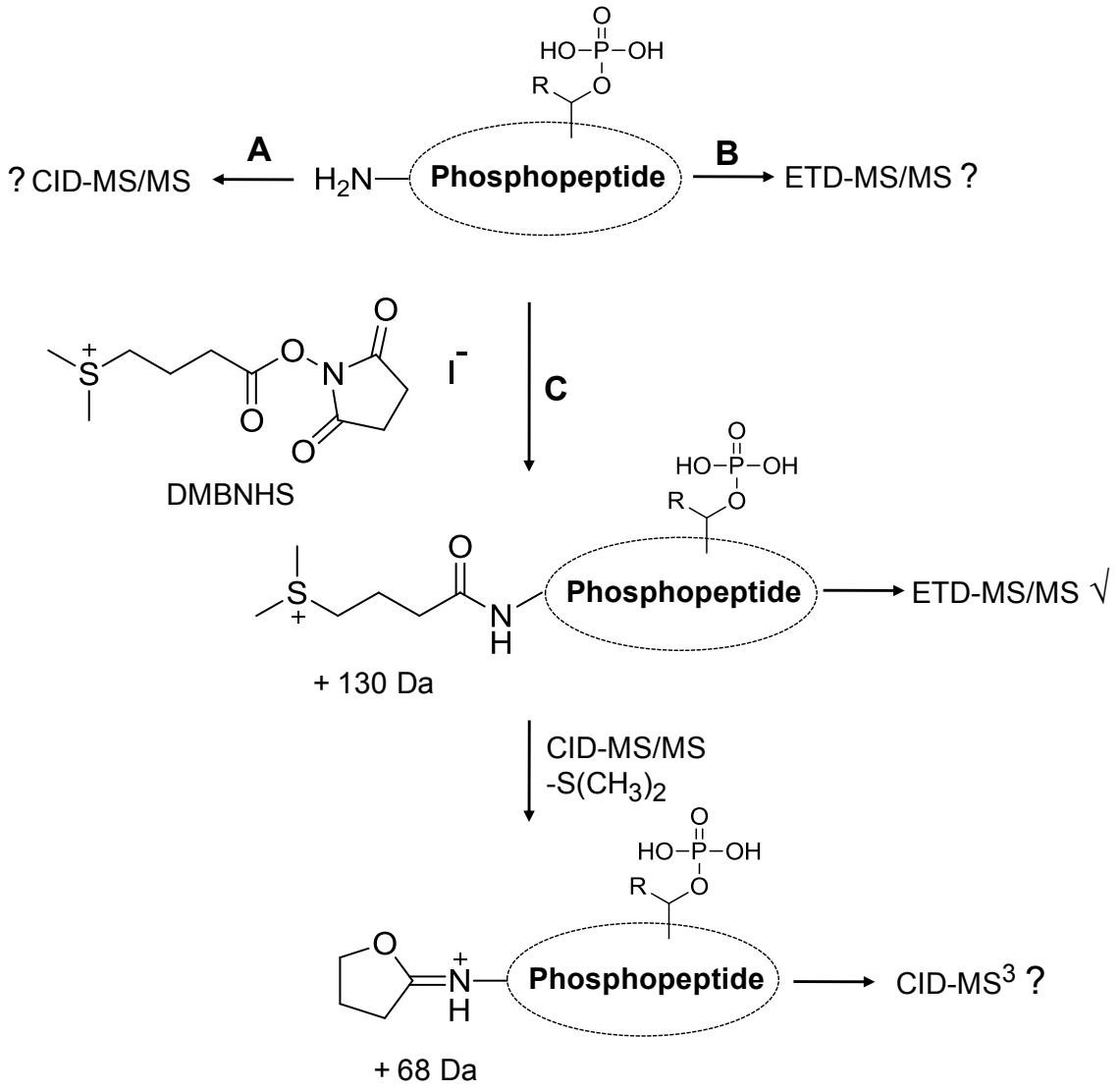

Scheme 6.1 General strategy for solution phase DMBNHS phosphopeptide labeling and gas-phase CID-MS/MS and ETD-MS/MS fragmentation of DMBNHS labeled phosphopeptide ions.

6.3 Optimization of DMBNHS Labeling Reaction Conditions

6.3.1 Effects of Phosphopeptide Concentration on Labeling Efficiency

In order to determine the optimum reaction conditions for phosphopeptides labeling using DMBNHS, the effect of the peptide concentration on labeling efficiency was first investigated. 100 μL of the synthetic phosphopeptide EDpSGTFSLGK (No. 4; Table 6.1) solution dissolved in PBS buffer at varying concentrations (100, 10, 1 and 0.25 μM peptide concentrations) was subjected to reaction with a 200-fold excess of DMBNHS. The modification was quenched after 1 hr and the reaction mixture was diluted (except for the case where the peptide concentration was 0.25 μM) and analyzed by HPLC-ESI-MS. Since phosphopeptides may contain different numbers of modifiable sites depending on the presence or absence of lysine residue, the ratios used here strictly denote the amount of reagent to the total number of primary amine groups present in phosphopeptides.

Table 6.1 Amino acid sequences of a mixture of six synthetic phosphopeptides.

Peptide No.	Sequence	Number of Potential Modification Sites
1	VIEDNEpYTAR	1
2	LNQSpSPDNVTDTK	2
3	TLSEVDpYAPAGPAR	1
4	EDpSGTFSLGK	2
5	LFTGHPEpSLER	1
6	SLSSPpTDNLELSLR	1

The base peak chromatograms obtained from HPLC-MS analysis of each of the labeled phosphopeptide are shown in Figure 6.1. Each peak was identified by analysis of the MS/MS and MS^3 product ion spectra and is discussed in detail later in this text. Phosphopeptide 4 has two potential modification sites; one is the N-terminal amino group and the other is the lysine residue at C-terminus. Complete reaction would result in a doubly modified peptide while an incomplete

labeling reaction would form two singly modified peptides with the same mass as each other, but with the modification at two different sites. Interestingly, the singly N-terminus-modified phosphopeptide 4 (4^{N}) was observed to have eluted temporally near to the unmodified peptide, whereas the singly lysine-modified phosphopeptide 4 (4^{K}) co-eluted with the doubly modified 4 ($4^{N,K}$) peptide about 1.4 min later than 4^{N}. The relative abundance of the base peak from the co-eluted species was marked in each chromatogram of Figure 6.1. It can be seen that the extent of modification decreases slightly with decreasing peptide concentration from 100 to 10 μM and then dropped sharply, even though the reagent excess was kept the same for each reaction. These results suggest that DMBNHS labeling yield is closely related to the concentration of the target amine groups.

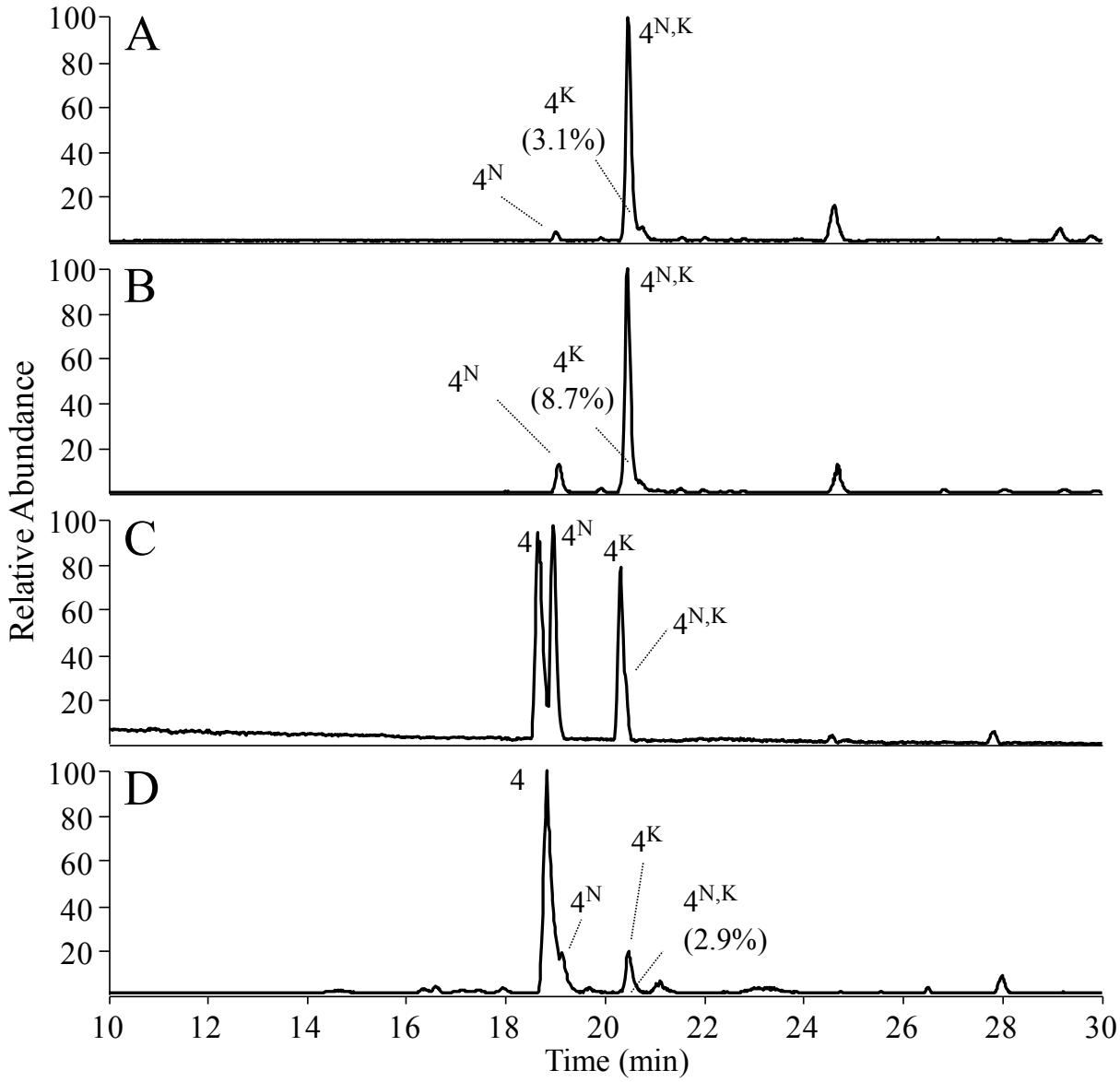

Figure 6.1 Base peak chromatograms of DMBNHS derivatized phosphopeptides EDpSGTFSLGK (No. 4) resulting from 1-hour reactions at varying peptide concentrations. (A) 100 µM, (B) 10 µM, (C) 1 µM, and (D) 0.25 µM. The ratio of reagent to primary amine group was kept at 200:1 for each reaction. The phosphopeptide is annotated by its number. A superscript "N" indicates the modification is on N-terminus of the peptide. A superscript "K" indicates the modification is on lysine residue of the peptide.

6.3.2 Optimization of Reaction Time and Molar Ratio of DMBNHS Labeling

A phosphopeptide mixture containing six synthetic phosphopeptides (No.1-6; Table 6.1) with equal concentrations dissolved in PBS buffer was used to determine the optimum reaction conditions for DMBNHS labeling. Based on the results described above, the extent of modification is highly dependent on the concentration of target amine groups, especially at low peptide concentrations. Typically, limited amounts of phosphoprotein samples can usually be obtained from sample preparation; however, the concentrations of target amine groups may be 1-2 orders higher than that of proteins after enzymatic digestion. Thus, 10 μL of phosphopeptide mix solution with concentrations of 1 μM of each peptide was subjected to derivatization using a molar ratio of 100:1 at reaction times from 15 to 60 min. Each reaction was immediately quenched then analyzed by HPLC-MS.

From the base peak chromatograms obtained from HPLC-MS analysis of each reaction shown in Figure 6.2, it was observed that most of the phosphopeptides were already modified at a reaction time as short as 15 min (Figure 6.2B). The reaction yield was slightly increased with a 30-min reaction time, but no significant improvement was observed at longer reaction times. Thus, a 30 min reaction time was applied in further studies. It should be noted that phosphopeptides containing two modifiable sites were less likely to undergo complete labeling compared to those phosphopeptides containing one modification site, which is consistent with typical reaction kinetics [394].

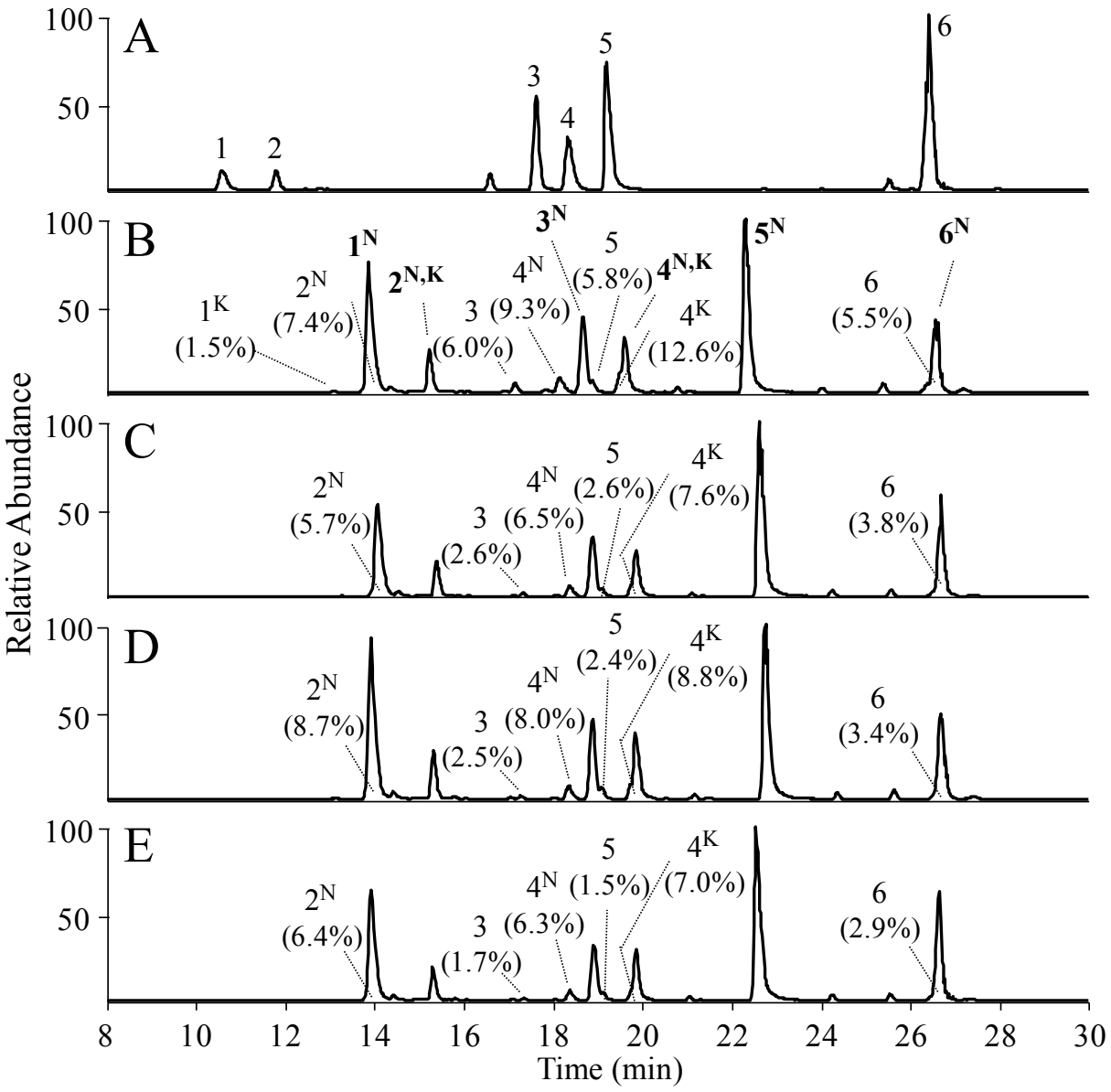

Figure 6.2 Base peak chromatograms of (A) underivatized phosphopeptide mix (No. 1-6) and derivatized phosphopeptide mix (No. 1-6, 1 μM each) using 100-fold of DMBNHS at varying reaction times of (B) 15 min, (C) 30 min, (D) 45 min, and (E) 60 min. The phosphopeptide is annotated by its number. The relative base peak abundances are indicated for low abundance or co-eluted phosphopeptides. The completely modified species are marked in bold. A superscript "N" indicates the modification is on N-terminus of the peptide. A superscript "K" indicates the modification is on lysine residue of the peptide.

The optimum molar ratio of DMBNHS to primary amino group for labeling a 6-phosphopeptide mix (No.1-6) was determined using molar ratios from 50 to 500 in a 30 min reaction. The base peak chromatograms obtained from HPLC-MS analysis of each reaction are shown in Figure 6.3. In order to monitor the change in the extent of modification with increasing molar ratios, the relative abundances of the base peak of each phosphopeptide and its derivatives are summarized in Table 6.2. Since the ionization efficiencies are different among phosphopeptide species and their labeled or partly labeled derivatives, the yields of labeling reaction for each phosphopeptide are not directly calculable. By comparing the relative abundances of peptide base peaks, the labeling reaction was observed to be essentially complete at a 200-fold molar excess of reagent to amino group, with limited improvement when using higher molar ratios. Based on these results, a 200-fold molar excess of DMBNHS reagent and a 30 min reaction period was considered suitable to satisfy the requirement for complete labeling of each of the phosphopeptides employed in this study. It is noted however, that individual peptides are expected to exhibit slightly different reactivity towards the derivatization reagent, due to differences in the pKa values of the amino functional group at each peptide.

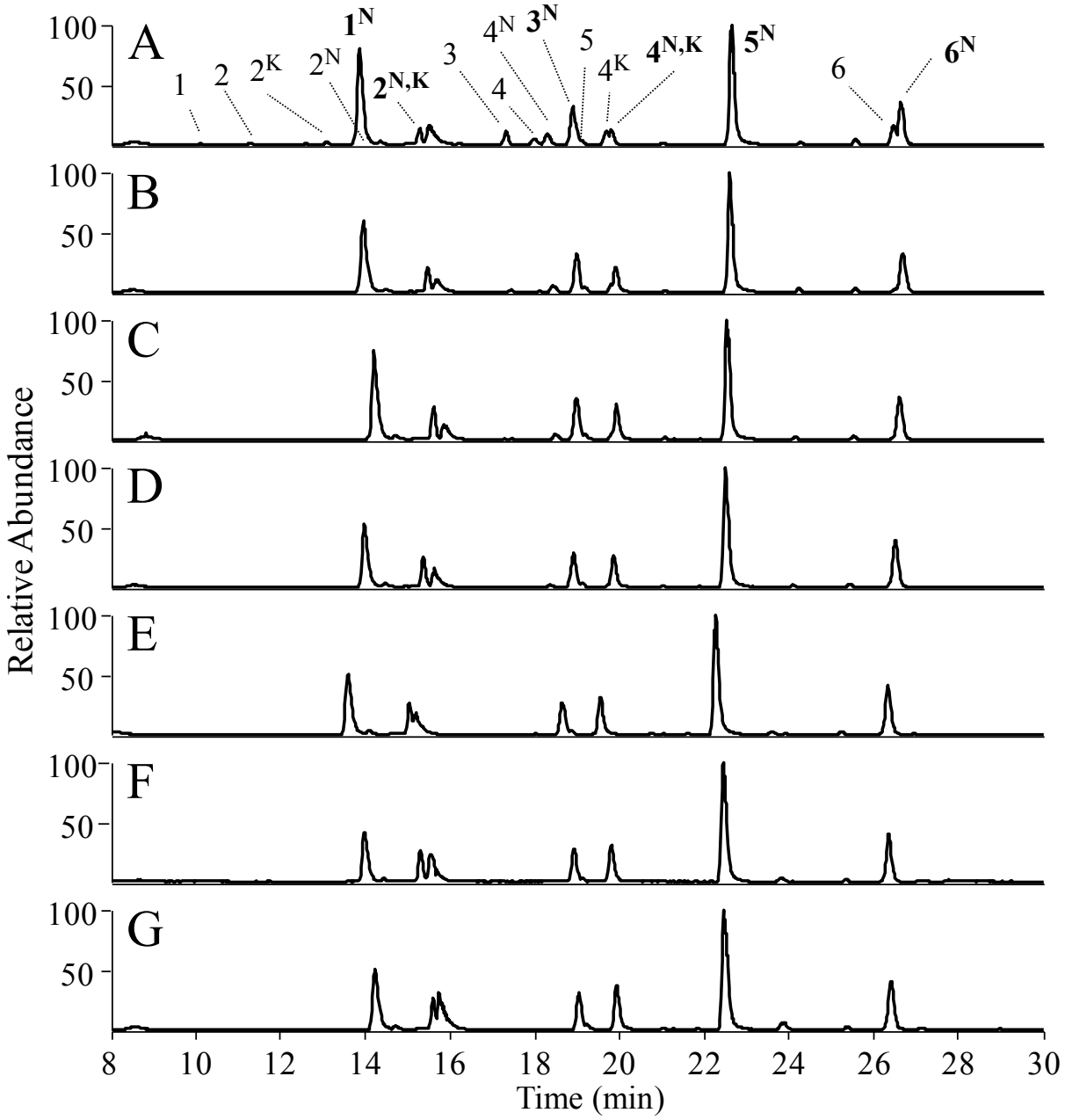

Figure 6.3 Base peak chromatograms of derivatized phosphopeptide mix (No. 1-6) using (A) 50-fold, (B) 100-fold, (C) 150-fold, (D) 200-fold, (E) 300-fold, (F) 400-fold, and (G) 500-fold excess of DMBNHS (30-min reaction). The phosphopeptide is annotated by its number. The completely modified species are marked in bold. A superscript "N" indicates the modification is on N-terminus of the peptide. A superscript "K" indicates the modification is on lysine residue of the peptide.

Table 6.2 Relative abundances obtained from base peak chromatograms of the six-phosphopeptide mixture modified with DMBNHS using various ratios.

Labeled	Part-labeled & Unlabled	DMBNHS-to-Primary Amino Group Ratio						
		50 : 1	100 : 1	150 : 1	200 : 1	300 : 1	400 : 1	500 : 1
1^{N}		81.3	60.8	75.5	52.9	51.2	42.1	50.8
	1	1.3	< 0.5	< 0.5	< 0.5	< 0.5	< 0.5	< 0.5
$2^{N,K}$		14.4	21.2	27.9	26.0	27.2	26.9	26.7
	2^{N}	12.4	6.6	6.1	3.0	1.7	1.1	1.0
	2^{K}	2.9	0.9	0.6	< 0.5	< 0.5	< 0.5	< 0.5
	2	1.6	< 0.5	< 0.5	< 0.5	< 0.5	< 0.5	< 0.5
3^{N}		32.3	32.7	35.1	29.4	27.6	28.2	32.0
	3	11.6	2.5	1.3	0.5	< 0.5	< 0.5	< 0.5
$4^{N,K}$		13.5	21.0	29.9	27.4	31.9	31.9	37.2
	4^{N}	9.8	5.8	5.0	2.4	1.2	0.8	0.6
	4^{K}	11.8	7.2	6.6	3.4	2.5	2.0	1.9
	4	5.6	1.3	0.8	< 0.5	< 0.5	< 0.5	< 0.5
5^{N}		100.0	100.0	100.0	100.0	100.0	100.0	100.0
	5	16.5	3.2	1.9	1.0	0.8	1.1	0.9
6^{N}		36.1	32.5	36.1	39.1	41.5	40.7	41.3
	6	16.5	3.5	1.8	1.0	0.6	0.6	0.7

* Six-phosphopeptide mixture with 1μM concentration of each peptide, 30-min reaction time.

** Superscript "N" indicates modification is on N-terminus of phosphopeptide. Superscript "K" indicates modification is on lysine residue of phosphopeptide. The sequences of the labeled phosphopeptides are contained in Table 6.1.

6.3.3 Picomole-Scale DMBNHS Labeling Reaction

The efficiency of DMBNHS labeling at the picomole-scale was examined using a 1 μM solution of the 6-phosphopeptide mix at volumes less than 10 μL reacted with a 100-fold excess of labeling reagent for each reaction. The base peak chromatograms following HPLC-MS analysis of each reaction are shown in Figure 6.4 and the relative abundances of base peaks of

labeled, partly labeled and unlabeled phosphopeptides are summarized in Table 6.3. Similar reaction efficiencies were observed for amounts from 8 pmol to 2 pmol for each phosphopeptide, comparable to that of the larger scale reactions under the same conditions. When the amount was 2 pmol for each phosphopeptide, the extent of labeling was slightly decreased for phosphopeptides containing one modifiable site; however there was some increase for phosphopeptides containing two modifiable sites. The observation of variances in labeling efficiencies might be related to increasing ratios of DMF volumes in reaction solutions since the volumes of peptide solution are decreased whereas DMF volume is all the 1 μL for each reaction. Although the reaction conditions require further optimization, the results shown here suggest the approach is amenable to low-picomole quantities of analyte.

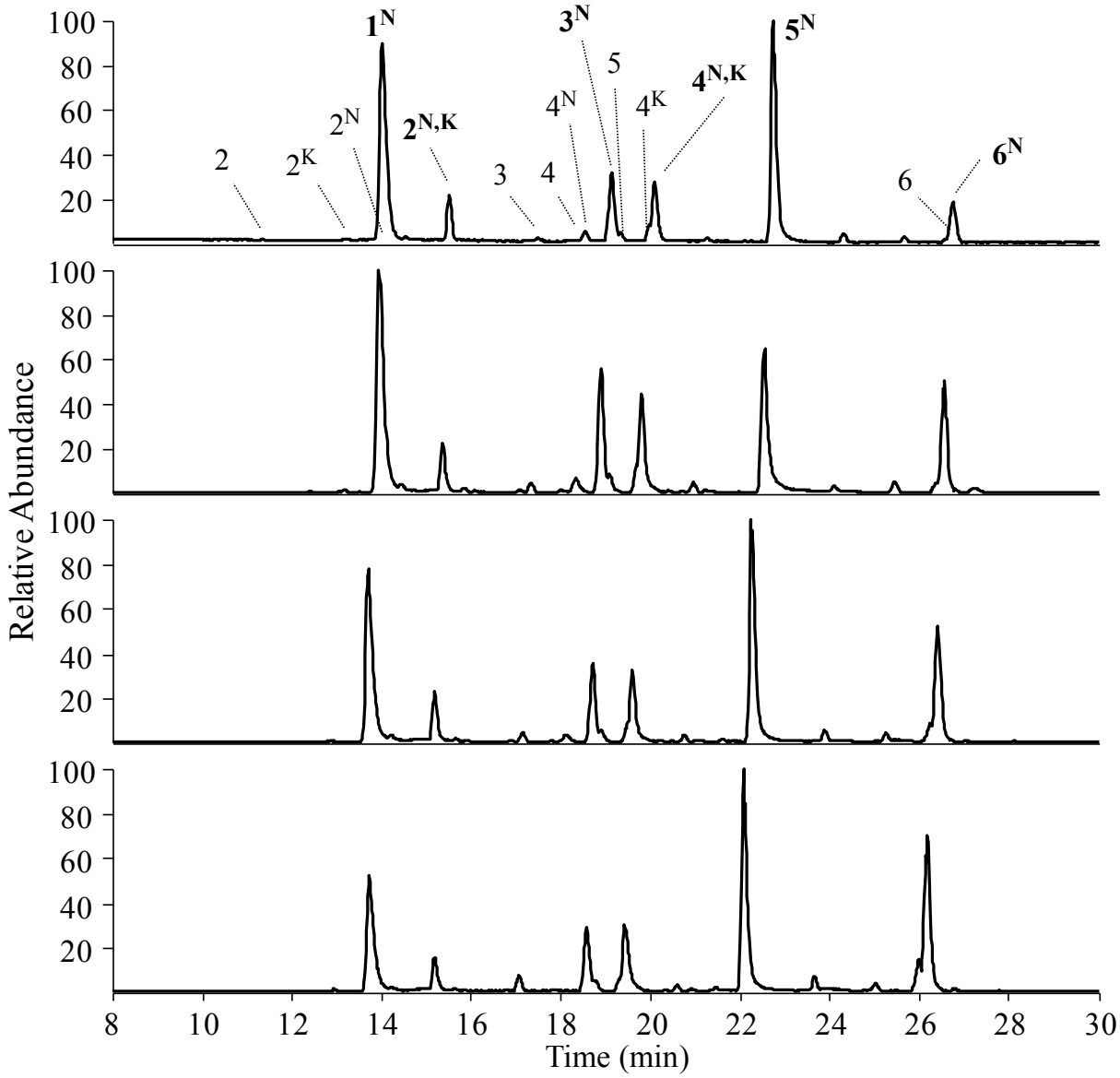

Figure 6.4 Base peak chromatograms of derivatized phosphopeptide mix (No. 1-6) using (A) 8 pmol, (B) 6 pmol, (C) 4 pmol, and (D) 2 pmol of each phosphopeptide and a 100-fold excess of DMBNHS (30-min reaction). The phosphopeptide is annotated by its number. The completely modified species are marked in bold. A superscript "N" indicates the modification is on N-terminus of the peptide. A superscript "K" indicates the modification is on lysine residue of the peptide.

Table 6.3 Relative abundances obtained from base peak chromatograms of the six-phosphopeptide mix modified with DMBNHS at low picomole quantities.

Labeled	Part-labeled & Unlabled	Six-Phosphopeptide Mix (1 μM)			
		8 pmol	6 pmol	4 pmol	2 pmol
1^{N}		90.0	100.0	77.9	52.4
	45	< 0.5	< 0.5	< 0.5	< 0.5
$2^{N,K}$		21.7	22.5	23.0	15.5
	46^{N}	7.0	8.2	3.7	< 0.5
	46^{K}	1.2	1.6	0.9	1.2
	46	< 0.5	< 0.5	< 0.5	< 0.5
3^{N}		32.0	56.0	35.8	29.0
	47	2.7	4.7	4.6	7.3
$4^{N,K}$		27.9	44.8	32.8	30.3
	48^{N}	5.8	6.9	3.5	0.6
	48^{K}	8.4	13.3	9.2	6.3
	48	1.2	1.4	0.7	< 0.5
5^{N}		100.0	65.0	100.0	100.0
	49	2.4	1.8	3.3	5.6
6^{N}		18.7	50.3	52.2	70.1
	50	2.1	4.5	8.6	14.6

* A superscipt “N” indicates modification is on N-terminus of phosphopeptide. A superscipt “K” indicates modification is on lysine residue of phosphopeptide. The sequences of the phosphopeptides are contained in Table 6.1.

6.4 Enrichment of DMBNHS Modified Phosphopeptides Using a TiO_2-Modified Membrane

The compatibility of the commonly used TiO_2-based methods for enrichment of DMBNHS modified phosphopeptides was investigated using an established TiO_2-modified Nylon membrane, the details of which are described elsewhere [395]. Briefly, a solution of 10 nmol of

phosphoangiotensin II (DRVpYIHPF) dissolved in 100 μL of PBS was modified by using 100-fold of DMBNHS. Following a 30 min reaction at room temperature, the modified phosphoangiotensin II was diluted in 4 mL of loading buffer (50% CH_3CN/50% H_2O/0.1 TFA, v/v) and 100 μL of this solution (containing 240 pmol of peptide) was passed through a TiO_2-modified Nylon membrane (0.02 cm^2 total working area) at a flow rate of 10 μL/min. The membrane was washed with 100 μL of washing buffer (same as the loading buffer) at a flow rate of 10 μL/min, and the bound peptides were then eluted from the membrane with 10 μL of 1 % NH_4OH in 50% CH_3CN / 50% H_2O (pH=10.9) at a flow rate of 2 μL/min.

To evaluate the recoveries of the modified phosphopeptides, the relative abundance of DMBNHS modified angiotensin II was measured by MALDI-MS before and after passing the solution through the membrane. D_3-DMBNHS labeled angiotensin II was used as an internal standard and was spiked into the sample immediately before the addition of MALDI matrix on plate, which is 0.5 μL of a 2,5-DHB solution (10 mg/mL in 50% CH_3CN/50 % H_2O/0.1% TFA v/v). From a triplicate measurement using different laser spots, an average recovery of 90.9 ± 1.9 % was obtained, suggesting the TiO_2-based methods are amenable to the enrichment of DMBNHS modified phosphopeptides.

6.5 ESI-MS Ionization Efficiency and Charge State Distribution upon Fixed Charge Derivatization

In order to evaluate the effect of DMBNHS labeling on ionization efficiency, the 6-phosphopeptide mix solution (No. 1-6) was modified with a 200-fold excess of DMBNHS reagent and then mixed with an equal amount of each of the underivatized phosphopeptide prior to injection of the sample for HPLC-MS analysis, following the approach described in Chapter Seven. The relative abundances of each phosphopeptide in underivatized and derivatized form are displayed in Figure 6.5, in an order corresponding to the increasing retention times of the underivatized species. An enhancement in total ionization efficiency (summed from all observed charge states) was observed from all six phosphopeptides present in the mixture; triplicate HPLC-MS analyses were found to result in less than 20% variation for each phosphopeptide in ionization efficiencies. Notably, the extent of the increased ionization efficiency was not the same for each phosphopeptide. For example, the total ionization efficiency increased 13-fold for phosphopeptide 1 (VIEDNEpYTAR) upon labeling, whereas less than a 2-fold enhancement was observed for phosphopeptides 3, 5 and 6. Compared to other phosphopeptides, phosphopeptide 1 exhibited an earlier retention time from a reverse-phase C18 column; evidently, the magnitude of enhancement in ionization efficiency upon DMBNHS labeling is related to a phosphopeptide's hydrophobicity, which will be discussed later in this text. Similar theoretical pI values were calculared for these six peptides using Compute pI/Mw tool (http://ca.expasy.org/tools/pi_tool.html), suggesting that acidity/basicity of the peptide doesn't play a significant role in affecting peptide ionization efficiencies by DMBNHS labeling.

An important aspect of the derivatization strategy is that the attachment of fixed charge sulfonium ion(s) to the phosphopeptides allows the peptide charge state distribution to be increased. This is reflected not only by the observation of increased high charge state peptide ion abundances, but also by the appearance of higher charge states which are not observed for the

unmodified phosphopeptides. For phosphopeptides 3, 5 and 6, the observed charge states did not change from labeling; however, there was a great enhancement in the relative abundances of the highest charge state present, i.e., triply charged peptide ions. Interestingly for phosphopeptides 1, 2 and 4, triply charged precursor ions were only observed for the labeled forms.

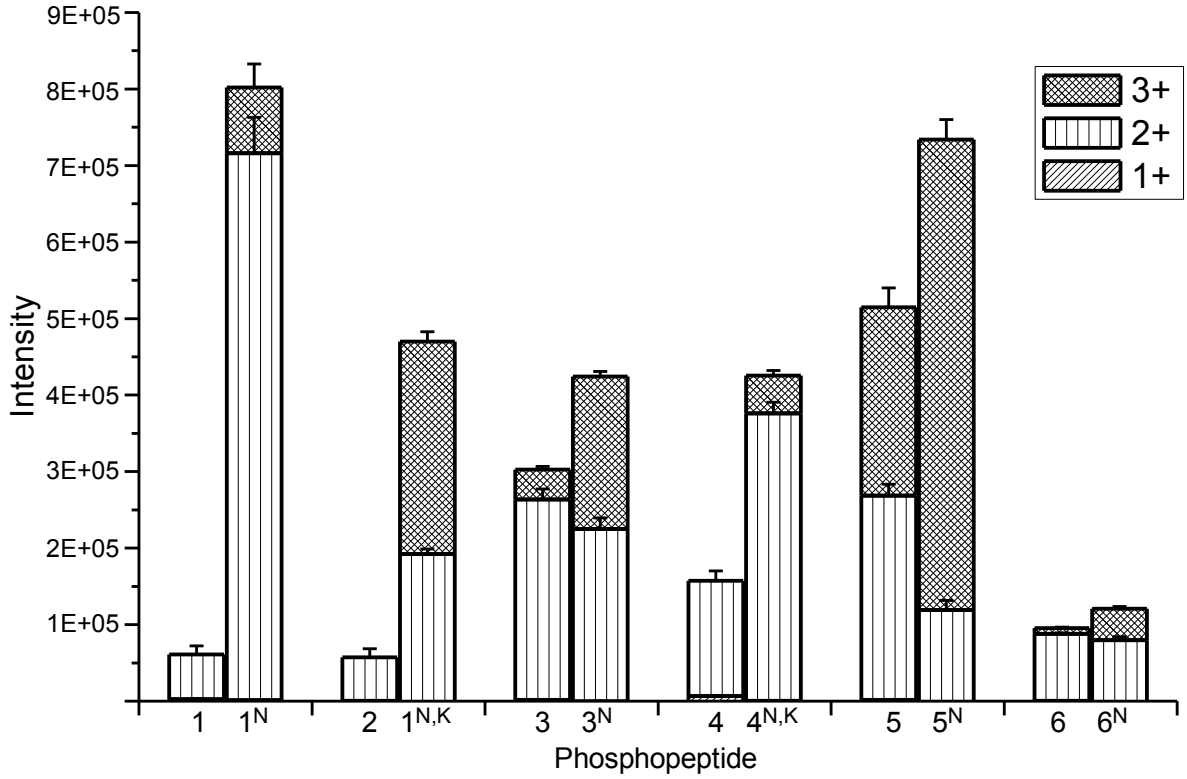

Figure 6.5 The ionization efficiency and charge state distribution of fixed charge labeled and unlabeled phosphopeptides following HPLC-MS analysis in triplicates. A superscript "N" indicates the modification is on N-terminus of the peptide. A superscript "K" indicates the modification is on lysine residue of the peptide. Error bars are shown as +SD. The sequences of the phosphopeptides are contained in Table 6.1.

To further examine the effectiveness of the DMBNHS labeling approach to enhance ionization efficiency and charge state distribution, 44 additional synthetic phosphopeptides were modified and mixed with equal amounts of underivatized phosphopeptides prior to injection for

HPLC-MS analysis. To avoid signal suppression among the co-eluted phosphopeptides, the 44 peptides were divided into 10 groups for modification reactions (some peptides were present in multiple mixtures in order to evaluate inter-sample variances), as described in Chapter Seven. The relative abundances of all the observed charge states from both unlabeled and labeled phosphopeptides are plotted in Figure 6.6 and summarized in Table 6.4, in order of increasing retention times of the unlabeled phosphopeptides from the reverse phase C18 column. These phosphopeptide sequences were selected as representative of a typical tryptic digest and cover a range of characteristics in terms of the type and number of phosphorylation sites, peptide mass, peptide charge states, potential for missed cleavages, etc. Of these phosphopeptides, an average 2.5-fold increase in total ionization efficiency was observed; a 1.8-fold enhancement for singly modified phosphopeptides (26 of 44), and a 3.5-fold enhancement for doubly modified species (18 of 44) was observed, suggesting an accumulation effect from multiple fixed charges.

Figure 6.6 Ionization efficiencies and charge state distributions of 44 phosphopeptides using fixed charge labeling following HPLC-MS analysis. The identities of the phosphopeptides are annotated by their numbers. The unlabeled peptide results are shown on the left hand side and the labeled peptide results are shown on the right hand side, for each peptide.

Figure 6.6 (cont'd)

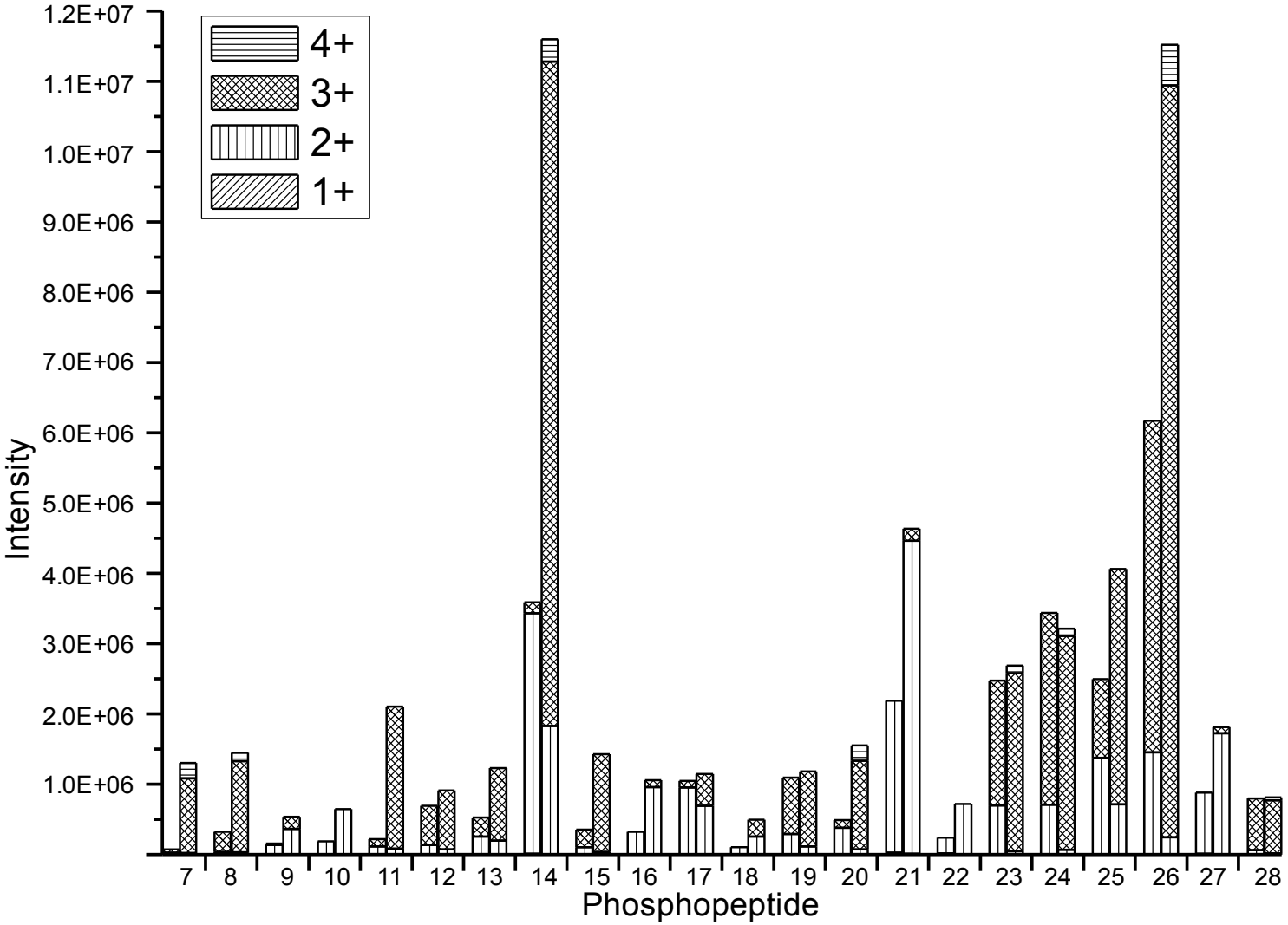

Figure 6.6 (cont'd)

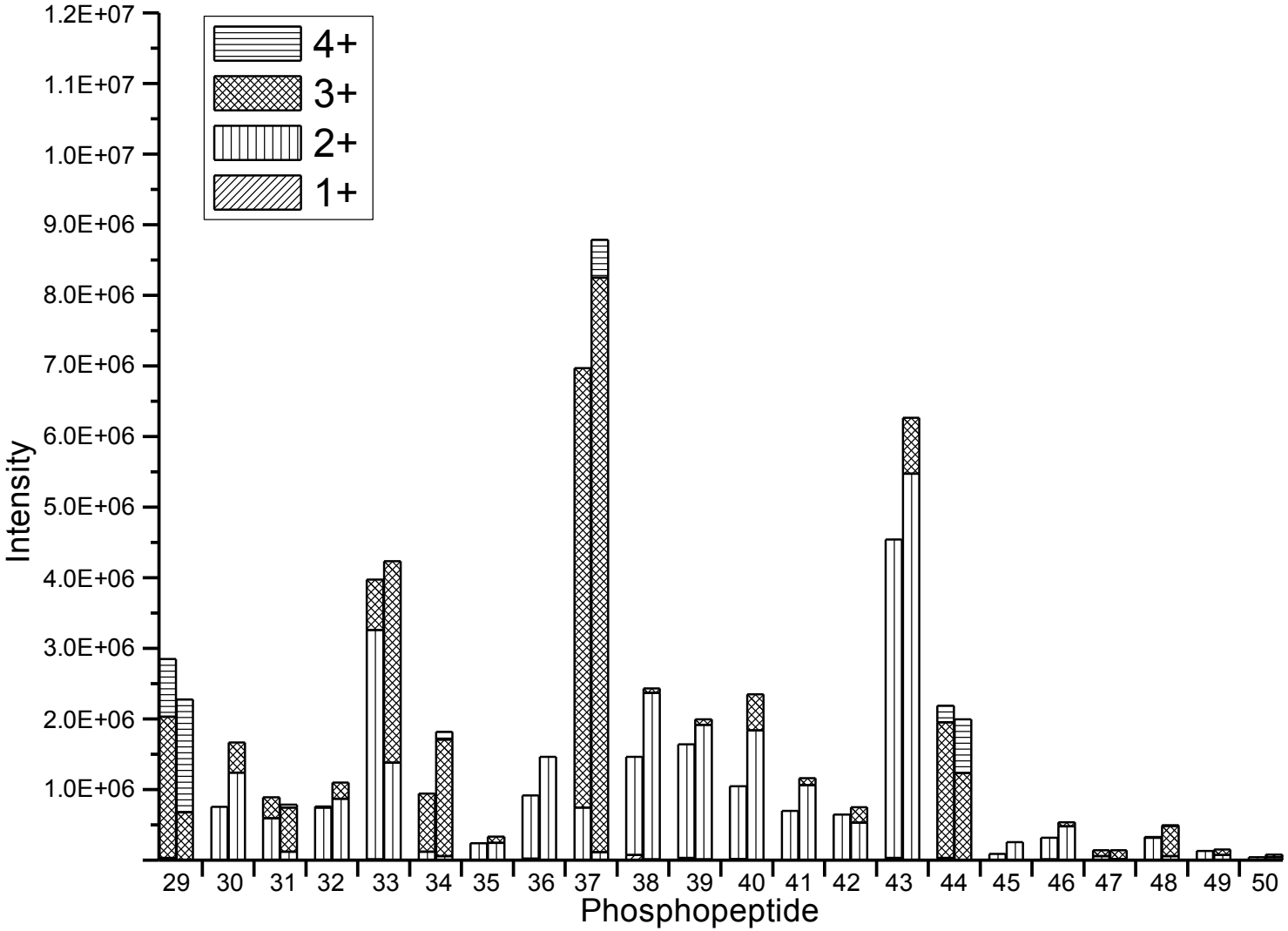

Table 6.4 Sequences and relative abundances of 44 unlabeled phosphopeptides and their fixed charge labeled counterparts following HPLC-MS analysis. The phosphopeptides are listed following the order of the retention times of their unlabeled forms. The ratio is the summed relative abundance of the labeled phosphopeptide to that of the unlabeled counterpart. A superscript "N" indicates the modification is on the N-terminus of the peptide. A superscript "N,K" indicates the modifications are on both the N-terminus and lysine residue of the peptide. N.D. = not detected.

Table 6.4 (cont'd)

No.	Sequence	Intensity					
		1+	2+	3+	4+	SUM	Ratio
7	ETEEQDpSDSAEQGDPAGEGK	0.00E+00	2.35E+04	4.77E+04	0.00E+00	7.12E+04	18.30
$7^{N,K}$		0.00E+00	2.17E+04	1.06E+06	2.21E+05	1.30E+06	
8	HGpSFVNKPTR	0.00E+00	3.70E+04	2.86E+05	0.00E+00	3.23E+05	4.49
$8^{N,K}$		0.00E+00	2.90E+04	1.30E+06	1.21E+05	1.45E+06	
9	ASGpSENEGDYNPGR	1.46E+02	1.36E+05	2.02E+04	0.00E+00	1.56E+05	3.43
9^{N}		0.00E+00	3.65E+05	1.72E+05	0.00E+00	5.37E+05	
10	NpYVTPVNR	2.05E+03	1.88E+05	0.00E+00	0.00E+00	1.90E+05	3.41
10^{N}		1.12E+03	6.47E+05	0.00E+00	0.00E+00	6.48E+05	
11	ApSPSLERPEK	2.53E+02	1.12E+05	1.04E+05	0.00E+00	2.16E+05	9.72
$11^{N,K}$		0.00E+00	8.25E+04	2.02E+06	0.00E+00	2.10E+06	
12	GpSPTRPNPPVR	3.46E+02	1.34E+05	5.59E+05	0.00E+00	6.93E+05	1.31
12^{N}		0.00E+00	7.42E+04	8.35E+05	0.00E+00	9.09E+05	
13	pSPQRPGWSR	5.34E+02	2.57E+05	2.68E+05	0.00E+00	5.26E+05	2.34
13^{N}		0.00E+00	2.00E+05	1.03E+06	0.00E+00	1.23E+06	
14	AEAPpSSPDVAPAGK	1.12E+04	3.42E+06	1.58E+05	0.00E+00	3.59E+06	3.23
$14^{N,K}$		0.00E+00	1.83E+06	9.45E+06	3.19E+05	1.16E+07	
15	pSDSELNNEVAARK	0.00E+00	1.04E+05	2.50E+05	0.00E+00	3.54E+05	4.04
$15^{N,K}$		0.00E+00	3.84E+04	1.39E+06	0.00E+00	1.43E+06	

Table 6.4 (cont'd)

No.	Sequence	Intensity					
		1+	2+	3+	4+	SUM	Ratio
16	ApSDLEDEESAAR	1.53E+03	3.23E+05	0.00E+00	0.00E+00	3.25E+05	3.26
16^{N}		2.08E+03	9.57E+05	9.86E+04	0.00E+00	1.06E+06	
17	PSApSPGDAGEQAIR	2.09E+03	9.52E+05	9.44E+04	0.00E+00	1.05E+06	1.09
17^{N}		0.00E+00	6.94E+05	4.53E+05	0.00E+00	1.15E+06	
18	pSQGGEEEGPLSDK	4.64E+02	1.03E+05	0.00E+00	0.00E+00	1.03E+05	4.78
$18^{N,K}$		0.00E+00	2.53E+05	2.42E+05	0.00E+00	4.95E+05	
19	pSPNNEGDVHFSR	0.00E+00	2.94E+05	7.99E+05	0.00E+00	1.09E+06	1.08
19^{N}		0.00E+00	1.12E+05	1.07E+06	0.00E+00	1.18E+06	
20	SApSSDTSEELNSQDSPPK	4.27E+02	3.78E+05	1.10E+05	0.00E+00	4.88E+05	3.17
$20^{N,K}$		0.00E+00	7.33E+04	1.26E+06	2.17E+05	1.55E+06	
21	pSNQIPTEVR	2.86E+04	2.16E+06	0.00E+00	0.00E+00	2.19E+06	2.12
21^{N}		1.30E+04	4.45E+06	1.71E+05	0.00E+00	4.63E+06	
22	DVYLpSPR	1.50E+04	2.25E+05	0.00E+00	0.00E+00	2.40E+05	2.99
22^{N}		2.96E+03	7.14E+05	0.00E+00	0.00E+00	7.17E+05	
23	SGSpSQELDVKPpSASPQER	0.00E+00	6.96E+05	1.78E+06	0.00E+00	2.48E+06	1.09
$23^{N,K}$		0.00E+00	4.58E+04	2.53E+06	1.13E+05	2.69E+06	
24	SGpSpSQELDVKPSASPQER	0.00E+00	7.09E+05	2.73E+06	0.00E+00	3.44E+06	0.93
$24^{N,K}$		0.00E+00	6.83E+04	3.04E+06	1.06E+05	3.21E+06	

Table 6.4 (cont'd)

No.	Sequence	Intensity					
		1+	2+	3+	4+	SUM	Ratio
25	pSFEEEGEHLGSR	3.66E+03	1.37E+06	1.12E+06	0.00E+00	2.49E+06	1.63
25^{N}		9.81E+02	7.10E+05	3.35E+06	0.00E+00	4.06E+06	
26	VGEEEHVpYSFPNK	3.22E+03	1.45E+06	4.72E+06	0.00E+00	6.17E+06	1.87
$26^{N,K}$		0.00E+00	2.44E+05	1.07E+07	5.79E+05	1.15E+07	
27	GDEpSLDNLDSPR	1.10E+04	8.68E+05	0.00E+00	0.00E+00	8.79E+05	2.06
27^{N}		2.61E+03	1.72E+06	9.17E+04	0.00E+00	1.81E+06	
28	DAHDVSPTSpTDpTEAQLTVER	0.00E+00	6.16E+04	7.34E+05	0.00E+00	7.96E+05	1.02
28^{N}		0.00E+00	1.69E+04	7.52E+05	4.36E+04	8.13E+05	
29	ALSGRApSPVPAPSSGLHAAVR	0.00E+00	3.25E+04	2.00E+06	8.14E+05	2.85E+06	0.80
29^{N}		0.00E+00	3.21E+03	6.75E+05	1.60E+06	2.28E+06	
30	ApSGVTVNDEVIK	4.81E+03	7.53E+05	0.00E+00	0.00E+00	7.58E+05	2.20
$30^{N,K}$		0.00E+00	1.24E+06	4.29E+05	0.00E+00	1.67E+06	
31	PpSPEADAPVLGSPEK	1.37E+03	5.91E+05	2.96E+05	0.00E+00	8.88E+05	0.88
$31^{N,K}$		0.00E+00	1.18E+05	6.25E+05	4.32E+04	7.86E+05	
32	VQIpSPDSGGLPER	2.32E+03	7.45E+05	1.48E+04	0.00E+00	7.62E+05	1.44
32^{N}		0.00E+00	8.70E+05	2.28E+05	0.00E+00	1.10E+06	
33	pYATPQVIQAPGPR	1.26E+04	3.25E+06	7.12E+05	0.00E+00	3.97E+06	1.06
33^{N}		2.54E+03	1.38E+06	2.85E+06	0.00E+00	4.23E+06	

Table 6.4 (cont'd)

No.	Sequence	Intensity					
		1+	2+	3+	4+	SUM	Ratio
34	DAHDVpSPTSpTDTEAQLTVER	0.00E+00	1.19E+05	8.22E+05	0.00E+00	9.41E+05	1.93
34^{N}		0.00E+00	5.88E+04	1.65E+06	1.09E+05	1.82E+06	
35	PGWAGMAApSSGSR	2.07E+03	2.37E+05	0.00E+00	0.00E+00	2.39E+05	1.38
35^{N}		0.00E+00	2.45E+05	8.61E+04	0.00E+00	3.31E+05	
36	LGpSVDSFER	1.90E+04	8.99E+05	0.00E+00	0.00E+00	9.18E+05	1.60
36^{N}		5.72E+03	1.46E+06	0.00E+00	0.00E+00	1.47E+06	
37	LSVPTpSDEEDEVPAPKPR	0.00E+00	7.47E+05	6.22E+06	0.00E+00	6.97E+06	1.26
$37^{N,K}$		0.00E+00	1.12E+05	8.14E+06	5.34E+05	8.79E+06	
38	pSPLQSVVVR	7.52E+04	1.39E+06	0.00E+00	0.00E+00	1.47E+06	1.66
38^{N}		1.07E+04	2.36E+06	6.22E+04	0.00E+00	2.43E+06	
39	pSGEGEVSGLMR	3.05E+04	1.61E+06	0.00E+00	0.00E+00	1.64E+06	1.22
39^{N}		8.59E+03	1.91E+06	7.52E+04	0.00E+00	1.99E+06	
40	pSPGAPGPLTLK	1.44E+04	1.03E+06	0.00E+00	0.00E+00	1.04E+06	2.25
$40^{N,K}$		0.00E+00	1.84E+06	5.09E+05	0.00E+00	2.35E+06	
41	NLpSPGAVESDVR	3.43E+03	6.94E+05	0.00E+00	0.00E+00	6.97E+05	1.67
41^{N}		0.00E+00	1.06E+06	1.02E+05	0.00E+00	1.16E+06	
42	NDpSGEENVPLDLTR	4.32E+03	6.44E+05	0.00E+00	0.00E+00	6.48E+05	1.16
42^{N}		0.00E+00	5.30E+05	2.20E+05	0.00E+00	7.50E+05	

Table 6.4 (cont'd)

No.	Sequence	Intensity					
		1+	2+	3+	4+	SUM	Ratio
43	ApSLEDAPVDDLTR	3.27E+04	4.51E+06	0.00E+00	0.00E+00	4.54E+06	1.38
43^{N}		5.25E+03	5.47E+06	7.90E+05	0.00E+00	6.27E+06	
44	LGHPEALSAGpTGSPQPPSFTYAQQR	0.00E+00	3.09E+04	1.92E+06	2.35E+05	2.19E+06	0.91
44^{N}		0.00E+00	5.27E+03	1.23E+06	7.57E+05	1.99E+06	
45	pSLGLDINMDSR	1.82E+03	8.43E+04	0.00E+00	0.00E+00	8.61E+04	2.97
45^{N}		0.00E+00	2.56E+05	0.00E+00	0.00E+00	2.56E+05	
46	ASpSLEDLVLK	8.12E+03	3.07E+05	0.00E+00	0.00E+00	3.15E+05	1.70
$46^{N,K}$		0.00E+00	4.79E+05	5.60E+04	0.00E+00	5.35E+05	
47	pSVNEALNHLLTEK	0.00E+00	5.66E+04	8.35E+04	0.00E+00	1.40E+05	1.00
$47^{N,K}$		0.00E+00	1.38E+04	1.27E+05	0.00E+00	1.41E+05	
48	SLGVLPFTLNSGpSPEK	1.13E+03	3.15E+05	1.03E+04	0.00E+00	3.26E+05	1.51
$48^{N,K}$		0.00E+00	5.91E+04	4.26E+05	7.99E+03	4.93E+05	
49	pSLPVSVPVWGFK	8.10E+02	1.31E+05	0.00E+00	0.00E+00	1.32E+05	1.13
$49^{N,K}$		0.00E+00	7.24E+04	7.62E+04	0.00E+00	1.49E+05	
50	AFLpSPPTLLEGPLR	0.00E+00	4.34E+04	0.00E+00	0.00E+00	4.34E+04	1.76
50^{N}		0.00E+00	3.96E+04	3.67E+04	0.00E+00	7.63E+04	

Further analysis of the data in Table 6.4 revealed an increased charge state distribution for all labeled phosphopeptides. It was determined that higher charge states appeared in 25 of 44 labeled phosphopeptides. For example, only singly and doubly charged species of phosphopeptide 40 (pSPGAPGPLTLK) were observed before derivatization (Figure 6.7 A). In contrast, the doubly modified phosphopeptide 40 resulted in a significant triply charged species and a 1.8-fold increase in the relative abundance of the doubly charged ion (Figure 6.7 B). Similarly, the appearance of the quadruply charged state and an enhancement in ionization efficiency of the triply charged ion was observed for labeled phosphopeptide 26 (VGEEEHVpYSFPNK) (Figure 6.7 D) compared to the unlabeled species (Figure 6.7 C). Although for a small number of the labeled phosphopeptides the appearance of higher charge states or increases in summed ionization efficiencies were not observed compared to the unlabeled species, enhanced relative abundances of the highest observable charge states were still achieved, as shown in Figure 6.8. In order to evaluate the charge state distributions before and after modification, the percentage of each charge state was calculated and averaged for labeled and unlabeled phosphopeptide species; the data listed in Table 6.5 indicate a dramatic shift towards higher charge states after labeling. Similar calculations were carried out separately for singly and doubly modified phosphopeptides (Table 6.6 and 6.7), and the results indicated that a double-modification was more effective than a single-modification to improve charge state distribution, which is consistent with the results described above regarding ionization efficiency.

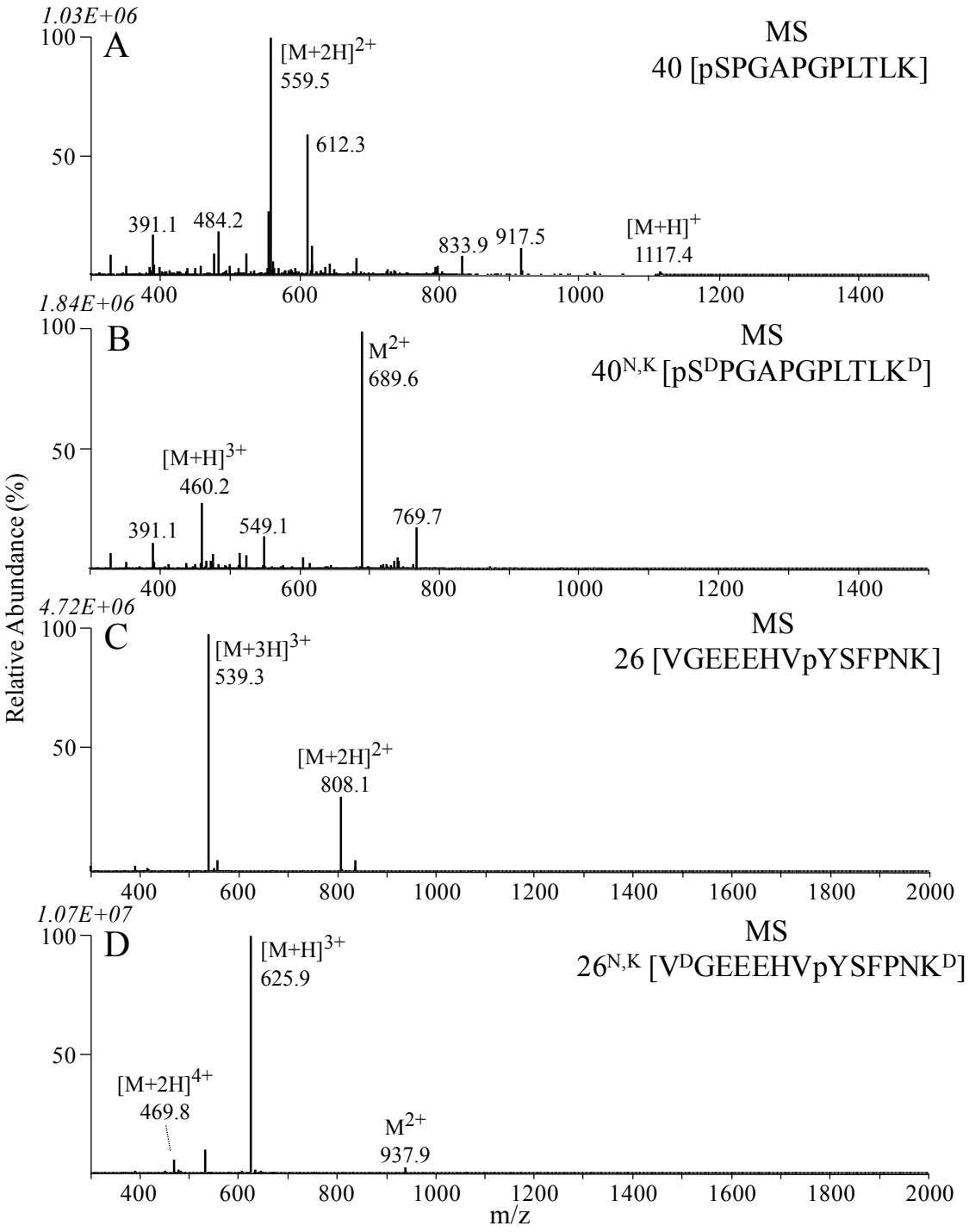

Figure 6.7 ESI-MS spectra of (A) native and (B) doubly modified phosphopeptide pSPGAPGPLTLK (No. 40), and (C) native and (D) doubly modified phosphopeptide VGEEEHVpYSFPNK (No. 26). A superscript "D" indicates the fixed charge modification. A superscript "N,K" indicates the modifications are on N-terminus and lysine residue of the peptide.

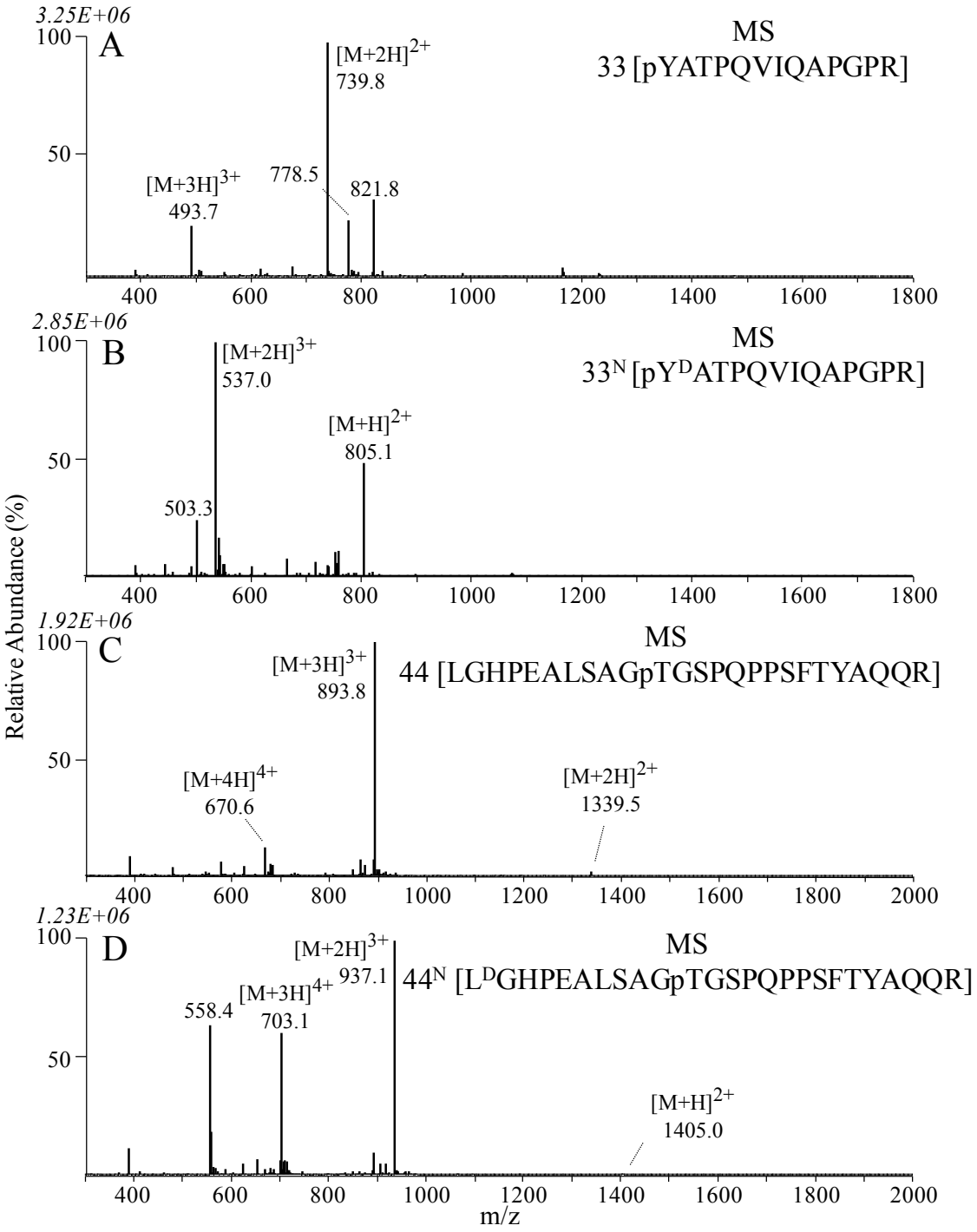

Figure 6.8 ESI-MS spectra of (A) native and (B) singly modified phosphopeptide pYATPQVIQAPGPR (No. 33), and (C) native and (D) singly modified phosphopeptide LGHPEALSAGpTGSPQPPSFTYAQQR (No. 44). A superscript "D" indicates the fixed charge modification. A superscript "N" indicates the modification is on N-terminus of the peptide.

Table 6.5 Average % charge state distribution from native and labeled phosphopeptides.

44 Phosphopeptides	Average %			
	1+	2+	3+	4+
Unlabeled	0.73 ± 1.28*	67.84 ± 36.56	30.53 ± 35.74	0.89 ± 4.57
Labeled	0.06 ± 0.13	44.60 ± 39.82	51.08 ± 36.95	4.03 ± 12.18
Ratio (Labeled/Unlabeled)	0.082	0.66	1.67	4.51

* ± Errors are expressed as standard deviations.

Table 6.6 Average % charge state distribution from native and labeled phosphopeptides containing one modifiable site.

Phosphopeptides containing 1 modifiable site (26)	Average %			
	1+	2+	3+	4+
Unlabeled	0.98 ± 1.54*	73.31 ± 37.03	24.20 ± 34.99	1.51 ± 5.91
Labeled	0.10 ± 0.16	59.45 ± 39.18	35.85 ± 34.82	4.78 ± 15.64
Ratio (Labeled/Unlabeled)	0.10	0.81	1.48	3.16

* ± Errors are expressed as standard deviations.

Table 6.7 Average % charge state distribution from native and labeled phosphopeptides containing two modifiable sites.

Phosphopeptides containing 2 modifiable sites (18)	Average %			
	1+	2+	3+	4+
Unlabeled	0.37 ± 0.65*	59.95 ± 35.38	39.68 ± 35.79	0.00 ± 0.00
Labeled	0.00 ±0.00	23.16 ± 30.47	73.08 ± 28.34	2.99 ±4.39
Ratio (Labeled/Unlabeled)	0.00	0.39	1.84	

* ± Errors are expressed as standard deviations.

It was noted that during HPLC-MS analysis, the DMBNHS labeled phosphopeptides (41 of 44) generally had longer retention times than their unlabeled counterparts, suggesting an increased hydrophobicity resulting from fixed charge labeling. This is probably due to the elongated carbon chain attached on the initial primary amine group since amine groups also carry a 'fixed charge' (i.e., a protonated ammonium group) under acidic mobile phase conditions. It was also observed that earlier-eluting phosphopeptides demonstrated a greater enhancement in ionization efficiency compared to later-eluting ones. For example, for phosphopeptides 7 (ETEEQDpSDSAEQGDPAGEGK) and 50 (AFLpSPPTLLEGPLR), which are the first and last eluted from the reverse phase C18 column among the 44 peptides examined here, the doubly modified peptide 7 experienced an 18.3-fold increase in total ionization efficiency; however, there was only a 1.76-fold increase for the singly modified peptide 50. An attempt to investigate the relationship between the potential for enhanced ionization efficiency by fixed charge DMBNHS labeling and peptide retention time is shown in Figure 6.9. In Figure 6.9, the y-axis shows the ratio of the summed relative abundances of the labeled and unlabeled phosphopeptides, while the x-axis is the retention time of the native phosphopeptides eluting from the reverse phase C18 column. A clear trend was observed in that the less-retained phosphopeptides tended to demonstrate greater improvements in ionization efficiency following fixed charge labeling. This enhancement of ionization trends downward with retention time until a minimum is reached at a roughly 2-fold increase. Typically, there is a linear relationship between peptide retention time in RP-HPLC and its hydrophobicity index [396]; hence, it may be concluded that the more hydrophilic phosphopeptides tend to be more effective for improved ionization efficiency by fixed charge DMBNHS labeling.

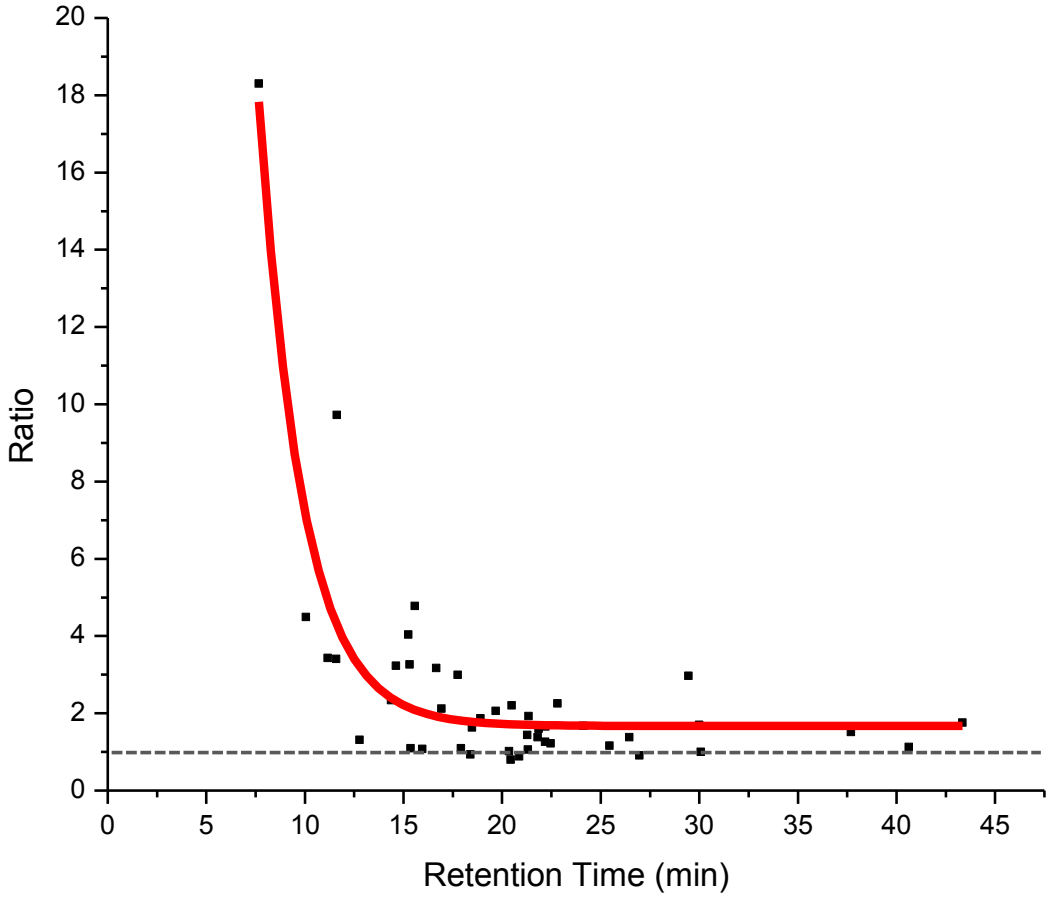

Figure 6.9 Plot of the ratio of total ion yields for DMBNHS labeled and unlabeled phosphopeptides versus the retention time of unlabeled phosphopeptides eluted from reverse phase C18 column. The trend line is simulated by Boltzmann fit, $R^2 = 0.80642$.

Thus, the contribution of DMBNHS derivatization to improved peptide ionization efficiency and charge state distribution is not due to the presence of the positively charged sulfonium ion, but also from the presence of the hydrophobic propyl chain within the tag attached to the modified amino group [397, 398]. In addition, due to their typical longer retention times, the labeled phosphopeptides are present in soluents containing a higher fraction of organic

solvent compared to their unlabeled forms, which also facilitates improved ESI efficiencies [399-401].

6.6 Fixed Charge Derivatization for Enhanced Collision Induced Dissociation (CID) and Electron Transfer Dissociation (ETD) Characterization of Phosphopeptide Ions

6.6.1 CID-MS/MS and -MS^3 Analysis of DMBNHS Labeled Phosphopeptides

Peptides were mass analyzed as they eluted from the column and entered the mass spectrometer. Following each MS scan, the three most abundant peptide ions were automatically subjected to CID-MS/MS, then the m/z of the selected precursor ions were added to a dynamic exclusion list. Then, in a data-dependent constant neutral loss scan (DDCNL) operation mode, if a defined neutral loss(es) corresponding to dimethylsulfide groups (see Table 7.2 in Experimental Chapter) were detected, the most abundant neutral loss product ion was automatically isolated and subjected to CID-MS^3.

CID-MS/MS and -MS^3 spectra of the singly DMBNHS modified phosphopeptide 44 (LGHPEALSAGpTGSPQPPSFTYAQQR) are shown in Figure 6.10A and B. The exclusive neutral loss of dimethylsulfide ($S(CH_3)_2$) was observed by dissociation of the triply charged $[44^N+2H]^{3+}$ (where the superscript "N" indicates modification on the peptide N-terminus) precursor ion (Figure 6.10A). The susceptibility of modified species to undergo cleavage resulting in the specific neutral loss of $S(CH_3)_2$ was found to significantly surpass any competing

loss of H_3PO_4, a finding consistent with previous studies which conclude that fragmentation of sulfonium ion derivatives is an energetically favorable process [170, 237, 239, 392].

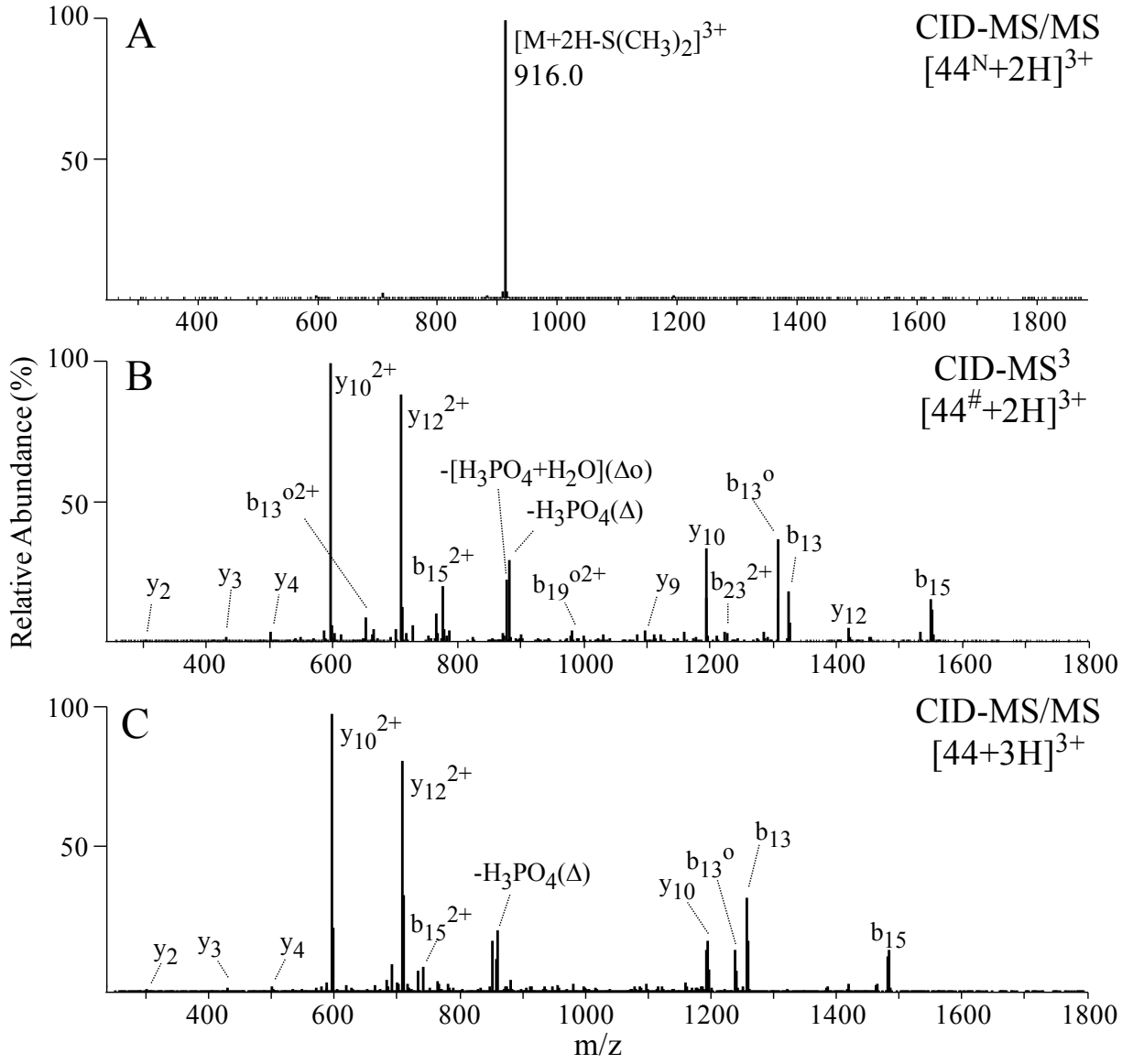

Figure 6.10 Multistage tandem mass spectra of triply charged phosphopeptide LGHPEALSAGpTGSPQPPSFTYAQQR (No. 44) species. (A) CID-MS/MS of singly modified phosphopeptide 44, (B) CID-MS^3 of neutral loss product ion resulted from (A), and (C) CID-MS/MS of native phosphopeptide 44. A superscript "N" indicates the modification is on N-terminus of the peptide. A superscript "#" indicates the iminohydrofuran (IHF) modification formed via the loss of dimethylsulfide during CID-MS/MS. Δ = -98 Da (-H_3PO_4 or - (HPO_3 + H_2O)); o = -18 Da (H_2O).

CID-MS^3 dissociation of the neutral loss product ion from Figure 6.10A gave rise to the spectrum shown in Figure 6.10B. A range of sequence product ions resulting from cleavage along the peptide backbone, together with nonsequence ions corresponding to loss of the phosphate group, were observed; the pattern was found to be very similar to that obtained by CID-MS/MS of the unmodified $[44+3H]^{3+}$ ion (Figure 6.10C). These results suggest that the five-membered cyclic iminohydrofuran (IHF) product formed via the loss of dimethylsulfide during CID-MS/MS is stable to dissociation during subsequent CID-MS^3. Furthermore, it is also evident that the IHF functionality has a limited influence on the formation of CID-MS^3 product ions.

Previous work in the Reid group using multistage MS/MS (i.e., MS^3) reactions of fixed charge sulfonium ion derivatization of peptide-specific functional groups (e.g., the side chains of methionine or cysteine residues) has demonstrated that selective side-chain fragmentation adjacent to the site of the fixed charge results in the formation of stable protonated cyclic five- or six-membered ring product ions [19, 236-239]. The Reilly group has also demonstrated that a "mobile" proton is generated with the loss of trimethylamine from fixed charge TMAB (4-trimethylammoniumbutyryl) derivatized peptides [402].

It is expected that as the proton affinity of the IHF-containing functional group is higher than that of an amino group [170], a potentially decreased "proton mobility" may result within the IHF-modified phosphopeptide product ion compared to the unmodified peptide of the same charge state. A decreased proton mobility within IHF-modified phosphopeptides may lead to a more favorable loss of the phosphate group under CID-MS^3 conditions [17], which therefore could limit the extent of sequence information obtained for phosphopeptide identification and

characterization. Consistent with this proposal, a higher magnitude of H_3PO_4 neutral loss was observed from CID-MS^3 spectrum of the labeled phosphothreonine-containing peptide 44 (Figure 6.10B) compared to that from CID-MS/MS spectrum of the unmodified peptide (Figure 6.10C), albeit a similar product ion pattern was observed.

Figure 6.11A shows the CID-MS/MS product ion spectrum obtained from the doubly modified phosphoserine-containing peptide ASpSLEDLVLK (No. 46). Two characteristic neutral loss product ions were observed, corresponding to sequential neutral losses of one and two $S(CH_3)_2$ molecules, indicating the presence of a lysine residue within the peptide. The most abundant neutral loss product ion from Figure 6.11A, i.e., loss of two $S(CH_3)_2$ groups, was selected for further fragmentation by CID-MS^3. As shown in Figure 6.11B, the appearance of the product ions following CID-MS^3 of doubly IHF-tagged peptide ions from Figure 6.11A indicated a dominant neutral loss of 98 Da; notably, this loss was minimal in the CID-MS/MS spectrum of the unmodified peptide 46 (Figure 6.11C), consistent with the observation described above.

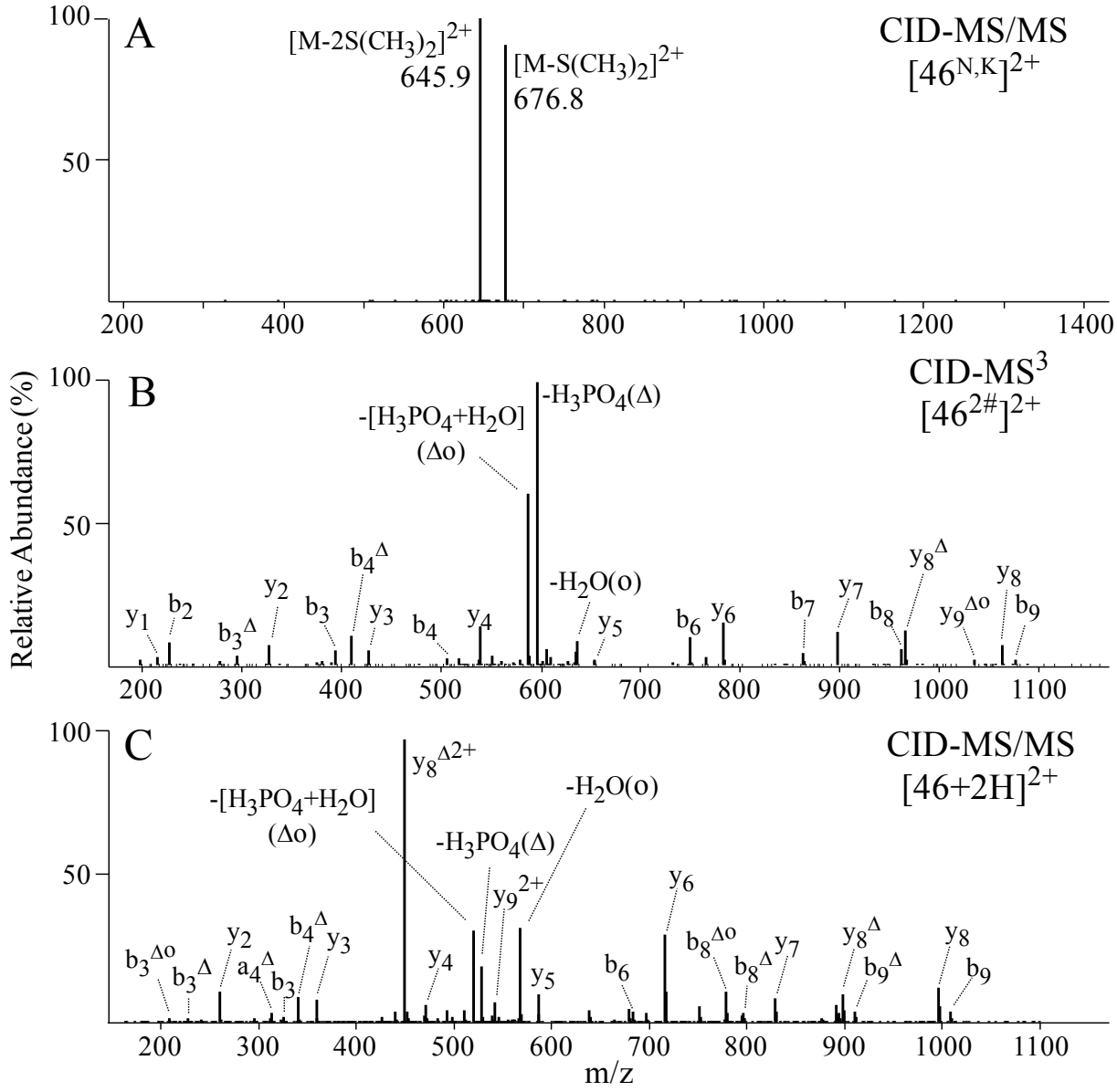

Figure 6.11 Multistage tandem mass spectra of doubly charged phosphopeptide ASpSLEDLVLK (No. 46) species. (A) CID-MS/MS of doubly modified phosphopeptide 46, (B) CID-MS^3 of neutral loss product ion resulted from (A), and (C) CID-MS/MS of native phosphopeptide 46. A superscript "N,K" indicates the modifications are on N-terminus and lysine residue of the peptide. A superscript "#" indicates the iminohydrofuran (IHF) modification formed via the loss of dimethylsulfide during CID-MS/MS. Δ = -98 Da (-H_3PO_4 or - (HPO_3 + H_2O)); o = -18 Da (H_2O).

The results presented here illustrate that CID-MS/MS of DMBNHS modified phosphopeptides give rise to exclusive neutral loss of dimethylsulfide groups; the propensity for preferential loss of $S(CH_3)_2$ is not significantly affected by the competing facile neutral loss of H_3PO_4. Such characteristic neutral losses of $S(CH_3)_2$ are useful in determining the presence and number of modifiable amino groups within phosphopeptides. Furthermore, the incorporation of differential isotope labels into the reagent may allow the approach to be extended to quantitative phosphoproteomics applications by permitting comparisons of the relative abundances of neutral loss products from CID-MS/MS of differentially-labeled phosphopeptides. However, compared to unmodified phosphopeptides, a decreased proton mobility may be exhibited by the $S(CH_3)_2$ neutral loss product, limiting the extent of sequence and phosphorylation site information which can be obtained by using CID-MS^3 of neutral loss product ions [170, 344].

6.6.2 ETD-MS/MS Analysis of DMBNHS Labeled Phosphopeptides

In a data-dependent operation mode, CID-MS/MS and ETD-MS/MS spectra were alternatively acquired for the five most abundant precursor ions following each MS scan as peptides eluted from column. ETD has been demonstrated to be a powerful dissociation technique for the identification of protein PTMs due to the retention of labile modifications during the fragmentation process. As described above, attaching a ‘fixed charge’ sulfonium ion derivative to the phosphopeptide leads to a significantly different fragmentation pattern from its native form when subjected to CID-MS/MS. However, at present, little is known about the ETD fragmentation behavior of fixed charge sulfonium ion modified peptide species. ETD

fragmentation efficiency is highly dependent on the charge density of precursor ions, and typically a charge state of 3+ of precursor ions is required to obtain ETD-MS/MS spectra with good quality. Thus, triply charged phosphopeptide ions are of most interest to investigate their ETD fragmentation behavior in this study. Fortunately, the addition of 'fixed charge' sulfonium ion(s) to a phosphopeptide can substantially increase the peptide charge state distribution, allowing the observation of triply charged peptide ions in high abundance.

Representative examples of the ETD-MS/MS product ion spectra for the unlabeled and singly labeled phosphoserine containing peptide LGHPEALSAGpTGSPQPPSFTYAQQR (No. 44) are shown in Figure 6.12A and B. ETD of the triply charged unlabeled phosphopeptide 44 (Figure 6.12A) gave rise to a series of singly charged z- and c-type product ions, and a doubly charged z_{23}^{2+} ion, suggesting charge locations are most probably at the basic Arg and His residues in addition to the N-terminus. Some y-ions are also present. The formation of y-type product ions by ETD hasve been previously reported due to peptide backbone dissociation induced by the addition of $H^{\bullet}$ to an amide nitrogen instead of the carbonyl group within the peptide [59, 60]. The observation of y-ions provides additional sequence information for peptide identification upon ETD; this is especially useful when c- or z-type ions are not formed from cleavages on the N-terminal side to proline residues, such as the y_{10} ion shown in Figure 6.12A. No phosphate loss was observed; however the presence of abundant hydroxyl groups within peptide 44 led to water loss product ions.

The ETD-MS/MS spectrum of singly modified phosphopeptide 44 (Figure 6.12B) displays some difference from that of its unlabeled counterpart; however, the differences were not as great as those observed resulting from CID-MS/MS experiments (i.e., no abundant phosphate

group neutral losses). The mass shift of 130 Da observed on all c product ions confirmed that the modification was located at the amino group of the N-terminus, and importantly, the sulfonium ion containing label was stable during the ETD process, which is distinctly different fragmentation behavior compared to that by CID. As a non-ergodic fragmentation technique, ETD allows the labile sulfonium moiety to be retained. It should be noted that the charge carrier for these c-ions are a fixed charge sulfonium ion instead of a proton. Thus, the disappearance of the doubly charged z_{23}^{2+} ion is probably due to the reduced number of ionizing protons present within the labeled peptide 44.

The addition of a fixed charge sulfonium ion modification to the peptides appeared to slightly reduce the abundance of the backbone fragment ions. For example, the c_5 ion underwent a decrease from 1.36 % to 0.83 % relative abundance, representing the biggest change among all sequence product ions. However, the numbers of observed c- and z-type ions were not compromised due to the labeling. In contrast, the appearance of low mass c-ions (e.g., c_2), which were not present in the ETD spectrum of unlabeled peptide 44, provided the potential to improve sequence coverage for phosphopeptide identification. Li et al. have reported that a greatly reduced abundance of backbone fragments was obtained from ECD of peptides labeled with 2,4,6-trimethylpyridine (TMP); and the authors reasoned that the pyridinium ion can form a stable radical upon capture of the electron such that further N-Cα dissociations are not likely to take place [76]. However, enhanced sequence coverage was observed from ECD of phosphonium labeled glycopeptides and phosphopeptides [73] as well as for the case of ETD from trimethylammonium group labeled cysteine containing peptides [70]. This might be attributable to the different recombination energies (i.e., energy released upon electron

attachment) of the introduced fixed charge containing functional groups compared to that of protonated basic groups within the peptides [73, 76].

Compared to the unlabeled phosphopeptide 44 (Figure 6.12A), the most significant difference observed in the ETD-MS/MS spectrum of the DMBNHS labeled counterpart is the presence of abundant methyl group and dimethylsulfide group losses from the charge reduced precursor ions (Figure 6.12B). Side chain or entire losses of the tag has been a common observation from previous reports regarding dissociation of fixed charge derivatized peptides by electron driven techniques [70, 73, 76]. These fragmentations likely result from initial capture of the electron by the fixed charge functional group residing at either aromatic rings or aliphatic chains. Similarly, the transfer of an electron from the anionic reagent to the fixed charge sulfonium ion may generate a hypervalent sulfur radical (Scheme 6.2), which triggers homolytic cleavage of the adjacent C-S bonds and gives rise to either a methyl radical loss or dimethylsulfide group loss. The presence of both sequence ions resulting from peptide backbone N-C_α cleavage and side-chain losses from cleavage on the sulfonium ion moiety suggest competition for the electron between the protonated peptide and the fixed charge tag. Interestingly, a low abundance dimethylsulfide neutral loss (3.2 % relative base peak abundance) was also found from intact precursor ions, similar to that observed from CID-MS/MS of DMBNHS labeled phosphopeptide, which was most likely generated by collisional activation during precursor ion isolation, or by the supplemental collisional activation applied in the ETD experiments.

Figure 6.12 ETD-MS/MS spectra of triply charged phosphopeptide LGHPEALSAGpTGSPQPPSFTYAQQR (No. 44) from (A) unmodified, and (B) singly DMBNHS modified form.

Figure 6.12 (cont'd)

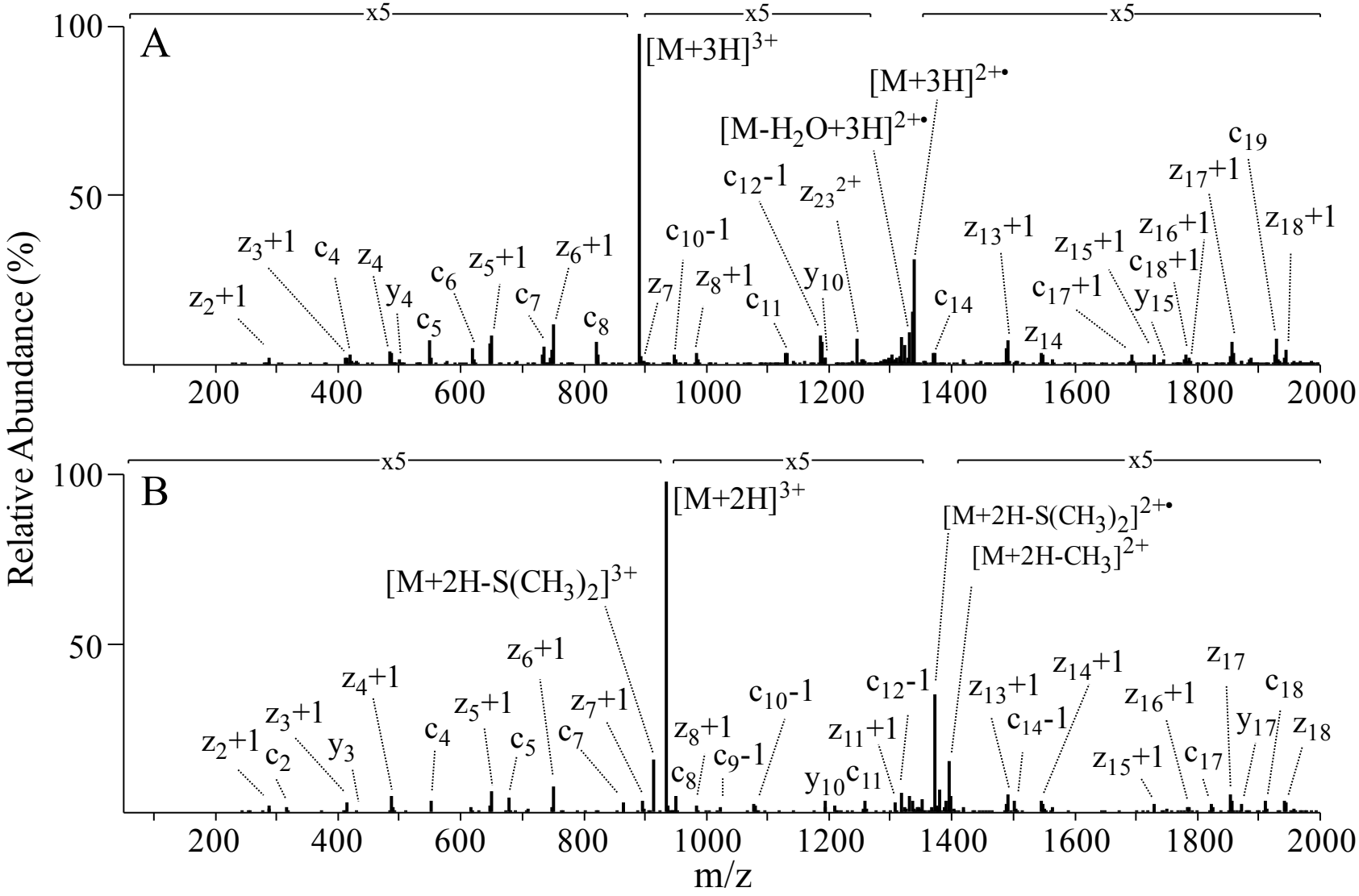

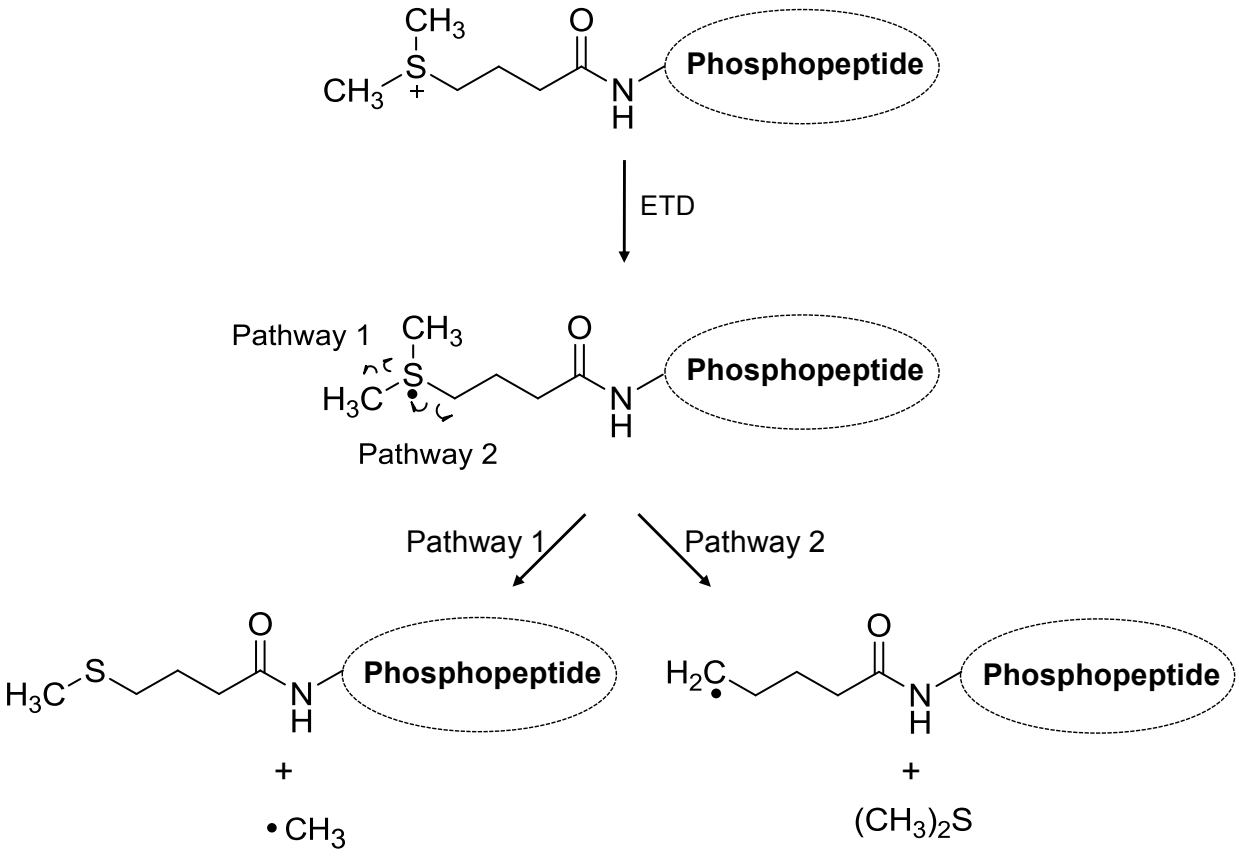

Scheme 6.2 Proposed mechanism for ETD fragmentation of the fixed charge sulfonium group.

Similar results were obtained when comparing the ETD-MS/MS of the unlabeled and doubly labeled phosphotyrosine containing peptide VGEEEHVpYSFPNK (No. 26), as shown in Figure 6.13 A and B. The addition of a second sulfonium ion containing tag did not cause a significant difference in peptide backbone cleavage, and the product ion pattern is similar to that of the singly modified phosphopeptides. A slight decrease in the relative abundance of some of the c- and z-type ions was observed, as well as the disappearance of doubly charged sequence product ions (e.g., z_{11}^{2+}, y_{11}^{2+}, c_{12}^{2+}, and z_{12}^{2+}). However, increased sequence coverage was achieved due to the appearance of low mass c_1, c_2 and z_1 ions.

Although the number of fixed charge labels had minimal influence on the peptide backbone cleavages using ETD, the side-chain losses became more complex due to the presence of the second sulfonium ion containing tag. Analysis of the ETD-MS/MS spectrum in Figure 6.13B suggests significant secondary tag losses (37.2 % summed relative base peak abundance) from charge-reduced species, albeit to an extent which is much weaker than the first methyl or dimethylsulfide loss (141.0 % summed relative base peak abundance). For doubly charged side-chain loss product ions, the loss of a second tag from the initial CH3• or $(CH_3)_2S$ loss product was probably a result of the applied supplemental collisional activation during ETD experiments since only one electron was transferred to the peptide precursor ion. However, for the singly charged side-chain loss product ions, attachment of a second electron likely induces cleavage on the second sulfonium ion tag. This was consistent with the fact that double CH_3• losses were mainly found in singly charged product ions.

Similar results were observed from ETD of the doubly modified phosphoserine containing peptide pSPGAPGPLTLK (No. 40) displayed in Figure 6.14A. For comparison, the ETD-MS/MS spectrum of the doubly charged unmodified peptide is shown in Figure 6.14B, since a 3+ precursor ion charge state was not observed. Limited sequence ions were observed, providing incomplete sequence coverage. In addition, these sequence ions were present at very low abundance. The attachment of two positively charged sulfonium ions into phosphopeptide 40 therefore allows increased sequence coverage by providing enhanced dissociation efficiencies at higher charge state.

Figure 6.13 ETD-MS/MS spectra of triply charged phosphopeptide VGEEEHVpYSFPNK (No. 26) from (A) unmodified, and (B) doubly DMBNHS modified form.

Figure 6.13 (cont'd)

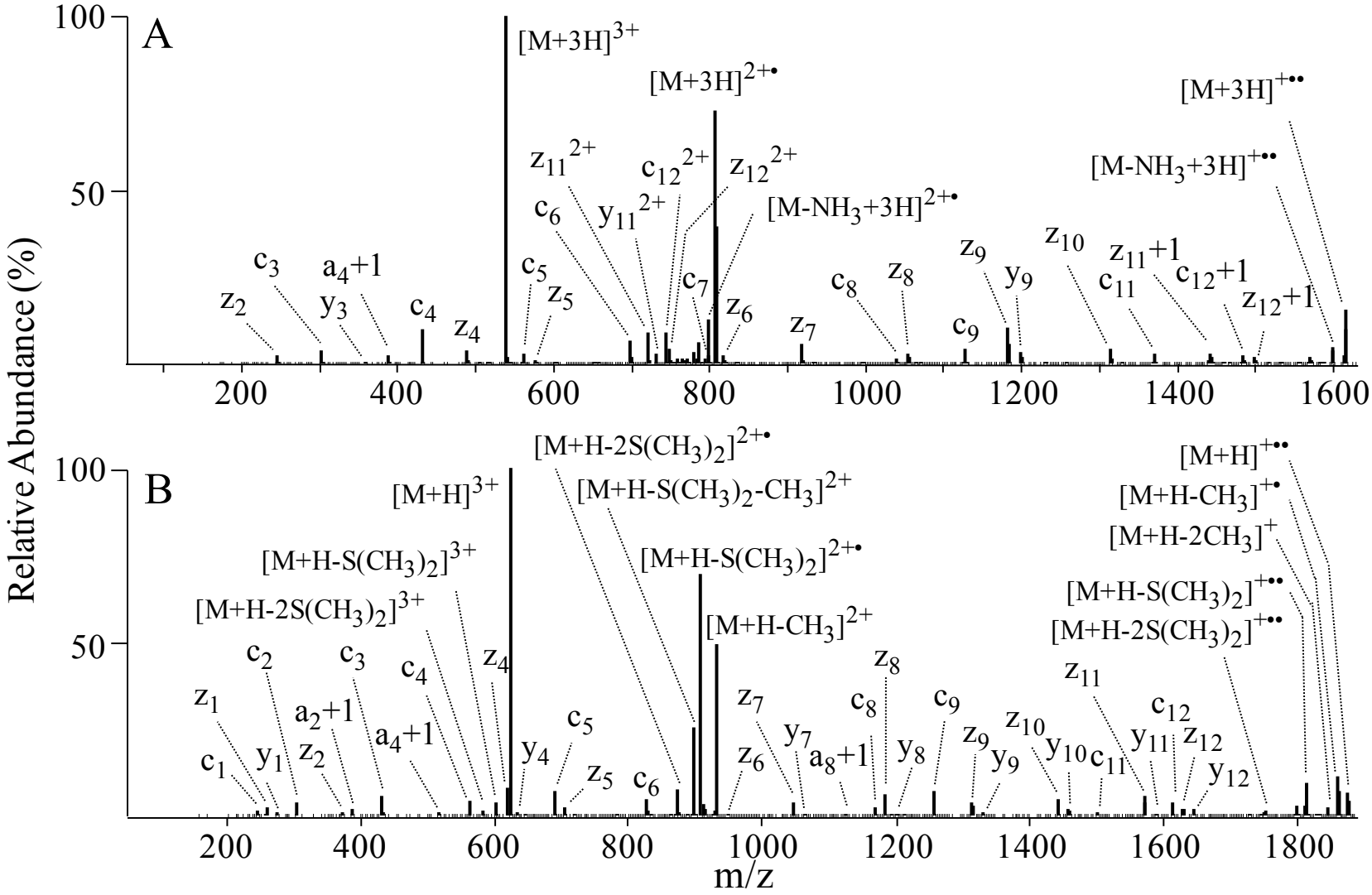

Figure 6.14 ETD-MS/MS spectra of (A) triply charged phosphopeptide pSPGAPGPLTLK (No. 40) from doubly DMBNHS modified form, and (B) doubly charged phosphopeptide 40 from unmodified form.

Figure 6.14 (cont'd)

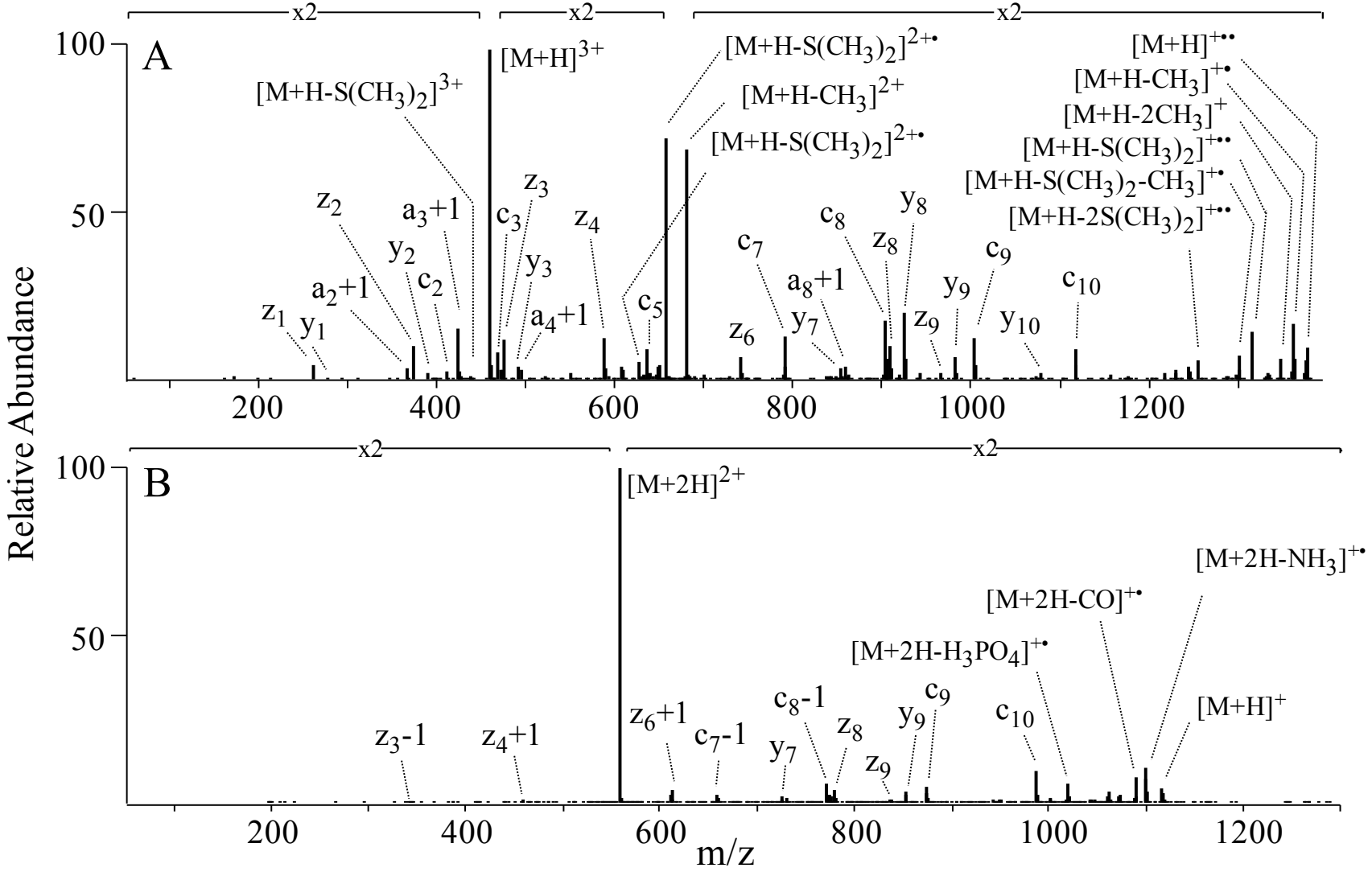

6.7 Fixed Charge Differential Isotope Labeling for Enhanced Collision Induced Dissociation (CID) and Electron Transfer Dissociation (ETD) Quantitative Analysis of Phosphopeptide

6.7.1 DMBNHS Differential Isotope Labeling Combined with CID-MS/MS for Relative Quantification of Phosphopeptides

As seen above, DMBNHS labeled phosphopeptides give rise to dominant or even exclusive $S(CH_3)_2$ neutral loss product ions upon CID-MS/MS. The structure of the DMBNHS reagent allows the introduction of six deuteriums into the dimethylsulfide neutral loss moiety or six deuteriums into the alkyl chain to provide two isobaric labeling reagents, i.e., D_6-heavy DMBNHS and D_6-light DMBNHS, respectively (Scheme 6.3). Thus, two neutral-loss product ions, corresponding to the loss of $S(CD_3)_2$ and $S(CH_3)_2$, will be generated from dissociation of isobarically DMBNHS labeled peptide ions during CID-MS/MS, which can be used for the relative quantification of phosphopeptides.

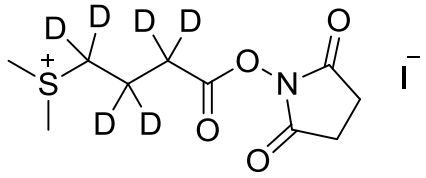

D_6-light DMBNHS

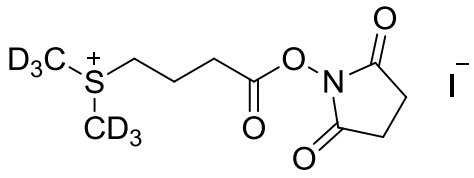

D_6-heavy DMBNHS

Scheme 6.3 Structure of stable isotope labeled DMBNHS reagents *S,S′*-dimethylthio-d_6-butanoylhydroxysuccinimide ester iodide (D_6-light DMBNHS; light neutral loss) and *S,S′*-d_6-dimethylthiobutanoylhydroxysuccinimide ester iodide (D_6-heavy DMBNHS; heavy neutral loss).

Proof of principle studies were carried out using a 6-synthetic phosphopeptide mixture (No.1-6) as described in the Chapter Seven. A range of phosphopeptide ratios from 1:5 to 5:1 were evaluated. Figure 6.15 shows a representative chromatogram of the 6-phosphopeptide mixture differentially labeled with D_6-light DMBNHS and D_6-heavy DMBNHS and mixed at a 1:1 ratio. It is known that using deuterated isotope labels canl cause some chromatographic separation of "light" and "heavy" labeled peptides [133, 138, 139]. The use of isobaric deuterated reagents may diminish or eliminate any shift in retention time of labeled peptides during LC separation. As shown in Figure 6.15, D_6-light and D_6-heavy DMBNHS labeled phosphopeptides co-eluted from the reverse phase C18 column and appeared as a single chromatographic peak for each peptide. Due to the isobaric feature, the differentially labeled peptides also appeared as single peaks in the MS scans (same m/z; data not shown), providing an enhanced peak capacity for detection.

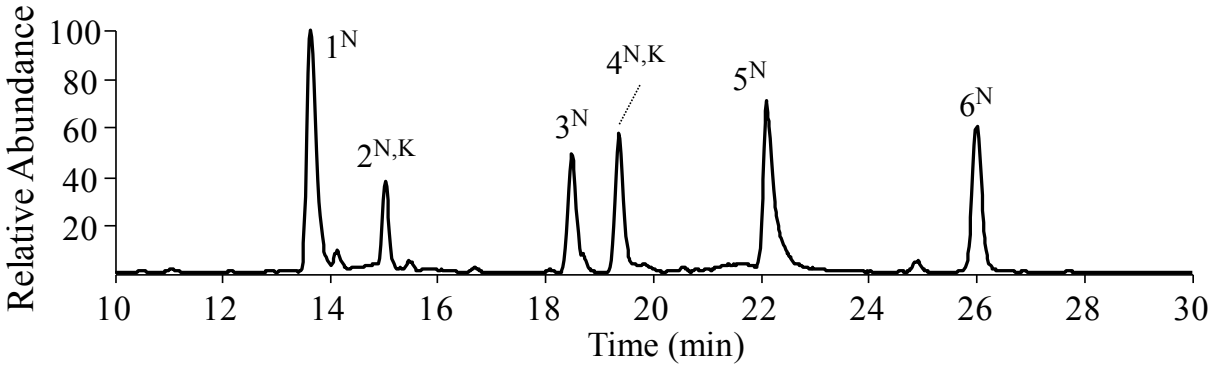

Figure 6.15 Base peak chromatogram of 6-phosphopeptide mixture (No.1-6) differentially labeled with D_6-light DMBNHS and D_6-heavy DMBNHS at a ratio of 1:1. A superscript "N" indicates the modification is on N-terminus of the peptide. A superscript "N,K" indicates the modifications are on N-terminus and lysine residue of the peptide.

Following acquisition of each MS scan, precursor ions were then analyzed by CID-MS/MS. The representative spectra shown in Figure 6.16 were obtained from dissociation of the triply charged phosphoserine containing peptide LFTGHPEpSLER (No. 5), labeled by D_6-light and D_6-heavy DMBNHS respectively, and mixed at varying ratios. As expected, two neutral loss product ions were observed, corresponding to the loss of $S(CH_3)_2$ and $S(CD_3)_2$ respectively. The quantification values extracted from the relative abundances of the two neutral loss product ions are consistent with the theoretical ratios. Similar results were also observed from CID-MS/MS of the doubly charged precursor ions (data not shown). It was found that the relative abundances of $S(CH_3)_2$ loss product ions resulting from dissociation of the D_6-light labeled phosphopeptide 5 were lower than the expected values; this was due to the presence of 12 % D_5-light DMBNHS impurities resulting from the incomplete deuterated starting material for synthesis. Thus, the relative abundances of $S(CH_3)_2$ loss product ions were corrected after taking into account the D_5-

light DMBNHS impurities (i.e., divided by 88 %). In addition, kinetic isotope effects on fragment ion yields corresponding to "light" and "heavy" dimethylsulfide loss might also contribute to this discrepancy. Thus, information about fragmentation efficiencies of D_6-light and D_6-heavy DMBNHS and their differentially labeled peptides need to be obtained to make corrections for this kinetic isotop effects, which is one of the aims in the future work. By examining each CID-MS/MS spectrum at different time points of the chromatographic peak, it was found the D_6-light labeled species eluted slightly earlier than the D_6-heavy labeled counterparts. The minor difference in retention time of differentially labeled phosphopeptides may bring some deviation to quantitative analysis; however, this feature was compensated by averaging all the MS/MS scans acquired across each chromatographic peak. Figure 6.17 shows the measured ratios obtained from phosphopeptide 5 (averaged over the 3+ and 2+ charge states) after correcting for each set of differentially labeled phosphopeptides. A linear relationship between measured ratio and experimental ratio of differentially labeled peptides was observed with $R = 0.99962$, indicating the reliability of the approach for quantitative phosphoproteome analysis.

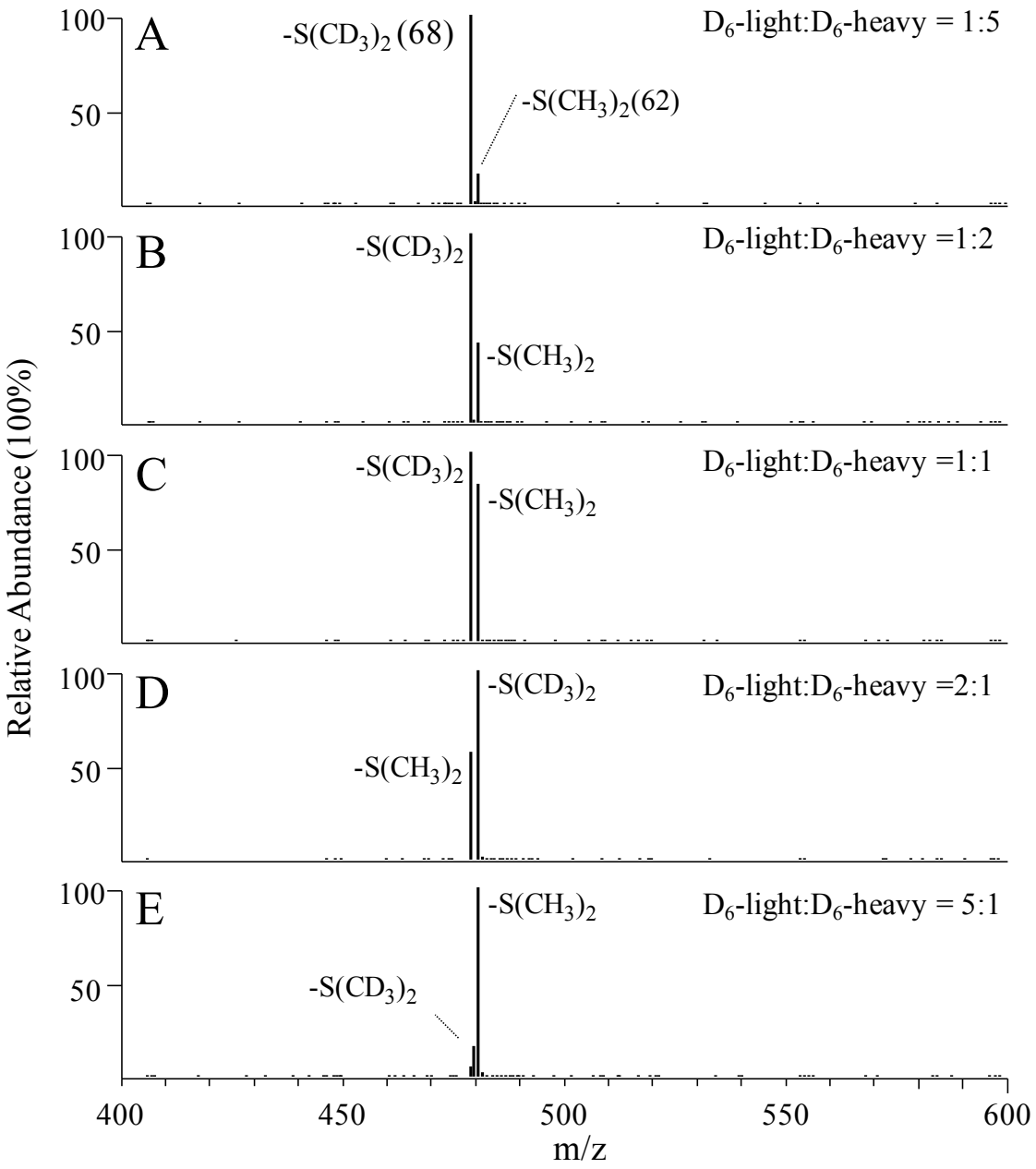

Figure 6.16 CID-MS/MS of triply charged phosphoserine containing peptide LFTGHPEpSLER (No. 5) labeled by D_6-light and D_6-heavy DMBNHS and mixed at a ratio of (A) D_6-light DMBNHS:D_6-heavy DMBNHS = 1:5, (B) D_6-light DMBNHS:D_6-heavy DMBNHS = 1:2, (C) D_6-light DMBNHS:D_6-heavy DMBNHS = 1:1, (D) D_6-light DMBNHS:D_6-heavy DMBNHS = 2:1, and (E) D_6-light DMBNHS:D_6-heavy DMBNHS = 5:1

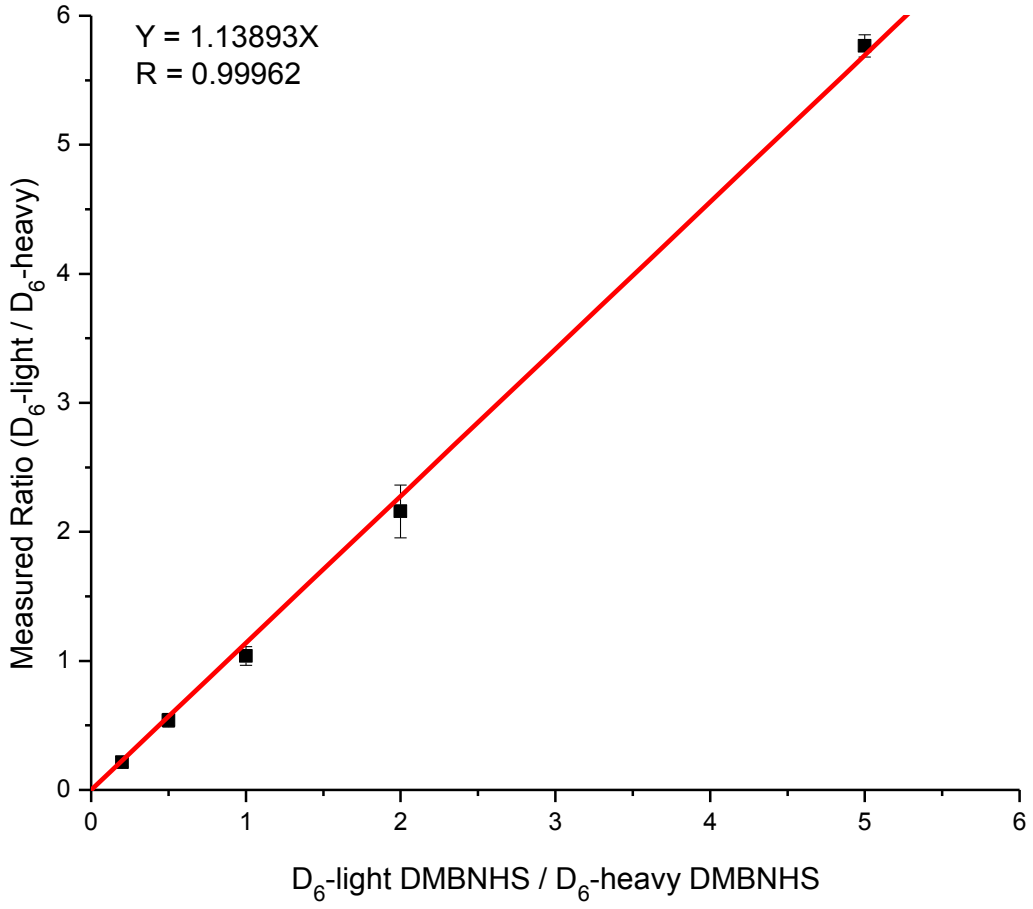

Figure 6.17 Measured ratios of D_6-light to D_6-heavy DMBNHS labeled phosphopeptide LFTGHPEpSLER (No. 5) using CID-MS/MS. Data shown are averaged over both 3+ and 2+ charge states and corrected for 12% D_5-light DMBNHS impurities. Error bars are expressed as standard deviations between two charge states.

6.7.2 Relative Quantification of Phosphopeptides Using Fixed Charge Differential Labeling and ETD-MS/MS

Based on the results obtained from ETD experiments with the natural abundance DMBNHS labeled phosphopeptides, an abundant $S(CH_3)_2$ loss was observed from charge

reduced precursor ions. Thus, an MS/MS based quantification strategy may also be applied with ETD using fragments arising from this loss. ETD-MS/MS spectra of the triply and doubly charged phosphopeptide LFTGHPEpSLER (No. 5) labeled by D_6-light and D_6-heavy DMBNHS at a ratio of 1:1 are displayed in Figure 6.18A and B. Together with a complementary series of c- and z-ions, abundant doubly charged product ions resulting from $S(CH_3)_2$ and $S(CD_3)_2$ losses were generated by ETD from the triply charged precursor ions (Figure 6.18A). Relative abundances calculated for the two tag losses was 0.84:1 after correction for D_5-light DMBNHS, which is comparable with the theoretical ratio of 1:1, suggesting that ETD-generated tag loss product ions may be quantitative. ETD-MS/MS of the doubly charged peptide ions (Figure 6.18B) provided less sequence information in comparison to that of triply charged species (Figure 6.18A); however, quantitative information was obtained by measuring the relative abundances of tag loss product ions to give a ratio of 1.04:1, further suggesting the ETD technique may be applied for quantitative analysis when combined with isotope labeled DMBNHS reagents.

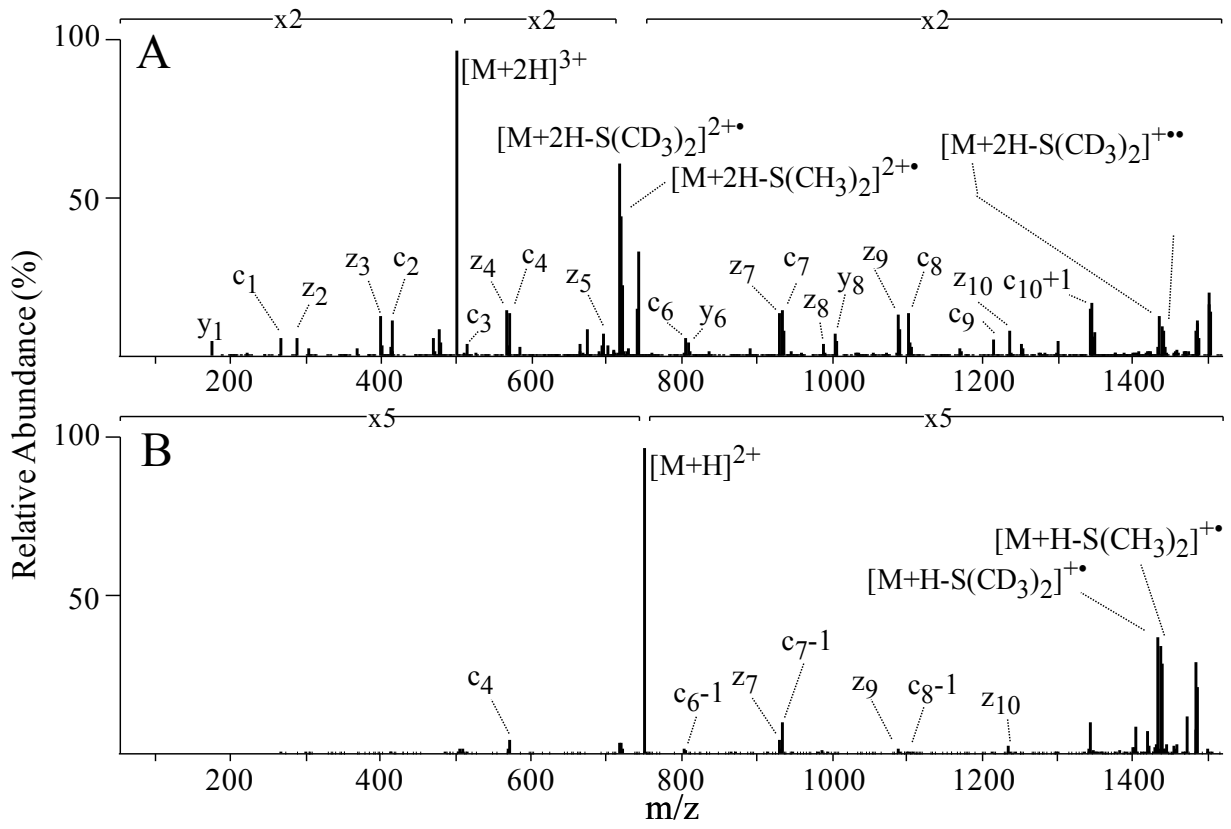

Figure 6.18 ETD-MS/MS of phosphoserine containing peptide LFTGHPEpSLER (No. 5) labeled by D_6-light and D_6-heavy DMBNHS and mixed at a ratio of D_6-light DMBNHS:D_6-heavy DMBNHS = 1:1 in (A) +3, and (B) +2 charge states. The superscript "N" indicates the modification is on N-terminus of the peptide.

To evaluate the quantitative capability of the sulfonium ion tag specific neutral loss product ions using ETD, the measured ratios of differentially labeled phosphopeptide 5 (averaged over the +3 and +2 charge states) versus the expected ratios are plotted and displayed in Figure 6.19. A linear relationship with an R = 0.99931 was obtained, comparable to the CID-MS/MS experiments (Figure 6.17). This although a less sensitive approach when compared to CID, the ETD fragmentation technique holds promise for simultaneous identification and relative

quantification of phosphopeptides with the combination of differential isotope labeled DMBNHS reagents.

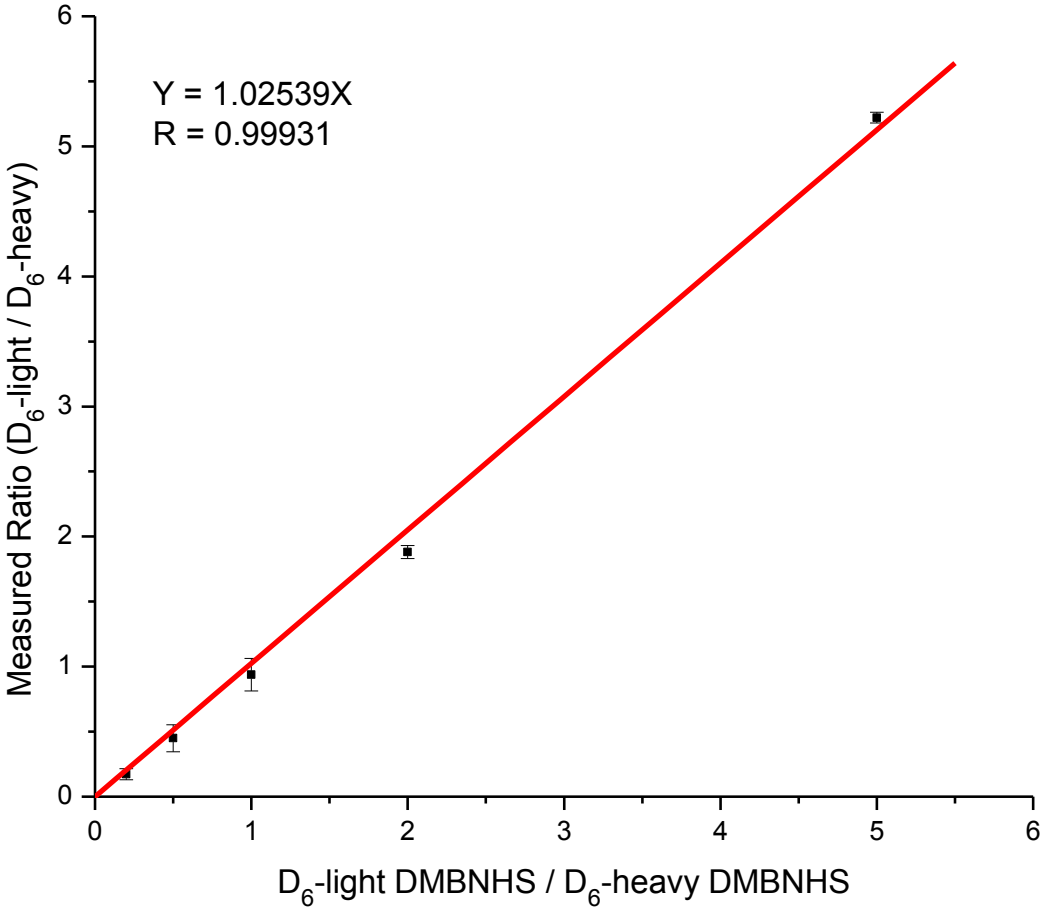

Figure 6.19 The measured ratios of D_6-light to D_6-heavy DMBNHS labeled phosphopeptide LFTGHPEpSLER (No. 5) using ETD-MS/MS. Data shown are averaged over 3+ and 2+ charge states and corrected for D_5-light DMBNHS impurities. Error bars are expressed as standard deviations between two charge states.

6.8 Summary and Future Aspects

The results described here have demonstrated that the fixed charge sulfonium ion containing labeling reagent DMBNHS reacts efficiently with peptide primary amine groups (N-termini and lysine side chains). The introduction of this fixed charge to phosphopeptides leads to improved ionization efficiencies (an average of 2.5 fold summed ionization efficiencies were observed from the analysis of 44 synthetic phosphopeptide products) and increases the abundance of high charge state precursor ions, or creates precursor ions of higher charge states than which are available from their unmodified counterparts. Upon CID-MS/MS, the exclusive neutral loss(es) of dimethylsulfide are observed, independently of the proton mobility of the phosphopeptide, while keeping the phosphate group(s) intact. The relative abundances of "light" versus "heavy" neutral loss product ions generated from CID-MS/MS of D_6-light and D_6-heavy DMBNHS labeled phosphopeptides enables differential quantitative analysis, whereas subsequent ETD-MS/MS of the intact precursor ion(s) allows phosphopeptide sequence identification and phosphorylation site characterization. Furthermore, characteristic losses observed from charge reduced precursor ions during ETD can be used for quantitative analysis, allowing the identification, characterization and quantification of phosphopeptides in one experiment.

In comparison to other derivatization methods, the DMBNHS labeling approach has the advantage of neutral loss specificity during collision induced gas-phase fragmentation along with an enhanced quantitation capability using both CID-MS/MS and ETD-MS/MS techniques. The reagent holds great promise for further studies of protein post-translational modifications.

CHAPTER SEVEN

EXPERIMENTAL METHODS FOR CHAPTER SIX

7.1 Materials

All chemicals were analytical reagent (AR) grade, or of a comparable or higher grade and used without further purification. N-hydroxysuccinimide (NHS), N,N′-dicyclohexylcarbodimide (DCC) and anhydrous dimethyl sulfoxide (DMSO) (stored over 3-Å molecular sieves) were purchased from Fluka (Buchs, Switzerland). Sodium methanethiolate, γ-butyrolactone, γ-butyrolactone-d_6, 4-bromobutyric acid, thiourea, iodomethane-d_3 and tris(hydroxymethyl)aminomethane (Tris) were from Sigma-Aldrich (St. Louis, MO, USA). Sodium hydroxide, sodium phosphate dibasic (crystal), potassium phosphate monobasic (crystal), magnesium sulfate (anhydrous) and formic acid (FA) were purchased from Spectrum Chemicals (Gardena, CA, USA). Sodium chloride, hydrochloric acid and potassium hydroxide were purchased from Columbus Chemical Industries (Columbus, WI, USA). Potassium chloride, sulfuric acid, N,N′-dimethyl formamide (DMF) and ethyl ether were purchased from Jade Scientific (Canton, MI, USA). Glacial acetic acid, dichloromethane, chloroform, methanol (anhydrous), ethanol, isopropyl alcohol and ethyl acetate were purchased from Mallinckrodt Chemicals (Phillipsburg, NJ, USA). Iodomethane and acetonitrile were purchased from EMD Chemicals (San Diego, CA, USA). Trifluoroacetic acid (TFA) was purchased from Pierce (Rockford, IL, USA). Recrystallized 2,5-dihydroxybenzoic acid (2,5-DHB) was purchased from Laser BioLabs (Sophia-Antipolis Cedex, France). All aqueous solutions were prepared by using

deionized water purified by a Barnstead nanopure diamond purification system (Dubuque, IA, USA).

The phosphoserine-containing peptide LFTGHPEpSLER (No. 5 in Table 6.1) was prepared 'in house' by manual stepwise Fmoc-based solid-phase peptide synthesis. All other phosphopeptides discussed in Chapter Six were synthesized either by Sigma-Genosys (The Woodlands, TX, USA) or by JPT Peptide Technologies GmbH (Berlin, Germany) and were used without further purification.

7.2 Synthesis of *S,S′*-Dimethylthiobutanoylhydroxysuccinimide Ester Iodide (DMBNHS) and *S,S′*-d_3-Dimethylthiobutanoylhydroxysuccinimide Ester Iodide (D_3-DMBNHS)

A sulfonium ion containing modification reagent, *S,S′*-dimethylthiobutanoylhydroxysuccinimide ester iodide (DMBNHS; **7**), with a three carbon alkyl chain was synthesized by Zhou *et al*. using the three-step process as shown in Scheme 7.1 below [170]. Based on the method of Musker *et al.* [403], 71.3 mmol sodium methanethiolate and 53.5 mmol of γ-butyrolactone were dissolved in 50 mL of dry DMSO. Then, the solution was stirred under an N_2 atmosphere at room temperature for 5 days. 125 mL of 1M HCl was added to the resulting slurry and the aqueous solution was extracted with 6 x 80 mL of diethyl ether. The solvent was evaporated under reduced pressure. The resulting viscous liquid was purified by silica gel column chromatography (100% ethyl acetate). The eluent containing the product was collected and concentrated under reduced pressure giving 6.6 g (92%) methylthiobutyric acid (**5**)

as a colorless oil. ^{1}H NMR (500 MHz, $CDCl_3$): δ 1.93 (qui, 2H, *J* = 7.0 Hz), 2.08 (s, 3H), 2.48 (t, 2H, *J* = 7.0 Hz), 2.54 (t, 2H, *J* = 7.0 Hz), 11.15 (s, br, 1H).

^{1}H-NMR spectra were obtained on Varian Inova 300 MHz or 500 MHz instruments and are reported in parts per million (ppm) relative to the solvents resonances (δ), with coupling constants (*J*) in Hertz (Hz).

5 was then esterified by reaction with N-hydroxysuccinimide (NHS) to yield methylthiobutyric hydroxysuccinimide ester (**6**). Under a N_2 atmosphere, 33 mmol of NHS and 30 mmol of **5** were dissolved in a mixture of 60 mL of $CHCl_3$ and 30 mL of CH_2Cl_2. The mixture was stirred for 5 minutes at room temperature. Then 33 mmol of N,N'-dicyclohexylcarbodiimide (DCC) was added and a precipitate formed immediately. The resulting slurry was stirred in a N_2 atmosphere. After 24 hrs, the mixture was filtered and the solution was collected and concentrated under reduced pressure. Then 5 mL of acetonitrile was added to the liquid and the precipitate was filtered out. The resultant solution was dried under vacuum, after which 6.08g (88%) product **6** was obtained as a white solid. ^{1}H NMR (500 MHz, $CDCl_3$): δ 2.02 (qui, 2H, *J* = 7.5 Hz), 2.09 (s, 3H), 2.59 (t, 2H, *J* = 7.0 Hz), 2.75 (t, 2H, *J* = 7.0 Hz), 2.82 (s, 4H).

Finally, **6** was reacted with methyl iodide to yield *S,S′*- dimethyl thiobutynolhydroxysuccinimide ester sulfonium iodide (DMBNHS; **7**). 1 mmol of methylthiobutyric hydroxysuccinimide ester (**6**) and 5 mmol of iodomethane were dissolved in 2 mL of CH_3CN then stirred in the dark at room temperature for 2 days. The resulting solution was then concentrated under reduced pressure. The resultant yellow solid was washed with 10 mL of dichloromethane then dried under vacuum over night to give 0.28 g (76%) product **7** as yellow

crystals. The product was stored in the dark. ^{1}H NMR (500 MHz, CD_3CN): δ 2.16 (qui, 2H, J = 7.5), 2.77 (s, 4H), 2.81 (s, 6H), 2.85 (t, 2H, J = 7.5), 3.29 (t, 2H, J = 7.5).

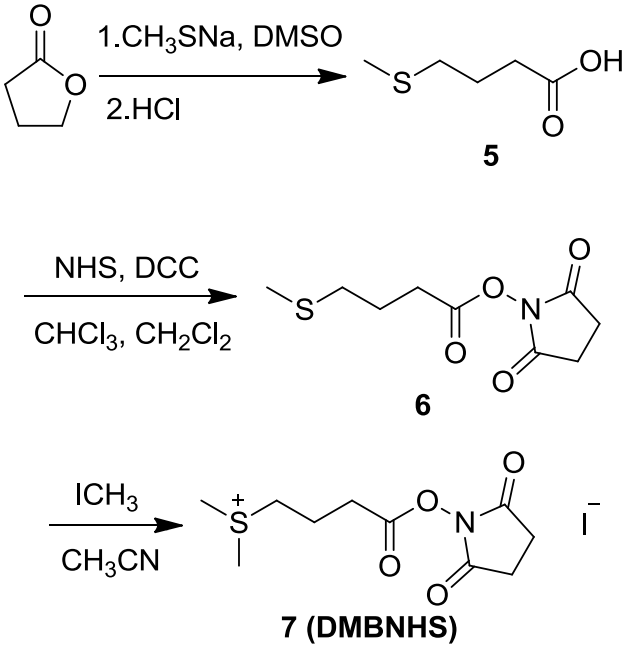

Scheme 7.1 Synthesis of the sulfonium ion containing derivatization reagent *S,S*′-dimethylthiobutanoylhydroxysuccinimide ester (DMBNHS; **7**).

S,S′-d_3-Dimethylthiobutanoylhydroxysuccinimide ester iodide (D_3-DMBNHS; **8**) was achieved by using iodomethane-d_3 as the alkylation reagent for **6** following the same procedures to **7**. 10 mmol of methylthiobutyric hydroxysuccinimide ester (**6**) and 10 mmol of iodomethane-d_3 dissolved in 6 mL of CH_3CN were employed for the reaction, and 2.84 g (76%) of yellow crystals were obtained. The product was stored in the dark. ^{1}H NMR (500MHz, CD_3CN): δ 2.16 (qui, 2H, J = 7.5), 2.77 (s, 4H), 2.82 (s, 3H), 2.85 (t, 2H, J = 7.5), 3.31 (t, 2H, J = 7.5).

7.3 Synthesis of *S,S′*-Dimethylthio-d_6-butanoylhydroxysuccinimide Ester Iodide (D_6-light DMBNHS)

The preparation of D_6-light DMBNHS (**11**) was started from γ-butyrolactone-d_6 as described for the synthesis of DMBNHS via a three-step process shown in Scheme 7.2.

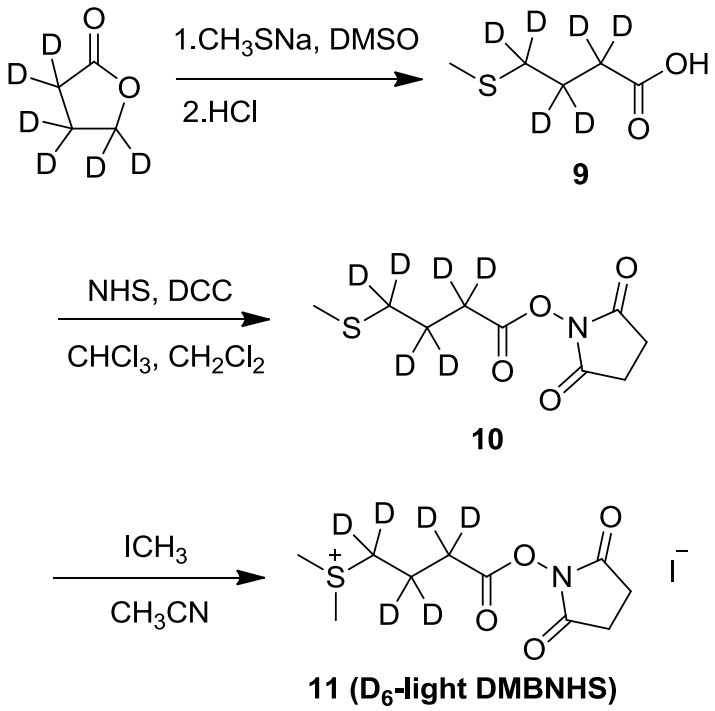

Scheme 7.2 Synthesis of the stable isotope encoded sulfonium ion containing derivatization reagent *S,S′*-dimethylthio-d_6-butanoylhydroxysuccinimide ester (D_6-light DMBNHS; **11**).

Using a procedure analogous to that for the acid **5**, to a solution of 2.72 g of sodium methanethiolate (34.9 mmol) in anhydrous DMSO (26 mL) under a N_2 atmosphere, γ-butyrolactone-d_6 (2.0 mL, 26.0 mmol) was added dropwise with stirring. The reaction was allowed to proceed at room temperature for 5 days, and then 65 mL of 1M HCl was added to the

resulting slurry. Following extraction with diethyl ether (6×40 mL) and solvent evaporation under reduced pressure, the crude product was redissolved in 100 mL of dichloromethane and washed with H_2O (3×25 mL). After drying with anhydrous $MgSO_4$ and solvent evaporation in vacuo, a colorless oil **9** was obtained in 90% yield (3.04g). ^{1}H NMR (500 MHz, $CDCl_3$): δ 2.06 (s, 3H), 11.27 (br, 1H). ^{2}H NMR (500 MHz, $CDCl_3$): δ 1.80 (s, 2H), 2.38 (s, 2H), 2.43 (s, broad, 2H).

NHS ester **10** was obtained in a similar manner to **6**, starting from 1.40 g of acid **7** (10.0 mmol) and 1.26 g of NHS (11.0 mmol) dissolved in 2:1 v/v mixture of chloroform and dichloromethane (30 ml). After 5-min stirring at room temperature, DCC (2.27 g, 11.0 mmol) was added, and the resultant suspension was stirred overnight under a N_2 atmosphere. The DCU precipitate was then filtered and the solution was concentrated in vacuo. After resuspending the crude product in 8 mL of CH_3CN, the remaining DCU was precipitated and removed by filtration. The solvent was then evaporated under reduced pressure to give a yellow solid in quantitative yield. ^{1}H NMR (500 MHz, $CDCl_3$): δ 2.07 (s, 3H), 2.82 (s, 4H).

The isotope encoded D_6-light DMBNHS (**11**) reagent was obtained by the method described for DMBNHS (**7**). A mixture of **10** (2.23 g, 9.4 mmol) and iodomethane (1.76 mL, 28.2 mmol) in CH_3CN (16 mL) was allowed to react at room temperature in the dark for 2 days. After solvent evaporation under reduced pressure, the resultant yellow solid was washed with dichloromethane and dried in vacuo to give pale-yellow crystals in 86% yield (3.06 g). The compound was stored in the dark for future use. ^{1}H NMR (500 MHz, CD_3CN): δ 2.77 (s, 4H), 2.83 (s, 6H).

7.4 Synthesis of *S,S′*-d_6-Dimethylthiobutanoylhydroxysuccinimide Ester Iodide (D_6-heavy DMBNHS)

Based on the method of Jessing *et al.* [255], 4-bromobutyric acid (8.35 g, 50.0 mmol) and thiourea (5.70 g, 75.0 mmol) were dissolved in 100 mL of ethanol and refluxed overnight (Scheme 7.3). The solvent was then evaporated under reduced pressure and 65 mL of 7.5 M NaOH (aq) was added. The mixture was refluxed at 90 ^{o}C under a N_2 atmosphere. After a 16 h reaction, 2M H_2SO_4 was added slowly while stirring in an ice bath until the pH = 1. The resulting mixture was extracted 4 times with 60 mL of CH_2Cl_2, dried over anhydrous $MgSO_4$, and concentrated *in vacuo* to give 5.27 g (88%) of thiobutyric acid (**12**) as a colorless oil. ^{1}H NMR (500 MHz, $CDCl_3$): δ 1.33 (t, 1H, *J* = 8.0 Hz), 1.93 (qui, 2H, *J* = 7.0 Hz), 2.50 (t, 2H, *J* = 7.0 Hz), 2.59 (q, 2H, *J* = 7.0 Hz), 11.28 (s, broad, 1H).

Adapted from the method of Crouch *et al.* [404], potassium hydroxide (1.31 g, 23.4 mmol) in 2 mL of methanol was added dropwise to **12** (1.08 g, 9 mmol) dissolved in 10 mL of methanol in an ice bath and stirred for 10 min. Iodomethane-d_3 (672.4 μL, 10.8 mmol) was added slowly over 10 min and the solution was stirred at room temperature overnight. After evaporating the solvent under reduced pressure, 12 mL of H_2O was added followed by 2M HCl until the pH = 1. The solution was extracted with 4 × 18 mL of diethyl ether. The organic extracts were combined and dried over anhydrous $MgSO_4$. The solvent was removed *in vacuo* and 858.2 mg (70%) of d_3-methylmercaptobutyric acid (**13**) was obtained as brown oil. ^{1}H NMR

(500 MHz, $CDCl_3$): δ 1.92 (qui, 2H, *J* = 7.0 Hz), 2.48 (t, 2H, *J* = 7.5 Hz), 2.53 (t, 2H, *J* = 7.5 Hz), 11.19 (s, broad, 1H).

Under a N_2 atmosphere, N-hydroxysuccinimide (792.4 mg, 6.89 mmol) and **13** (858.2 mg, 6.26 mmol) were dissolved in a mixture of $CHCl_3$ (15 mL) and CH_2Cl_2 (10 mL). The mixture was stirred for 5 minutes at room temperature, then DCC (1419.5 mg, 6.89 mmol) was added and a precipitate formed immediately. The resulting slurry was stirred in a N_2 atmosphere. After 18 hrs, the mixture was filtered, then the filtrate was collected and concentrated under reduced pressure. Then CH_3CN (3 mL) was added and the precipitate was filtered out. The solvent was removed *in vacuo* to yield d_3-methylmercaptobutyric hydroxysuccinimide ester (**14**) as a yellow solid with a quantitative yield. ^{1}H NMR (500 MHz, $CDCl_3$): δ 2.02 (qui, 2H, *J* = 7.5 Hz), 2.58 (t, 2H, *J* = 7.5 Hz), 2.74 (t, 2H, *J* = 7.0 Hz), 2.82 (s, 4H).

Finally, **14** (933.6 mg, 3.99 mmol) and d_3-iodomethane (1.16 g, 7.98 mmol) were dissolved in CH_3CN (8 mL) and stirred in the dark at room temperature for 2 days. The resulting solution was concentrated under reduced pressure. The resultant yellow solid was washed with dichloromethane and then dried *in vacuo* over night to yield 1.19 g (79%) of *S,S*′-d_6-dimethylthiobutanoylhydroxysuccinimide ester iodide (D_6-heavy DMBNHS; **15**) as a white solid. The product was stored in the dark. ^{1}H NMR (500 MHz, CD_3CN): δ 2.16 (qui, 2H, *J* = 7.5 Hz), 2.77 (s, 4H), 2.85 (t, 2H, *J* = 7.5 Hz), 3.30 (m, 2H).

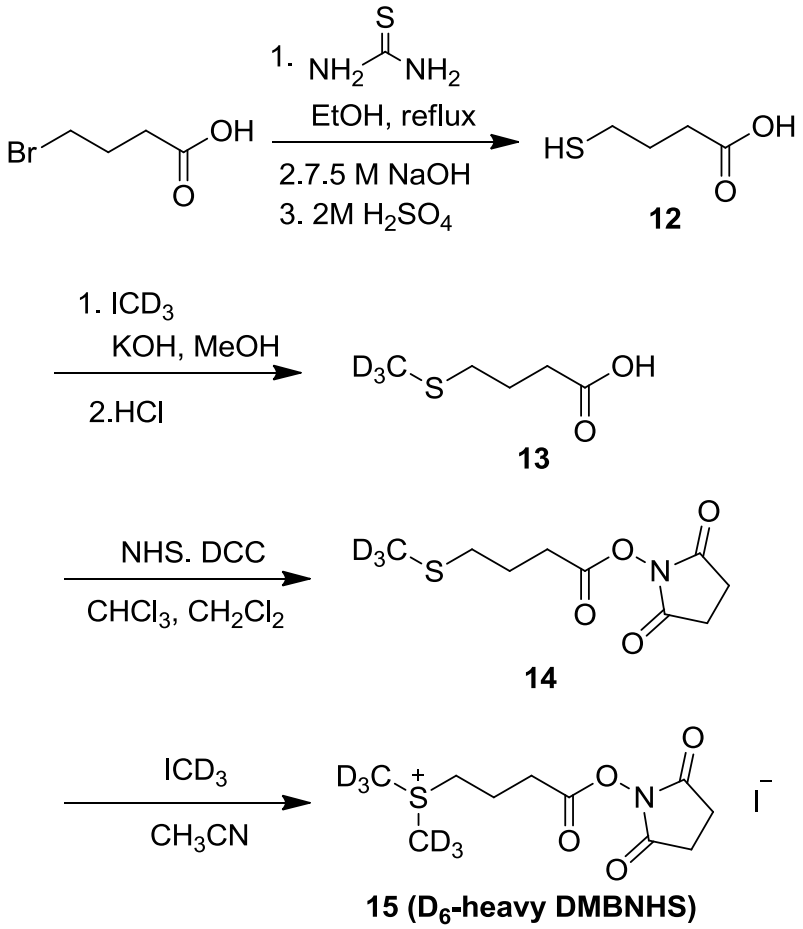

Scheme 7.3 Synthesis of the stable isotope encoded sulfonium ion containing derivatization reagent *S,S′*-d_6-dimethylthiobutanoylhydroxysuccinimide ester (D_6-heavy DMBNHS; **15**).

7.5 Phosphopeptide Derivatization Reactions and Sample Preparation

7.5.1 Phosphopeptide Derivatization Reactions for Determination of the Optimum Labeling Conditions

For DMBNHS derivatization reactions, preliminary experiments were performed using a 6-phosphopeptide mixture (No. 1-6, Table 6.1) with a concentration of 1 μM for each peptide

dissolved in phosphate-buffered saline (PBS, 800 mg of NaCl, 217 mg of $Na_2HPO_4 \cdot 7H_2O$, 20 mg of KCl, and 20 mg of KH_2PO_4 per 100 ml, pH 7.5). In order to determine optimal conditions for derivatization, 1 μL of freshly prepared DMBNHS solution (8 mM in DMF) was added to 10 μL of peptide mix, to produce a 100-molar excess of DMBNHS relative to the primary amine group. The reactions were allowed to proceed for 15, 30, 45 and 60 min at room temperature in the dark. Each reaction was quenched by the addition of a 160-molar excess of Tris (0.5 M, pH 8.26 at 25 ˚C) and incubated at room temperature for 10 min to ensure complete deactivation of derivatization reagent. The reaction products were then diluted to a final concentration of 0.2 μM with 3% acetic acid/5% CH_3CN before HPLC-MS analysis. The appropriate DMBNHS-to-primary amine ratio was determined by the addition of various DMBNHS amounts contained in 1 μL of DMF to 10 μL of peptide mix solution to produce final ratios of 1:50, 1:100, 1:150, 1:200, 1:300, 1:400 and 1:500. All reactions were incubated at room temperature for 30 min followed by quenching and dilution as described above.

7.5.2 Sample Preparation for Comparing Ionization Efficiencies between Underivatized and Derivatized Phosphopeptides

For the 6-phosphopeptide mix (No. 1-6), derivatization was performed by combining a 10 μL PBS solution containing 100 pmol of each peptide mixed with 1 μL of DMBNHS solution (0.16 M in DMF) in a 200-molar excess of reagent to primary amine. After incubation at room temperature in the dark for 30 min and quenching with Tris, an underivatized 6-phosphopeptide mix (No. 1-6) solution also containing 100 pmol of each phosphopeptide, was spiked into the

solution. The working solution was then diluted to a final concentration of 0.2 μM for analysis by LC-MS, in triplicate.

Forty-four phosphopeptides (No. 1-44, the sequences of which are shown in Table 6.4), which were divided into 10 mixtures (some peptides were present in multiple mixtures to make 10 × 5-phosphopeptide mixtures) with a concentration of 10 μM for each peptide in PBS buffer, were derivatized by the procedures described above for the 6-phosphopeptide mix (No. 1-6) using a 0.2 M DMBNHS solution. As each phosphopeptide contains one or two target primary amine groups, the ratios of reagent to primary amine were within 200:1 to 400:1 ranges to ensure complete derivatization for each phosphopeptide. Following similar quenching and spiking of equal amounts of underivatized phosphopeptides, each solution was diluted to a final concentration of 0.5 pmol/μL for further analysis.

7.5.3 Sample Preparation for Quantitative Analysis of Stable Isotope Differentially Labeled Phosphopeptides

The same procedures as described above in Section 7.5.2 were used for differential isotope labeling of the 6-phosphopeptide mix (No. 1-6), using either D_6-light DMBNHS or D_6-heavy DMBNHS reagent. 40 μL of peptide mix solution with a concentration of 25 μM of each peptide was used for each derivatization reaction, and combined with 4 μL of reagent solution (0.4 M in DMF) to maintain a 200-molar excess of reagent to primary amine group. Following incubation (30 min) and quenching (10 min) under the same conditions, the D_6-light DMBNHS and D_6-heavy DMBNHS labeled phosphopeptide mixtures were pooled in 1:5, 1:2, 1:1, 2:1 and 5:1

molar ratios. Each solution was then diluted to the final concentrations as listed in Table 7.1 prior to HPLC-MS analysis.

Table 7.1 Final concentrations of D_6-light DMBNHS and D_6-heavy DMBNHS labeled phosphopeptides prior to HPLC-MS analysis.

D_6-light DMBNHS Labeled Phosphopeptides (μM)	D_6-heavy DMBNHS Labeled Phosphopeptides (μM)	Ratio
0.10	0.50	1:5
0.15	0.30	1:2
0.20	0.20	1:1
0.30	0.15	2:1
0.50	0.10	5:1

7.6 Mass Spectrometry

Mass spectrometry analysis was performed using either an LTQ linear quadrupole ion trap mass spectrometer equipped with nano electrospray ionization (nESI), or an LTQ XL linear quadrupole ion trap mass spectrometer equipped with a chip-based nESI source (Advion NanoMate, Ithaca, NY, USA) with ETD capabilities. Both mass spectrometers were manufactured by Thermo Fisher Scientific (San Jose, CA, USA). The MS and MS/MS spectra collected from infusion injections are typically the average of 30-50 scans. Repeated analysis of individual samples resulted in less than 5% variation in relative product ion abundances.

7.6.1 Tandem Mass Spectrometry Performed by Direct Infusion

For direct infusion experiments, all reaction products were desalted by Sep-pak (Waters, Milford, MA) purification, with elution using 40, 60 and 80% CH_3CN (aq) containing 0.05% formic acid prior to mass spectrometry analysis.

CID-MS/MS and -MS^3 analysis was performed by introducing samples (~10 μM) into the LTQ mass spectrometers at a flow rate of 0.5 μL/min. The spray voltage was maintained at 2.5 kV, while the capillary temperature was set at 180 ˚C. Precursor ions were isolated at an isolation window of 1.5-2 m/z, and subjected to CID by using helium as a collision gas, at an activation *q* value of 0.25 and an activation time of 30 ms. Collision energies were individually optimized for each compound of interest.

For ETD-MS/MS experiments, samples (~10 μM) were loaded into a Whatman Multichem 96-well plate (Fisher Scientific, Pittsburgh, PA) and introduced into the LTQ XL mass spectrometer via a chip-based nESI source. Infusion operation was achieved by using an ESI chip, a spray voltage of 1.5 kV, a gas pressure of 0.3 psi and an air gap of 3 μL. ETD-MS/MS and -MS^3 data were acquired on mass selected precursor ions using a isolation window of 3 m/z. Fluoranthene anions were introduced as the electron-transfer reagent for ETD experiments, with reaction times of 100 ms. Supplemental collisional activation of ETD products (ETcaD), whereby low energy collisional activation is used to break up ETD products which could not overcome non-covalent interactions, was carried out for doubly charged precursor ions using standard conditions [363, 364].

7.6.2 HPLC-ESI-MS, CID-MS/MS and -MS^3 for Phosphopeptide Analysis

HPLC-MS, -MS/MS and -MS^3 analysis was performed using an LTQ mass spectrometer coupled with a Paradigm MS4 capillary RP-HPLC system (Michrom Bioresources, Auburn, CA, USA) equipped with an Advance nESI source. The phosphopeptide mixtures were separated on a 200 μm i.d. × 50 mm fused silica column packed with Magic C18 (3 μm, 200 Å; Michrom Bioresources, Auburn, CA, USA). Gradient elution was performed linearly over a 45-min period from 95% solvent A (0.1% formic acid in H_2O) to 50% solvent B (0.1% formic acid in CH_3CN) at a flow rate of 2 μL min^{-1}. The ion transfer tube of the mass spectrometer was set at 180 °C and the spray voltage was maintained at 2.0 kV. All data were acquired automatically using methods created with Xcalibur software (Thermo Fisher Scientific, San Jose, CA, USA). The top three parent ions from each MS scan above a threshold of 10,000 counts were selected for CID-MS/MS using standard conditions. The isolation window was maintained at 2.0 m/z and the normalized collision energy was set at 25. The LTQ was operated in a data-dependent constant neutral loss scan mode (DDCNL), developed in our laboratory [170]. If neutral losses with a m/z variance of ±0.5 according to the defined values listed in Table 7.2 or Table 7.3 were detected above a threshold of 10,000, CID-MS^3 was automatically initiated to further fragment the most abundant neutral loss product ion. The neutral loss values listed in Table 7.2 account for single, double, triple and quadruple $S(CH_3)_2$ neutral losses resulted from non-isotope encoded DMBNHS derivatization experiments; otherwise, the numbers shown in Table 7.3 were corresponding to $S(CH_3)_2$ and $S(CD_3)_2$ neutral losses for the quantitative analysis of phosphopeptides employing D_6-light DMBNHS and D_6-heavy DMBNHS derivatization reagents. Dynamic exclusion was enabled to allow a maximum of five analyses of the selected m/z within 30 s before it was placed on a dynamic exclusion list for a period of 10 s.

Table 7.2 Summary of the data dependent constant neutral loss (DDCNL) MS/MS values employed for the identification of DMBNHS derivatized phosphopeptides.

Neutral loss (m/z)	Number of $S(CH_3)_2$ neutral losses	Charge state of precursor ion
62.00	1	1+
	2	2+
	3	3+
	4	4+
49.60	4	5+
46.50	3	4+
41.33	2	3+
37.20	3	5+
31.00	1	2+
	2	4+
24.80	2	5+
20.67	1	3+
15.50	1	4+
12.40	1	5+

Table 7.3 Summary of the data dependent constant neutral loss (DDCNL) MS/MS values employed for the identification of D_6-light DMBNHS and D_6-heavy DMBNHS derivatized phosphopeptides.

Neutral loss (m/z)	Number of neutral losses	Charge state of precursor ion
68.06	1 $S(CD_3)_2$	1+
	2 $S(CD_3)_2$	2+
	3 $S(CD_3)_2$	3+
62.02	1 $S(CH_3)_2$	1+
	2 $S(CH_3)_2$	2+
	3 $S(CH_3)_2$	3+
45.37	2 $S(CD_3)_2$	3+
41.35	2 $S(CH_3)_2$	3+
34.03	1 $S(CD_3)_2$	2+
	2 $S(CD_3)_2$	4+
31.01	1 $S(CH_3)_2$	2+
	2 $S(CH_3)_2$	4+
22.69	1 $S(CD_3)_2$	3+
20.67	1 $S(CH_3)_2$	3+

7.6.3 HPLC-ESI-MS, CID-MS/MS and ETD–MS/MS for Phosphopeptide Analysis

LC-MS, CID-MS/MS and ETD-MS/MS analysis was performed using a LTQ XL mass spectrometer coupled with a Paradigm MS4 capillary RP-HPLC system (Michrom Bioresources, Auburn, CA, USA) equipped with an Advance nESI source. Chromatographic separation was performed using a C18 stationary phase column, 50 mm length × 200 μm i.d. The mobile phase consisted of 2% CH_3CN and 0.1% formic acid in H_2O (A) and 5% H_2O and 0.1 % formic acid in CH_3CN (B). Gradient elution was performed by increasing the mobile-phase composition from 2% to 46% B over 44 min at a flow rate of 2 μL min^{-1}.

The ion transfer tube of the mass spectrometer was set at 200 °C while the spray voltage was maintained at 1.4 kV. All MS and MS/MS spectra were collected automatically using methods created with Xcalibur software (Thermo, San Jose, CA, USA) and all spectra were recorded in centroid mode. The LTQ XL was operated in Nth Order Double Play With ETD mode, whereby the top five parent ions from each MS scan above a threshold abundance of 10,000 counts were selected for sequential alternating CID-MS/MS and ETD-MS/MS, with the isolation window maintained at 2.0 m/z. The normalized collision energy was set at 30 for CID experiments. ETD experiments were carried out by using fluoranthene anions as the electron-transfer reagent with optimized reaction times of 30 ms and ETcaD enabled.

7.7 Data Analysis

7.7.1 Quantitative Analysis of Phosphopeptide Ion Abundances

In order to evaluate the peptide ionization efficiency upon 'fixed charge' derivatization, the average ratio of the relative abundances (summed from all observed charge states) were determined from derivatized and underivatized phosphopeptide forms. Since the same charge states could not always be observed from particular phosphopeptide pairs, the ratios of the average percent charge state were calculated to highlight the charge state distributions of derivatized phosphopeptides compared with underivatized ones. All relative abundances were determined from full mass spectra averaged over the corresponding chromatographic peaks.

7.7.2 Relative Quantitative Analysis of Phosphopeptides by Differential Isotope Labeling

Note that for quantitative analysis experiments, the precursor ions have the same m/z in the ESI-MS spectra due to the isobaric nature of the two isotope labeling reagents. Thus, quantitative analysis was achieved by calculating the ratio of the "light" and "heavy" labeled neutral-loss (i.e., $S(CH_3)_2$ and $S(CD_3)_2$) product ion abundances which were determined following HPLC-CID-MS/MS analysis of D_6-light and D_6-heavy DMBNHS labeled phosphopeptides for all available charge states. Successive target neutral losses were observed from multiply modified phosphopeptides. Sometimes the targeted neutral losses also appeared together with other neutral losses such as H_2O and NH_3. In these cases, the summed abundances from all product ions resulting from the loss of $S(CH_3)_2$ or $S(CD_3)_2$ were used for determination of the ratio. During ETD-MS/MS experiments, neutral losses of $S(CH_3)_2$ or $S(CD_3)_2$ were also observed from charge

reduced species of precursor ions which contain the fixed charge derivative. In these cases, the same calculations as those described above were applied as an alternative tool for relative quantitative analysis.

REFERENCES

1. Anderson, N. L.; Anderson, N. G., Proteome and Proteomics: New Technologies, New Concepts, and New Words. *Electrophoresis* **1998,** 19, 1853-1861.

2. Cox, J.; Mann, M., Is Proteomics the New Genomics? *Cell* **2007,** 130, 395-398.

3. Aebersold, R.; Mann, M., Mass Spectrometry-Based Proteomics. *Nature* **2003,** 422, 198-207.

4. Cañas, B.; López-Ferrer, D.; Ramos-Fernández, A.; Camafeita, E.; Calvo, E., Mass Spectrometry Technologies for Proteomics. *Brief. Funct. Genomic. Proteomic.* **2006,** 4, 295-320.

5. Cravatt, B. F.; Simon, G. M.; Yates, J. R., III, The Biological Impact of Mass-Spectrometry-Based Proteomics. *Nature* **2007,** 450, 991-1000.

6. Baker, M., Mass Spectrometry for Biologists. *Nat. Methods* **2010,** 7, 157-161.

7. Fenn, J. B.; Mann, M.; Meng, C. K.; Wong, S. F.; Whitehouse, C. M., Electrospray Ionization for Mass Spectrometry of Large Biomolecules. *Science* **1989,** 246, 64-71.

8. Karas, M.; Hillenkamp, F., Laser Desorption Ionization of Proteins with Molecular Masses Exceeding 10 000 Daltons. *Anal. Chem.* **1988,** 60, 2299-2301.

9. Tanaka, K.; Waki, H.; Ido, Y.; Akita, S.; Yoshida, Y.; Yoshida, T., Protein and Polymer Analyses up to mlz 100 000 by Laser Ionization Time-of-flight Mass Spectrometry. *Rapid Commun. Mass Spectrom.* **1988,** 2, 151-153.

10. Mirza, S. P.; Olivier, M., Methods and Approaches for the Comprehensive Characterization and Quantification of Cellular Proteomes using Mass Spectrometry. *Physiol Genomics* **2008,** 33, 3-11.

11. Mann, M.; Jensen, O. N., Proteomic Analysis of Post-Translational Modifications. *Nat. Biotechnol.* **2003,** 21, 255-261.

12. Cox, K. A.; Gaskell, S. J.; Morris, M.; Whiting, A., Role of the Site of Protonation in the Low-Energy Decompositions of Gas-Phase Peptide Ions. *J. Am. Soc. Mass Spectrom.* **1996,** 7, 515-612.

13. Wysocki, V. H.; Tsaprailis, G.; Smith, L. L.; Breci, L. A., Mobile and Localized Protons: A Framework for Understanding Peptide Dissociation. *J. Mass Spectrom.* **2000,** 35, 1399-1406.

14. Kapp, E. A.; Schütz, F.; Reid, G. E.; Eddes, J. S.; Moritz, R. L.; O'Hair, R. A. J.; Speed, T. P.; Simpson, R. J., Mining a Tandem Mass Spectrometry Database To Determine the Trends and Global Factors Influencing Peptide Fragmentation. *Anal. Chem.* **2003,** 75, 6251-6264.

15. Hung, C.-W.; Schlosser, A.; Wei, J.; Lehmann, W. D., Collision-Induced Reporter Fragmentations for Identification of Covalently Modified Peptides. *Anal. Bioanal. Chem.* **2007,** 389, 1003-1016.

16. Annan, R. S.; Carr, S. A., Phosphopeptide Analysis by Matrix-Assisted Laser Desorption Time-of-Flight Mass Spectrometry. *Anal. Chem.* **1996,** 68, 3413-3421.

17. Palumbo, A. M.; Tepe, J. J.; Reid, G. E., Mechanistic Insights into the Multistage Gas-Phase Fragmentation Behavior of Phosphoserine- and Phosphothreonine-Containing Peptides. *J. Proteome Res.* **2008,** 7, 771-779.

18. Reid, G. E.; Roberts, K. D.; Kapp, E. A.; Simpson, R. J., Statistical and Mechanistic Approaches to Understanding the Gas-Phase Fragmentation Behavior of Methionine Sulfoxide Containing Peptides. *J. Proteome Res.* **2004,** 3, 751-759.

19. Froelich, J. M.; Kaplinghat, S.; Reid, G. E., Automated Neutral Loss and Data Dependent Energy Resolved "Pseudo MS^3" for the Targeted Identification, Characterization and Quantitative Analysis of Methionine-Containing Peptides *Eur. J. Mass Spectrom.* **2008,** 14, 219-229.

20. Ong, S.-E.; Mann, M., Mass Spectrometry-Based Proteomics Turns Quantitative. *Nat. Chem. Biol.* **2005,** 1, 252-262.

21. Elliott, M. H.; Smith, D. S.; Parker, C. E.; Borchers, C., Current Trends in Quantitative Proteomics. *J. Mass Spectrom.* **2009,** 44, 1637-1660.

22. Gingras, A.-C.; Gstaiger, M.; Raught, B.; Aebersold, R., Analysis of Protein Complexes Using Mass Spectrometry. *Nat. Rev. Mol. Cell Bio.* **2007,** 8, 645-654.

23. Leitner, A.; Lindner, W., Current Chemical Tagging Strategies for Proteome Analysis by Mass Spectrometry. *J. Chromatogr. B* **2004,** 813, 1-26.

24. Leitner, A.; Lindner, W., Chemistry Meets Proteomics: The Use of Chemical Tagging Reactions for MS-Based Proteomics. *Proteomics* **2006,** 6, 5418-5434.

25. Froelich, J. M.; Lu, Y.; Reid, G. E., *Chemical Derivatization and Multistage Tandem Mass Spectrometry for Protein Structural Characterization*. CRC Press: 2009; Vol. V Applications of Ion Trapping Devices.

26. Roth, K. D. W.; Huang, Z. H.; Sadagopan, N.; Watson, J. T., Charge Derivatization of Peptides for Analysis by Mass Spectrometry. *Mass Spectrom. Rev.* **1998,** 17, 255-274.

27. Zhao, Y.; Jensen, O. N., Modification-Specific Proteomics: Strategies for Characterization of Post-Translational Modifications Using Enrichment Techniques. *Proteomics* **2009,** 9, 4632-4641.

28. Lill, J., Proteomic Tools for Quantitation by Mass Spectrometry. *Mass Spectrom. Rev.* **2003,** 22, 182-194.

29. Mendoza, V. L.; Vachet, R. W., Probing Protein Structure by Amino Acid-Specific Covalent Labeling and Mass Spectrometry. *Mass Spectrom. Rev.* **2009,** 28, 785-815.

30. Seidler, J.; Zinn, N.; Boehm, M. E.; Lehmann, W. D., *De Novo S*equencing of Peptides by MS/MS. *Proteomics* **2010,** 10, 634-649.

31. Hunt, D. F.; Yates, J. R., III; Shabanowitz, J.; Winston, S.; Hauer, C. R., Protein Sequencing by Tandem Mass Spectrometry. *Proc. Natl. Acad. Sci. USA* **1986,** 83, 6233-6237.

32. Steen, H.; Mann, M., The ABC's (and XYZ's) of Peptide Sequencing. *Nat. Rev. Mol. Cell Bio.* **2004,** 5, 699-711.

33. Renzone, G.; Salzano, A. M.; Arena, S.; Ambrosio, C. D.; Scaloni, A., Mass Spectrometry-Based Approaches for Structural Studies on Protein Complexes at Low-Resolution. *Current Proteomics* **2007,** 4, 1-16.

34. Dikler, S.; Kelly, J. W.; Russell, D. H., Improving Mass Spectrometric Sequencing of Arginine-containing Peptides by Derivatization with Acetylacetone. *J. Mass Spectrom.* **1997,** 32, 1337-1349.

35. Foettinger, A.; Leitner, A.; Lindner, W., Derivatisation of Arginine Residues with Malondialdehyde for the Analysis of Peptides and Protein Digests by LC-ESI-MS/MS. *J. Mass Spectrom.* **2006,** 41, 623-632.

36. Kuyama, H.; Sonomura, K.; Shima, K.; Nishimura, O.; Tsunasawa, S., An Improved Method for d*e Novo* Sequencing of Arginine-Containing, N^{α}-Tris(2,4,6-trimethoxyphenyl)-Phosphonium-Acetylated Peptides. *Rapid Commun. Mass Spectrom.* **2008,** 22, 2063-2072.

37. Keough, T.; Youngquist, R. S.; Lacey, M. P., A Method for High-Sensitivity Peptide Sequencing Using Postsource Decay Matrix-Assisted Laser Desorption Ionization Mass Spectrometry. *Proc. Natl. Acad. Sci. USA* **1999,** 96, 7131-7136.

38. Huang, Z.-H.; Wu, J.; Roth, K. D. W.; Yang, Y.; Gage, D. A.; Watson, J. T., A Picomole-Scale Method for Charge Derivatization of Peptides for Sequence Analysis by Mass Spectrometry. *Anal. Chem.* **1997,** 69, 137-144.

39. Münchbach, M.; Quadroni, M.; Miotto, G.; James, P., Quantitation and Facilitated de Novo Sequencing of Proteins by Isotopic N-Terminal Labeling of Peptides with a Fragmentation-Directing Moiety. *Anal. Chem.* **2000,** 72, 4047-4057.

40. Keough, T.; Youngquist, R. S.; Lacey, M. P., Sulfonic Acid Derivatives for Peptide Sequencing by MALDI MS. *Anal. Chem.* **2003,** 75, 156A-165A.

41. Keough, T.; Lacey, M. P.; Youngquist, R. S., Derivatization Procedures to Facilitate *de Novo* Sequencing of Lysine-Terminated Tryptic Peptides Using Postsource Decay Matrix-

Assisted Laser Desorption/Ionization Mass Sspectrometry. *Rapid Commun. Mass Spectrom.* **2000,** 14, 2348-2356.

42. Samyn, B.; Debyser, G.; Sergeant, K.; Devreese, B.; Beeumen, J. V., A Case Study of De Novo Sequence Analysis of N-Sulfonated Peptides by MALDI TOF/TOF Mass Spectrometry. *J. Am. Soc. Mass Spectrom.* **2004,** 15, 1838-1852.

43. Keough, T.; Lacey, M. P.; Strife, R. J., Atmospheric Pressure Matrix-Assisted Laser Desorption/Ionization Ion Trap Mass Spectrometry of Sulfonic Acid Derivatized Trptic Peptides. *Rapid Commun. Mass Spectrom.* **2001,** 15, 2227-2239.

44. Gevaert, K.; Demol, H.; Martens, L.; Hoorelbeke, B.; Puype, M.; Goethals, M.; Damme, J. V.; Boeck, S. D.; Vandekerckhove, J., Protein Identification Based on Matrix Assisted Laser Desorption/Ionization-Post Source Decay Mass Spectrometry. *Electrophoresis* **2001,** 22, 1645-1651.

45. Wang, D.; Kalb, S. R.; Cotter, R. J., Improved Procedures for N-Terminal Sulfonation of Peptides for Matrix-Assisted Laser Desorption/Ionization Post-Source Decay Peptide Sequencing. *Rapid Commun. Mass Spectrom.* **2004,** 18, 96-102.

46. Marekov, L. N.; Steinert, P. M., Charge Derivatization by 4-Sulfophenyl Isothiocyanate Enhances Peptide Sequencing by Post-Source Decay Matrix-Assisted Laser Desorption/Ionization Time-of-Flight Mass Spectrometry. *J. Mass Spectrom.* **2003,** 38, 373-377.

47. Lee, Y. H.; Kim, M.-S.; Choie, W.-S.; Min, H.-K.; Lee, S.-W., Highly Informative Proteome Analysis by Combining Improved N-Terminal Sulfonation for *de Novo* Peptide Sequencing and Online Capillary Reverse-Phase Liquid Chromatography/Tandem Mass Spectrometry. *Proteomics* **2004,** 4, 1684-1694.

48. William R. Alley, J.; Mechref, Y.; Klouckova, I.; Novotny, M. V., Improved Collision-Induced Dissociation Analysis of Peptides by Matrix-Assisted Laser Desorption/Ionization Tandem Time-of-Flight Mass Spectrometry through 3-Sulfobenzoic Acid Succinimidyl Ester Labeling. *J. Proteome Res.* **2007,** 6, 124-132.

49. Franck, J.; Ayed, M. E.; Wisztorski, M.; Salzet, M.; Fournier, I., On-Tissue N-Terminal Peptide Derivatizations for Enhancing Protein Identification in MALDI Mass Spectrometric Imaging Strategies. *Anal. Chem.* **2009,** 81, 8305-8317.

50. Liao, P.-C.; Huang, Z.-H.; Allison, J., Charge Remote Fragmentation of Peptides Following Attachment of a Fixed Positive Charge: A Matrix-Assisted Laser Desorption / Ionization Postsource Decay Study. *J. Am. Soc. Mass Spectrom.* **1997,** 8, 501-509.

51. Adamczyk, M.; Gebler, J. C.; Wu, J., Charge Derivatization of Peptides to Simplify their Sequencing with an Ion Trap Mass Spectrometer. *Rapid Commun. Mass Spectrom.* **1999,** 13, 1413-1422.

52. Huang, Z.-H.; Shen, T.; Wu, J.; Cage, D. A.; Watson, J. T., Protein Sequencing by Matrix-Assisted Laser Desorption Ionization-Postsource Decay-Mass Spectrometry Analysis of the *N*-Tris(2,4,6-trimethoxyphenyl)phosphine-Acetylated Tryptic Digests. *Anal. Biochem.* **1999,** 268, 305-317.

53. Shen, T. L.; Allison, J., Interpretation of Matrix-Assisted Laser Desorption/Ionization Postsource Decay Spectra of Charge-Derivatized Peptides: Some Examples of Tris[(2,4,6-Trimethoxyphenyl) Phosphonium]-Tagged Proteolytic Digestion Products of Phosphoenolpyruvate Carboxykinase. *J. Am. Soc. Mass Spectrom.* **2000,** 11, 145-152.

54. Sadagopan, N.; Watson, J. T., Investigation of the Tris(trimethoxyphenyl)phosphonium Acetyl Charged Derivatives of Peptides by Electrospray Ionization Mass Spectrometry and Tandem Mass Spectrometry. *J. Am. Soc. Mass Spectrom.* **2000,** 11, 107-119.

55. Chen, W.; Lee, P. J.; Shion, H.; Ellor, N.; Gebler, J. C., Improving de Novo Sequencing of Peptides Using a Charged Tag and C-Terminal Digestion. *Anal. Chem.* **2007,** 79, 1583-1590.

56. Harrison, A. G.; Young, A. B.; Bleiholder, C.; Suhai, S.; paizs, B., Scrambling of Sequence Information in Collision-Induced Dissociation of Peptides. *J. Am. Chem. Soc.* **2006,** 128, 10364-10365.

57. Samgina, T. Y.; Kovalev, S. V.; Gorshkov, V. A.; Artemenko, K. A.; Poljakov, N. B.; Lebedeva, A. T., N-Terminal Tagging Strategy for *De Novo* Sequencing of Short Peptides by ESI-MS/MS and MALDI-MS/MS. *J Am. Soc. Mass Spectrom.* **2010,** 21, 104-111.

58. Zubarev, R. A.; Kelleher, N. L.; McLafferty, F. W., Electron Capture Dissociation of Multiply Charged Protein Cations. A Nonergodic Process. *J. Am. Chem. Soc.* **1998,** 120, 3265-3266.

59. Syka, J. E. P.; Coon, J. J.; Schroeder, M. J.; Shabanowitz, J.; Hunt, D. F., Peptide and Protein Sequence Analysis by Electron Transfer Dissociation Mass Spectrometry. *Proc. Natl. Acad. Sci. USA* **2004,** 101, 9528-9533.

60. Zubarev, R. A.; Kruger, N. A.; Fridriksson, E. K.; Lewis, M. A.; Horn, D. M.; Carpenter, B. K.; McLafferty, F. W., Electron Capture Dissociation of Gaseous Multiply-Charged Proteins Is Favored at Disulfide Bonds and Other Sites of High Hydrogen Atom Affinity. *J. Am. Chem. Soc.* **1999,** 121, 2857-2862.

61. Horn, D. M.; Zubarev, R. A.; McLafferty, F. W., Automated *de Novo* Sequencing of Proteins by Tandem High-Resolution Mass Spectrometry. *Proc. Natl. Acad. Sci. USA* **2000,** 97, 10313-10317.

62. Zubarev, R. A.; Horn, D. M.; Fridriksson, E. K.; Kelleher, N. L.; Kruger, N. A.; Lewis, M. A.; Carpenter, B. K.; McLafferty, F. W., Electron Capture Dissociation for Structural Characterization of Multiply Charged Protein Cations. *Anal. Chem.* **2000,** 72, 563-573.

63. Cooper, H. J.; Håkansson, K.; Marshall, A. G., The Role of Electron Capture Dissociation in Biomolecular Analysis. *Mass Spectrom. Rev.* **2005,** 24, 201-222.

64. Mikesh, L. M.; Ueberheide, B.; Chi, A.; Coon, J. J.; Syka, J. E. P.; Shabanowitz, J.; Hunt, D. F., The Utility of ETD Mass Spectrometry in Proteomic Analysis. *Biochim. Biophys. Acta* **2006,** 1764, 1811-1822.

65. Good, D. M.; Wirtala, M.; McAlister, G. C.; Coon, J. J., Performance Characteristics of Electron Transfer Dissociation Mass Spectrometry. *Mol. Cell. Proteomics* **2007,** 6, 1942-1951.

66. Zubarev, R. A.; Zubarev, A. R.; Savitski, M. M., Electron Capture/Transfer versus Collisionally Activated/Induced Dissociations: Solo or Duet? *J. Am. Soc. Mass Spectrom.* **2008,** 19, 753-761.

67. Pitteri, S. J.; Chrisman, P. A.; Hogan, J. M.; McLuckey, S. A., Electron Transfer Ion/Ion Reactions in a Three-Dimensional Quadrupole Ion Trap: Reactions of Doubly and Triply Protonated Peptides with $SO_2^{\cdot-}$. *Anal. Chem.* **2005,** 77, 1831-1839.

68. Pitteri, S. J.; Chrisman, P. A.; McLuckey, S. A., Electron-Transfer Ion/Ion Reactions of Doubly Protonated Peptides: Effect of Elevated Bath Gas Temperature. *Anal. Chem.* **2005,** 77, 5662-5669.

69. Ueberheide, B. M.; Fenyö, D.; Alewood, P. F.; Chait, B. T., Rapid Sensitive Analysis of Cysteine Rich Peptide Venom Components. *Proc. Natl. Acad. Sci. USA* **2009,** 106, 6910-6915.

70. Vasicek, L.; Brodbelt, J. S., Enhanced Electron Transfer Dissociation through Fixed Charge Derivatization of Cysteines. *Anal. Chem.* **2009,** 81, 7876-7884.

71. Madsen, J. A.; Brodbelt, J. S., Simplifying Fragmentation Patterns of Multiply Charged Peptides by N-Terminal Derivatization and Electron Transfer Collision Activated Dissociation. *Anal. Chem.* **2009,** 81, 3645-3653.

72. Hennrich, M. L.; Boersema, P. J.; van den Toorn, H.; Mischerikow, N.; Heck, A. J. R.; Mohammed, S., Effect of Chemical Modifications on Peptide Fragmentation Behavior upon Electron Transfer Induced Dissociation. *Anal. Chem.* **2009,** 81, 7814-7822.

73. Chamot-Rooke, J.; van der Rest, G.; Dalleu, A.; Bayc, S.; Lemoineb, J., The Combination of Electron Capture Dissociation and Fixed Charge Derivatization Increases Sequence Coverage for *O*-Glycosylated and *O*-Phosphorylated Peptides. *J. Am. Soc. Mass Spectrom.* **2007,** 18, 1405-1413.

74. Chamot-Rooke, J.; Malosse, C.; Frison, G.; Tureček, F., Electron Capture in Charge-Tagged Peptides. Evidence for the Role of Excited Electronic States. *J. Am. Soc. Mass Spectrom.* **2007,** 18, 2146-2161.

75. Jones, J. W.; Sasaki, T.; Goodlett, D. R.; Tureček, F., Electron Capture in Spin-Trap Capped Peptides. An Experimental Example of Ergodic Dissociation in Peptide Cation-Radicals. *J. Am. Soc. Mass Spectrom.* **2007,** 18, 432-444.

76. Li, X.; Cournoyer, J. J.; Lin, C.; O'Connor, P. B., The Effect of Fixed Charge Modifications on Electron Capture Dissociation. *J. Am. Soc. Mass Spectrom.* **2008,** 19, 1514-1526.

77. Sohn, C. H.; Chung, C. K.; Yin, S.; Ramachandran, P.; Loo, J. A.; Beauchamp, J. L., Probing the Mechanism of Electron Capture and Electron Transfer Dissociation Using Tags with Variable Electron Affinity. *J. Am. Chem. Soc.* **2009,** 131, 5444-5459.

78. Xia, Y.; Gunawardena, H. P.; Erickson, D. E.; McLuckey, S. A., Effects of Cation Charge-Site Identity and Position on Electron-Transfer Dissociation of Polypeptide Cations. *J. Am. Chem. Soc.* **2007,** 129, 12232-12243.

79. Gunawardena, H. P.; Gorenstein, L.; Erickson, D. E.; Xia, Y.; McLuckey, S. A., Electron Transfer Dissociation of Multiply Protonated and Fixed Charge Disulfide Linked Polypeptides. *Int. J. Mass Spectrom.* **2007,** 265, 130-138.

80. Chung, T.; Tureček, F., Selecting Fixed-Charge Groups for Electron-Based Peptide Dissociations A Computational Study of Pyridinium Tags. *Int. J. Mass Spectrom.* **2008,** 276, 127-135.

81. Little, D. P.; Speir, J. P.; Senko, M. W.; O'Connor, P. B.; McLafferty, F. W., Infrared Multiphoton Dissociation of Large Multiply Charged Ions for Biomolecule Sequencing. *Anal. Chem.* **1994,** 66, 2809-2815.

82. Thompson, M. S.; Cui, W.; Reilly, J. P., Fragmentation of Singly Charged Peptide Ions by Photodissociation at λ=157 nm. *Angew. Chem. Int. Ed.* **2004,** 43, 4791-4794.

83. Brodbelt, J. S.; Wilson, J. J., Infrared Multiphoton Dissociation in Quadrupole Ion Traps. *Mass Spectrom. Rev.* **2009,** 28, 390-424.

84. Reilly, J. P., Ultraviolet Photofragmentation of Biomolecular Ions. *Mass Spectrom. Rev.* **2009,** 28, 425-447.

85. Oh, J. Y.; Moon, J. H.; Kim, M. S., Chromophore Effect in Photodissociation at 266 nm of Protonated Peptides Generated by Matrix-Assisted Laser Desorption Ionization (MALDI). *J. Mass Spectrom.* **2005,** 40, 899-907.

86. Tecklenburg, R. E., Jr., Miller, M. N.; Russell, D. H., Laser Ion Beam Photodissociation Studies of Model Amino Acids and Peptides. *J. Am. Chem. Soc.* **1989,** 111, 1161-1171.

87. Oh, J. Y.; Moon, J. H.; Lee, Y. H.; Hyung, S.-W.; Lee, S.-W.; Kim, M. S., Photodissociation Tandem Mass Spectrometry at 266nm of an Aliphatic Peptide Derivatized with Phenyl Isothiocyanate and 4-Sulfophenyl Isothiocyanate. *Rapid Commun. Mass Spectrom.* **2005,** 19, 1283-1288.

88. Wilson, J. J.; Brodbelt, J. S., Infrared Multiphoton Dissociation for Enhanced de Novo Sequence Interpretation of N-Terminal Sulfonated Peptides in a Quadrupole Ion Trap. *Anal. Chem.* **2006,** 78, 6855-6862.

89. Wilson, J. J.; Brodbelt, J. S., MS/MS Simplification by 355 nm Ultraviolet Photodissociation of Chromophore-Derivatized Peptides in a Quadrupole Ion Trap. *Anal. Chem.* **2007,** 79, 7883-7892.

90. Vasicek, L. A.; Wilson, J. J.; Brodbelt, J. S., Improved Infrared Multiphoton Dissociation of Peptides through N-Terminal Phosphonite Derivatization. *J. Am. Soc. Mass Spectrom.* **2009,** 20, 377-384.

91. Ly, T.; Julian, R. R., Residue-Specific Radical-Directed Dissociation of Whole Proteins in the Gas Phase. *J. Am. Chem. Soc.* **2008,** 130, 351-358.

92. Diedrich, J. K.; Julian, R. R., Site-Selective Fragmentation of Peptides and Proteins at Quinone-Modified Cysteine Residues Investigated by ESI-MS. *Anal. Chem.* **2010,** 82, 4006-4014.

93. Seo, J.; Lee, K.-J., Post-translational Modifications and Their Biological Functions: Proteomic Analysis and Systematic Approaches. *J. Biochem. Mol. Biol.* **2004,** 37, 35-44.

94. Czeszak, X.; Morelle, W.; Ricart, G.; Tétaert, D.; Lemoine, J., Localization of the O-Glycosylated Sites in Peptides by Fixed-Charge Derivatization with a Phosphonium Group. *Anal. Chem.* **2004,** 76, 4320-4324.

95. Mega, T.; Nakamura, N.; Ikenaka, T., Modifications of Substituted Seryl and Threonyl Residues in Phosphopeptides and a Polysialoglycoprotein by β-Elimination and Nucleophile Additions. *J. Biochem.* **1990,** 107, 68-72.

96. Zhou, H.; D.Watts, J.; Aebersold, R., A Systematic Approach to the Analysis of Protein Phosphorylation. *Nat. Biotechnol.* **2001,** 19, 375-378.

97. Tao, W. A.; Wollscheid, B.; O'Brien, R.; Eng, J. K.; Li, X.-j.; Bodenmiller, B.; Watts, J. D.; Hood, L.; Aebersold, R., Quantitative Phosphoproteome Analysis Using a Dendrimer Conjugation Chemistry and Tandem Mass Spectrometry. *Nat. Methods* **2005,** 2, 591-598.

98. van der Veken, P.; Dirksen, E. H. C.; Ruijter, E.; Elgersma, R. C.; Heck, A. J. R.; Rijkers, D. T. S.; Slijper, M.; Liskamp, R. M. J., Development of a Novel Chemical Probe for the Selective Enrichment of Phosphorylated Serine and Threonine-Containing Peptides. *ChemBioChem* **2005,** 6, 2271-2280.

99. Oda, Y.; Nagasu, T.; Chait, B. T., Enrichment Analysis of Phosphorylated Proteins as a Tool for Probing the Phosphoproteome. *Nat. Biotechnol.* **2001,** 19, 379-382.

100. Goshe, M. B.; Veenstra, T. D.; Panisko, E. A.; Conrads, T. P.; Angell, N. H.; Smith, R. D., Phosphoprotein Isotope-Coded Affinity Tags: Application to the Enrichment and Identification of Low-Abundance Phosphoproteins. *Anal. Chem.* **2002,** 74, 607-616.

101. McLachlin, D. T.; Chait, B. T., Improved β-Elimination-Based Affinity Purification Strategy for Enrichment of Phosphopeptides. *Anal. Chem.* **2003,** 75, 6826-6836.

102. Chowdhury, S. M.; Munske, G. R.; Siems, W. F.; Bruce, J. E., A New Maleimide-Bound Acid-Cleavable Solid-Support Reagent for Profiling Phosphorylation. *Rapid Commun. Mass Spectrom.* **2005,** 19, 899-909.

103. Steen, H.; Mann, M., A New Derivatization Strategy for the Analysis of Phosphopeptides by Precursor Ion Scanning in Positive Ion Mode. *J. Am. Soc. Mass Spectrom.* **2002,** 13, 996-1003.

104. Arrigoni, G.; Resjö, S.; Levander, F.; Nilsson, R.; Degerman, E.; Quadroni, M.; Pinna, L. A.; James, P., Chemical Derivatization of Phosphoserine and Phosphothreonine containing

Peptides to Increase Sensitivity for MALDI-Based Analysis and for Selectivity of MS/MS Analysis. *Proteomics* **2006,** 6, 757-766.

105. Amoresano, A.; Monti, G.; Cirulli, C.; Marino, G., Selective detection and identification of phosphopeptides by dansyl MS/MS/MS fragmentation. *Rapid Commun. Mass Spectrom.* **2006,** 20, 1400-1404.

106. Reinders, J.; Meyer, H. E.; Sickmann, A., Applications of Highly Sensitive Phosphopeptide Derivatization Methods Without the Need for Organic Solvents. *Proteomics* **2006,** 6, 2647-2649.

107. Mano, N.; Aoki, S.; Yamazaki, T.; Nagaya, Y.; Mori, M.; Abe, K.; Shimada, M.; Yamaguchi, H.; Goto, T.; Goto, J., Analysis of Phosphorylated Peptides by Double Pseudoneutral Loss Extraction Coupled with Derivatization Using *N*-(4-Bromobenzoyl)aminoethanethiol. *Anal. Chem.* **2009,** 81, 9395-9401.

108. Rusnak, F.; Zhou, J.; Hathaway, G. M., Identification of Phosphorylated and Glycosylated Sites in Peptides by Chemically Targeted Proteolysis. *J. Biomol. Tech.* **2002,** 13, 228-237.

109. Rusnak, F.; Zhou, J.; Hathaway, G. M., Reaction of Phosphorylated and *O*-Glycosylated Peptides by Chemically Targeted Identification at Ambient Temperature. *J. Biomol. Tech.* **2004,** 15, 296-304.

110. Knight, Z. A.; Schilling, B.; Row, R. H.; Kenski, D. M.; Gibson, B. W.; Shokat, K. M., Phosphospecific Proteolysis for Mapping Sites of Protein Phosphorylation. *Nat. Biotechnol.* **2003,** 21, 1047-1054.

111. McCormick, D. J.; Holmes, M. W.; Muddiman, D. C.; Madden, B. J., Mapping Sites of Protein Phosphorylation by Mass Spectrometry Utilizing a Chemical-Enzymatic Approach: Characterization of Products from α-S1Casein Phosphopeptides. *J. Proteome Res.* **2005,** 4, 424-434.

112. Tsumoto, H.; Ra, M.; Samejima, K.; Taguchi, R.; Kohda, K., Chemical Derivatization of Peptides Containing Phosphorylated Serine/Threonine for Efficient Ionization and Quantification in Matrix-Assisted Laser Desorption/Ionization Time-of-Flight Mass Spectrometry. *Rapid Commun. Mass Spectrom.* **2008,** 22, 965-972.

113. Weckwerth, W.; Willmitzer, L.; Fiehn, O., Comparative Quantification and Identification of Phosphoproteins Using Stable Isotope Labeling and Liquid Chromatography/Mass Spectrometry. *Rapid Commun. Mass Spectrom.* **2000,** 14, 1677-1681.

114. Adamczyk, M.; Gebler, J. C.; Wu, J., Identification of Phosphopeptides by Chemical Modification with an Isotopic Tag and Ion Trap Mass Spectrometer. *Rapid Commun. Mass Spectrom.* **2002,** 16, 999-1001.

115. Greis, K. D.; Hayes, B. K.; Comer, F. I.; Kirk, M.; Barnes, S.; Lowary, T. L.; Hart, G. W., Selective Detection and Site-Analysis of O-GlcNAc-Modified Glycopeptides by β-Elimination and Tandem Electrospray Mass Spectrometry. *Anal. Biochem.* **1996,** 234, 38-49.

116. Rademaker, G. J.; Pergantis, S. A.; Blok-Tip, L.; Langridge, J. I.; Kleen, A.; Thomas-Oates, J. E., Mass Spectrometric Determination of the Sites of O-Glycan Attachment with Low Picomolar Sensitivity. *Anal. Biochem.* **1998,** 257, 149-160.

117. Mirgorodskaya, E.; Hassan, H.; Clausen, H.; Roepstorff, P., Mass Spectrometric Determination of O-Glycosylation Sites Using β-Elimination and Partial Acid Hydrolysis. *Anal. Chem.* **2001,** 73, 1263-1269.

118. Zheng, Y.; Guo, Z.; Cai, Z., Combination of β-Elimination and Liquid Chromatography/Quadrupole Time-of-Flight Mass Spectrometry for the Determination of O-Glycosylation Sites. *Talanta* **2009,** 78, 358-363.

119. Czeszak, X.; Ricart, G.; Tetaert, D.; Michalski, J. C.; Lemoine, J., Identification of Substituted Sites on MUC5AC Mucin Motif Peptides after Enzymatic O-Glycosylation Combining β-Elimination and Fixed-Charge Derivatization. *Rapid Commun. Mass Spectrom.* **2002,** 16, 27-34.

120. Cauet, G.; Strub, J.-M.; Leize, E.; Wagner, E.; Dorsselaer, A. V.; Lusky, M., Identification of the Glycosylation Site of the Adenovirus Type 5 Fiber Protein. *Biochemistry* **2005,** 44,, 5453-5460.

121. Wells, L.; Vosseller, K.; Cole, R. N.; Cronshaw, J. M.; Matunis, M. J.; Hart, G. W., Mapping Sites of *O*-GlcNAc Modification Using Affinity Tags for Serine and Threonine Post-translational Modifications. *Mol. Cell. Proteomics* **2002,** 1, 791-804.

122. Zhang, Q.; Qian, W.-J.; Knyushko, T. V.; Clauss, T. R. W.; Purvine, S. O.; Moore, R. J.; Sacksteder, C. A.; Chin, M. H.; Smith, D. J.; Camp, D. G.; Bigelow, D. J.; Smith, R. D., A Method for Selective Enrichment and Analysis of Nitrotyrosine-Containing Peptides in Complex Proteome Samples. *J. Proteome Res.* **2007,** 6, 2257-2268.

123. Derakhshan, B.; Wille, P. C.; Gross, S. S., Unbiased Identification of Cysteine *S*-Nitrosylation Sites on Proteins. *Nat. Protoc.* **2007,** 2, 1685-1691.

124. Roth, A. F.; Wan, J.; Bailey, A. O.; Sun, B.; Kuchar, J. A.; Green, W. N.; Phinney, B. S.; Yates, J. R. III; Davis, N. G., Global Analysis of Protein Palmitoylation in Yeast. *Cell* **2006,** 125, 1003-1013.

125. Kang, R.; Wan, J.; Arstikaitis, P.; Takahashi, H.; Huang, K.; Bailey, A. O.; Thompson, J. X.; Roth, A. F.; Drisdel, R. C.; Mastro, R.; Green, W. N.; Yates, J. R., III; Davis, N. G.; EI-Husseini, A., Neural Palmitoyl-Proteomics Reveals Dynamic Synaptic Palmitoylation. *Nature* **2008,** 456, 904-909.

126. Yates, J. R. III; Ruse, C. I.; Nakorchevsky, A., Proteomics by Mass Spectrometry: Approaches, Advances, and Applications. *Annu. Rev. Biomed. Eng.* **2009,** 11, 49-79.

127. Chelius, D.; Zhang, T.; Wang, G.; Shen, R.-F., Global Protein Identification and Quantification Technology Using Two-Dimensional Liquid Chromatography Nanospray Mass Spectrometry. *Anal. Chem.* **2003,** 75, 6658-6665.

128. Old, W. M.; Meyer-Arendt, K.; Aveline-Wolf, L.; Pierce, K. G.; Mendoza, A.; Sevinsky, J. R.; Resing, K. A.; Ahn, N. G., Comparison of Label-free Methods for Quantifying Human Proteins by Shotgun Proteomics. *Mol. Cell. Proteomics* **2005,** 4, 1487-1502.

129. Julka, S.; Regnier, F., Quantification in Proteomics through Stable Isotope Coding: A Review. *J. Proteome Res.* **2004** 3, 350-363.

130. Gygi, S. P.; Rist, B.; Gerber, S. A.; Turecek, F.; Gelb, M. H.; Aebersold, R., Quantitative Analysis of Complex Protein Mixtures Using Isotope-Coded Affinity Tags. *Nat. Biotechnol.* **1999,** 17, 994-999.

131. Zhang, R.; Sioma, C. S.; Wang, S.; Regnier, F. E., Fractionation of Isotopically Labeled Peptides in Quantitative Proteomics. *Anal. Chem.* **2001,** 73, 5142-5149.

132. Zhang, R.; Sioma, C. S.; Thompson, R. A.; Xiong, L.; Regnier, F. E., Controlling Deuterium Isotope Effects in Comparative Proteomics. *Anal. Chem.* **2002,** 74, 3662-3669.

133. Zhang, R.; Regnier, F. E., Minimizing Resolution of Isotopically Coded Peptides in Comparative Proteomics. *J. Proteome Res.* **2002,** 1, 139-147.

134. Che, F.-Y.; Fricker, L. D., Quantitative Peptidomics of Mouse Pituitary: Comparison of Different Stable Isotopic Tags. *J. Mass Spectrom.* **2005,** 40, 238-249.

135. Gygi, S. P.; Rist, B.; Griffin, T. J.; Eng, J.; Aebersold, R., Proteome Analysis of Low-Abundance Proteins Using Multidimensional Chromatography and Isotope-Coded Affinity Tags. *J. Proteome Res.* **2002,** 1, 47-54.

136. Han, D. K.; Eng, J.; Zhou, H.; Aebersold, R., Quantitative Profiling of Differentiation-Induced Microsomal Proteins Using Isotope-Coded Affinity Tags and Mass Spectrometry. *Nat. Biotechnol.* **2001,** 19, 946-951.

137. Guina, T.; Purvine, S. O.; Yi, E. C.; Eng, J.; Goodlett, D. R.; Aebersold, R.; Miller, S. I., Quantitative Proteomic Analysis Indicates Increased Synthesis of a Quinolone by *Pseudomonas Aeruginosa* Isolates from Cystic Fibrosis Airways. *Proc. Natl. Acad. Sci. USA* **2003,** 100, 2771-2776.

138. Hansen, K. C.; Schmitt-Ulms, G.; Chalkley, R. J.; Hirsch, J.; Baldwin, M. A.; Burlingame, A. L., Mass Spectrometric Analysis of Protein Mixtures at Low Levels Using Cleavable ^{13}C-Isotope-coded Affinity Tag and Multidimensional Chromatography. *Mol. Cell. Proteomics* **2003,** 2, 299-314.

139. Li, J.; Steen, H.; Gygi, S. P., Protein Profiling with Cleavable Isotope-coded Affinity Tag (cICAT) Reagents. *Mol. Cell. Proteomics* **2003,** 2, 1198-1204.

140. Oda, Y.; Owa, T.; Sato, T.; Boucher, B.; Daniels, S.; Yamanaka, H.; Shinohara, Y.; Yokoi, A.; Kuromitsu, J.; Nagasu, T., Quantitative Chemical Proteomics for Identifying Candidate Drug Targets. *Anal. Chem.* **2003,** 75, 2159-2165.

141. Ross, P. L.; Huang, Y. N.; Marchese, J. N.; Williamson, B.; Parker, K.; Hattan, S.; Khainovski, N.; Pillai, S.; Dey, S.; Daniels, S.; Purkayastha, S.; Juhasz, P.; Martin, S.; Bartlet-Jones, M.; He, F.; Jacobson, A.; Pappin, D. J., Multiplexed Protein Quantitation in *Saccharomyces cerevisiae* Using Amine-reactive Isobaric Tagging Reagents. *Mol. Cell. Proteomics* **2004,** 4, 1154-1169.

142. Wu, W. W.; Wang, G.; Baek, S. J.; Shen, R.-F., Comparative Study of Three Proteomic Quantitative Methods, DIGE, cICAT, and iTRAQ, Using 2D Gel- or LC-MALDI TOF/TOF. *J. Proteome Res.* **2006,** 5, 651-658.

143. Sachon, E.; Mohammed, S.; Bache, N.; Jensen, O. N., Phosphopeptide Quantitation Using Amine-Reactive Isobaric Tagging Reagents and Tandem Mass Spectrometry: Application to Proteins Isolated by Gel Electrophoresis. *Rapid Commun. Mass Spectrom.* **2006,** 20, 1127-1134.

144. Choe, L.; Ascenzo, M. D.; Relkin, N. R.; Pappin, D.; Ross, P.; Williamson, B.; Guertin, S.; Pribil, P.; Lee, K. H., 8-Plex Quantitation of Changes in Cerebrospinal Fluid Protein Expression in Subjects Undergoing Intravenous Immunoglobulin Treatment for Alzheimer's Disease. *Proteomics* **2007,** 7, 3651-3660.

145. Nilsson, C. L.; Dillon, R.; Devakumar, A.; Shi, S. D.-H.; Greig, M.; Rogers, J. C.; Krastins, B.; Rosenblatt, M.; Kilmer, G.; Major, M.; Kaboord, B. J.; Sarracino, D.; Rezai, T.; Prakash, A.; Lopez, M.; Ji, Y.; Priebe, W.; Lang, F. F.; Colman, H.; Conrad, C. A., Quantitative Phosphoproteomic Analysis of the STAT3/IL-6/HIF1α Signaling Network: An Initial Study in GSC11 Glioblastoma Stem Cells. *J. Proteome Res.* **2010,** 9, 430-443.

146. Thompson, A.; Schäfer, J.; Kuhn, K.; Kienle, S.; Schwarz, J.; Schmidt, G.; Neumann, T.; Hamon, C., Tandem Mass Tags: A Novel Quantification Strategy for Comparative Analysis of Complex Protein Mixtures by MS/MS. *Anal. Chem.* **2003,** 75, 1895-1904.

147. Dayon, L.; Hainard, A.; Licker, V.; Turck, N.; Kuhn, K.; Hochstrasser, D. F.; Burkhard, P. R.; Sanchez, J.-C., Relative Quantification of Proteins in Human Cerebrospinal Fluids by MS/MS Using 6-Plex Isobaric Tags. *Anal. Chem.* **2008,** 80, 2921-2931.

148. Li, S.; Zeng, D., CILAT - A New Reagent for Quantitative Proteomics. *Chem. Commun.* **2007,** 21, 2181-2183.

149. Han, H.; Pappin, D. J.; Ross, P. L.; McLuckey, S. A., Electron Transfer Dissociation of iTRAQ Labeled Peptide Ions. *J. Proteome Res.* **2008,** 7, 3643-3648.

150. Phanstiel, D.; Zhang, Y.; Marto, J. A.; Coon, J. J., Peptide and Protein Quantification Using iTRAQ with Electron Transfer Dissociation. *J. Am. Soc. Mass Spectrom.* **2008,** 19, 1255-1262.

151. Phanstiel, D.; Unwin, R.; McAlister, G. C.; Coon, J. J., Peptide Quantification Using 8-Plex Isobaric Tags and Electron Transfer Dissociation Tandem Mass Spectrometry. *Anal. Chem.* **2009,** 81, 1693-1698.

152. Viner, R. I.; Zhang, T.; Second, T.; Zabrouskov, V., Quantification of Post-Translationally Modified Peptides of Bovine α-Crystallin Using Tandem Mass Tags and Electron Transfer Dissociation. *J. Proteomics* **2009,** 72, 874-885.

153. Englander, S. W., Hydrogen Exchange and Mass Spectrometry: A Historical Perspective. *J. Am. Soc. Mass Spectrom.* **2006,** 17, 1481-1489.

154. Wales, T. E.; Engen, J. R., Hydrogen Exchange Mass Spectrometry for the Analysis of Protein Dynamics. *Mass Spectrom. Rev.* **2006,** 25, 158-170.

155. Engen, J. R., Analysis of Protein Conformation and Dynamics by Hydrogen/Deuterium Exchange MS. *Anal. Chem.* **2009,** 81, 7870-7875.

156. Xu, G.; Chance, M. R., Hydroxyl Radical-Mediated Modification of Proteins as Probes for Structural Proteomics. *Chem. Rev.* **2007,** 107, 3514-3543.

157. Konermann, L.; Stocks, B. B.; Pan, Y.; Tong, X., Mass Spectrometry Combined with Oxidative Labeling for Exploring Protein Structure and Folding. *Mass Spectrom. Rev.* **2010,** 29, 651-667.

158. Sinz, A., Chemical Cross-Linking and Mass Spectrometry to Map Three-Dimensional Protein Structures and Protein-Protein Interactions. *Mass Spectrom. Rev.* **2006,** 25, 663-682.

159. Tullius, T. D.; Dombroski, B. A., Hydroxyl Radical "Footprinting": High-Resolution Information about DNA-Protein Contacts and Application to λ Repressor and Cro Protein. *Proc. Natl. Acad. Sci. USA* **1986,** 83, 5469-5473.

160. Tsai, C.-J.; Lin, S. L.; Wolfson, H. J.; Nussinov, R., Studies of Protein-Protein Interfaces: A Statistical Analysis of the Hydrophobic Effect. *Protein Sci.* **1997,** 6, 53-64.

161. Jones, S.; Heyningen, P. v.; Berman, H. M.; Thornton, J. M., Protein-DNA Interactions: A Structural Analysis. *J. Mol. Biol.* **1999,** 287, 877-896.

162. Suckau, D.; Mak, M.; Przybylski, M., Protein Surface Topology-Probing by Selective Chemical Modification and Mass Spectrometric Peptide Mapping. *Proc. Natl. Acad. Sci. USA* **1992,** 89, 5630-5634.

163. Izumi, S.; Kaneko, H.; Yamazaki, T.; Hirata, T.; Kominami, S., Membrane Topology of Guinea Pig Cytochrome P450 17α Revealed by a Combination of Chemical Modifications and Mass Spectrometry. *Biochemistry* **2003,** 42, 14663-14669.

164. Novak, P.; Kruppa, G. H.; Young, M. M.; Schoeniger, J., A Top-Down Method for the Determination of Residue-Specific Solvent Accessibility in Proteins. *J. Mass Spectrom.* **2004,** 39, 322-328.

165. Carven, G. J.; Stern, L. J., Probing the Ligand-Induced Conformational Change in HLA-DR1 by Selective Chemical Modification and Mass Spectrometric Mapping. *Biochemistry* **2005,** 44, 13625-13637.

166. Shell, S. M.; Hess, S.; Kvaratskhelia, M.; Zou, Y., Mass Spectrometric Identification of Lysines Involved in the Interaction of Human Replication Protein A with Single-Stranded DNA. *Biochemistry* **2005,** 44, 971-978.

167. Scholten, A.; Visser, N. F. C.; van der Heuvel, R. H. H.; Heck, A. J. R., Analysis of Protein-Protein Interaction Surfaces Using a Combination of Efficient Lysine Acetylation and nanoLC-MALDI-MS/MS Applied to the E9:Im9 Bacteriotoxin-Immunity Protein Complex. *J. Am. Soc. Mass Spectrom.* **2006,** 17, 983-994.

168. McKee, C. J.; Kessl, J. J.; Norris, J. O.; Shkriabai, N.; Kvaratskhelia, M., Mass Spectrometry-Based Footprinting of Protein-Protein Interactions. *Methods* **2009,** 47, 304-307.

169. Janecki, D. J.; Beardsley, R. L.; Reilly, J. P., Probing Protein Tertiary Structure with Amidination. *Anal. Chem.* **2005,** 77, 7274-7281.

170. Zhou, X.; Lu, Y.; Wang, W.; Borhan, B.; Reid, G. E., 'Fixed Charge' Chemical Derivatization and Data Dependant Multistage Tandem Mass Spectrometry for Mapping Protein Surface Residue Accessibility. *J. Am. Soc. Mass Spectrom.* **2010,** 21, 1339-1351.

171. Glocker, M. O.; Borchers, C.; Fiedler, W.; Suckau, D.; Przybylski, M., Molecular Characterization of Surface Topology in Protein Tertiary Structures by Amino-Acylation and Mass Spectrometric Peptide Mapping. *Bioconjugate Chem.* **1994,** 5, 583-590.

172. Hochleitner, E. O.; Borchers, C.; Parkrer, C.; Bienstock, R. J.; Tomer, K. B., Characterization of a Discontinuous Epitope of the Human Immunodeficiency Virus (HIV) Core Protein p24 by Epitope Excision and Differential Chemical Modification Followed by Mass Spectrometric Peptide Mapping Analysis. *Protein Sci.* **2000,** 9, 487-496.

173. Petrotchenko, E. V.; Borchers, C. H., Crosslinking Combined with Mass Spectrometry for Structural Proteomics. *Mass Spectrom. Rev.* **2010**, 29, 862-876.

174. Horton, H. R.; Moran, L. A.; Ochs, R. S.; Rawn, J. D.; Scrimgeour, K. G., Principles of Biochemistry, 3rd edition, Pearson Education, Inc., Prentice Hall. **2002**, Page 51.

175. Trakselis, M. A.; Alley, S. C.; Ishmael, F. T., Identification and Mapping of Protein-Protein Interactions by a Combination of Cross-Linking, Cleavage, and Proteomics. *Bioconjugate Chem.* **2005,** 16, 741-750.

176. Bader, G. D.; Hogue, C. W. V., Analyzing Yeast Protein-Protein Interaction Data Obtained from Different Sources. *Nature Biotech.* **2002,** 20, 991-997.

177. Qian, B.; Raman, S.; Das, R.; Bradley, P.; McCoy, A. J.; Read, R. J.; Baker, D., High-Resolution Structure Prediction and the Crystallographic Phase Problem. *Nature* **2007,** 450, 259-264.

178. Young, M. M.; Tang, N.; Hempel, J. C.; Oshiro, C. M.; Taylor, E. W.; Kuntz, I. D.; Gibson, B. W.; Dollinger, G., High Throughput Protein Fold Identification by Using Experimental Constraints Derived from Intramolecular Cross-Links and Mass Spectrometry. *Proc. Natl. Acad. Sci. USA* **2000,** 97, 5802-5806.

179. Chakravarti, B.; Lewis, S. J.; Chakravarti, D. N.; Raval, A., Three Dimensional Structures of Proteins and Protein Complexes from Chemical Cross-Linking and Mass Spectrometry: A Biochemical and Computational Overview. *Current Proteomics* **2006,** 3, 1-21.

180. Cross-Linking Reagents Technical Handbook, Pierce. **2005**, Page 3.

181. Lomant, A. J.; Fairbanks, G., Chemical Probes of Extended Biological Structures : Synthesis and Properties of the Cleavable Protein Cross-linking Reagent [^{35}S]Dithiobis (succinimidyl propionate). *J. Mol. Biol.* **1976,** 104, 243-261.

182. Bich, C.; Maedler, S.; Chiesa, K.; DeGiacomo, F.; Bogliotti, N.; Zenobi, R., Reactivity and Applications of New Amine Reactive Cross-Linkers for Mass Spectrometric Detection of Protein-Protein Complexes. *Anal. Chem.* **2010,** 82, 172-179.

183. Alley, S. C.; Ishmael, F. T.; Jones, A. D.; Benkovic, S. J., Mapping Protein-Protein Interactions in the Bacteriophage T4 DNA Polymerase Holoenzyme Using a Novel Trifunctional Photo-cross-linking and Affinity Reagent. *J. Am. Chem. Soc.* **2000,** 122, 6126-6127.

184. Trester-Zedlitz, M.; Kamada, K.; Burley, S. K.; Fenyö, D.; Chait, B. T.; Muir, T. W., A Modular Cross-Linking Approach for Exploring Protein Interactions. *J. Am. Chem. Soc.* **2003,** 125, 2416 -2425.

185. Sinz, A., Chemical Cross-Linking and Mass Spectrometry for Mapping Three-Dimensional Structures of Proteins and Protein Complexes. *J. Mass Spectrom.* **2003,** 38, 1225-1237.

186. Schilling, B.; Row, R. H.; Gibson, B. W.; Guo, X.; Young, M. M., MS2Assign, Automated Assignment and Nomenclature of Tandem Mass Spectra of Chemically Crosslinked Peptides. *J. Am. Soc. Mass Spectrom.* **2003,** 14, 834–850.

187. Sinz, A.; Kalkhof, S.; Ihling, C., Mapping Protein Interfaces by a Trifunctional Cross-Linker Combined with MALDI-TOF and ESI-FTICR Mass Spectrometry. *J. Am. Soc. Mass Spectrom.* **2005,** 16, 1921-1931.

188. Ahrends, R.; Kosinski, J.; Kirsch, D.; Manelyte, L.; Giron-Monzon, L.; Hummerich, L.; Schulz, O.; Spengler, B.; Friedhoff, P., Identifying an Interaction Site Between MutH and the C-terminal Domain of MutL by Crosslinking, Affinity Purification, Chemical Coding and Mass Spectrometry. *Nucleic Acids Res.* **2006,** 34, 3169-3180.

189. Kang, S.; Mou, L.; Lanman, J.; Velu, S.; Brouillette, W. J.; Peter E. Prevelige, J., Synthesis of Biotin-Tagged Chemical Cross-Linkers and their Applications for Mass Spectrometry. *Rapid Commun. Mass Spectrom.* **2009,** 23, 1719-1726.

190. Chowdhury, S. M.; Munske, G. R.; Tang, X.; Bruce, J. E., Collisionally Activated Dissociation and Electron Capture Dissociation of Several Mass Spectrometry-Identifiable Chemical Cross-Linkers. *Anal. Chem.* **2006,** 78, 8183-8193.

191. Chu, F.; Mahrus, S.; Craik, C. S.; Burlingame, A. L., Isotope-Coded and Affinity-Tagged Cross-Linking (ICATXL): An Efficient Strategy to Probe Protein Interaction Surfaces. *J. Am. Chem. Soc.* **2006,** 128, 10362-10363.

192. Zhang, H.; Tang, X.; Munske, G. R.; Tolic, N.; Anderson, G. A.; Bruce, J. E., Identification of Protein-Protein Interactions and Topologies in Living Cells with Chemical Cross-linking and Mass Spectrometry. *Mol. Cell. Proteomics* **2009,** 8, 409-420.

193. Chowdhury, S. M.; Du, X.; Tolić, N.; Wu, S.; Moore, R. J.; Mayer, M. U.; Smith, R. D.; Adkins, J. N., Identification of Cross-Linked Peptides after Click-Based Enrichment Using Sequential Collision-Induced Dissociation and Electron Transfer Dissociation Tandem Mass Spectrometry. *Anal. Chem.* **2009,** 81, 5524-5532.

194. Reynolds, K. J.; Yao, X.; Fenselau, C., Proteolytic ^{18}O Labeling for Comparative Proteomics: Evaluation of Endoprotease Glu-C as the Catalytic Agent. *J. Proteome Res.* **2002,** 1, 27-33.

195. Back, J. W.; Notenboom, V.; de Koning, L. J.; Muijsers, A. O.; Sixma, T. K.; de Koster, C. G.; de Jong, L., Identification of Cross-Linked Peptides for Protein Interaction Studies Using Mass Spectrometry and ^{18}O Labeling. *Anal. Chem.* **2002,** 74, 4417 -4422.

196. Chen, X.; Chen, Y. H.; Anderson, V. E., Protein Cross-Links: Universal Isolation and Characterization by Isotopic Derivatization and Electrospray Ionization Mass Spectrometry. *Anal. Biochem.* **1999,** 273, 192-203.

197. Taverner, T.; Hall, N. E.; O' Hair, R. A. J.; Simpson, R. J., Characterization of an Antagonist Interleukin-6 Dimer by Stable Isotope Labeling, Cross-linking, and Mass Spectrometry. *J. Biol. Chem.* **2002,** 277, 46487-46492.

198. Müller, D. R.; Schindler, P.; Towbin, H.; Wirth, U.; Voshol, H.; Hoving, S.; Steinmetz, M. O., Isotope-Tagged Cross-Linking Reagents. A New Tool in Mass Spectrometric Protein Interaction Analysis. *Anal. Chem.* **2001,** 73, 1927 -1934.

199. Pearson, K. M.; Pannell, L. K.; Fales, H. M., Intramolecular Cross-Linking Experiments on Cytochrome C and Ribonuclease A Using an Isotope Multiplet Method *Rapid Commun. Mass Spectrom.* **2002,** 16, 149-159.

200. Seebacher, J.; Mallick, P.; Zhang, N.; Eddes, J. S.; Aebersold, R.; Gelb, M. H., Protein Cross-Linking Analysis Using Mass Spectrometry, Isotope-Coded Cross-Linkers, and Integrated Computational Data Processing. *J. Proteome Res.* **2006** 5, 2270-2282.

201. Petrotchenko, E. V.; Olkhovik, V. K.; Borchers, C. H., Isotopically Coded Cleavable Cross-linker for Studying Protein-Protein Interaction and Protein Complexes. *Mol. Cell. Proteomics* **2005,** 4, 1167 - 1179.

202. Müller, M. Q.; de Koning, L. J.; Schmidt, A.; Ihling, C.; Syha, Y.; Rau, O.; Mechtler, K.; Schubert-Zsilavecz, M.; Sinz, A., An Innovative Method To Study Target Protein-Drug Interactions by Mass Spectrometry. *J. Med. Chem,* **2009,** 52, 2875-2879.

203. Bennett, K. L.; Kussmann, M.; Björk, P.; Godzwon, M.; Mikkelsen, M.; Sørensen, P.; Roepstorff, P., Chemical Cross-Linking with Thiol-Cleavable Reagents Combined with Differential Mass Spectrometric Peptide Mapping-A Novel Approach to Assess Intermolecular Protein Contacts. *Protein Sci.* **2000,** 9, 1503 - 1518.

204. Back, J. W.; Sanz, M. A.; de Jong, L.; de Koning, L. J.; Nijtmans, L. G. J.; de Koster, C. G.; Grivell, L. A.; van der Spek, H.; Muijsers, A. O., A Structure for the Yeast Prohibitin Complex: Structure Prediction and Evidence from Chemical Crosslinking and Mass Spectrometry. *Protein Sci.* **2002,** 11, 2471-2478.

205. Peterson, J. J.; Young, M. M.; Takemoto, L. J., Probing α-Crystallin Structure Using Chemical Cross-Linkers and Mass Spectrometry. *Mol. Vision* **2004,** 10, 857-866.

206. Kasper, P. T.; Back, J. W.; Vitale, M.; Hartog, A. F.; Roseboom, W.; de Koning, L. J.; van Maarseveen, J. H.; Muijsers, A. O.; de Koster, C. G.; de Jong, L., An Aptly Positioned Azido Group in the Spacer of a Protein Cross-Linker for Facile Mapping of Lysines in Close Proximity. *ChemBioChem* **2007,** 8, 1281-1292.

207. Back, J. W.; Hartog, A. F.; Dekker, H. L.; Muijsers, A. O.; de Koning, L. J.; de Jong, L., A New Crosslinker for Mass Spectrometric Analysis of the Quaternary Structure of Protein Complexes. *J. Am. Soc. Mass Spectrom.* **2001,** 12, 222-227.

208. Tang, X.; Munske, G. R.; Siems, W. F.; Bruce, J. E., Mass Spectrometry Identifiable Cross-Linking Strategy for Studying Protein-Protein Interactions. *Anal. Chem.* **2005,** 77, 311-318.

209. Zhang, H.; Tang, X.; Munske, G. R.; Zakharova, N.; Yang, L.; Zheng, C.; Wolff, M. A.; Tolic, N.; Anderson, G. A.; Shi, L.; Marshall, M. J.; Fredrickson, J. K.; Bruce, J. E., In Vivo Identification of the Outer Membrane Protein OmcA-MtrC Interaction Network in Shewanella oneidensis MR-1 Cells Using Novel Hydrophobic Chemical Cross-Linkers. *J. Proteome Res.* **2008,** 7, 1712-1720.

210. Soderblom, E. J.; Goshe, M. B., Collision-Induced Dissociative Chemical Cross-Linking Reagents and Methodology: Applications to Protein Structural Characterization Using Tandem Mass Spectrometry Analysis. *Anal. Chem.* **2006,** 78, 8059-8068.

211. Soderblom, E. J.; Bobay, B. G.; Cavanagh, J.; Goshe, M. B., Tandem Mass Spectrometry Acquisition Approaches to Enhance Identification of Protein-Protein Interactions Using Low-Energy Collision-Induced Dissociative Chemical Crosslinking Reagents. *Rapid Commun. Mass Spectrom.* **2007,** 21, 3395-3408.

212. Dreiocker, F.; Müller, M. Q.; Sinz, A.; Schäfer, M., Collision-Induced Dissociative Chemical Cross-Linking Reagent for Protein Structure Characterization: Applied Edman Chemistry in the Gas Phase. *J. Mass Spectrom.* **2010,** 45, 178-189.

213. Gardner, M. W.; Vasicek, L. A.; Shabbir, S.; Anslyn, E. V.; Brodbelt, J. S., Chromogenic Cross-Linker for the Characterization of Protein Structure by Infrared Multiphoton Dissociation Mass Spectrometry. *Anal. Chem.* **2008,** 80, 4807-4819.

214. Díaz, D. D.; Rajagopal, K.; Strable, E.; Schneider, J.; Finn, M. G., "Click" Chemistry in a Supramolecular Environment: Stabilization of Organogels by Copper(I)-Catalyzed Azide-Alkyne [3 + 2] Cycloaddition. *J. Am. Chem. Soc.* **2006,** 128, 6056-6057.

215. Iglesias, A. H.; Santos, L. F. A.; Gozzo, F. C., Collision-Induced Dissociation of Lys-Lys Intramolecular Crosslinked Peptides. *J Am Soc Mass Spectrom* **2009,** 20, 557-566.

216. Iglesias, A. H.; Santos, L. F. A.; Gozzo, F. C., Identification of Cross-Linked Peptides by High-Resolution Precursor Ion Scan. *Anal. Chem.* **2010,** 82, 909-916.

217. Tang, X.; Bruce, J. E., A New Cross-Linking Strategy: Protein Interaction Reporter (PIR) Technology for Protein - Protein Interaction Studies. *Mol. BioSyst.* **2010,** 6, 939-947.

218.Petrotchenko, E. V.; Xiao, K.; Cable, J.; Chen, Y.; Dokholyan, N. V.; Borchers, C. H., BiPS, a Photocleavable, Isotopically Coded, Fluorescent Cross-linker for Structural Proteomics. *Mol. Cell. Proteomics* **2009,** 8, 273-286.

219. Henzel, W. J.; Billeci, T. M.; Stults, J. T.; Wong, S. C.; Grimley, C.; Watanabe, C., Identifying Proteins from Two-Dimensional Gels by Molecular Mass Searching of Peptide Fragments in Protein Sequence Databases. *Proc. Natl. Acad. Sci. USA* **1993,** 90, 5011-5015.

220. Eng, J. K.; McCormack, A. L.; Yates, J. R., III, An Approach to Correlate Tandem Mass Spectral Data of Peptides with Amino Acid Sequences in a Protein Database. *J. Am. Soc. Mass Spectrom.* **1994,** 5, 976-989.

221. Mann, M.; Wilm, M., Error-Tolerant Identification of Peptides in Sequence Databases by Peptide Sequence Tags. *Anal. Chem.* **1994,** 66, 4390-4399.

222. Johnson, R. S.; Martin, S. A.; Biemann, K., Novel Fragmentation Process of Peptides by Collision-Induced Decomposition in a Tandem Mass Spectrometer: Differentiation of Leucine and Isoleucine. *Anal. Chem.* **1987,** 59, 2621-2625.

223. Simpson, R. J.; Connolly, L. M.; Eddes, J. S.; Pereira, J. J.; Moritz, R. L.; Reid, G. E., Proteomic Analysis of the Human Colon Carcinoma Cell Line (LIM 1215): Development of a Membrane Protein Database. *Electrophoresis* **2000,** 21, 1707-1732.

224. Boersema, P. J.; Mohammed, S.; Hecka, A. J. R., Phosphopeptide Fragmentation and Analysis by Mass Spectrometry. *J. Mass Spectrom.* **2009,** 44, 861-878.

225. Palumbo, A. M.; Smith, S. A.; Kalcic, C. L.; Dantus, M.; Stemmer, P. M.; Reid, G. E., Tandem Mass Spectrometry Strategies for Phosphoproteome Analysis. *Mass Spectrom. Rev.* **2010**, in press, DOI 10.1002/mas.20310.

226. Biemann, K.; Papayannopous, I. A., Amino Acid Sequencing of Proteins. *Acc. Chem. Res.* **1994,** 27, 370-378.

227. Paizs, B.; Suhai, S., Fragmentation Pathways of Protonated Peptides. *Mass Spectrom. Rev.* **2005,** 24, 508-548.

228. Dongré, A. R.; Jones, J. L.; Somogyi, A.; Wysocki, V. H., Influence of Peptide Composition, Gas-Phase Basicity, and Chemical Modification on Fragmentation Efficiency: Evidence for the Mobile Proton Model. *J. Am. Chem. Soc.* **1996,** 118, 8365-8374.

229. O'Hair, R. A. J., The Role of Nucleophile-Electrophile Interactions in the Unimolecular and Bimolecular Gas-Phase Ion Chemistry of Peptides and Related Systems. *J. Mass Spectrom.* **2000,** 35, 1377-1381.

230. Schlosser, A.; Lehmann, W. D., Five-Membered Ring Formation in Unimolecular Reactions of Peptides: A Key Structural Element Controlling Low-Energy Collision-Induced Dissociation of Peptides. *J. Mass Spectrom.* **2000,** 35, 1382-1390.

231. Lioe, H.; O'Hair, R. A. J., A Novel Salt Bridge Mechanism Highlights the Need for Nonmobile Proton Conditions to Promote Disulfide Bond Cleavage in Protonated Peptides Under Low-Energy Collisional Activation. *J. Am. Soc. Mass Spectrom.* **2007,** 18, 1109-1123.

232. Lee, Y. J., Mass Spectrometric Analysis of Cross-Linking Sites for the Structure of Proteins and Protein Complexes. *Mol. BioSyst.* **2008,** 4, 816-823.

233. Singh, P.; Panchaud, A.; Goodlett, D. R., Chemical Cross-Linking and Mass Spectrometry As a Low-Resolution Protein Structure Determination Technique. *Anal. Chem.* **2010,** 82, 2636-2642.

234. Gao, Q.; Xue, S.; Doneanu, C. E.; Shaffer, S. A.; Goodlett, D. R.; Nelson, S. D., Pro-CrossLink. Software Tool for Protein Cross-Linking and Mass Spectrometry. *Anal. Chem.* **2006,** 78, 2145-2149.

235. Rinner, O.; Seebacher, J.; Walzthoeni, T.; Mueller, L.; Beck, M.; Schmidt, A.; Mueller, M.; Aebersold, R., Identification of Cross-Linked Peptides from Large Sequence Databases. *Nat. Meth.* **2008,** 5, 315-318.

236. Reid, G. E.; Roberts, K. D.; Simpson, R. J.; O'Hair, R. A. J., Selective Identification and Quantitative Analysis of Methionine Containing Peptides by Charge Derivatization and Tandem Mass Spectrometry. *J. Am. Soc. Mass Spectrom.* **2005,** 16, 1131-1150.

237. Amunugama, M.; Roberts, K. D.; Reid, G. E., Mechanisms for the Selective Gas-Phase Fragmentation Reactions of Methionine Side Chain Fixed Charge Sulfonium Ion Containing Peptides. *J. Am. Soc. Mass Spectrom.* **2006,** 17, 1631-1642.

238. Sierakowski, J.; Amunugama, M.; Roberts, K. D.; Reid, G. E., Substituent Effects on the Gas-Phase Fragmentation Reactions of Sulfonium Ion Containing Peptides. *Rapid Commun. Mass Spectrom.* **2007,** 21, 1230-1238.

239. Roberts, K. D.; Reid, G. E., Leaving Group Effects on the Selectivity of the Gas-Phase Fragmentation Reactions of Side Chain Fixed-Charge-Containing Ppeptide Ions. *J. Mass Spectrom.* **2007,** 42, 187-198.

240. Anderson, G. W.; Zimmerman, J. E.; Callahan, F. M., The Use of Esters of N-Hydroxysuccinimide in Peptide Synthesis. *J. Am. Chem. Soc.* **1964,** 86, 1839-1842.

241. Oae, S.; Ed., *Organic Chemistry of Sulfur*. Plenum Press: New York, 1977.

242. Gorham, J., Separation of Plant Betaines and Their Sulphur Analogues by Cation-Exchange High-Performance Liquid Chromatography. *J. Chromatogr.* **1984,** 281, 345-451.

243. Gaucher, S. P.; Hadi, M. Z.; Young, M. M., Influence of Crosslinker Identity and Position on Gas-Phase Dissociation of Lys–Lys Crosslinked Peptides. *J. Am. Soc. Mass Spectrom.* **2006,** 17, 395-405.

244. Guo, X.; Bandyopadhyay, P.; Schilling, B.; Young, M. M.; Fujii, N.; Aynechi, T.; Guy, R. K.; Kuntz, I. D.; Gibson, B. W., Partial Acetylation of Lysine Residues Improves Intraprotein Cross-Linking. *Anal. Chem.* **2008,** 80, 951 -960.

245. Novak, P.; Young, M. M.; Schoeniger, J. S.; Kruppa, G. H., A Top-Down Approach to Protein Structure Studies Using Chemical Cross-Linking and Fourier Transform Mass Spectrometry. *Eur. J. Mass Spectrom.* **2003** 9, 623-631.

246. Swaim, C. L.; Smith, J. B.; Smith, D. L., Unexpected Products from the Reaction of the Synthetic Cross-Linker 3,3'- Dithiobis(Sulfosuccinimidyl Propionate), DTSSP with Peptides. *J. Am. Soc. Mass Spectrom.* **2004,** 15, 736–749

247. Leavell, M. D.; Novak, P.; Behrens, C. R.; Schoeniger, J. S.; Kruppa, G. H., Strategy for Selective Chemical Cross-Linking of Tyrosine and Lysine Residues. *J. Am. Soc. Mass Spectrom.* **2004,** 15, 1604-1611.

248. Kalkhof, S.; Sinz, A., Chances and Pitfalls of Chemical Cross-Linking with Amine-Reactive N-Hydroxysuccinimide Esters. *Anal. Bioanal. Chem.* **2008,** 392, 305-312.

249. Mädler, S.; Bich, C.; Touboul, D.; Zenobi, R., Chemical Cross-Linking with NHS Esters: A Systematic Study on Amino Acid Reactivities. *J. Mass Spectrom.* **2009,** 44, 694-706.

250. Mädler, S.; Gschwind, S.; Zenobi, R., Role of Arginine in Chemical Cross-Linking with N-Hydroxysuccinimide Esters. *Anal. Biochem.* **2010,** 398, 123-125.

251. Qin, J.; Chait, B. T., Preferential Fragmentation of Protonated Gas-Phase Peptide Ions Adjacent to Acidic Amino Acid Residues. *J. Am. Chem. Soc.* **1995,** 117, 5411-5412.

252. Yu, W.; Vath, J. E.; Huberty, M. C.; Martin, S. A., Identification of the Facile Gas-Phase Cleavage of the Asp-Pro and Asp-Xxx Peptide Bonds in Matrix-Assisted Laser Desorption Time-of-Flight Mass Spectrometry. *Anal. Chem.* **1993,** 65, 3015-3023.

253. Sullivan, A. G.; Brancia, F. L.; Tyldesley, R.; Bateman, R.; Sidhu, K.; Hubbard, S. J.; Oliver, S. G.; Gaskell, S. J., The Exploitation of Selective Cleavage of Singly Protonated Peptide Ions Adjacent to Aspartic Acid Residues Using a Quadrupole Orthogonal Time-Of-

Flight Mass Spectrometer Equipped with a Matrix-Assisted Laser Desorption/Ionization Source. *Int. J. Mass Spectrom.* **2001,** 210, 665-676.

254. Lee, S.-W.; Kim, H. S.; Beauchamp, J. L., Salt Bridge Chemistry Applied to Gas-Phase Peptide Sequencing: Selective Fragmentation of Sodiated Gas-Phase Peptide Ions Adjacent to Aspartic Acid Residues. *J. Am. Chem. Soc.* **1998,** 120, 3188-3195.

255. Jessing, M.; Brandt, M.; Jensen, K. J.; Christensen, J. B.; Boas, U., Thiophene Backbone Amide Linkers, a New Class of Easily Prepared and Highly Acid-Labile Linkers for Solid-Phase Synthesis. *J. Org. Chem.* **2006,** 71, 6734-6741.

256. Rabinovich, M. S.; Levimov, M. M.; Kulikova, G. N.; Yakushina, L. M.; Verkhovtseva, T. P.; Meller, F. M., An Investigation in the Field of the Synthesis of Precursors and Fragments of Antibiotics VII. Carboxy Derivatives of Mercaptoacetic Acid. . *Zhurnal Obshchei Khimii* **1962,** 32, 1167-1172.

257. Zhang, J.; Jing, B.; Tokutake, N.; Regen, S. L., Transbilayer Complementarity of Phospholipids. A Look beyond the Fluid Mosaic Model. *J. Am. Chem. Soc.* **2004,** 126, 10856-10857.

258. Numata, M.; Koumoto, K.; Mizu, M.; Sakurai, K.; Shinkai, S., Parallel vs. Anti-Parallel Orientation in a Curdlan/Oligo(dA) Complex as Estimated by a FRET Technique. *Org. Biomol. Chem.* **2005,** 3, 2255 - 2261.

259. Ficarro, S. B.; McCleland, M. L.; Stukenberg, P. T.; Burke, D. J.; Ross, M. M.; Shabanowitz, J.; Hunt, D. F.; White, F. M., Phosphoproteome Analysis by Mass Spectrometry and its Application to *Saccharomyces cerevisiae*. *Nat. Biotechnol.* **2002,** 20, 301-305.

260. He, T.; Alving, K.; Feild, B.; Norton, J.; Joseloff, E. G.; Patterson, S. D.; Domon, B., Quantitation of Phosphopeptides Using Affinity Chromatography and Stable Isotope Labeling. *J. Am. Soc. Mass Spectrom.* **2004,** 15, 363-373.

261. Hnízda, A.; Šantrůček, J.; Šanda, M.; Strohalm, M.; Kodíček, M., Reactivity of Histidine and Lysine Side-Chains with Diethylpyrocarbonate - A Method to Identify Surface-Exposed Residues in Proteins. *J. Biochem. Biophys. Methods* **2008,** 70, 1091-1097.

262. Lundblad, R. L., *Chemical Reagents for Protein Modification. 2nd edition*. CRC Press: 1991.

263. de Hoffmann, E.; Stroobant, V., Mass Spectrometry Principles and Applications. 3rd edition, John Wiley and Sons, New York.

264. March, R. E., An Introduction to Quadrupole Ion Trap Mass Spectrometry. *J. Mass Spectrom.* **1997,** 32, 351-369.

265. Hager, J. W., A New Linear Ion Trap Mass Spectrometer. *Rapid Commun. Mass Spectrom.* **2002,** 16, 512-526.

266. Schwartz, J. C.; Senko, M. W.; Syka, J. E. P., A Two-Dimensional Quadrupole Ion Trap Mass Spectrometer. *J. Am. Soc. Mass Spectrom.* **2002,** 13, 659-669.

267. Spickett, C. M.; Pitt, A. R.; Morrice, N.; Kolch, W., Proteomic Analysis of Phosphorylation, Oxidation and Nitrosylation in Signal Transduction. *Biochim. Biophys. Acta* **2006,** 1764, 1823-1841.

268. Hunter, T., Signaling-2000 and Beyond. *Cell* **2000,** 100, 113-127.

269. Reinders, J.; Sickmann, A., State-of-the-Art in Phosphoproteomics. *Proteomics* **2005,** 5, 4052-4061.

270. Paradela, A.; Albar, J. P., Advances in the Analysis of Protein Phosphorylation. *J. Proteome Res.* **2008,** 7, 1809-1818.

271. McLachlin, D. T.; Chait, B. T., Analysis of Phosphorylated Proteins and Peptides by Mass Spectrometry. *Curr. Opin. Chem. Biol.* **2001,** 5, 591-602.

272. Mann, M.; Ong, S.-E.; Grønborg, M.; Steen, H.; Jensen, O. N.; Pandey, A., Analysis of Protein Phosphorylation Using Mass Spectrometry: Deciphering the Phosphoproteome. *Trends Biotechnol.* **2002,** 20, 261-268.

273. Leitner, A., Phosphopeptide Enrichment Using Metal Oxide Affinity Chromatography. *Trends Anal. Chem.* **2010,** 29, 177-185.

274. Hunter, T., Protein Kinases and Phosphatases: The Yin and Yang of Protein Phosphorylation and Signaling. *Cell, Vol.* **1995,** 80, 225-236.

275. Kalume, D. E.; Molina, H.; Pandey, A., Tackling the Phosphoproteome: Tools and Strategies. *Curr. Opin. Chem. Biol.* **2003,** 7, 64-69.

276. Goshe, M. B., Characterizing Phosphoproteins and Phosphoproteomes Using Mass Spectrometry. *Brief. Funct. Genomic. Proteomic.* **2006,** 4, 363-376.

277. Thingholm, T. E.; Jensen, O. N.; Larsen, M. R., Analytical Strategies for Phosphoproteomics. *Proteomics* **2009,** 9, 1451-1468.

278. Dunn, J. D.; Reid, G. E.; Bruening, M. L., Techniques for Phosphopeptide Enrichment Prior to Analysis by Mass Spectrometry. *Mass Spectrom. Rev.* **2010,** 29, 29-54.

279. Nita-Lazar, A.; Saito-Benz, H.; White, F. M., Quantitative Phosphoproteomics by Mass Spectrometry: Past, Present, and Future. *Proteomics* **2008,** 8, 4433-4443.

280. Rush, J.; Moritz, A.; Lee, K. A.; Guo, A.; Goss, V. L.; Spek, E. J.; Zhang, H.; Zha, X.-M.; Polakiewicz, R. D.; Comb, M. J., Immunoaffinity Profiling of Tyrosine Phosphorylation in Cancer Cells. *Nat. Biotechnol.* **2005,** 23, 94-101.

281. Lind, S. B.; Molin, M.; Savitski, M. M.; Emilsson, L.; Åström, J.; Hedberg, L.; Adams, C.; Nielsen, M. L.; Engström, Å.; Elfineh, L.; Andersson, E.; Zubarev, R. A.; Pettersson, U., Immunoaffinity Enrichments Followed by Mass Spectrometric Detection for Studying Global Protein Tyrosine Phosphorylation. *J. Proteome Res.* **2008,** 7, 2897-2910.

282. Olsen, J. V.; Blagoev, B.; Gnad, F.; Macek, B.; Kumar, C.; Mortensen, P.; Mann, M., Global, In Vivo, and Site-Specific Phosphorylation Dynamics in Signaling Networks. *Cell* **2006,** 127, 635-648.

283. Andersson, L.; Porath, J., Isolation of Phosphoproteins by Immobilized Metal (Fe^{3+}) Affinity Chromatography. *Anal. Biochem.* **1986,** 154, 250-254.

284. Posewitz, M. C.; Tempst, P., Immobilized Gallium(III) Affinity Chromatography of Phosphopeptides. *Anal. Chem.* **1999,** 71, 2883-2892.

285. Matsudah, H.; Nakamura, H.; Nakajima, T., New Ceramic Titania: Selective Adsorbent for Organic Phosphates Hisashi. *Anal. Sci.* **1990,** 6, 911-912.

286. Ikeguchi, Y.; Nakamura, H., Determination of Organic Phosphates by Column-Switching High Performance Anion-Exchange Chromatography Using On-Line Preconcentration on Titania. *Anal. Sci.* **1997,** 13, 479-483.

287. Kweon, H. K.; Håkansson, K., Selective Zirconium Dioxide-Based Enrichment of Phosphorylated Peptides for Mass Spectrometric Analysis. *Anal. Chem.* **2006,** 78, 1743-1749.

288. Ficarro, S. B.; Parikh, J. R.; Blank, N. C.; Marto, J. A., Niobium(V) Oxide (Nb_2O_5): Application to Phosphoproteomics. *Anal. Chem.* **2008,** 80, 4606-4613.

289. Neville, D. C. A.; Rozanas, C. R.; Price, E. M.; Gruis, D. B.; Verkman, A. S.; Townsend, R. R., Evidence for Phosphorylation of Serine 753 in CFTR Using a Novel Metal-Ion Affinity Resin and Matrix-Assisted Laser Desorption Mass Spectrometry. *Protein Sci.* **1997,** 6, 2436-2445.

290. Li, S.; Dass, C., Iron(III)-Immobilized Metal Ion Affinity Chromatography and Mass Spectrometry for the Purification and Characterization of Synthetic Phosphopeptides. *Anal. Biochem.* **1999,** 270, 9-14.

291. Nühse, T. S.; Stensballe, A.; Jensen, O. N.; Peck, S. C., Large-scale Analysis of in Vivo Phosphorylated Membrane Proteins by Immobilized Metal Ion Affinity Chromatography and Mass Spectrometry. *Mol. Cell. Proteomics* **2003,** 2, 1234-1243.

292. Zhou, H.; Xu, S.; Ye, M.; Feng, S.; Pan, C.; Jiang, X.; Li, X.; Han, G.; Fu, Y.; Zou, H., Zirconium Phosphonate-Modified Porous Silicon for Highly Specific Capture of Phosphopeptides and MALDI-TOF MS Analysis. *J. Proteome Res.* **2006,** 5, 2431-2437.

293. Feng, S.; Ye, M.; Zhou, H.; Jiang, X.; Jiang, X.; Zou, H.; Gong, B., Immobilized Zirconium Ion Affinity Chromatography for Specific Enrichment of Phosphopeptides in Phosphoproteome Analysis. *Mol. Cell. Proteomics* **2007,** 6, 1656-1665.

294. Riggs, L.; Sioma, C.; Regnier, F. E., Automated Signature Peptide Approach for Proteomics. *J. Chromatogr. A* **2001,** 924, 359-368.

295. Garcia, B. A.; Busby, S. A.; Barber, C. M.; Shabanowitz, J.; Allis, C. D.; Hunt, D. F., Characterization of Phosphorylation Sites on Histone H1 Isoforms by Tandem Mass Spectrometry. *J. Proteome Res.* **2004,** 3, 1219-1227.

296. Li, X.; Gerber, S. A.; Rudner, A. D.; Beausoleil, S. A.; Haas, W.; Villén, J.; Elias, J. E.; Gygi, S. P., Large-Scale Phosphorylation Analysis of α-Factor-Arrested *Saccharomyces cerevisiae*. *J. Proteome Res.* **2007,** 6, 1190-1197.

297. Raska, C. S.; Parker, C. E.; Dominski, Z.; Marzluff, W. F.; Glish, G. L.; Pope, R. M.; Borchers, C. H., Direct MALDI-MS/MS of Phosphopeptides Affinity-Bound to Immobilized Metal Ion Affinity Chromatography Beads. *Anal. Chem.* **2002,** 74, 3429-3433.

298. Moser, K.; White, F. M., Phosphoproteomic Analysis of Rat Liver by High Capacity IMAC and LC-MS/MS. *J. Proteome Res.* **2006,** 5, 98-104.

299. Ndassa, Y. M.; Orsi, C.; Marto, J. A., Improved Immobilized Metal Affinity Chromatography for Large-Scale Phosphoproteomics Applications. *J. Proteome Res.* **2006,** 5, 2789-2799.

300. Stewart, I. I.; Thomson, T.; Figeys, D., ^{18}O Labeling: A Tool for Proteomics. *Rapid Commun. Mass Spectrom.* **2001,** 15, 2456-2465.

301. Kokubu, M.; Ishihama, Y.; Sato, T.; Nagasu, T.; Oda, Y., Specificity of Immobilized Metal Affinity-Based IMAC/C18 Tip Enrichment of Phosphopeptides for Protein Phosphorylation Analysis. *Anal. Chem.* **2005,** 77, 5144-5154.

302. Pinkse, M. W. H.; Uitto, P. M.; Hilhorst, M. J.; Ooms, B.; Heck, A. J. R., Selective Isolation at the Femtomole Level of Phosphopeptides from Proteolytic Digests Using 2D-NanoLC-ESI-MS/MS and Titanium Oxide Precolumns. *Anal. Chem.* **2004,** 76, 3935-3943.

303. Ikeguchi, Y.; Nakamura, H., Selective Enrichment of Phospholipids by Titania. *Anal. Sci.* **2000,** 16, 541-543.

304. Sano, A.; Nakamura, H., Chemo-affinity of Titania for the Column-Switching HPLC Analysis of Phosphopeptides. *Anal. Sci.* **2004,** 20, 565-566.

305. Larsen, M. R.; Thingholm, T. E.; Jensen, O. N.; Roepstorff, P.; Jørgensen, T. J. D., Highly Selective Enrichment of Phosphorylated Peptides from Peptide Mixtures Using Titanium Dioxide Microcolumns. *Mol. Cell. Proteomics* **2005,** 4, 873-886.

306. Thingholm, T. E.; Jørgensen, T. J. D.; Jensen, O. N.; Larsen, M. R., Highly Selective Enrichment of Phosphorylated Peptides Using Titanium Dioxide. *Nat. Protoc.* **2006,** 1, 1929-1935.

307. Jensen, S. S.; Larsen, M. R., Evaluation of the Impact of Some Experimental Procedures on Different Phosphopeptide Enrichment Techniques. *Rapid Commun. Mass Spectrom.* **2007,** 21, 3635-3645.

308. Sugiyama, N.; Masuda, T.; Shinoda, K.; Nakamura, A.; Tomita, M.; Ishihama, Y., Phosphopeptide Enrichment by Aliphatic Hydroxy Acid-modified Metal Oxide Chromatography for Nano-LC-MS/MS in Proteomics Applications. *Mol. Cell. Proteomics* **2007,** 6, 1103-1109.

309. Lo, C.-Y.; Chen, W.-Y.; Chen, C.-T.; Chen, Y.-C., Rapid Enrichment of Phosphopeptides from Tryptic Digests of Proteins Using Iron Oxide Nanocomposites of Magnetic Particles Coated with Zirconia as the Concentrating Probes. *J. Proteome Res.* **2007,** 6, 887-893.

310. Zhou, H.; Tian, R.; Ye, M.; Xu, S.; Feng, S.; Pan, C.; Jiang, X.; Li, X.; Zou, H., Highly Specific Enrichment of Phosphopeptides by Zirconium Dioxide Nanoparticles for Phosphoproteome Analysis. *Electrophoresis* **2007,** 28, 2201-2215.

311. Li, Y.; Leng, T.; Lin, H.; Deng, C.; Xu, X.; Yao, N.; Yang, P.; Zhang, X., Preparation of Fe_3O_4@ZrO_2 Core-Shell Microspheres as Affinity Probes for Selective Enrichment and Direct Determination of Phosphopeptides Using Matrix-Assisted Laser Desorption Ionization Mass Spectrometry. *J. Proteome Res.* **2007,** 6, 4498-4510.

312. Wolschin, F.; Wienkoop, S.; Weckwerth, W., Enrichment of Phosphorylated Proteins and Peptides from Complex Mixtures Using Metal Oxide/Hydroxide Affinity Chromatography (MOAC). *Proteomics* **2005,** 5, 4389-4397.

313. Röhrig, H.; Colby, T.; Schmidt, J.; Harzen, A.; Facchinelli, F.; Bartels, D., Analysis of Desiccation-Induced Candidate Phosphoproteins from *Craterostigma plantagineum* Isolated with a Modified Metal Oxide Affinity Chromatography Procedure. *Proteomics* **2008,** 8, 3548-3560.

314. Wang, Y.; Chen, W.; Wu, J.; Guo, Y.; Xia, X., Highly Efficient and Selective Enrichment of Phosphopeptides Using Porous Anodic Alumina Membrane for MALDI-TOF MS Analysis. *J. Am. Soc. Mass Spectrom.* **2007,** 18, 1387-1395.

315. Jeong, N. C.; Lee, J. S.; Tae, E. L.; Lee, Y. J.; Yoon, K. B., Acidity Scale for Metal Oxides and Sanderson's Electronegativities of Lanthanide Elements. *Angew. Chem. Int. Ed.* **2008,** 47, 10128-10132.

316. Bodenmiller, B.; Mueller, L. N.; Mueller, M.; Domon, B.; Aebersold, R., Reproducible Isolation of Distinct, Overlapping Segments of the Phosphoproteome. *Nat. Meth.* **2007,** 4, 231-237.

317. Carr, S. A.; Annan, R. S.; Huddleston, M. J., Mapping Posttranslational Modifications of Proteins by MS-Based Selective Detection: Application to Phosphoproteomics. *Methods Enzymol.* **2005,** 405, 82-115.

318. Han, X.; Aslanian, A.; Yates, J. R., III, Mass Spectrometry for Proteomics. *Curr. Opin. Chem. Biol.* **2008,** 12, 483-490.

319. Liao, P.-C.; Leykam, J.; Andrews, P. C.; Gage, D. A.; Allison, J., An Approach to Locate Phosphorylation Sites in a Phosphoprotein: Mass Mapping by Combining Specific Enzymatic Degradation with Matrix-Assisted Laser Desorption/Ionization Mass Spectrometry. *Anal. Biochem.* **1994,** 219, 9-20

320. Larsen, M. R.; Sørensen, G. L.; Fey, S. J.; Larsen, P. M.; Roepstorff, P., Phospho-Proteomics: Evaluation of the Use of Enzymatic De-Phosphorylation and Differential Mass Spectrometric Peptide Mass Mapping for Site Specific Phosphorylation Assignment in Proteins Separated by Gel Electrophoresis. *Proteomics* **2001,** 1, 223-238.

321. Pyatkivskyy, Y.; Ryzhov, V., Coupling of Ion-Molecule Reactions with Liquid Chromatography on a Quadrupole Ion Trap Mass Spectrometer. *Rapid Commun. Mass Spectrom.* **2008,** 22, 1288-1294.

322. Wells, J. M.; McLuckey, S. A., Collision-Induced Dissociation (CID) of Peptides and Proteins. *Methods Enzymol.* **2005,** 402, 148-185.

323. Sweet, S. M. M.; Cooper, H. J., Electron Capture Dissociation in the Analysis of Protein Phosphorylation. *Expert Rev. Proteomic.* **2007,** 4, 149-159.

324. Wiesner, J.; Premsler, T.; Sickmann, A., Application of Electron Transfer Dissociation (ETD) for the Analysis of Posttranslational Modifications. *Proteomics* **2008,** 8, 4466-4483.

325. Kalcic, C. L.; Gunaratne, T. C.; Jones, A. D.; Dantus, M.; Reid, G. E., Femtosecond Laser-Induced Ionization/Dissociation of Protonated Peptides. *J. Am. Chem. Soc.* **2009,** 131, 940-942.

326. Smith, S. A.; Kalcic, C. L.; Safran, K. A.; Stemmer, P. M.; Dantus, M.; Reid, G. E., Enhanced Characterization of Singly Protonated Phosphopeptide Ions by Femtosecond Laser-induced Ionization/Dissociation Tandem Mass Spectrometry (fs-LID-MS/MS). *J. Am. Soc. Mass Spectrom.* **2010,** 21, 2031-2040.

327. McLuckey, S. A.; Goeringer, D. E., Slow Heating Methods in Tandem Mass Spectrometry. *J. Mass Spectrom.* **1997,** 32, 461-474.

328. Reid, G. E.; Simpson, R. J.; Hair, R. A. J. O., Leaving Group and Gas Phase Neighboring Group Effects in the Side Chain Losses from Protonated Serine and its Derivatives. *J. Am. Soc. Mass Spectrom.* **2000,** 11, 1047-1060.

329. Flora, J. W.; Muddiman, D. C., Determination of the Relative Energies of Activation for the Dissociation of Aromatic versus Aliphatic Phosphopeptides by ESI-FTICR-MS and IRMPD. *J. Am. Soc. Mass Spectrom.* **2004,** 15, 121-127.

330. Huddleston, M. J.; Annan, R. S.; Bean, M. F.; Carr, S. A., Selective Detection of Phosphopeptides in Complex Mixtures by Electrospray Liquid Chromatography/Mass Spectrometry. *J. Am. Soc. Mass Spectrom.* **1993,** 4, 710-717.

331. Edelson-Averbukh, M.; Pipkorn, R.; Lehmann, W. D., Phosphate Group-Driven Fragmentation of Multiply Charged Phosphopeptide Anions. Improved Recognition of Peptides Phosphorylated at Serine, Threonine, or Tyrosine by Negative Ion Electrospray Tandem Mass Spectrometry. *Anal. Chem.* **2006,** 78, 1249-1256.

332. Carr, S. A.; Huddleston, M. J.; Annan, R. S., Selective Detection and Sequencing of Phosphopeptides at the Femtomole Level by Mass Spectrometry. *Anal. Biochem.* **1996,** 239, 180-192.

333. Schlosser, A.; Pipkorn, R.; Bossemeyer, D.; Lehmann, W. D., Analysis of Protein Phosphorylation by a Combination of Elastase Digestion and Neutral Loss Tandem Mass Spectrometry. *Anal. Chem.* **2001,** 73, 170-176.

334. Hogan, J. M.; Pitteri, S. J.; McLuckey, S. A., Phosphorylation Site Identification via Ion Trap Tandem Mass Spectrometry of Whole Protein and Peptide Ions: Bovine α-Crystallin A Chain. *Anal. Chem.* **2003,** 75, 6509-6516.

335. Bateman, R. H.; Carruthers, R.; Hoyes, J. B.; Jones, C.; Langridge, J. I.; Millar, A.; Vissers, J. P. C., A Novel Precursor Ion Discovery Method on a Hybrid Quadrupole Orthogonal Acceleration Time-of-Flight (Q-TOF) Mass Spectrometer for Studying Protein Phosphorylation. *J. Am. Soc. Mass Spectrom.* **2002,** 13, 792-803.

336. Chang, E. J.; Archambault, V.; McLachlin, D. T.; Krutchinsky, A. N.; Chait, B. T., Analysis of Protein Phosphorylation by Hypothesis-Driven Multiple-Stage Mass Spectrometry. *Anal. Chem.* **2004,** 76, 4472-4483.

337. Schroeder, M. J.; Shabanowitz, J.; Schwartz, J. C.; Hunt, D. F.; Coon, J. J., A Neutral Loss Activation Method for Improved Phosphopeptide Sequence Analysis by Quadrupole Ion Trap Mass Spectrometry. *Anal. Chem.* **2004,** 76, 3590-3598.

338. Beausoleil, S. A.; Villén, J.; Gerber, S. A.; Rush, J.; Gygi, S. P., A Probability-Based Approach for High-Throughput Protein Phosphorylation Analysis and Site Localization. *Nat. Biotechnol.* **2006,** 24, 1285-1292.

339. Ulintz, P. J.; Yocum, A. K.; Bodenmiller, B.; Aebersold, R.; Andrews, P. C.; Nesvizhskii, A. I., Comparison of MS^2-Only, MSA, and MS^2/MS^3 Methodologies for Phosphopeptide Identification. *J. Proteome Res.* **2009,** 8, 887-899.

340. Steen, H.; Küster, B.; Fernandez, M.; Pandey, A.; Mann, M., Detection of Tyrosine Phosphorylated Peptides by Precursor Ion Scanning Quadrupole TOF Mass Spectrometry in Positive Ion Mode. *Anal. Chem.* **2001,** 73, 1440-1448.

341. Steen, H.; Küster, B.; Fernandez, M.; Pandey, A.; Mann, M., Tyrosine Phosphorylation Mapping of the Epidermal Growth Factor Receptor Signaling Pathway. *J. Biol. Chem.* **2002,** 277, 1031-1039.

342. Steen, H.; Küster, B.; Mann, M., Quadrupole Time-of-Flight versus Triple-Quadrupole Mass Spectrometry for the Determination of Phosphopeptides by Precursor Ion Scanning. *J. Mass Spectrom.* **2001,** 36, 782-790.

343. DeGnore, J. P.; Qin, J., Fragmentation of Phosphopeptides in an Ion Trap Mass Spectrometer. *J. Am. Soc. Mass Spectrom.* **1998,** 9, 1175-1188.

344. Palumbo, A. M.; Reid, G. E., Evaluation of Gas-Phase Rearrangement and Competing Fragmentation Reactions on Protein Phosphorylation Site Assignment Using Collision Induced Dissociation-MS/MS and MS^3. *Anal. Chem.* **2008,** 80, 9735-9747.

345. Edelson-Averbukh, M.; Shevchenko, A.; Pipkorn, R.; Lehmann, W. D., Gas-Phase Intramolecular Phosphate Shift in Phosphotyrosine-Containing Peptide Monoanions. *Anal. Chem.* **2009,** 81, 4369-4381.

346. Leitner, A.; Foettinger, A.; Lindner, W., Improving Fragmentation of Poorly Fragmenting Peptides and Phosphopeptides During Collision-Induced Dissociation by Malondialdehyde Modification of Arginine Residues. *J. Mass Spectrom.* **2007,** 42, 950-959.

347. Gronert, S.; Renee Huang; Li, K. H., Gas Phase Derivatization in Peptide Analysis I: The Utility of Trimethyl Borate in Identifying Phosphorylation Sites. *Int. J. Mass Spectrom.* **2004,** 231, 179-187.

348. Gronert, S.; Li, K. H.; Horiuchi, M., Manipulating the Fragmentation Patterns of Phosphopeptides via Gas-Phase Boron Derivatization: Determining Phosphorylation Sites in Peptides with Multiple Serines. *J. Am. Soc. Mass Spectrom.* **2005,** 16, 1905-1914.

349. McLafferty, F. W.; Horn, D. M.; Breuker, K.; Ge, Y.; Lewis, M. A.; Cerda, B.; Zubarev, R. A.; Carpenter, B. K., Electron Capture Dissociation of Gaseous Multiply Charged Ions by Fourier-Transform Ion Cyclotron Resonance. *J. Am. Soc. Mass Spectrom.* **2001,** 12, 245-249.

350. Syrstad, E. A.; Tureček, F., Toward a General Mechanism of Electron Capture Dissociation. *J. Am. Soc. Mass Spectrom.* **2005,** 16, 208-224.

351. Stensballe, A.; Jensen, O. N.; Olsen, J. V.; Haselmann, K. F.; Zubarev, R. A., Electron Capture Dissociation of Singly and Multiply Phosphorylated Peptides. *Rapid Commun. Mass Spectrom.* **2000,** 14, 1793-1800.

352. Shi, S. D.-H.; Hemling, M. E.; Carr, S. A., Phosphopeptide/Phosphoprotein Mapping by Electron Capture Dissociation Mass Spectrometry. *Anal. Chem.* **2001,** 73, 19-22.

353. Sweet, S. M. M.; Mardakheh, F. K.; Ryan, K. J. P.; Langton, A. J.; Heath, J. K.; Cooper, H. J., Targeted Online Liquid Chromatography Electron Capture Dissociation Mass Spectrometry for the Localization of Sites of in Vivo Phosphorylation in Human Sprouty2. *Anal. Chem.* **2008,** 80, 6650-6657.

354. Sweet, S. M. M.; Creese, A. J.; Cooper, H. J., Strategy for the Identification of Sites of Phosphorylation in Proteins: Neutral Loss Triggered Electron Capture Dissociation. *Anal. Chem.* **2006,** 78, 7563-7569.

355. Sweet, S. M. M.; Bailey, C. M.; Cunningham, D. L.; Heath, J. K.; Cooper, H. J., Large Scale Localization of Protein Phosphorylation by Use of Electron Capture Dissociation Mass Spectrometry. *Mol. Cell. Proteomics* **2009,** 8, 904-912.

356. Chi, A.; Huttenhower, C.; Geer, L. Y.; Coon, J. J.; Syka, J. E. P.; Bai, D. L.; Shabanowitz, J.; Burke, D. J.; Troyanskaya, O. G.; Hunt, D. F., Analysis of Phosphorylation Sites on Proteins from *Saccharomyces cerevisiae* by Electron Transfer Dissociation (ETD) Mass Spectrometry. *Proc. Natl. Acad. Sci.* **2007,** 104, 2193-2198.

357. Molina, H.; Horn, D. M.; Tang, N.; Mathivanan, S.; Pandey, A., Global Proteomic Profiling of Phosphopeptides Using Electron Transfer Dissociation Tandem Mass Spectrometry. *Proc. Natl. Acad. Sci.* **2007,** 104, 2199-2204.

358. Swaney, D. L.; Wenger, C. D.; Thomson, J. A.; Coon, J. J., Human Embryonic Stem Cell Phosphoproteome Revealed by Electron Transfer Dissociation Tandem Mass Spectrometry. *Proc. Natl. Acad. Sci.* **2009,** 106, 995-1000.

359. Chalmers, M. J.; Håkansson, K.; Johnson, R.; Smith, R.; Shen, J.; Emmett, M. R.; Marshall, A. G., Protein kinase A Phosphorylation Characterized by Tandem Fourier Transform Ion Cyclotron Resonance Mass Spectrometry. *Proteomics* **2004,** 4, 970-981.

360. Kweon, H. K.; Håkansson, K., Metal Oxide-Based Enrichment Combined with Gas-Phase Ion-Electron Reactions for Improved Mass Spectrometric Characterization of Protein Phosphorylation. *J. Proteome Res.* **2008,** 7, 749-755.

361. Swaney, D. L.; McAlister, G. C.; Coon, J. J., Decision Tree-Driven Tandem Mass Spectrometry for Shotgun Proteomics. *Nat. Meth.* **2008,** 5, 959-964.

362. Horn, D. M.; Ge, Y.; McLafferty, F. W., Activated Ion Electron Capture Dissociation for Mass Spectral Sequencing of Larger (42 kDa) Proteins. *Anal. Chem.* **2000,** 72, 4778-4784.

363. Swaney, D. L.; McAlister, G. C.; Wirtala, M.; Schwartz, J. C.; Syka, J. E. P.; Coon, J. J., Supplemental Activation Method for High-Efficiency Electron-Transfer Dissociation of Doubly Protonated Peptide Precursors. *Anal. Chem.* **2007,** 79, 477-485.

364. Han, H.; Xia, Y.; McLuckey, S. A., Beam-Type Collisional Activation of Polypeptide Cations that Survive Ion/Ion Electron Transfer. *Rapid Commun. Mass Spectrom.* **2007,** 21, 1567-1573.

365. Bushey, J. M.; Baba, T.; Glish, G. L., Simultaneous Collision Induced Dissociation of the Charge Reduced Parent Ion during Electron Capture Dissociation. *Anal. Chem.* **2009,** 81, 6156-6164.

366. Xu, Y.; Zhang, L.; Lu, H.; Yang, P., Mass Spectrometry Analysis of Phosphopeptides after Peptide Carboxy Group Derivatization. *Anal. Chem.* **2008,** 80, 8324-8328.

367. Zhang, L.; Xu, Y.; Lu, H.; Yang, P., Carboxy Group Derivatization for Enhanced Electrontransfer Dissociation Mass Spectrometric Analysis of Phosphopeptides. *Proteomics* **2009,** 9, 4093-4097.

368. Kjeldsen, F.; Giessing, A. M. B.; Ingrell, C. R.; Jensen, O. N., Peptide Sequencing and Characterization of Post-Translational Modifications by Enhanced Ion-Charging and Liquid Chromatography Electron-Transfer Dissociation Tandem Mass Spectrometry. *Anal. Chem.* **2007,** 79, 9243-9252.

369. Crowe, M. C.; Brodbelt, J. S., Differentiation of Phosphorylated and Unphosphorylated Peptides by High-Performance Liquid Chromatography-Electrospray Ionization-infrared Multiphoton Dissociation in a Quadrupole Ion Trap. *Anal. Chem.* **2005,** 77, 5726-5734.

370. Flora, J. W.; Muddiman, D. C., Selective, Sensitive, and Rapid Phosphopeptide Identification in Enzymatic Digests Using ESI-FTICR-MS with Infrared Multiphoton Dissociation. *Anal. Chem.* **2001,** 73, 3305-3311.

371. Flora, J. W.; Muddiman, D. C., Gas-Phase Ion Unimolecular Dissociation for Rapid Phosphopeptide Mapping by IRMPD in a Penning Ion Trap: An Energetically Favored Process. *J. Am. Chem. Soc.* **2002,** 124, 6546-6547.

372. Chalmers, M. J.; Quinn, J. P.; Blakney, G. T.; Emmett, M. R.; Mischak, H.; Gaskell, S. J.; Marshall, A. G., Liquid Chromatography-Fourier Transform Ion Cyclotron Resonance Mass Spectrometric Characterization of Protein Kinase C Phosphorylation. *J. Proteome Res.* **2003,** 2, 373-382.

373. Crowe, M. C.; Brodbelt, J. S., Infrared Multiphoton Dissociation (IRMPD) and Collisionally Activated Dissociation of Peptides in a Quadrupole Ion Trap with Selective IRMPD of Phosphopeptides. *J. Am. Soc. Mass Spectrom.* **2004,** 15, 1581-1592.

374. Kim, T.-Y.; Reilly, J. P., Time-Resolved Observation of Product Ions Generated by 157 nm Photodissociation of Singly Protonated Phosphopeptides. *J. Am. Soc. Mass Spectrom.* **2009,** 20, 2334-2341.

375. Diedrich, J. K.; Julian, R. R., Site-Specific Radical Directed Dissociation of Peptides at Phosphorylated Residues. *J. Am. Chem. Soc.* **2008,** 130, 12212-12213.

376. Shin, Y. S.; Moon, J. H.; Kima, M. S., Observation of Phosphorylation Site-Specific Dissociation of Singly Protonated Phosphopeptides. *J. Am. Soc. Mass Spectrom.* **2010,** 21, 53-59.

377. Schulenberg, B.; Goodman, T. N.; Aggeler, R.; Capaldi, R. A.; Patton, W. F., Characterization of Dynamic and Steady-State Protein Phosphorylation Using a Fluorescent Phosphoprotein Gel Stain and Mass Spectrometry. *Electrophoresis* **2004,** 25, 2526-2532.

378. Chitteti, B. R.; Peng, Z., Proteome and Phosphoproteome Differential Expression under Salinity Stress in Rice (*Oryza sativa*) Roots. *J. Proteome Res.* **2007,** 6, 1718-1727.

379. Ong, S.-E.; Blagoev, B.; Kratchmarova, I.; Kristensen, D. B.; Steen, H.; Pandey, A.; Mann, M., Stable Isotope Labeling by Amino Acids in Cell Culture, SILAC, as a Simple and Accurate Approach to Expression Proteomics. *Mol. Cell. Proteomics* **2002,** 1, 376-386.

380. Ong, S.-E.; Mann, M., A Practical Recipe for Stable Isotope Labeling by Amino Acids in Cell Culture (SILAC). *Nat. Protoc.* **2006,** 1, 2650-2660.

381. Hoof, D. V.; Muñoz, J.; Braam, S. R.; Pinkse, M. W. H.; Linding, R.; Heck, A. J. R.; Mummery, C. L.; Krijgsveld, J., Phosphorylation Dynamics during Early Differentiation of Human Embryonic Stem Cells. *Cell Stem Cell* **2009,** 5, 214-226.

382. Krüger, M.; Moser, M.; Ussar, S.; Thievessen, I.; Luber, C. A.; Forner, F.; Schmidt, S.; Zanivan, S.; Fässler, R.; Mann, M., SILAC Mouse for Quantitative Proteomics Uncovers Kindlin-3 as an Essential Factor for Red Blood Cell Function. *Cell* **2008,** 134, 353-364.

383. Riggs, L.; Seeley, E. H.; Regnier, F. E., Quantification of Phosphoproteins with Global Internal Standard Technology. *J. Chromatogr. B* **2005,** 817, 89-96.

384. Previs, M. J.; VanBuren, P.; Begin, K. J.; Vigoreaux, J. O.; LeWinter, M. M.; Matthews, D. E., Quantification of Protein Phosphorylation by Liquid Chromatography-Mass Spectrometry. *Anal. Chem.* **2008,** 80, 5864-5872.

385. Goshe, M. B.; Conrads, T. P.; Panisko, E. A.; Angell, N. H.; Veenstra, T. D.; Smith, R. D., Phosphoprotein Isotope-Coded Affinity Tag Approach for Isolating and Quantitating Phosphopeptides in Proteome-Wide Analyses. *Anal. Chem.* **2001,** 73, 2578-2586.

386. Qian, W.-J.; Goshe, M. B.; Camp, D. G., II; Yu, L.-R.; Tang, K.; Smith, R. D., Phosphoprotein Isotope-Coded Solid-Phase Tag Approach for Enrichment and Quantitative Analysis of Phosphopeptides from Complex Mixtures. *Anal. Chem.* **2003,** 75, 5441-5450.

387. Yao, X.; Freas, A.; Ramirez, J.; Demirev, P. A.; Fenselau, C., Proteolytic ^{18}O Labeling for Comparative Proteomics: Model Studies with Two Serotypes of Adenovirus. *Anal. Chem.* **2001,** 73, 2836-2842.

388. Zhang, Y.; Wolf-Yadlin, A.; Ross, P. L.; Pappin, D. J.; Rush, J.; Lauffenburger, D. A.; White, F. M., Time-resolved Mass Spectrometry of Tyrosine Phosphorylation Sites in the Epidermal Growth Factor Receptor Signaling Network Reveals Dynamic Modules. *Mol. Cell. Proteomics* **2005,** 4, 1240-1250.

389. Thingholm, T. E.; Palmisano, G.; Kjeldsen, F.; Larsen, M. R., Undesirable Charge-Enhancement of Isobaric Tagged Phosphopeptides Leads to Reduced Identification Efficiency. *J. Proteome Res.* **2010,** 9, 4045-4052.

390. Shi, Y.; Yao, X., Oxygen Isotopic Substitution of Peptidyl Phosphates for Modification-Specific Mass Spectrometry. *Anal. Chem.* **2007,** 79, 8454-8462.

391. Ramos, A. A.; Yang, H.; Rosen, L. E.; Yao, X., Tandem Parallel Fragmentation of Peptides for Mass Spectrometry. *Anal. Chem.* **2006,** 78, 6391-6397.

392. Lu, Y.; Tanasova, M.; Borhan, B.; Reid, G. E., Ionic Reagent for Controlling the Gas-Phase Fragmentation Reactions of Cross-Linked Peptides. *Anal. Chem.* **2008,** 80, 9279-9287.

393. Ren, D.; Julka, S.; Inerowicz, H. D.; Regnier, F. E., Enrichment of Cysteine-Containing Peptides from Tryptic Digests Using a Quaternary Amine Tag. *Anal. Chem.* **2004,** 76, 4522-4530.

394. House, J. E., *Principles of chemical kinetics*. Amsterdam; Boston: Elsevier/Academic Press: 2007.

395. Tan, Y.-J.; Wang, W.-H.; Palumbo, A.; Reid, G. E.; Bruening, M. L., Phosphopeptide Enrichment with a Titanium Dioxide-Modified Nylon Membrane. *Manuscipt in Preparation*.

396. Krokhin, O. V.; Craig, R.; Spicer, V.; Ens, W.; Standing, K. G.; Beavis, R. C.; Wilkins, J. A., An Improved Model for Prediction of Retention Times of Tryptic Peptides in Ion Pair Reversed-phase HPLC. *Mol. Cell. Proteomics* **2004,** 3, 908-919.

397. Cech, N. B.; Enke, C. G., Pratical Implications of Some Recent Studies in Electrospray Ionization Fundamentals. *Mass Spectrom. Rev.* **2001,** 20, 362-387.

398. Frahm, J. L.; Bori, I. D.; Comins, D. L.; Hawkridge, A. M.; Muddiman, D. C., Achieving Augmented Limits of Detection for Peptides with Hydrophobic Alkyl Tags. *Anal. Chem.* **2007,** 79, 3989-3995.

399. Cech, N. B.; Enke, C. G., Relating Electrospray Ionization Response to Nonpolar Character of Small Peptides. *Anal. Chem.* **2000,** 72, 2717-2723.

400. Cech, N. B.; Enke, C. G., Effect of Affinity for Droplet Surfaces on the Fraction of Analyte Molecules Charged during Electrospray Droplet Fission. *Anal. Chem.* **2001,** 73, 4632-4639.

401. Cech, N. B.; Krone, J. R.; Enke, C. G., Predicting Electrospray Response from Chromatographic Retention Time. *Anal. Chem.* **2001,** 73, 208-213.

402. He, Y.; Reilly, J. P., Does a Charge Tag Really Provide a Fixed Charge? *Angew. Chem. Int. Ed.* **2008,** 47, 2463-2465.

403. Williams, K. A.; Doi, J. T.; Musker, W. K., Neighboring-Group Participation in Organic Redox Reactions. 10. The Kinetic and Mechanistic Effects of Imidazole and Benzimidazole Nitrogen on Thioether Oxidations. *J. Org. Chem.* **1985,** 50, 4-10.

404. Crouch, N. P.; Adlington, R. M.; Baldwin, J. E.; Lee, M.-H.; MacKinnon, C. H., A Mechanistic Rationalisation for the Substrate Specificity of Recombinant Mammalian 4-Hydroxyphenylpyruvate Dioxygenase (4-HPPD). *Tetrahedron* **1997,** 53, 6993-7010.